2020

Metagenomic identification and characterisation of emerging and re-emerging viruses causing disease in febrile patients.

Wise, Emma Louise

UNIVERSITY OF PLYMOUTH

METAGENOMIC IDENTIFICATION AND CHARACTERISATION OF EMERGING AND RE-EMERGING VIRUSES CAUSING DISEASE IN FEBRILE PATIENTS

by

EMMA LOUISE WISE

A thesis submitted to the University of Plymouth in partial fulfilment for the degree of

DOCTOR OF PHILOSOPHY

School of Biomedical Sciences

[In collaboration with Public Health England]

January 2020

ACKNOWLEDGEMENTS

This project would not have been possible without the people of Ecuador and Sierra Leone, to whom this project is dedicated. The Zika outbreak in the Americas and the Ebola outbreak in West Africa caused untold suffering, the extent of which is difficult to grasp for those fortunate enough to live without the daily threat of infectious disease. The strength of character of those I met in Sierra Leone in 2015 is a testament to human resilience.

Thank you to my supervisors Steve Pullan, Christopher Logue, Gyuri Fejer and Simon Jackson for your involvement in the project and your belief that I could carry it out. Your encouragement, suggestions, knowledge and experience have been invaluable to me, as have your support and guidance throughout.

Thank you to Dan Carter for selflessly giving up your time despite having a full-time job and your own PhD project. Thanks in particular for staying late as my CL3 'buddy' and for helping with a mammoth number of plaque assays, I appreciate it hugely. Thank you to the rest of the genomics team; Kuia Lewandowski, Mike Elmore, Mia White, Karen Osman, Tom Hender and Liana Kafetzopoulou for looking after me when I first joined, training me and supporting me. I feel lucky to have been part of the team and I will miss you all.

Thank you to my colleagues at the Universidad San Francisco de Quito, particularly Sully Márquez, Sonia Zapata and Gabriel Trueba, for your ongoing support and enthusiasm for the project and for hosting me in the summer of 2018.

Thank you to Barry Atkinson for your time, effort and planning in making the OROV time-course experiment happen and for your insightful comments and suggestions. Thank

you to everyone at Public Health England that helped me in one way or another, particularly the Virology and Pathogenesis group, the National Collection of Pathogenic Viruses and the European Collection of Authenticated Cell Cultures. Thank you to the Sierra Leone Ministry of Health and Sanitation (MoSH) and the PHE-MoSH biobank committee for granting permission to use Sierra Leonean patient plasma samples.

Thank you to my family and friends for the support, understanding and love you have shown me throughout. Thank you to my wonderful mum for the myriad ways in which you supported me and showed me that you are proud of me. Thank you to Tom for being so excited for me to do this, for compromising, for making me laugh and for lending an interested ear and an analytical mind.

AUTHOR'S DECLARATION

At no time during the registration for the degree of Doctor of Philosophy has the author been registered for any other University award without prior agreement of the Doctoral College Quality Sub-Committee.

Work submitted for this research degree at the University of Plymouth has not formed part of any other degree either at the University of Plymouth or at another establishment.

This study was funded by a studentship from Public Health England PhD studentship fund and carried out in collaboration with Public Health England.

Publications

1. **Wise EL**, Pullan ST, Márquez S, Paz V, Mosquera JD, Zapata S, *et al.* Isolation of Oropouche Virus from Febrile Patient, Ecuador. Emerg Infect Dis. 2018 May;24(5):935–7. doi:10.3201/eid2405.171569.

2. Gutierrez B, **Wise EL**, Pullan ST, Logue CH, Bowden TA, Escalera-Zamudio M, et al. The evolutionary dynamics of Oropouche Virus in South America. J Virol. Dec 2019, JVI.01127-19; doi: 10.1128/JVI.01127-19.

3. **Wise EL**, Márquez S, Mellors J, Paz V, Atkinson B, Gutierrez B, *et al.* Oropouche virus cases identified in Ecuador using an optimised qRT-PCR informed by metagenomic sequencing. PLOS Neglected Tropical Diseases 14(1): e0007897. doi: 10.1371/journal.pntd.0007897.

Publications not included as examined elements of the thesis itself that were published during the research registration period:

1. **Wise EL**, Marston DA, Banyard AC, Goharriz H, Selden D, Maclaren N, Goddard T, Johnson N, McElhinney LM, Brouwer A, Aegerter JN, Smith GC, Horton DL, Breed AC, Fooks AR. Passive surveillance of United Kingdom bats for lyssaviruses (2005-2015). Epidemiol Infect. 2017 Jul 24:1-13. doi: 10.1017/S0950268817001455.

Training courses completed

Title	Date	Duration	Location
Train the trainer	12/09/17	2 days	PHE Porton Down
1st medical entomology course "Insects and vector-borne diseases in Amazonia and the Caribbean: from field to lab"	18/09/17	12 days	Institut Pasteur de la Guyane, French Guiana
The transfer process	06/10/18	1 day	Plymouth University
Fundamentals of cell culture: Key principles and practice	10/10/17	4 days	PHE Porton Down
How to write a research paper	24/10/17	1 day	PHE Porton Down
STEM ambassador induction training	16/11/17	0.5 day	Winchester Science Centre & Planetarium
Practical training in PMBC isolation, viral stimulation and flow cytometry	26/02/18	2 days	Plymouth University
MinION research and development day	20/04/18	1 day	London
Risk assessment for risk assessors	30/10/18	2 days	PHE Porton Down
'Stand up for Science' workshop on public engagement	14/11/18	1 day	London

Conference attendance (presentations listed in 'research presentations' table)

Title	Date	Duration	Location
20th Conference in Genomics and Proteomics of Human Pathogens	22/06/17	1 day	PHE Colindale, London
PHE PhD student conference 2018	07/02/18	1 day	PHE Chilton, Oxfordshire
9th European meeting on viral zoonoses	29-02/10/19	4 days	Saint-Raphael, France

Research presentations

Title	Date	Type	Location
Characterisation of the human virome in febrile patients	22/06/17	Poster	20th Conference in Genomics and Proteomics of Human Pathogens, PHE Colindale
First identification of Oropouche virus in Ecuador	04/12/17	Poster	Postgraduate Society research showcase, Plymouth University
First identification of Oropouche virus in Ecuador	07/02/18	Poster (awarded runner up prize)	PHE PhD student conference 2018
Real-time infectious disease sequencing demonstration	11&12/09/18	Demonstration	PHE conference, Warwick University
Identification of a cluster of Oropouche orthobunyavirus cases in Ecuador	07/03/19	Talk (awarded 1st place)	PHE PhD student conference 2019
Identification of a cluster of Oropouche orthobunyavirus cases in Ecuador	14/05/19	Talk	Internal seminar, PHE
Oropouche virus cases identified in Ecuador using an optimised qRT-PCR informed by metagenomic sequencing.	01/10/19	Talk	9th European meeting on viral zoonoses, Saint-Raphael, France
Metagenomic identification of pathogens causing disease in Ebola-negative patients	21/11/19	Talk	Sierra Leone Ebola Biobank Governance Group meeting, PHE

Teaching presentations

Title	Role	Date	Event	Location
Virus hazard groups, good microbiological practice, RNA extraction	Lead	5-8/09/17	Virology training course	PHE Porton Down
Hazard criteria and categorisation of microbes	Speaker	3-6 monthly from Sep 2017 – Feb 2019	ISTR Level 1 Biosafety Practitioner course/Containment level 3 training course	PHE Porton Down
Ebola training lab session	Lead	05/10/17	PHE Schools day	PHE Porton Down
Good microbiological practice, working in a microbiological safety cabinet, emergency procedures	Lead and assist	20-24/11/17	Biosafety & biosecurity train the trainer course	Republican Center of Quarantine and Especially Dangerous Infections, Bishkek, Kyrgyzstan
'How can you help stop a disease outbreak?'	Lead	15/03/18	British science week 2018	All Saints Academy, Cheltenham
'Why work in science?'	Speaker	16/04/18	Leicester University student visit	PHE Porton Down
'DNA: the stuff of life'	Speaker	3-6 monthly from April 2018 – May 2019	Hitchhikers guide to microbiology course	PHE Porton Down
'The world of viruses'	Speaker	18/04/18	Hitchhikers guide to microbiology course	PHE Porton Down

ZIKV plaque assay	Assist	14-25/05/18	MSc Animal Virology	USFQ, Ecuador
Undergraduate student coursework	Assist	14-25/05/18	MSc Animal Virology	USFQ, Ecuador
qRT-PCR and metagenomic sequencing training for Sully Marquez – visiting scientist from USFQ	Lead and assist	09-23/05/19	Training visit	PHE Porton Down

Word count of main body of thesis: 56,075

Signed: E.L. Wise

Date: 06/01/2020

ABSTRACT

Emma Louise Wise

Metagenomic identification and characterisation of emerging and re-emerging viruses causing disease in febrile patients.

Emerging infectious diseases (EID) significantly impact public health and have the potential to cause pandemics. Outbreaks of EID have increased in recent decades, with RNA viruses responsible for a substantial proportion of them. Outbreaks are more likely to occur in areas with high biodiversity, poor sanitation and public health infrastructure, and limited resources for EID control. Furthermore, clinical symptoms of many viral infections overlap, making them challenging to diagnose correctly.

Metagenomic sequencing (metagenomics) negates the need for targeted detection assays, generates virus genome information and can detect novel or genetically divergent viruses. Through combining targeted PCR-based assays with untargeted metagenomics, this project aimed to detect infections in two cohorts of patients with fever from low-and-middle income countries (Sierra Leone and Ecuador), characterise any viruses identified and pursue further knowledge relevant to EID.

Plasmodium, *Leptospira* and Ebola virus (EBOV) infections were detected in Sierra Leonean patient samples using PCR-based assays. Human immunodeficiency virus, GB virus C (human pegivirus) and hepatitis B virus were identified in 36 PCR-negative Sierra Leonean patient samples using metagenomics. The detection of EBOV was surprising because the patients tested negative for EBOV RNA using a qRT-PCR assay at the time of sampling; further investigation suggested the discrepancies were related to assay sensitivity.

This project detected and isolated Oropouche virus (OROV), an emerging arbovirus, from a patient from Ecuador for the first time. Metagenomics revealed that the Ecuadorian strain was divergent from other strains at an established diagnostic qRT-PCR binding site. This information allowed the optimisation of a qRT-PCR assay, which subsequently identified further OROV infections within the patient cohort. Adoption of this assay in relevant countries could enhance OROV surveillance and diagnosis. This demonstrates the value of using metagenomics alongside PCR-based assays in screening studies to ensure diagnostic assays can detect current strains. In addition to OROV, Dengue virus, Hepatitis A virus, Zika virus, and *Leptospira* were identified in Ecuadorian patient samples.

Phylogenetic analyses of OROV sequences suggested that an OROV outbreak occurred in Esmeraldas, Ecuador in 2016. OROV vector *Culicoides paraensis* is not present in this area, raising the question of alternative insect vectors. Experiments demonstrated that OROV replicates in *Aedes* spp. cell lines. These species are important mosquito vectors of other arboviral diseases and this finding warrants further investigation. Further experimental work identified human fibroblasts and hepatocytes as potentially relevant to OROV pathogenesis in humans.

LIST OF CONTENTS

LIST OF FIGURES

LIST OF TABLES

ABBREVIATIONS

ADE	Antibody-dependant enhancement
AIDS	Acquired immunodeficiency syndrome
AUFI	Acute undifferentiated febrile illness
BHQ1	Black hole quencher 1
bp	Base pair
CCHFV	Crimean-congo haemorrhagic fever orthonairovirus
CDC	Centers for Disease Control and Prevention
cDNA	Complementary DNA
CFR	Case fatality rate
CHHF	Chapare virus
CHIKV	Chikungunya virus
CL	Containment level
CNS	Central nervous system
CPE	Cytopathic effect
Cq	Cycle quantification
CSF	Cerebrospinal fluid
DALYs	Disability-adjusted life years
DC	Dendritic cells
Dcr2	Dicer 2
DENV	Dengue virus
DMEM	Dulbecco's modified eagle medium
DMSO	Dimethyl sulfoxide
DNA	Deoxyribonucleic acid
dNTPs	Deoxyribonucleotide triphosphates
D-PBS	Dulbecco's phosphate-buffered saline
dpi	Days post-infection
DRC	Democratic Republic of Congo
ECACC	European Collection of Authenticated Cell Cultures
ECSA	East/Central/South Africa
EDTA	Ethylene diamine tetraacetic acid
EID	Emerging infectious disease
ELISA	Enzyme-linked immunosorbent assay
EMEM	Eagle's minimum essential medium
ETC	Ebola treatment centre
EVD	Ebola virus disease
EW	Epidemiological week
FAM	6-carboxyfluorescein
FBS	Foetal bovine serum
GBVC	GB virus C (human pegivirus)
GMEM	Glasgow minimum essential medium
GP	Glycoprotein
GTOV	Guanarito virus

HAV	Hepatovirus A virus
HBV	Hepatitis B virus
HFRS	Haemorrhagic fever with renal syndrome
HHV-8	Human herpesvirus-8
HIV-1	Human immunodeficiency virus type 1
HKGF	Human keratinocyte growth supplement
hpi	Hours post-infection
HPS	Hantavirus pulmonary syndrome
IAV	Influenza A virus
IFN	Interferon
IL	Interleukin
IOM	Institute of Medicine
IQTV	Iquitos virus
IRF	Interferon regulatory factor
JEV	Japanese encephalitis virus
JUNV	Junin virus
LASV	Lassa mammarenavirus
MACV	Machupo virus
MARV	Marburg marburgvirus
MAVS	Mitochondrial antiviral signalling protein
MAYV	Mayaro virus
MEM	Minimum essential medium
MGB	Minor groove binder
MgSO4	Magnesium sulphate
MOI	Multiplicity of infection
mRNA	Messenger RNA
NBCS	New born calf serum
NCPV	National Collection of Pathogenic Viruses
NEAA	Non-essential amino acids
NF-κB	Nuclear factor kappa-light-chain-enhancer of activated B cells
ng	Nanograms
NGO	Non-governmental organisation
NGS	Next generation sequencing
NP	Nucleoprotein
nt	Nucleotide
NTC	No template control
NXC	Negative extraction control
ONNV	O'nyong-nyong virus
ONT	Oxford Nanopore Technologies
ORF	Open reading frame
OROV	Oropouche orthobunyavirus
P	Passage
PBMCs	Peripheral blood mononuclear cells
PBS-A	Phosphate buffered saline with 1% bovine albumin
PCR	Polymerase chain reaction
pfu	Plaque forming units
PHE	Public Health England

pmol	Picomoles
PRNT	Plaque reduction neutralisation test
pVHF	Pan-viral haemorrhagic fever
QOS	Qiagen One-Step RT-PCR kit
qRT-PCR	Real-time reverse transcription PCR
R group	Reactive group
RACE	Random amplification of cDNA ends
RDT	Rapid device test
RIG-I	Retinoic acid-inducible gene I
RIP	Recombinant Identification Programme
RIPL	Rare and Imported Pathogen Laboratories
RNA	Ribonucleic acid
RNAi	RNA interference
rpm	Revolutions per minute
RPMI	Roswell Park Memorial Park 1640 medium
rRNA	Ribosomal RNA
RT	Reverse transcription
RT-PCR	Reverse transcription polymerase chain reaction
RVFV	Rift Valley fever phlebovirus
s	Seconds
SABV	Sabia virus
SARS	Severe acute respiratory syndrome
SISPA	Sequence-Independent, Single-Primer Amplification
SNP	Single nucleotide polymorphism
SSIII	Superscript III Platinum One-step quantitative RT-PCR kit
TB	Tuberculosis
TBEV	Tick-borne encephalitis virus
TMRCA	Time to most recent common ancestor
TNF-α	Tumour necrosis-factor-alpha
TPB	Tryptose phosphate broth
UK	United Kingdom
USA	United states of America
USD	United States Dollars
USFQ	Universidad San Francisco de Quito
UTR	Untranslated region
VEGF	Vascular endothelial growth factor
WHO	World Health Organisation
ZIKV	Zika virus

CHAPTER 1: INTRODUCTION

1.1 EMERGING INFECTIOUS DISEASE

In recent decades, improved living conditions and advances in medicine and technology have reduced the burden of infectious disease at a global level (1,2). Despite this, morbidity and mortality caused by infectious disease remains a significant problem, particularly in low-or-middle-income countries in which resources are limited and healthcare systems are often under-funded and overstretched (3). Compounding this is the disease burden that occurs during outbreaks of emerging or re-emerging infectious disease (EID). The World Health Organisation (WHO) defines EID as "one that either has appeared and affected a population for the first time, or has existed previously but is rapidly spreading, either in terms of the number of people getting infected, or to new geographical areas" (4). Outbreaks of EID have a major immediate impact on public health in affected countries, place substantial pressure on healthcare systems during an outbreak and have wider implications in the form of pandemic potential.

An analysis of EID origin events (5) revealed that the number of events increased decade on decade from the 1940's to the 2000's (corrected for reporting bias), suggesting that the threat to global public health from EID is increasing over time (Figure 1.1). A systematic review identified nearly 1,400 species of human pathogen in the literature, of which 87 were first reported in humans after 1980, of which 58 were viruses. Of these novel virus species, 45 had single-stranded ribonucleic acid (RNA) genomes (6).

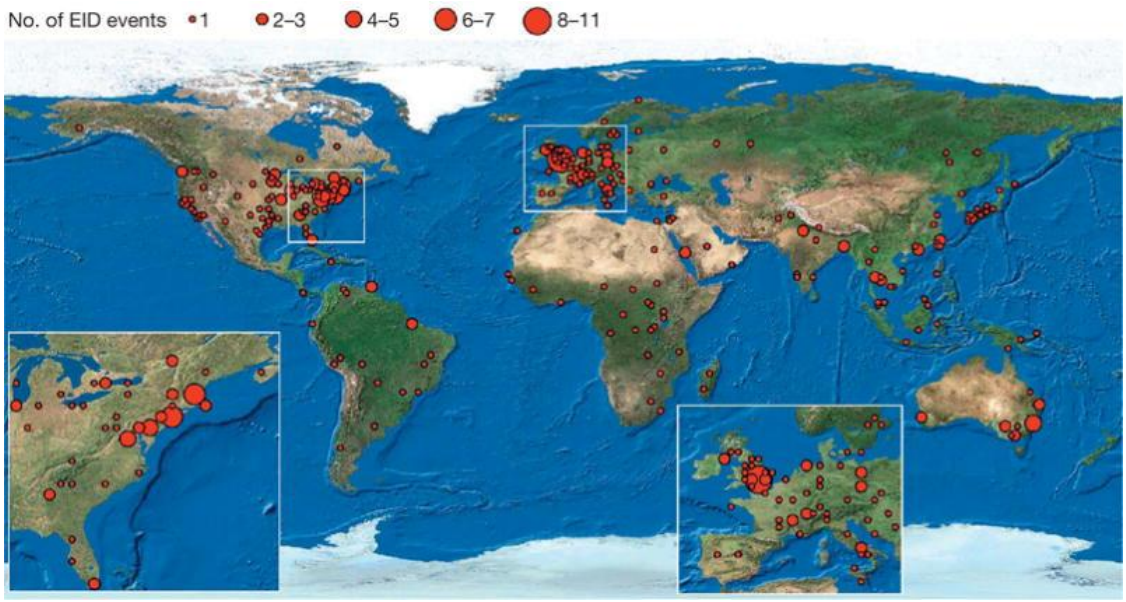

Figure 1.1 A map of the geographic origins of EID events (1940 – 2004) caused by all pathogen types. Circles represent one-degree grid cells and the area of the circle is proportional to the number of events in the cell. This figure is reproduced from Jones *et al.* (2008) (5).

The over-representation of viruses, particularly RNA viruses, in the pool of emerging pathogens is often explained in terms of the genetic plasticity afforded to them by their genomes. All viruses are obligate intracellular parasites and must create an environment in the host cell that enables replication of the viral genome and proteins, effective packaging of new virions and virion release from the cell. Viruses with deoxyribonucleic acid (DNA) genomes may use a host or viral polymerase for genome replication, RNA viruses always encode an RNA-dependant RNA polymerase for this purpose since these enzymes do not exist in the host (7). RNA-dependant polymerases have low fidelity, resulting in many more mutations per replication cycle compared to DNA-dependant polymerases, which have a proofreading capability the former enzymes lack (8). The

average rate of RNA virus genome nucleotide substitution is estimated to be 1.0e-2 to 1.0e-5 nucleotide substitutions per site/year (9,10). A single infected cell can produce thousands of virions from one cycle of replication (11), meaning that the population of viruses within a host is genetically diverse. In addition to high mutation rates, RNA virus replication cycles occur within a matter of hours, meaning mutations are accumulated over short periods of time, making them easy to observe and measure (12). Furthermore, in viruses with segmented genomes, genetic diversity is increased by reassortment; the process of genome segment exchange that can occur when two viruses infect the same cell. This viral population diversity confers the ability to adapt when selection pressures are present because of the presence of many genetic variants. This means that a minor variant in the population may survive and expand as a result of pressures such as immune response, drug treatment, or a change in host species.

1.1.1 ZOONOSES AND PATHOGEN EMERGENCE

Of all pathogens known to infect humans, only an estimated 50-100 are specific to humans (6), the remaining vast majority are zoonotic. The WHO defines a zoonosis as "any disease or infection that is naturally transmissible from vertebrate animals to humans" (13). A spillover is a transmission event that occurs when a pathogen previously restricted to animals infects a human. Zoonotic transmission ranges from pathogens that are primarily animal infections but occasionally spill over into humans (e.g. rabies virus), to those that are largely human pathogens but are also capable of infecting animals (e.g. rubella virus) (6). The latter are sometimes referred to as 'reverse zoonoses'. Of the 87 human pathogens discovered since 1980, 80% are zoonotic (6).

A chain of events must happen for a zoonotic pathogen to emerge and become established in the human population. Gardy and Loman (2018) (14) outline three phases of disease emergence (Figure 1.2): Pre-emergence, in which the pathogen population expands, possibly into a new geographic region and/or a new host, usually as a result of changing land use or demographics. Localised emergence may follow, in which spillover to humans occurs, resulting from human contact with infected animals or their bodily fluids, but this does not result in person-to-person transmission. Finally, in pandemic emergence, the pathogen infects multiple humans in sustained chains of transmission, often facilitated by the movement of infected people (15).

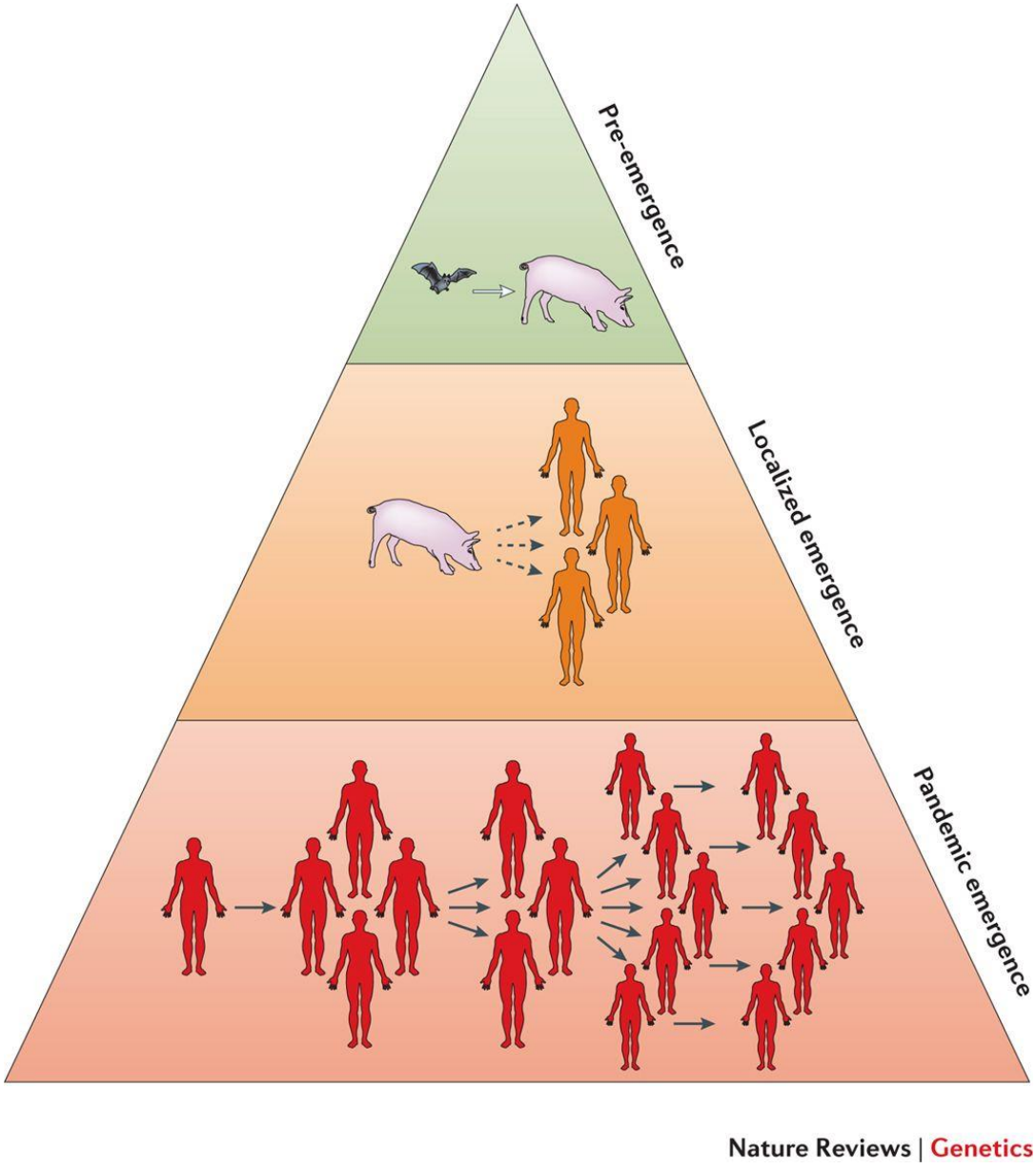

Figure 1.2 Emergence of a zoonotic pathogen from an animal reservoir into the human population. Reproduced from Gardy and Loman (2018) (14).

1.1.2 DRIVERS OF EMERGENCE

EID events tend to occur in hot spots that are defined by environmental, ecological and socioeconomic characteristics (5). A landmark report published by the Institute of Medicine (IOM) in 2003 proposed the 'convergence model' that explained the interactions of genetic, biological, environmental, ecological, social, political and economic factors associated with human infection with a new pathogen (Figure 1.3). The 2003 report built on previous work to identify thirteen key drivers of disease emergence (16). A common theme was change: change in climate and weather, changing ecosystems, economic development and land use, international travel and commerce, changing human demographics and behaviour (17). The commonality in these factors is an increase in the number of opportunities for humans and pathogens to interact, as well as an increased number of interactions between humans. This leads to a higher chance of spillover events occurring which are subsequently passed from person-to-person. Jones *et al.* (2008) identified areas at high risk of spillover as those with a high diversity of wildlife species in which recent changes in demographic or farming have occurred (5). This was corroborated by a biogeographic analysis showing that mammalian biodiversity was the strongest predictor of disease co-occurrence (18). An additional driver of outbreaks is inadequate sanitation and hygiene in the context of the breakdown or absence of public health systems, which was the largest contributor in nearly 40% of 400 public health events of international concern (19). Overall, these observations suggest that surveillance for EID is best targeted to areas with high biodiversity, poor sanitation and public health infrastructure, and limited resources for EID control (14,19).

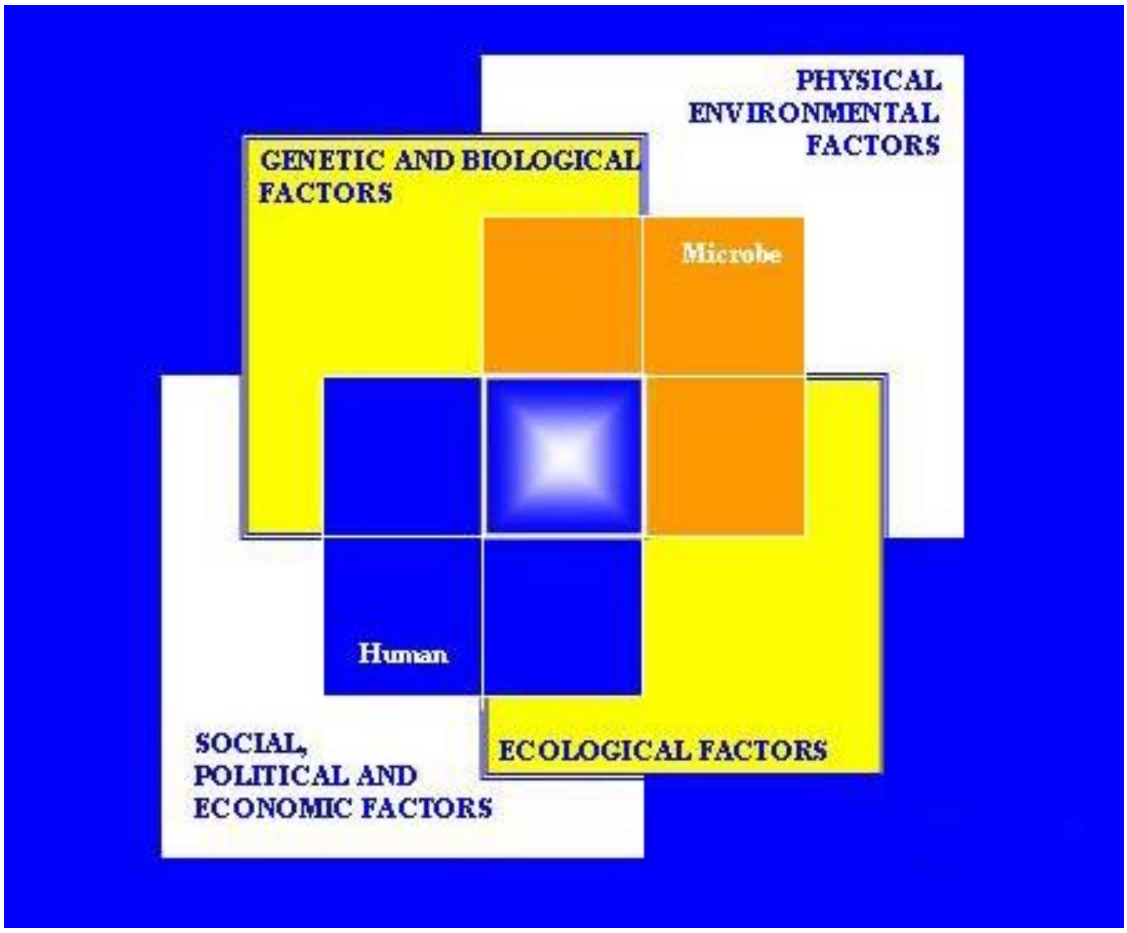

Figure 1.3 The convergence model of disease emergence proposed by the Institute of Medicine. Reproduced from Kimball (2004) (20), adapted from (17).

Seasonality is a phenomenon observed for numerous infectious diseases including those that cause food-borne illnesses, respiratory infections and vector-borne diseases (21). Knowledge of the seasonal trends of infectious disease within endemic countries is important to be able to effectively target surveillance, plan vector control strategies and guide laboratory testing and diagnosis of patients. The factors leading to seasonality can be complex and commonly include human behaviours, climate, environment, and vector abundance (21). The latter is particularly important in arbovirus seasonality. This has

been studied for mosquito-borne viruses including dengue virus (DENV) (1,21–23), chikungunya virus (CHIKV) (24,25) and Zika virus (ZIKV) (26), midge-borne viruses including Bluetongue virus and Akabane virus in Australia (27), and Oropouche virus (OROV) in Brazil, outbreaks of which tend to occur during the rainy season between January and June due to an increased number of vector breeding sites (28). In West Africa, Lassa fever incidence is seasonal, with outbreaks occurring yearly in Nigeria and cases peaking around March, during the transition from the dry season to the wet season (29,30). Malaria incidence has seasonal patterns similar to some arboviruses and higher mosquito abundance correlates with more malaria transmission (31). EBOV seasonality has recently been investigated using a statistical modelling approach to look at previous outbreaks and spillover events (32). The authors found that EBOV spillover intensity is highest during transitions between wet and dry seasons, adding weight to the theory that there may be seasonality in EBOV spillover events (32–34). Understanding seasonal patterns of disease in endemic areas is important to be able to plan effective surveillance programmes.

A valid question regarding EID is why focus on pathogens that cause relatively low mortality and morbidity compared to huge global health burdens such as malaria, tuberculosis, and hepatitis B infection? Most emerging pathogens do not result in global pandemics, but those that do can have devastating and long-term consequences on the human population. For example the emergence of human immunodeficiency virus-1 (HIV-1) last century, which since its discovery has resulted in 32 million deaths and as of 2018, 37.9 million people living with the infection (35). In 2016, HIV was the 4th most common cause of death in low-income countries (36). Furthermore, significant economic and political damage can result from disease outbreaks and the public's

reaction to them (6). The economic cost of the 2003 severe acute respiratory syndrome (SARS) coronavirus outbreak, which caused fewer than 1000 deaths, was estimated at billions of dollars (37), and the outbreak of variant CJD resulting from prion infection in the United Kingdom (UK), causing approximately 100 deaths, had a similar economic cost (6). Although EID events are more likely to occur in certain geographical areas (18), globalisation and the increasingly interconnected nature of the modern world means that the spread of a newly emerged pathogen to geographically distant parts of the globe can happen extremely quickly. This has been demonstrated many times in recent years, notably the global spread of SARS coronavirus in 2003 (38), the emergence and subsequent pandemic of influenza A (H1N1) virus in 2009 (39), the export of EBOV to multiple countries from West Africa during the outbreak of 2014-2016 (40,41), and imported Zika virus cases with subsequent autochthonous transmission in the United States of America (USA) and Europe (42,43). Control of EID is a complex, global issue that requires collaborative working across borders. To combat EID effectively, surveillance on a local level must be combined with rapid, globally co-ordinated interventions to detect and control outbreaks at an early stage.

1.1.3 ACUTE UNDIFFERENTIATED FEBRILE ILLNESS

Acute undifferentiated febrile illness (AUFI) is a widely-used term used to describe an undiagnosed, non-specific clinical presentation. Despite there being no widely-accepted, universal definition, AUFI is typically defined as an illness that includes fever, has an abrupt-onset and lasts less than two weeks (44). Illness of this kind can be caused by a wide range of infectious agents that have an overlapping clinical spectrum, making accurate diagnosis challenging. One quarter of all deaths in low-income countries are

attributed to diseases that present as AUFI, including malaria, vector-borne viral diseases, diarrhoeal diseases and respiratory tract infections (1,45); demonstrating the need for improved diagnosis and treatment for AUFI patients.

Diagnosis of AUFI patients is commonly performed using a combination of clinical observations, history, and laboratory tests. Suspected pathogens are identified based on clinical factors, from which appropriate laboratory tests are identified. The tests that are used depend on the resources and capabilities of the laboratory, the sample type available, and the time between the onset of symptoms and sampling. The kinetics of a viral infection varies between virus species, but the majority show a similar pattern, involving a phase of viraemia that peaks days-to-weeks following exposure (Figure 1.4). At this time virus is present in the blood and nucleic acid-based tests that detect viral RNA/DNA are useful, and virus isolation in cell culture is possible (Figure 1.4). As viraemia declines approximately a week after the onset of symptoms, IgM antibody titres rise and become measurable, followed by a longer-lived IgG antibody response (Figure 1.4). Following the decline of viraemia, serological tests that detect IgM and IgG are much more reliable than nucleic acid-based tests, however they are often not as specific because of antibody cross-reactivity to antigenically similar viruses (46). Plasma or serum are common sample types used for the detection of viruses using molecular methods, although urine, saliva or cerebrospinal fluid (CSF) may be used depending on the suspected virus and clinical picture. Assay validation must be performed on any non-standard sample types to be able to provide a reliable diagnostic result.

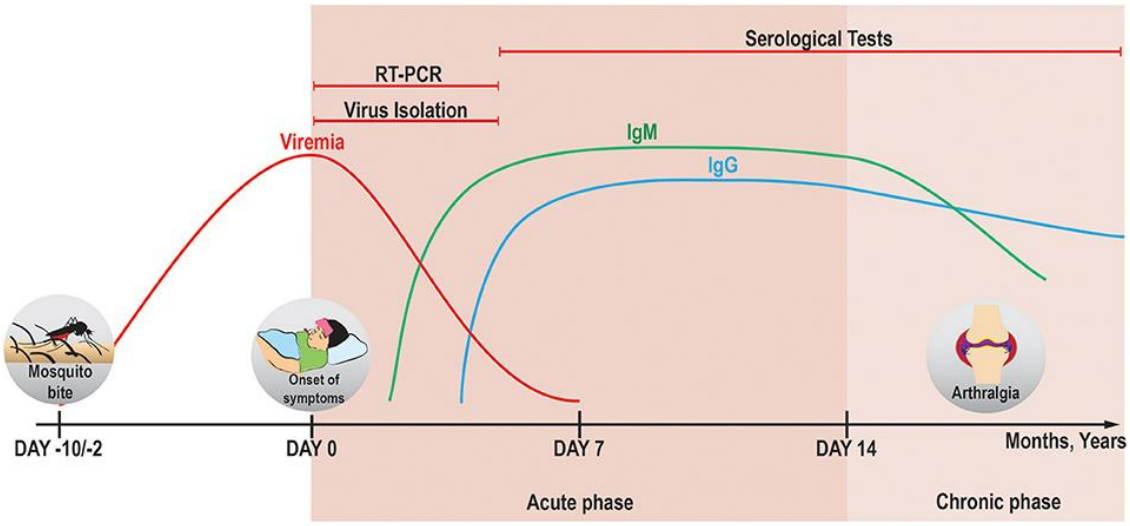

Figure 1.4 Suitable laboratory diagnostic techniques at each stage of a viral infection, in this instance CHIKV. Reproduced from Tanabe *et al.* (2018) (47).

Diagnosing the causative agent of AUFI can be challenging. The majority of current diagnostic methods rely on prior knowledge of the causative agent (e.g. genome sequence information, known epitopes), and many cases remain undiagnosed, potentially leading to inaccurate reporting of disease incidence and in particular the underreporting of infectious diseases (48). Misdiagnosis may lead to inappropriate treatment, with potentially serious consequences to the patient and wasting of valuable resources.

1.2 VIRAL CAUSES OF AUFI

This section provides an overview of a select group of viruses that cause an AUFI-like clinical picture in humans, focussing on emerging viruses of current global clinical importance.

1.2.1 ALPHAVIRUSES

CHIKUNGUNYA VIRUS (CHIKV) is an enveloped, single stranded, positive-sense RNA virus that belongs to the genus *Alphavirus*, family *Togaviridae* (49). It is a member of the Semliki Forest virus complex which includes the closely related Ross River virus, O'nyong'nyong virus and Semliki Forest virus. CHIKV was first isolated in 1952 from a febrile patient in Tanzania (50) shortly followed by detection in *Aedes aegypti* mosquitoes (51), and has since been detected in more than 100 countries across all continents (Figure 1.5) (52). Transmission is via a mosquito-vector, principally *Ae. aegypti* and *Ae. albopictus*. Both sylvatic (in which wildlife act as the major host) and urban (in which humans are the host) cycles exist (Figure 1.6) (53). The sylvatic cycle exists mainly in Africa and involves transmission between vertebrate hosts, principally non-human primates (54) but also rodents and possibly bats (52). *Aedes* species mosquitoes (*Ae. albopictus, Ae. furcifer, Ae africanus, Ae. taylori*) are the vector (55). Transmission in rural environments is between humans as the host and infected mosquito vectors, often *Ae. albopictus* (55). Larger outbreaks in urban areas are often the result of the movement of infected humans into high density urban areas where *Ae. aegypti* and *Ae. albopictus* are present (52). Since 2005, the role of *Ae. albopictus* in CHIKV transmission has substantially increased, because of the spread of this species into Africa and Europe, and adaptive mutations in the envelope glycoproteins (56–58)

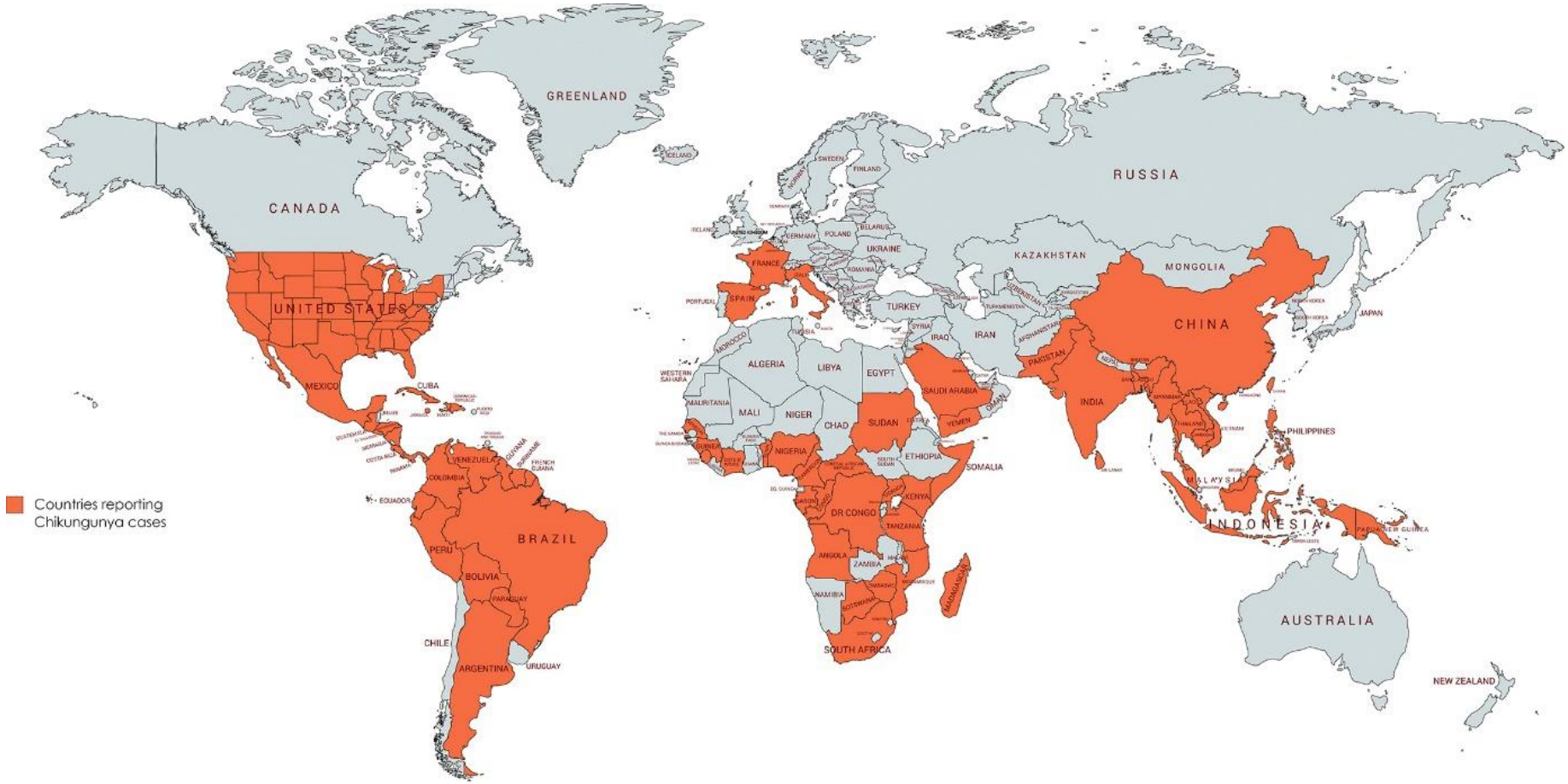

Figure 1.5 The global distribution of CHIKV, shown as countries and territories reporting CHIKV. Reproduced from Vairo *et al.* (2019) (52), data from the Centers for Disease Control and Prevention (59).

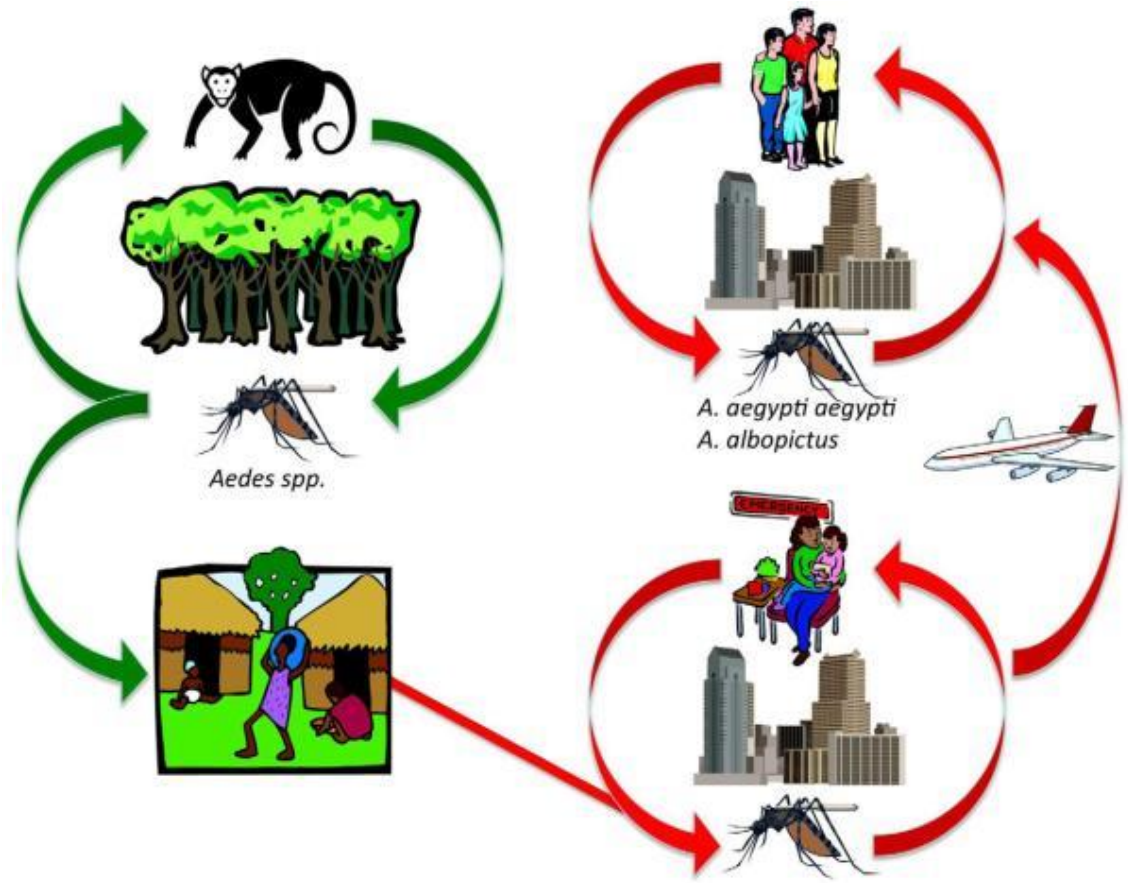

Figure 1.6 CHIKV transmission cycles. The sylvatic cycle (green) is present in Africa only. The endemic/epidemic urban cycle (red) is widespread throughout the world. Figure reproduced from Weaver *et al.* (2012) (54), adapted from the version originally published (60).

Separate lineages of CHIKV exist in Africa, which are restricted to West and East/Central/South Africa (ECSA) (52). The latter clade was responsible for an epidemic spreading into Asia in the 1950s (52). More recently, numerous large CHIKV epidemics have occurred. Transport of CHIKV from Kenya to Lamu island in 2004, then Réunion island and others in the Indian ocean caused a series of explosive epidemics (52). In a separate introduction from Kenya to India in 2005, millions of people were infected as a result of autochthonous transmission that continues to the present day (60). A number

of independent introductions occurred in the years following, resulting from infected travellers returning to Europe, Southeast Asia and the Americas from India, with onward local transmission occurring in Southeast Asia, Italy and France (61–63). In 2013, the ECSA lineage was detected in the Americas, preceding widespread transmission across the continent with 2.9 million cases and 296 deaths as of July 2016 (64), however, the number of deaths is thought to have been largely underestimated (65).

The clinical picture of CHIKV infection in humans is like that of several other arboviruses but with some distinctions. The classic symptoms associated with acute infection are fever, severe arthralgia and a rash (66). This phase typically lasts 7-10 days, followed by a chronic stage lasting months to years, characterised by joint pain and fatigue (67). Atypical presentations have been reported including cardiac, neurological and haemorrhagic manifestations (66), however these are not common. The case fatality rate (CFR) calculated from the Réunion Island outbreak was 1 in 1000 (68), but this figure can be higher in vulnerable populations including elderly people and neonates (67). It is estimated that 50-97% of infections are symptomatic (69). Treatment of CHIKV infection is symptomatic and no specific antiviral treatments exist (70). The field of CHIKV vaccine development has produced a number of promising candidate vaccines, however the completion of phase III trials is challenging because of the low number of cases observed between epidemics (70).

Because clinical symptoms of CHIKV and other pathogens that circulate in similar geographic areas are shared, laboratory confirmation is important. The most commonly used laboratory methods for diagnosis of CHIKV are molecular tests (detection of viral RNA, typically from serum and plasma samples) and serological assays that detect IgM and IgG antibodies (70). Virus isolation and antigen detected methods are also used but

are less common (70). Detection of CHIKV using metagenomic sequencing has recently been reported (71).

CHIKV replicates in a number of human cell types including epithelial and endothelial cells and monocyte-derived macrophages, but not lymphoid or monocytoid cells (68). However, replication in human monocytes is debated; one study demonstrated that CHIKV infects and replicates in human monocytes *in vitro*, albeit at a low level (72). Following initial infection, the virus travels to the lymph nodes then disseminates to other tissues via the blood, where it replicates in organs and causes viraemia (67). The inflammation observed during CHIKV infection is thought to contribute to the joint pain experienced by chronic CHIKV patients. Cytokines tumour necrosis-factor-alpha (TNF-α), interleukin (IL) -6, and IL-1, released during infection, promote osteoclast activity and are associated with the development of joint pain (73).

MAYARO VIRUS (MAYV) is an alphavirus that was first isolated from forest workers in Mayaro, Trinidad, in 1954 (74). Since then sporadic outbreaks of Mayaro fever have been reported from Brazil, and one small outbreak occurred in Bolivia (75–80). Phylogenetic analyses based on partial envelope (E1-E2) sequences demonstrated the existence of three genotypes; D, L and N (Figure 1.7). Virus or antibodies have been detected from Brazil, Bolivia, Colombia, Ecuador, French Guiana, Haiti, Mexico, Peru, Surinam, Trinidad and Venezuela (Figure 1.7) (81–91). The enzootic transmission cycle of MAYV is not well characterised, however, transmission is thought to occur between infected mosquitoes (primarily *Haemagogus* genus) and non-human primates (76,92). Human cases have thus far been associated with forest and rural areas only, however,

concerns exist over the potential of the virus to cause outbreaks in new areas, particularly as previous outbreaks have involved high numbers of cases (79,93) and *Ae. aegypti* have been demonstrated to be moderately competent vectors in the laboratory (94). This raises concerns that an urban transmission cycle could emerge between humans and *Ae. aegypti* in the future (95).

Mayaro fever typically manifests as fever, headache, rash and arthralgia, the latter of which can continue for months or years (96). The overlap in clinical picture between MAYV and other arboviruses means infection can easily be mis-diagnosed, particularly as a lesser-known cause of disease. Furthermore, cross-reactivity between antibodies against MAYV and other alphaviruses such as CHIKV make serological testing challenging (97,98). Molecular testing can overcome this problem but currently reverse transcription-polymerase chain reaction (RT-PCR) assays are not widely available in the relevant areas (96). Long-term arthralgia is noted in over half of MAYV infected patients (93) and in a study evaluating patient immune response to MAYV, infection was associated with the release of inflammatory cytokines including IL-13, IL-7, and vascular endothelial growth factor (VEGF) (99). MAYV is poorly represented in the literature, however the molecular mechanisms of pathogenesis are assumed to be similar to that seen in other alphaviruses until further evidence can be produced (100).

Figure 1.7 The known distribution of MAYV genotypes. Reproduced from Pezzi *et al.* (2019) (96).

1.2.2 ARENAVIRUSES

LASSA MAMMARENAVIRUS (LASV) belongs to the *Mammarenavirus* genus, family *Arenaviridae*. Mammarenaviruses are enveloped, single stranded, negative-sense RNA viruses with a bi-segmented genome (large and small segments), that infect mammalian hosts (101). LASV was first discovered in Nigeria in 1969 following cases of febrile illness in missionary nurses, subsequently named Lassa fever (102). LASV is endemic in West Africa, cases have been reported from Benin, Ghana, Guinea, Liberia, Mali, Nigeria, Senegal, and Sierra Leone (103–105). Insufficient surveillance, civil unrest, lack of point-of-care diagnostic tests and a wide spectrum of clinical presentations (including asymptomatic infections) makes it very difficult to understand the true distribution of LASV (106). Similarly, estimates of annual Lassa fever incidence are crude because surveillance in endemic areas is not standardised, however, the Center for Disease Control (CDC) estimates that each year the virus infects between 100,000 and 300,000 people, 5,000 of whom die as a result (103). A small number of travel-associated cases have been documented from countries in the Americas and Europe (107,108).

The primary reservoir species for LASV is *Mastomys natalensis*, the multimammate rat (Figure 1.8), in which infection is asymptomatic but virus is shed in urine and faeces, which is usually the source of human infection (109). Interactions with *Mastomys* rodents frequently occur in rural areas with poor sanitation or crowded conditions. Rodents invade human homes in search of food and exposure to contaminated rodent bodily fluids occurs, resulting in infection (106). Following a zoonotic transmission, human-to-human transmission is possible via infected bodily fluids, though less common (101). Nosocomial outbreaks have occurred, facilitated by poor infection control and barrier nursing practices (110).

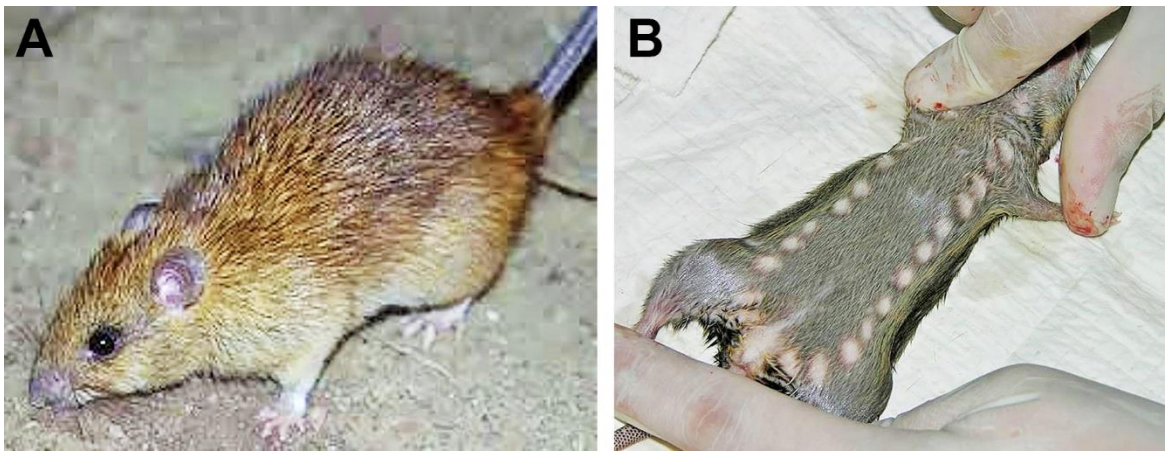

Figure 1.8 The LASV reservoir species multimammate rat *Mastomys natalensis*. B: Ventral surface of *M. natalensis* showing two rows of mammary glands. Reproduced from Asogun *et al.* (2019) (106).

The onset of Lassa fever typically occurs 2-21 days following exposure (103,104). The disease has a wide clinical spectrum, ranging from asymptomatic infection to severe haemorrhagic disease (110). Common symptoms include fever, headache, myalgia, sore throat and gastrointestinal symptoms (111–113). More specific symptoms, associated with severe disease, are present in less than a third of Lassa fever patients and can include conjunctival infection, facial swelling and haemorrhagic manifestations such as mucosal or gastrointestinal bleeding (114). CFRs in hospitalised patients range from 10 – 20%, if death occurs it results from shock and multi-organ system failure (114,115). Ribavirin is used to treat LASV infection and is most effective in the 6 days following onset of symptoms (116). No vaccine is currently available although some monoclonal antibody therapies have shown promise (117,118). Many survivors of Lassa fever experience neurological sequelae, with 25% experiencing deafness as a result of infection (101,119,120).

Mammarenaviruses are separated into 'Old World' and 'New World' groups based on genetic and geographic factors (121). LASV belongs to the Old World group, alongside Lymphocytic choriomeningitis virus and Lujo virus. Within the LASV species itself, a high degree of genetic diversity is observed with multiple lineages circulating in West Africa (122), which presents substantial challenges to developing diagnostic tests capable of detecting all known lineages. This is important because Lassa fever is very difficult to diagnose based on clinical symptoms alone, due to the wide spectrum of disease and symptoms, therefore laboratory diagnosis is required to confirm an infection. The gold standard test is RT-PCR for detection of LASV RNA (123). Complementary testing includes serological tests, antigen detection, or immunohistochemistry on post-mortem samples (106). Virus isolation can only take place in biosafety level 4 containment laboratories (106).

The mammarenavirus life cycle is relatively well understood (Figure 1.9). Virus enters the host via inhalation, where it is infects alveolar macrophages which move to the draining lymph node, disseminating virus to various tissues throughout the body (101). The major cellular receptor for LASV is α-dystroglycan (124) and virus enters the cell via a clatherin-independent pathway (125). Viral genome replication takes place in the cytoplasm and is initiated by the nucleoprotein (NP) and the large RNA-dependent RNA polymerase complex, acquiring 5' caps from host messenger RNA (mRNA) (101). During replication, arenaviruses evade the mammalian immune system in several ways. The NP limits the type I interferon (IFN) response by inhibiting activation of downstream genes (101). The New World mammarenavirus Z protein inhibits the IFN response by binding to retinoic acid-inducible gene I (RIG-I), preventing RIG-I binding to mitochondrial

antiviral signalling protein (MAVS) and halting the signalling cascade that usually results in the production of IFNβ (101).

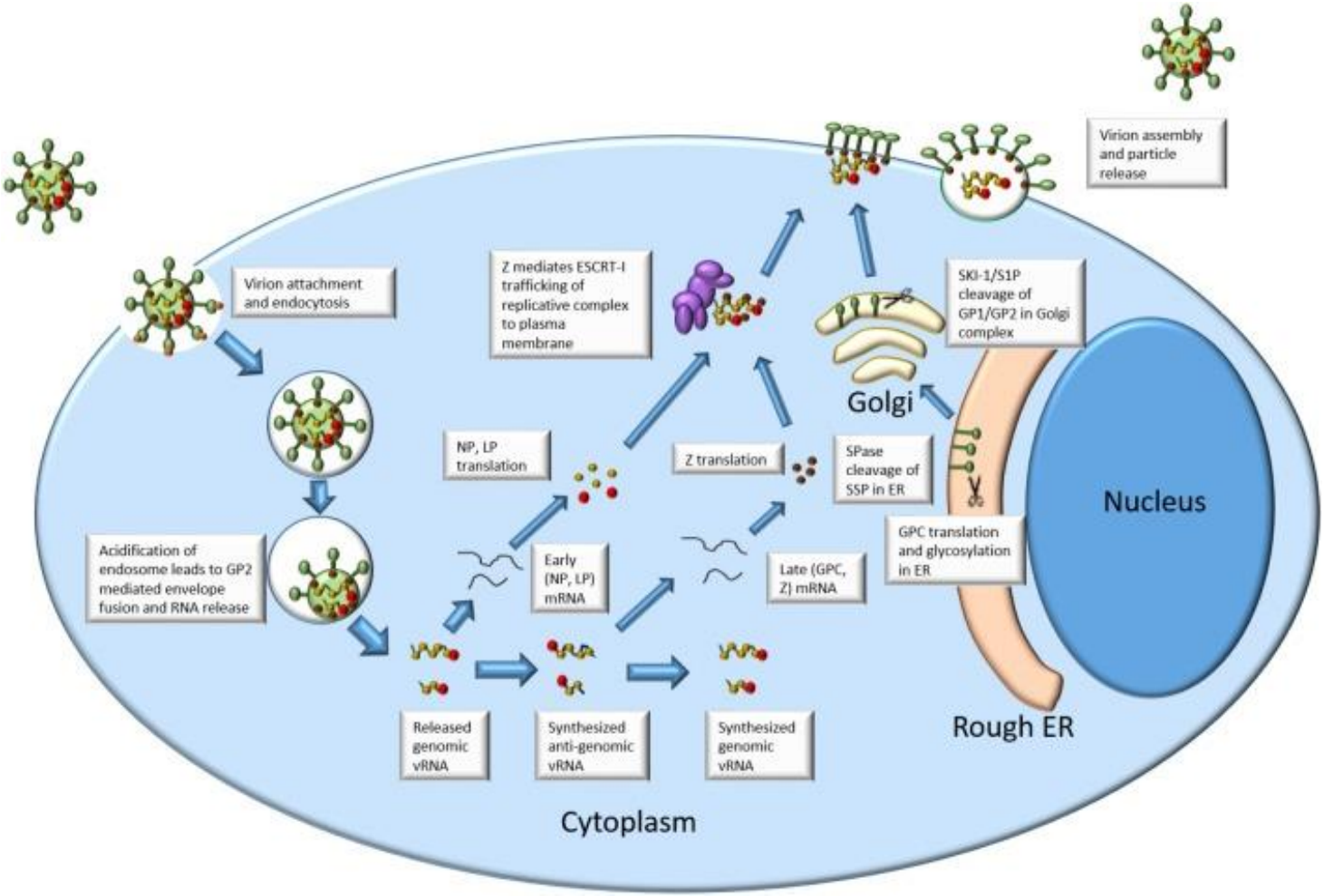

Figure 1.9 The arenavirus life cycle. Reproduced from Hallam *et al.* (2018) (101).

JUNIN VIRUS (JUNV) is a New World mammarenavirus capable of causing haemorrhagic disease in humans. The other New World viruses in the *Mammarenavirus* genus are Machupo virus (MACV), Guanarito virus (GTOV), Sabia virus (SABV), and Chapare virus (CHHF), all of which are capable of causing similar disease. This viruses are the causative agents of Argentine Haemorrhagic Fever (JUNV), Bolivian Haemorrhagic Fever (MACV), Venezuelan Haemorrhagic Fever (GTOH) and Brazilian Haemorrhagic Fever (SABV) (101). They are found in the Americas and have higher CFRs (15-33%) than those seen from Old World viruses, however, they cause fewer infections annually (101,126,127). The primary animal reservoirs are mice species belonging to sub-family *Sigmodontinae,* family *Muridae;* JUNV infection is associated with agricultural activities that result in exposure to infected mouse urine and/or faeces (101).

1.2.3 BUNYAVIRUSES

CRIMEAN-CONGO HAEMORRHAGIC FEVER ORTHONAIROVIRUS (CCHFV) is an enveloped, single stranded, negative-sense RNA virus with three genomic segments, belonging to the genus *Orthonairovirus*, family *Nairoviridae*, order *Bunyavirales.* A febrile illness of unknown aetiology occurred in soviet troops re-occupying the Crimean peninsula in 1944, resulting in approximately 200 hospitalisations with a 10% CFR (128). The disease was linked to tick bites however CCHFV itself was not identified until 1967 when it was isolated from a patient in Uzbekistan (129). CCHFV has been found over a wide geographical area including many regions of Africa, Eastern Europe, the Middle East and Asia, however the majority of reported cases have been from Turkey (130,131).

CCHFV is spread via the bite of an infected *Hyalomma* species tick and is maintained in a sylvatic cycle with domestic livestock (131). It is thought that many human infections are subclinical; one study investigating seroprevalence in Turkey during 2009 estimated that 88% of infections were asymptomatic (132). Disease in symptomatic patients ranges from mild to severe. Symptoms observed in severe disease include bleeding and typically develop 3-6 days following the onset of symptoms (Figure 1.10) (130). Reported CFRs range from 4%-20% (133). Treatment is frequently with ribavirin, however it is not clear whether this is effective (134). A CCHFV vaccine was developed and approved in the Soviet Union in 1970 and a similar vaccine has been in use in Bulgaria, however the efficacy of these have not been fully evaluated (135,136). Modern attempts to develop a vaccine have been impeded by the lack of animal models for CCHFV (135).

Figure 1.10 Clinical presentation of Crimean-Congo haemorrhagic fever in a severely ill patient. Patient shows ecchymosis (discolouration of the skin resulting from bleeding underneath) not seen in other types of viral haemorrhagic fever. Reproduced from Bente *et al.* (2013) (135).

CCHFV has the highest degree of sequence diversity seen in any arbovirus, up to 31% in the M-segment (135). Six viral lineages exist based on the complete sequences of each genome segment. Generally (but not always), viruses from similar locations cluster in the same lineage (135). This genetic diversity presents challenges for diagnostic tests based on RNA detection but despite this, RT-PCR using a serum sample is considered the gold standard test. Previously the gold standard was virus isolation, however this is constrained by the requirement for a biosafety level 4 containment laboratory (135). Serological detection of virus-specific IgM and/or IgG is a useful complementary test (135).

CCHFV targets Kupffer cells, hepatic endothelial cells and hepatocytes (131). An increase in liver enzymes is detected during infection, which is related to necrosis of hepatocytes (131). Vascular leakage during infection is caused by both the virus itself and the immune response; in particular high levels of cytokines IL-1, IL-6, and TNF-α are observed. Levels of IL-6 and TNF-α are higher in fatal cases (137,138).

HANTAVIRUSES are a group of 36 virus species within the genus *Orthohantavirus*, family *Hantaviridae*, order *Bunyavirales* (49). The geographical distribution of the hantaviruses is related to the distribution of their animal reservoir and they are widely distributed across parts of Asia, Europe, Africa and the Americas (139,140). Hantaviruses are usually closely associated with a specific rodent species, resulting from co-evolution between virus and host (141). Known reservoir species include the bank vole *Myodes glareolus* (Puumala virus) (142), *Apodemus flavicollis* (Dobrava virus) (143), *Rattus norvegicus* (Seoul virus) (144) and the deer mouse *Peromyscus maniculatus* (Sin Nombre virus)

(145). Hantaviruses infect approximately 200,000 people each year (146), with Sin Nombre virus and Andes virus responsible for hantavirus pulmonary syndrome (HPS) in the Americas, Hantaan virus causing haemorrhagic fever with renal syndrome (HFRS) in Asia, Puumala virus and Dobrava virus causing HFRS in Europe, and Seoul virus causing HFRS globally (147). Hantavirus infections are thought to be highly underreported due to the lack of comprehensive epidemiological data from many countries, particularly in Europe where it is estimated that only 20% of all Puumala virus infections are diagnosed (148).

In recent years Seoul virus was identified in the UK, first in wild rats (149) and then independently in a breeding colony of pet rats (150,151) following three linked cases of HFRS. These cases demonstrate the continued emergence of hantaviruses and the potential for interaction between humans and reservoir species.

Human hantavirus infection usually results from exposure to infected animals, their urine, faeces or virus-contaminated aerosols (Figure 1.11) (147). Human-to-human transmission has only been recorded for Andes virus (152). Depending on hantavirus species, human infection can result in serious disease, manifesting as HPS, or HFRS (147), with CRFs of up to 40% and 12%, respectively (147). Diagnosis of hantavirus infection is based on clinical and epidemiological information combined with laboratory tests; commonly detection of IgM and IgG antibodies in patient serum (153). Commercially available rapid tests exist which detect IgM antibodies at point-of-care (154,155). Molecular detection using RT-PCR is common and can detect infection before the presence of specific antibodies (156,157). There is no specific therapy for hantavirus infection and only one vaccine (Hantavax) which is licensed for human use in the Republic of Korea only (147).

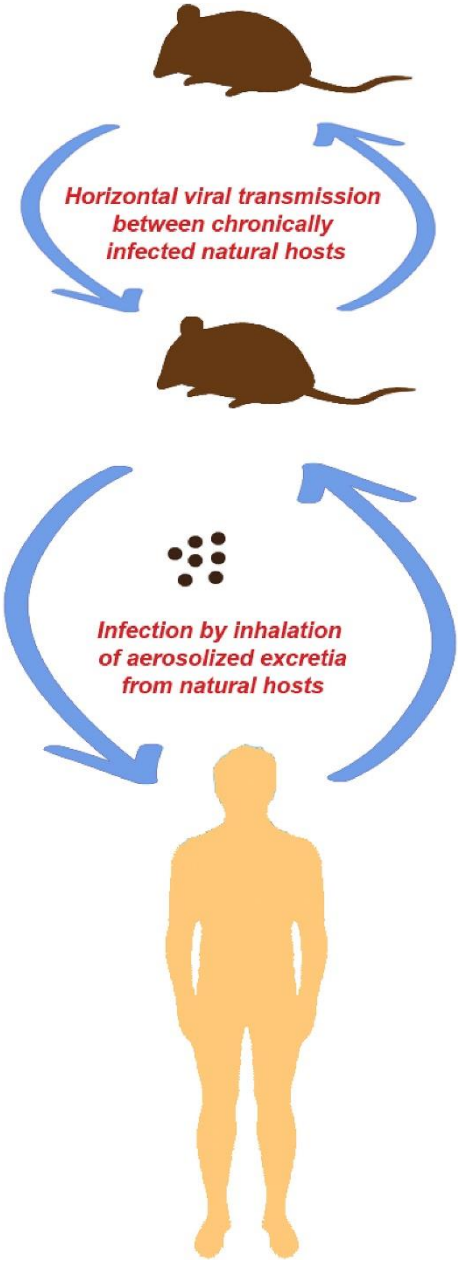

Figure 1.11 Hantavirus life cycle and spillover infection to humans. Reproduced from Avsic-Zupanic *et al.* (2019) (153).

Pathogenic hantaviruses suppress the innate immune response. The early IFN response is abrogated by viral interference with interferon regulatory factor (IRF)-3 and NF-κB (Nuclear factor kappa-light-chain-enhancer of activated B cells) signalling pathways (158). The cytoplasmic tail of the Gn glycoprotein has been implicated in this inhibition of IFN response and this is thought to be necessary for hantavirus replication in endothelial cells, the primary site of infection (158). Additionally, some hantaviruses are known to infect dendritic cells (DCs); Hantaan virus induces maturation in infected DCs which may lead to dissemination of the virus following DC migration to lymph nodes (159,160).

RIFT VALLEY FEVER PHLEBOVIRUS (RVFV) belongs to the genus *Phlebovirus*, family *Phenuiviridae*, order *Bunyavirales.* RVFV was first described in 1930 following disease and abortions in sheep in Kenya (161), but was not isolated until 1967 from a case in Nigeria (162). Outbreaks have since been reported from West Africa, South Africa, Madagascar, Egypt, Saudi Arabia and Yemen (163,164). Rift Valley fever is primarily a disease of livestock, however, it be transmitted to humans through direct contact with infected animal blood or carcasses, or a bite from an infected mosquito. Vertebrates act as hosts, in which infection is asymptomatic or causes mild disease, and the virus has been detected in a wide range of species including camels, lions, elephants and bats (165–167). *Aedes* species mosquitoes are the primary enzootic reservoir and vector for RVFV, with *Culex*, *Anopheles* and *Mansonia* mosquitoes acting as secondary vectors, playing a role in the amplification of epidemics (164). Aside from mosquitoes, virus has been isolated from midges, flies and ticks, although their role in transmission remains unknown (162).

Disease in humans is usually mild with non-specific 'flu-like' symptoms, although in rare cases severe disease develops, manifesting as one or more of three clinical syndromes; ocular disease, meningoencephalitis, or haemorrhagic fever (162). Fatalities are rare (<1%) but occur most commonly in patients with haemorrhagic fever (163). Treatment for severe disease is supportive; the administration of ribavirin has been shown to increase the chance of neurological disease developing (168). A formalin-inactivated vaccine is used to protect lab workers and those at high risk of exposure, however it is not suitable for animal use due to the requirement for three inoculations to establish effective immunity (169,170). A number of modern vaccine candidates have been developed that show promise and some have undergone field testing, however financial investment is required to get these to a point where they could be applied effectively in endemic countries (171–173). Diagnosis in humans is performed on blood samples using RT-PCR, ELISA to detect viral antigen, or serology to detect IgM or IgG antibodies (162).

As with other bunyaviruses, the non-structural NSs protein is the major virulence factor for RVFV and plays a role in innate immune evasion (174). Animal studies have demonstrated a protective role for type I IFNs in phlebovirus infection, which is typically induced by detection of viral RNA by RIG-I, as well as the cytoplasmic RNA helicase/MAVS axis (175).

OROPOUCHE ORTHOBUNYAVIRUS (OROV) belongs to the genus *Orthobunyavirus*, family *Peribunyaviridae*, order *Bunyavirales*. At least 30 viruses within this genus can cause human disease (176), many of these are within the Simbu serogroup including Simbu virus, Shamonda virus, OROV, and recombinant orthobunyaviruses such as Iquitos virus

(IQTV, Figure 1.12). OROV infection in humans causes an acute febrile illness, Oropouche fever, which has infected more than 500,000 people since its discovery in Trinidad and Tobago in 1955, where it was isolated from a febrile patient (28,177). OROV has caused multiple epidemics in Brazil and Peru, as well as a single epidemic in Panama (28). In 2016 the WHO announced that the emergence of OROV in new areas was a significant risk, in large part due to the wide geographical spread of the biting midge vector *Culicoides paraensis* (178). OROV is of particular interest in the context of EID because the clinical picture is similar to that of other arboviral diseases circulating in the same geographical locations, meaning OROV may not be considered as a cause of infection in febrile patients because of the higher prevalence and awareness of other infections such as dengue fever and malaria (28).

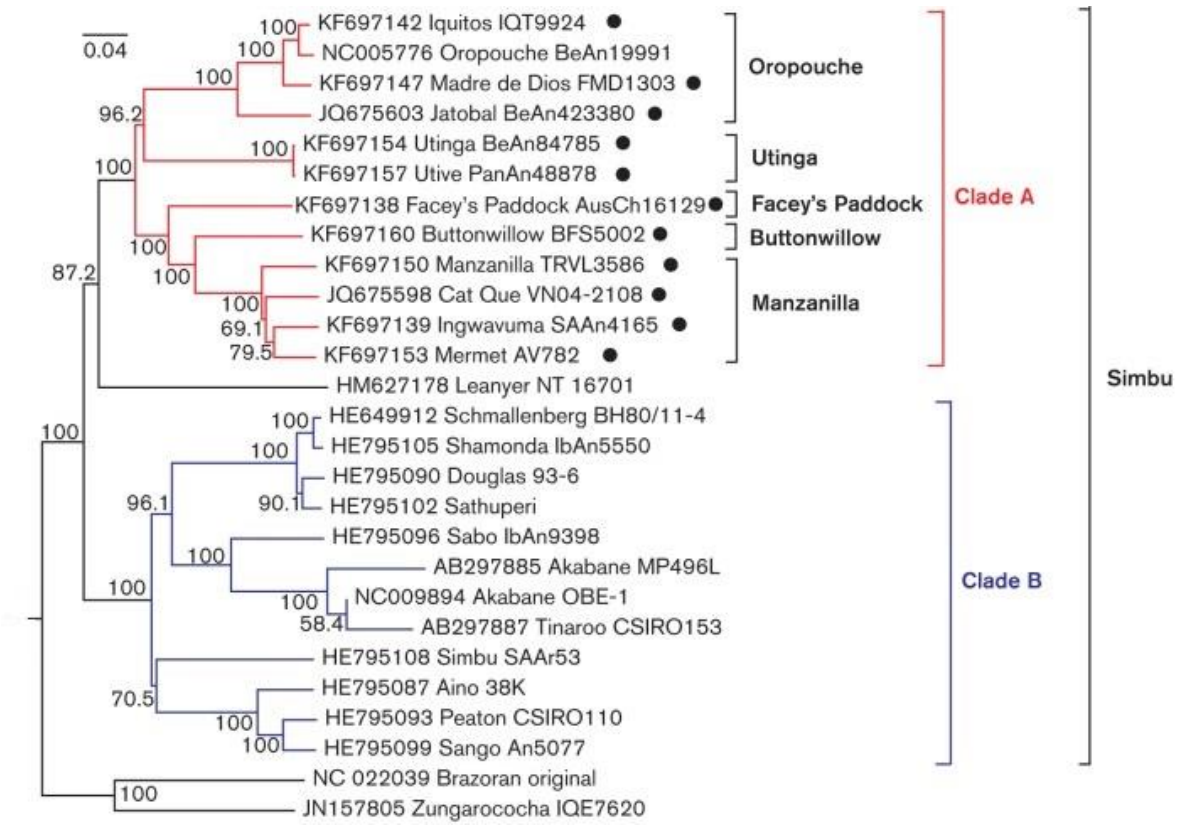

Figure 1.12 Phylogenetic tree of members of the Simbu serogroup, genus *Orthobunyavirus*, based on the protein-coding portion of the genomic L segment. Modified from Ladner *et al.* 2014 (179).

In the urban transmission cycle, humans act as hosts and *C. paraensis* is the vector, although there is some debate as to the existence of other vector species, particularly the mosquito *Culex quinquefasciatus* (28,180). OROV is maintained in a sylvatic cycle that is not well understood, but thought to involve numerous vertebrate host species and insect vectors (181). Urban outbreaks occur when a person becomes infected from an insect bite in a forested or rural area then moves into an urban area where the vector species is present (182).

Oropouche fever is typically self-limiting and relatively mild in nature. An incubation period of four to eight days after exposure precedes non-specific systemic symptoms which can include fever, headache, myalgia, arthralgia, anorexia, dizziness, chills, and photophobia. Viraemia is typically seen 2-4 days following the onset of symptoms (28). There are no reports of death from OROV infection; however infections of the central nervous system (CNS) and meningitis have been reported in rare cases (183,184). No treatments or vaccines are available for OROV infection, although a virus particle production assay and an OROV rescue system have been developed in recent years (185,186), which may be useful for developing a recombinant vaccine as well as improving knowledge of OROV pathogenesis.

Studies have identified several factors involved in OROV pathogenesis and immune response. *In vitro* studies in HeLa cells demonstrated that OROV induces apoptosis by triggering an intracellular pathway involving mitochondria (187), while a mouse study showed that OROV infection advances from the posterior to the anterior of the brain, crossing the blood-brain-barrier and spreading into the brain parenchyma, which is associated with more severe clinical signs (188). Activation of MAVS, IRF-3 and IRF-7, and production of type I IFNs are implicated in controlling infection (189).

1.2.4 FILOVIRUSES

EBOLAVIRUS (EBOV) is a genus of enveloped, single stranded negative-sense RNA viruses with non-segmented genomes and a characteristic filament shape. The genus belongs to the family *Filoviridae* and contains five viral species; *Zaire ebolavirus*, *Sudan ebolavirus*, *Bundibugyo ebolavirus*, *Taï Forest ebolavirus* and *Reston ebolavirus* (190).

Since the first detection of EBOV in 1976, ebolaviruses Zaire, Sudan and Bundibugyo have been responsible for sporadic, relatively small outbreaks of haemorrhagic fever in humans. These outbreaks have typically been limited to rural areas in Sudan, Democratic Republic of Congo (DRC), Republic of Congo, Gabon and Uganda (Table 1.1) (41,191). An exception to the typical small, contained outbreaks was the West African Ebola virus outbreak, the largest outbreak to date, that occurred between 2014-2016. This affected urban as well as rural areas and resulted in 28,646 cases and 11,323 deaths (Table 1.1) (192). Blood samples from EBOV-negative patients are used in this project and the outbreak is introduced in more detail in Chapter 3. At the time of writing, the second largest EBOV outbreak on record is ongoing in the DRC and as of 26th December 2019, 3,366 cases and 2,227 deaths have been reported (193).

Year began	Country	Ebolavirus species	Cases	Deaths	Case fatality rate (%)
2019	Uganda	Zaire	4	3	75
2018	DRC	Zaire	3,366†	2,227†	66†
2017	DRC	Zaire	8	4	50
2015	Italy	Zaire	1	0	0
2014	DRC	Zaire	66	49	74
2014	Spain	Zaire	1	0	0
2014	UK	Zaire	1	0	0
2014	USA	Zaire	4	1	25
2014	Senegal	Zaire	1	0	0
2014	Mali	Zaire	8	6	75
2014	Nigeria	Zaire	20	8	40
2014	Sierra Leone	Zaire	14,124*	3,956*	28
2014	Liberia	Zaire	10,675*	4,809*	45
2014	Guinea	Zaire	3,811*	2,543*	67
2012	DRC	Bundibugyo	57	29	51
2012	Uganda	Sudan	7	4	57
2012	Uganda	Sudan	24	17	71
2011	Uganda	Sudan	1	1	100
2008	DRC	Zaire	32	14	44
2007	Uganda	Bundibugyo	149	37	25
2007	DRC	Zaire	264	187	71
2005	Congo	Zaire	12	10	83
2004	Sudan	Sudan	17	7	41

2003	Congo	Zaire	35	29	83
2003	Congo	Zaire	143	128	90
2001	Congo	Zaire	59	44	75
2001	Gabon	Zaire	65	53	82
2000	Uganda	Sudan	425	224	53
1996	South Africa (ex-Gabon)	Zaire	1	1	100
1996	Gabon	Zaire	60	45	75
1996	Gabon	Zaire	31	21	68
1995	DRC	Zaire	315	254	81
1994	Côte d'Ivoire	Taï Forest	1	0	0
1994	Gabon	Zaire	52	31	60
1979	Sudan	Sudan	34	22	65
1977	DRC	Zaire	1	1	100
1976	Sudan	Sudan	284	151	53
1976	DRC	Zaire	318	280	88

Table 1.1 Recorded Ebola virus disease outbreaks. Table adapted from WHO (194). †Outbreak ongoing, figures correct as of 26th December 2019. *Includes suspect, probable and confirmed Ebolavirus disease (EVD) cases. 2018 and 2017 DRC outbreak data from (193) and (195), respectively.

Bats are strongly indicated to be reservoirs for EBOV; numerous studies have shown evidence of EBOV-antibodies in bats (196–200), viral RNA has been detected from bat samples (201) and experimental studies have shown that EBOV can infect bats without causing clinical disease (202). Non-human primates are also susceptible to infection

(203). Outbreaks of Ebolavirus disease (EVD) in humans begins with a spillover event where a person is infected through contact with an infected animal, or contaminated faeces, urine or blood. Following this, human-to-human transmission may occur via contaminated bodily fluids (204).

EVD in humans begins with symptoms including fever, chills, myalgia and malaise (205). Progression of disease leads to multi-system involvement including respiratory, gastrointestinal, vascular, postural, and neurological symptoms. Haemorrhagic manifestations may be observed from the peak of disease onwards (205). Previous outbreaks have recorded CFRs of 25-90% (204) with an average of 65% (206).

There are no approved therapies for the treatment of EVD, which is currently largely supportive (41). However, the West African EBOV outbreak highlighted the need for effective EBOV vaccines and therapeutic agents. During the outbreak, collaborative working led to rapid progress in clinical trials, including phase II vaccine trials in West Africa and a ring vaccination phase III trial in Guinea (207). Despite best efforts, the majority of trials took place towards the end of the outbreak, when it was difficult to recruit sufficient numbers to demonstrate statistically significant results, as was the case for the ZMapp monoclonal antibody trial (207). Most recently, the recombinant vesicular stomatitis virus - Zaire ebolavirus vaccine developed by Merck has been used on a large scale for the first time during the ongoing EBOV outbreak in DRC, where more than quarter of a million people were vaccinated between August-December 2019 (193,208). Full analyses will be published in time, but an initial report shows that the vaccine is well-tolerated and accepted by the community (209). Despite these advances, no vaccines or therapeutics have been licensed as of the time of writing (210), although the European medicines agency has recommended conditional marketing authorisation

for the Merck vaccine (211) and the WHO has given it prequalification status, recognising that it meets standards for quality, safety and efficacy (212).

Filoviruses infect cells of myeloid lineage including DCs, monocytes and macrophages early in the course of infection. In the later stages, cell tropism becomes more broad and non-lymphocytic cell types are susceptible to infection (213). Filoviruses can abrogate the innate immune response by preventing the production of type I IFNs and blocking the induction of an anti-viral state (214), allowing the virus to replicate rapidly and to a high titre. Furthermore, the filovirus glycoprotein (GP) is able to evade the immune response in a number of ways, perhaps most notably by the production of a soluble form of GP which competes for antibodies that would otherwise bind to and possibly neutralise whole virions (213).

MARBURG MARBURGVIRUS (MARV) forms a distinct genus (*Marburgvirus*) within the *Filoviridae* family and causes a similar disease in humans to that caused by EBOV, however, the average CFR is slightly lower at 54% (206). The virus was discovered following simultaneous outbreaks in Germany and Serbia in 1967 as a result of transmission from monkeys imported from Uganda (215). Outbreaks and sporadic cases of MARV have since been reported from Angola, DRC, Kenya, Uganda, and South Africa (in one person with recent travel to Zimbabwe) (215). Bats of the genus *Rousettus* are known reservoirs for MARV, whether other wildlife reservoirs exist has yet to be proven (206).

1.2.5 FLAVIVIRUSES

DENGUE VIRUS (DENV) is an enveloped, single stranded, positive-sense RNA virus with a non-segmented genome, within the *Flavivirus* genus, family *Flaviviridae* (49). DENV has five known antigenically distinct serotypes (DENV1-5), the most recently discovered of which, DENV-5, was identified in 2013 (216). DENV serotypes 1-4 circulate in urban and peri-urban environments around the world (217), whereas DENV-5 has only been detected in rural parts of Sarawak state, Malaysia (216). DENV is responsible for a huge burden of disease and is widespread throughout tropical and sub-tropical regions, currently endemic in more than 100 countries and showing increased incidence in recent decades (218). 70% of the burden of disease is in Asia, although the Americas and Western Pacific regions are also seriously affected (Figure 1.13) (218). The epidemiology of DENV in Africa is poorly characterised, reflected by the lack of distribution data for this continent (Figure 1.13), however, 32 countries have reported cases of DENV since 1960 (219). All four serotypes have been detected in Africa, although DENV-2 is most common (219). Accurate DENV case estimation is difficult, however, the WHO estimates that 390 million infections occur annually across the world, with 3.9 billion people at risk of infection (22,218).

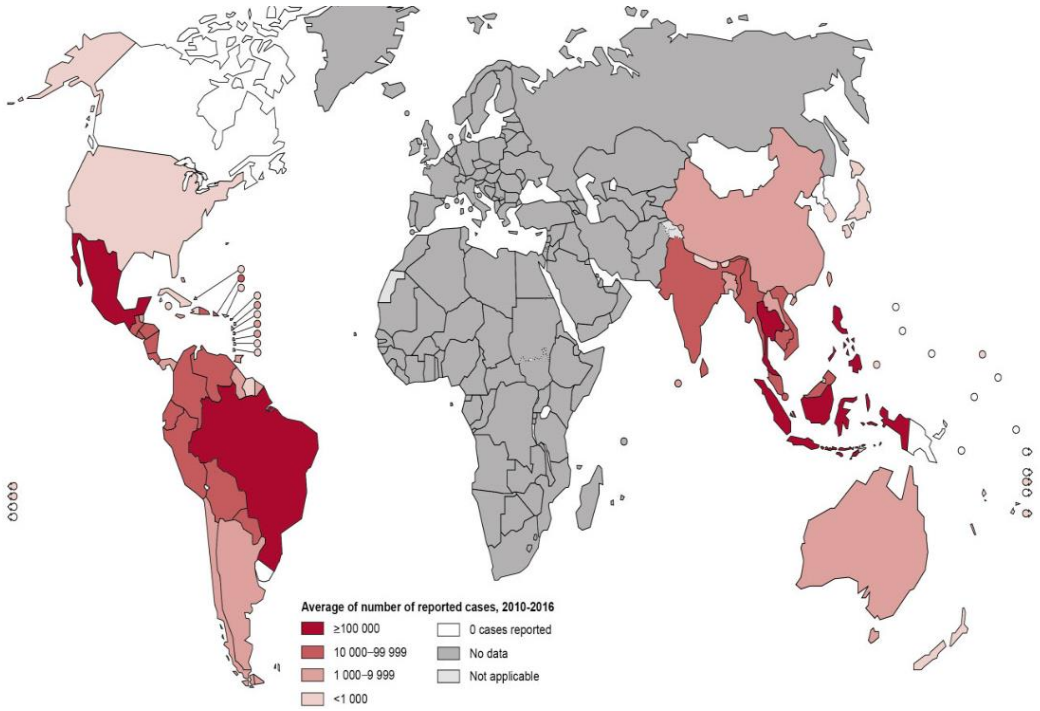

Figure 1.13 Distribution of dengue fever in 2016. Colour shows the average number of suspected or confirmed dengue cases, reported to WHO 2010-2016. Available at https://www.who.int/denguecontrol/epidemiology/en/.

DENV is frequently transmitted to humans from a bite by an infected *Ae. aegypti* mosquito, which acts as the primary vector (217). *Ae. albopictus* is also a vector but to a lesser extent than *Ae. aegypti* (218), and sexual transmission has been reported (220). Transmission occurs in cycles between wild vertebrates and mosquito vectors (wild cycle) and humans and mosquito vectors (epizootic cycle) (217).

DENV infection in humans causes dengue fever which has a broad clinical spectrum, ranging from a non-serious 'flu-like' illness to severe forms which can be fatal. Typically, non-serious symptoms last for 2-7 days and include fever, headache, muscle and joint pain, nausea and rash. Severe dengue involves complications resulting from fluid accumulation, plasma leaking, severe bleeding and organ impairment (218). The WHO

estimates that half a million people are hospitalised with severe dengue each year, of which 2.5% die as a result (218). Between 2010 and 2016, a decline in the CFR was recorded, believed to result from improved case management in dengue endemic countries (218). There is no specific treatment for dengue fever, however in 2015 the first DENV vaccine (Dengvaxia CYD-TDV) was registered for use in endemic areas of some countries (218). In line with WHO recommendations, laboratory diagnosis of DENV is carried out through a combination of serological testing to detect anti-DENV IgM and/or IgG antibodies, and RT-PCR to detect viral RNA (221). Virus isolation is also often carried out (221).

Immunopathogenesis plays a role in severe dengue, which occurs more frequently in patients that have had a previous DENV infection. The mechanism of antibody-dependant enhancement (ADE) is well understood (222). Antibodies against viral precursor membrane and envelope proteins, made during the immune response to a primary infection, are likely to poorly neutralise a subsequent DENV infection due to high viral genetic and antigenic variation and low antibody titres (222). During a subsequent infection, opsonisation of virions into cells in which they can replicate, such as macrophages, increases viral entry and replication (223–225). In addition, the resulting induction of inflammatory cytokines contributes to the 'cytokine storm' often seen accompanying the onset of severe symptoms in patients with severe dengue (222,226). Evidence suggests DENV-specific antibodies also enhance ZIKV infection (227,228), a related flavivirus that co-circulates with DENV in several countries, however no evidence from cases of natural infection is available as of yet (222).

JAPANESE ENCEPHALITIS VIRUS (JEV) is a member of the *Flavivirus* genus (Figure 1.14) that can infect the human CNS and is a major cause of viral encephalitis in Asia, with an estimated 68,000 cases occurring annually (229). Four genotypes exist, named I-IV, of which genotype III historically caused the large majority of cases, however genotype I has become more prevalent in recent decades (230,231). JEV is endemic in 25 countries in South Asia, South-East Asia and Western Pacific regions and may be seasonal or year-round depending on the climate, which influences vector populations (229,232). Transmission to humans occurs via the bite of an infected *Culex* species mosquito. Humans do not develop viraemia of sufficient titre to infect biting mosquitoes, which themselves become infected when feeding on infected pigs or water-birds (229).

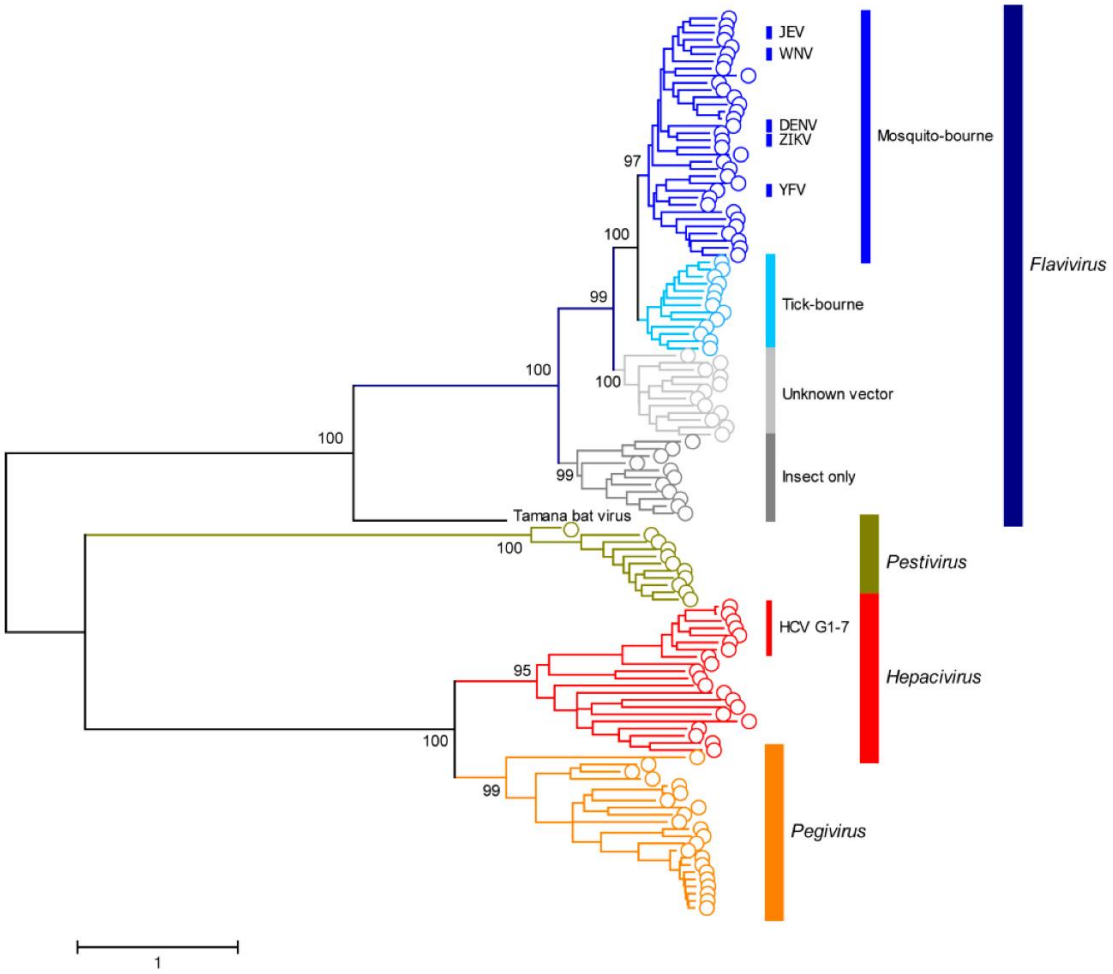

Figure 1.14 Phylogenetic relationships within the *Flaviviridae*. Reproduced from Kleinert *et al.* (2019) (233).

Most infections are asymptomatic or mild but in rare cases severe disease develops, the most common form of which is acute encephalitis syndrome, characterised by severe headache, malaise and the inability to think clearly, which may progress to flaccid paralysis (231). The CFR is up to 30% in severe disease and permanent sequelae including paralysis and recurrent seizures are seen in 20-30% of survivors (229). Several safe and effective JEV vaccines exist, of which the most widely used is the live attenuated SA14-

14-2 vaccine (231). No effective anti-viral treatment exists (229). Laboratory diagnosis is usually by detection of IgM antibodies, however because of antibody cross-reactivity with other flaviviruses, a plaque reduction neutralisation test (PRNT) should also be performed to confirm the presence of JEV (231). RT-PCR is often not appropriate because viraemia subsides by the time sever disease manifests, however it shows better utility with CSF samples than blood (231).

The dermis is the primary site of infection for JEV, in which the virus replicates in currently undefined cell types before being transported to lymphoid organs via infected immune cells (234). Low-level viraemia occurs and the virus may replicate in lymphocytes, although this is not thought to be a major site of replication (235,236). JEV enters the brain through a poorly-understood mechanism, where it can be detected primarily in the nuclear grey matter (237). CNS inflammation is a hallmark of JEV infection, in which brain-infiltrating monocytes, macrophages and microglia play a major role (237).

TICK-BORNE ENCEPHALITIS VIRUS (TBEV) is a flavivirus found in central, eastern and northern Europe and Asia. There are three genetic subtypes; European (mainly transmitted by *Ixodes ricinus* ticks), Siberian and Far Eastern (mainly transmitted by *Ixodes persulcatus*) (238). TBEV belongs to the TBEV serocomplex; a group of closely related tick-borne flaviviruses including: Powassan/deer tick virus, Omsk haemorrhagic fever virus, Kyasanur Forest disease virus, louping ill virus, and Langat virus (239). In 2019, Public Health England (PHE) announced that cases of TBEV had been detected in the UK for the first time (240), in ticks from southern England (241). The recent expansion of

the disease into new regions in Europe is thought to be a result of the spread of tick populations, likely caused by climate change and change in land use (238).

Disease in humans results from a bite from an infected tick. Cases of TBEV have increased in recent years, the WHO estimates that 10,000-12,000 clinical cases occur annually, although this is believed to be an underestimate (242). The initial disease is a typical 'flu-like' illness, which may be followed by infection of the CNS resulting in meningitis, encephalitis or meningoencephalitis, with CFR estimates of 1-20% depending on the virus (238,243). Survivors of neuro-invasive TBEV infection experience long-term sequelae in 25-40% of cases (243). Currently there are no effective antiviral treatments for TBEV, but there is an effective vaccine (238). Diagnosis of TBEV is performed through a combination of clinical and laboratory findings. IgM and IgG antibody detection in patient CSF is considered a reliable method (244). Similar to JEV, neuronal damage and immunopathology is thought to be responsible for the clinical symptoms and disease progression in TBEV infection (239).

WEST NILE VIRUS (WNV) is a flavivirus that was discovered in Uganda in 1937, causing epidemics in Africa, Europe, the Middle East and Asia in the following decades (245). In 1999 WNV was introduced to the United States, possibly from the Middle East, where it caused a large outbreak, subsequently becoming endemic and spreading through North, Central and South America (246). Infection is maintained in a complex sylvatic cycle involving multiple species of mosquitoes and birds and as such, outbreak localities are usually on major birds migratory routes (246,247).

WNV transmission to non-reservoir host species has resulted in significant morbidity and mortality in equine and bird species; large declines in numbers have been reported in 23 bird species (248,249). WNV is transmitted to humans through the bite of infected *Culex* species mosquitoes (250,251). Humans are not reservoir hosts and most infections are asymptomatic, however, 20% of individuals experience symptoms including rash, headache and fever (246). Severe neurological disease is rare but can be fatal and is seen in <1% of cases. Symptoms may include encephalitis, meningitis and acute flaccid paralysis. There are currently no effective treatments or vaccines available (246) and sequelae are seen in approximately 50% of survivors (245). Laboratory diagnosis is performed using ELISA to detect IgM or IgG antibodies in serum or CSF, PRNT, virus isolation in cell culture or RT-PCR to detect viral RNA (246).

WNV replicates in keratinocytes and DCs at the site of infection, then migrates to lymph nodes in activated Langerhans cells (234). Viraemia and virus dissemination to organs, including the kidneys and spleen, follows (234). WNV can cross the blood-brain-barrier but the mechanism is not well understood. The neuropathology seen during infection is thought to be at least partly caused by the immune response, either from CNS-resident cells or from infiltrating leukocytes (245). Some recovering patients develop chronic kidney disease or long-term neurological sequelae; the mechanisms are not well understood but it is suggested that generation of IL-1 by astrocytes negatively impacts neuronal progenitor cells, which may contribute to neurological impairment (252).

YELLOW FEVER VIRUS (YFV) is a flavivirus found in tropical regions of Africa, and Central and South America (Figure 1.15) (253). YFV was once considered a forgotten disease but has re-emerged in recent years, likely due to a decrease in vaccination coverage in endemic areas. This can occur, for example as seen in Southern Sudan, because of political unrest and population movement of unvaccinated people (254). Very recently, in 2016-2018, re-emergence in non-endemic areas and endemic areas with low levels of vaccination coverage has highlighted the need for better understanding and surveillance of YFV infection (255).

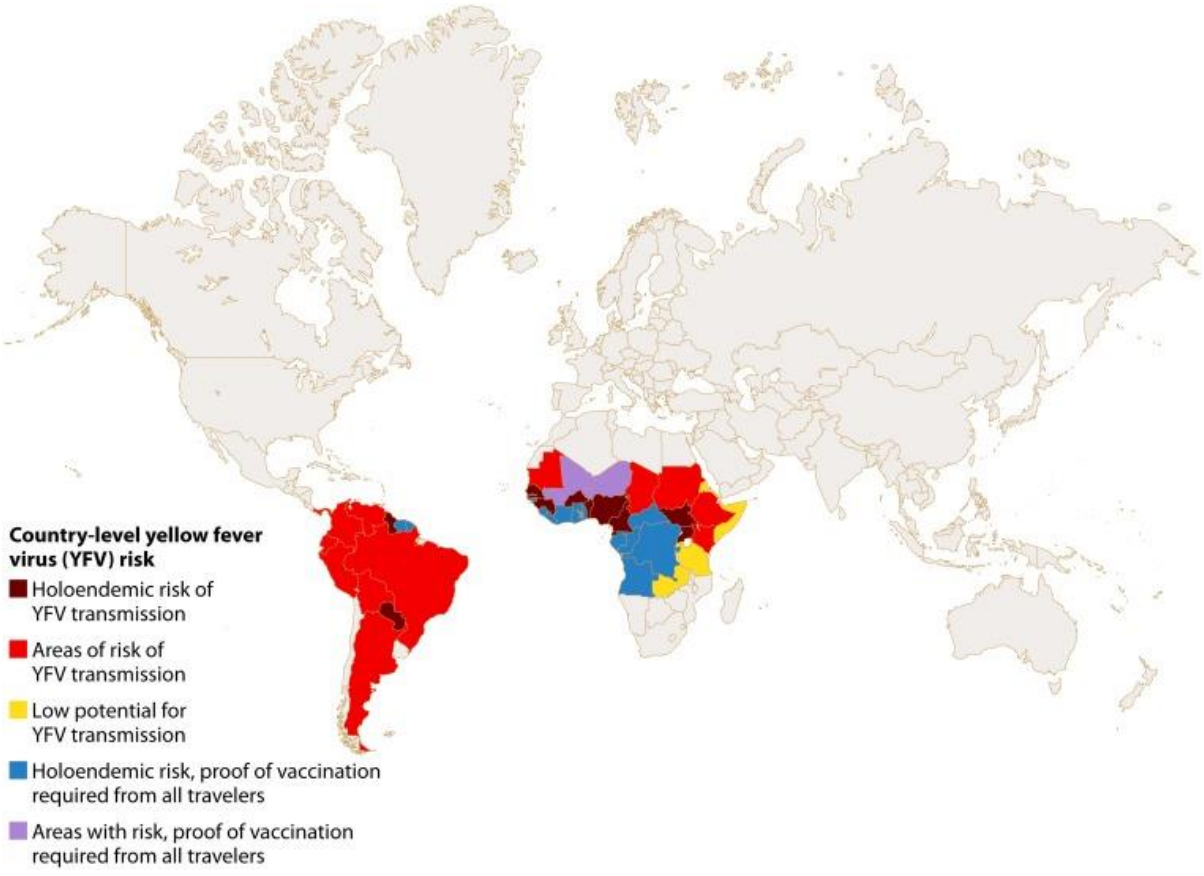

Figure 1.15 Countries with areas of endemic YFV and countries with requirements for proof of vaccination from incoming travellers (as of July 2018). Reproduced from Waggoner *et al.* (2018) (256).

YFV is transmitted by mosquitoes in the *Haemogogus, Sabethes* and *Aedes* genera (255). The virus is maintained in a sylvatic cycle between mosquitoes and non-human primates, and in an urban cycle between mosquitoes and humans (255). The annual number of YFV cases globally is estimated at 80,000-200,000 (257). Yellow fever disease presents as a 'flu-like' illness commonly observed in flavivirus infection and usually improves within five days. In approximately 15% of patients, symptoms quickly recur and may become more severe, including jaundice, bleeding, liver and kidney damage. In patients who develop severe disease the CFR is approximately 50% (253). A live-attenuated YFV vaccine (YFV-17D) is widely available and was used successfully in mass vaccination campaigns during the 1940-1950s and 2000s (258,259). YFV diagnosis is performed through a combination of clinical observations and laboratory tests, including virus culture, serology, molecular testing, and antigen detection (256).

In humans YFV replicates primarily in the liver (260). To reach this organ, the virus infects DCs in dermal tissue at the site of infection which migrate to lymph nodes, priming an adaptive immune response prior to spreading virus through the bloodstream to the liver (255). Studies in human cells and humanised mice show that YFV has a broad tropism and can replicate in hepatocytes, haemopoietically-derived cells including DCs, monocyte-derived macrophages, T-cells, Kupffer cells and endothelial cells (261–266). Studies of tissue biopsies from YFV fatalities, in addition to evidence from animal models, suggest that hepatocyte apoptosis is important in YFV pathogenesis and that the immune-response contributes to disease through an unbalanced cytokine response (260,267,268).

ZIKA VIRUS (ZIKV) is an emerging flavivirus that was first detected in Uganda in 1947 in a sentinel rhesus macaque, followed shortly after by detection in humans in Nigeria in 1953 (269). In the following decades, sporadic cases were reported from Africa and South-east Asia, then in 2007 a major outbreak occurred in Yap Island, Micronesia (270), followed by an outbreak in French Polynesia in 2013-2014, during which two thirds of the population were infected (271). In 2015 the first cases of ZIKV were reported from Brazil; following this the virus spread rapidly through the Americas (269). Since 2015, 55 countries reported autochthonous, vector-borne transmission of ZIKV, of which 48 are in the Americas or the Caribbean (272). Additionally, 5 countries reported sexual ZIKV transmission (272). This outbreak is introduced in more detail in Chapter 4.

ZIKV transmission cycles are not fully understood, however sylvatic and urban cycles are known to exist, in which ZIKV transmission is maintained between vertebrate hosts and mosquito vectors. Vertical and venereal ZIKV transmission occurs within vector populations (Figure 1.16) (269). In urban cycles, the primary method of transmission is a bite from an infected female mosquito (typically the anthropophilic species *Ae. aegypti*), however sexual transmission from person-to-person also occurs (273).

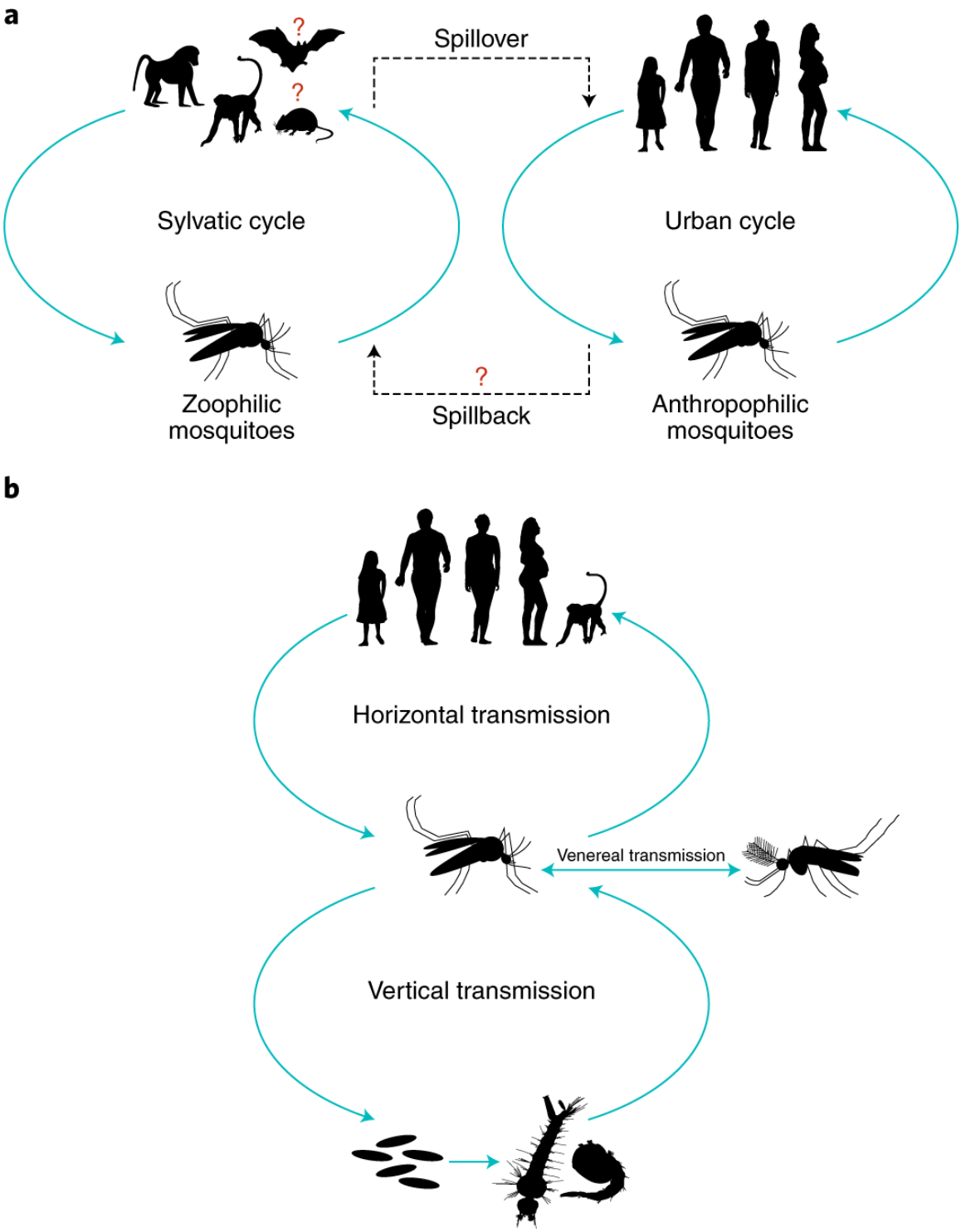

Figure 1.16 ZIKV transmission cycles. A) Horizontal transmission occurs in sylvatic and urban cycles **B)** Vector-borne transmission occurs via horizontal transmission between vertebrates and vectors, and via vertical and venereal transmission between mosquitoes. Reproduced from Gutiérrez-Bugallo *et al.* (2019) (269).

ZIKV in humans is asymptomatic in 80% of infections, while the remaining 20% experience a mild disease lasting between two and seven days, characterised by rash, fever, arthralgia, conjunctivitis and other minor symptoms (274). During the French Polynesian outbreak, an increase in patients presenting with severe neurological conditions including Guillain-Barré syndrome, encephalitis, meningoencephalitis, and myelitis was reported. An association between ZIKV infection and microcephaly was made in 2016, when a 20-fold increase in congenital defects in the USA was recorded by the CDC (275). A link between ZIKV infection, Guillain-Barré syndrome and microcephaly was reported in a number of studies (276–278). ZIKV is closely related to DENV, and questions exist over whether cross-reactive antibodies could have a protective effect, or whether ADE and resulting pathology occur, as seen in sequential infection with different DENV serotypes (222). A recent review of the evidence surmised that current knowledge is inadequate to draw a clear conclusion on this (279). Currently, there are no licensed treatments or vaccines for ZIKV infection (280). The laboratory testing protocols recommended by the WHO are nucleic-acid tests for patients <7 days from the onset of symptoms, and serological and/or nucleic-acid tests in patients ≥7 days from onset of symptoms (281).

The pathogenesis of ZIKV is the subject of much research, though not yet fully understood. Axl (a phosphatidylserine receptor) enables viral entry in permissive cells including dermal fibroblasts and a number of cell types in the CNS (282). ZIKV activates toll-like receptor 3 and indirectly causes apoptosis (273). An increase of cytokines including IL-1β, IL-2, IL-4, IL-6, IL-9, IL-10, IL13, IL-17, IFN-γ-induced protein 10, chemokine (C-C motif) ligand 5 (CCL5), macrophage inflammatory protein 1 alpha, and VEGF has been observed in serum of patients in the acute phase of ZIKV infection, which

returned to baseline levels during recovery (283). ZIKV antagonises type I IFN signalling in human cells by the viral NS5 protein binding to signal transducer and activator of transcription 2 (STAT2), leading to its degradation. In this way the upregulation of IFN-stimulated genes is attenuated (273).

1.2.6 NON-VIRAL INFECTIOUS CAUSES OF AUFI

Although viruses are responsible for a substantial burden of AUFI-like disease (284,285), non-viral agents play a large part. Malaria has historically been a huge problem in tropical regions, however, global efforts to control transmission have resulted in a significant decline in cases in recent years (286). Despite this, malaria is still a serious issue, causing 219 million infections and 435,000 deaths in 2017 (287). *Plasmodium falciparum* is responsible for the vast majority of malaria burden, transmitted by *Anopheles* spp. mosquitoes (288). A plateau in the rate of case decline was observed between 2015-2017 (286), highlighting the need to continue investing in malaria surveillance, vector control, treatment and eradication efforts.

A review of studies looking at the aetiology of >80,000 AUFI patients in Asia identified dengue fever as the most common aetiology (12%), with leptospirosis, typhoid and scrub typhus following, all of which are bacterial infections (284). Leptospirosis is a zoonosis resulting from infection with *Leptospira* spp., which are distributed worldwide although incidence is poorly understood in affected regions (289). Transmission occurs when humans are exposed to urine from infected rodents, often via contaminated water, but does not occur from person-to-person (290). Typhoid is caused by *Salmonella* Typhi, transmitted via contaminated food or water and can be life-threatening (291).

Annually it is responsible for 11-20 million cases and 128,000 – 161,000 deaths, primarily in developing areas of Africa, the Americas, South-East Asia and Western Pacific regions (291). Antibiotic treatment is usually effective and two licensed vaccines exist (291). Scrub typhus, caused by *Orientia tsutsugamushi* infection, is transmitted to humans via larval mites and infections are most commonly seen in rural areas of Southeast Asia, Indonesia, China, Japan, India, and northern Australia (292).

O. tsutsugamushi belongs to the *Rickettsiaceae* family of Gram-negative bacilli, which includes the genus *Rickettsia*. Bacteria responsible for several different diseases belong to the *Rickettsia* genus, including epidemic typhus or louse-borne typhus fever (*R. prowazekii*), murine typhus fever *(R. typhii*), rickettsialpox (*R. akari)* and Rocky Mountain spotted fever (*R. rickettsia)*. The geographic distribution of rickettsial disease is determined by the range of the vector, which are ectoparasites or arthropods (hard or soft ticks, mosquitoes, mites, lice, and fleas) that transmit the bacteria via biting (293).

1.3 METAGENOMIC SEQUENCING AND VIRUS DETECTION

1.3.1 CURRENT NEXT GENERATION SEQUENCING TECHNOLOGIES

Sanger's dideoxy chain termination method of DNA sequencing (1st generation sequencing) was developed the 1970s and widely used in the following decades, making the sequencing of bacterial and eukaryotic genomes possible and enabling the completion of the first human genome sequence in 2001 (294). The development of next-generation sequencing (NGS) began in 2005 with second-generation sequencing technologies such as the Roche 454 sequencing system, which utilised a pyrosequencing approach, and the Illumina sequencing-by-synthesis chemistry, now widely used in molecular biology laboratories (Table 1.2) (295). Third generation sequencing technologies were developed shortly afterwards from 2009, encompassing novel approaches that remove the amplification step used in second generation approaches. Although the costs associated with NGS are high, the development of this technology has resulted in a dramatic decrease in the cost of DNA sequencing per megabase. 'Moore's law', coined to describe the long-term trend in computer power doubling every two years, is commonly used to observe and project technology improvements. Those that follow Moore's law are considered to be doing extremely well in terms of speed of development. The cost per megabase of DNA fitted well with Moore's law between 2001 and 2008, following which a dramatic drop in cost occurred, far outpacing Moore's law (Figure 1.17) and coinciding with the transition from Sanger to NGS (296).

Sequencing platform	Sequencing generation	Amplification method	Sequencing method	Read length (bp)	Error rate (%)	Error type	Number of reads per run	Time per run (hours)
Sanger ABI 3730xl	1st	PCR	Dideoxy chain termination	600–1000	0.001	Indel–Substitution	96	0.5–3
454 Roche GS FLX +	2nd	PCR	Pyrosequencing	700	1	Indel	1.00E+06	23
Illumina MiSeq	2nd	PCR	Synthesis	2 × 300	0.1	Substitution	4.4-5.0E+07	56
Oxford Nanopore MinION	3rd	None	Nanopore	~ 200–20,000	5	Indel–Substitution	0.7–1.2e+07	0.1-50

Table 1.2 Comparison of widely used 1st, 2nd and 3rd generation sequencing technologies. Adapted from Derocles *et al.* 2018 (297). PCR = polymerase chain reaction. Updates to the table were made from the following sources: read length – MinION (298), error rate – MinION (299), number of reads per run – Illumina Miseq (300), MinION (301), time per run – Illumina Miseq (300).

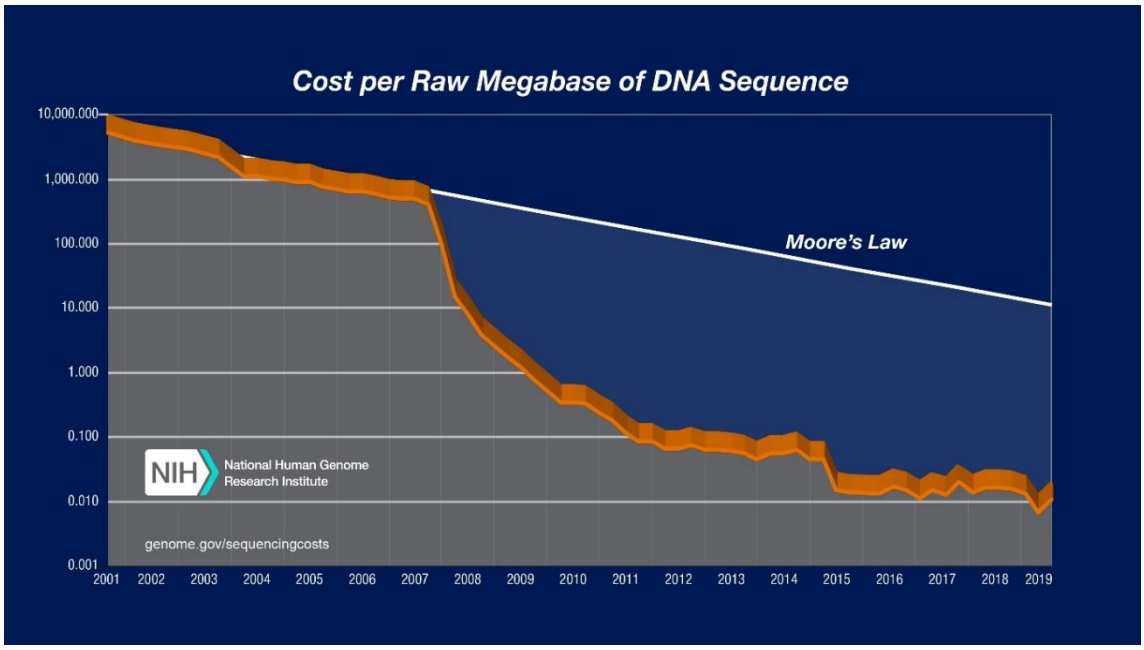

Figure 1.17 Sequencing costs per megabase of DNA, 2001 - August 2019. The dramatic decrease in cost seen from 2008 coincides with the transition from Sanger to NGS. Data from the National Human Genome Research Institute, figure reproduced from https://www.genome.gov/about-genomics/fact-sheets/DNA-Sequencing-Costs-Data

Illumina and Nanopore are probably the most widely used sequencing technologies in the field of virus genome sequencing at present. In Illumina's sequencing-by-synthesis chemistry, DNA is prepared by generating sequencing libraries, where DNA is fragmented into 200-300 bp and adapters are ligated to the ends of the fragments (Figure 1.18). The library is applied to a solid surface (the flow cell) where adapters enable the DNA bind to the surface of the flow cell. DNA is amplified in a polymerase chain reaction (PCR) known as 'cluster generation', where approximately one million copies of each DNA fragment are generated on the flow cell surface (Figure 1.18). The

sequencing reaction works in a similar way to the Sanger method; it uses deoxyribonucleotide triphosphates (dNTPs) that contain a fluorescently labelled terminator, which prevents further DNA polymerisation after a single base has been incorporated (Figure 1.18). Unlike Sanger sequencing, the termination is reversible, and fluorescence is detected optically following the addition of dNTPS, after which the terminator is removed before another cycle of dNTP addition begins. Millions of sequencing reactions occur simultaneously on the flowcell and the resulting reads are uniform in length due to the single base addition performed during each cycle.

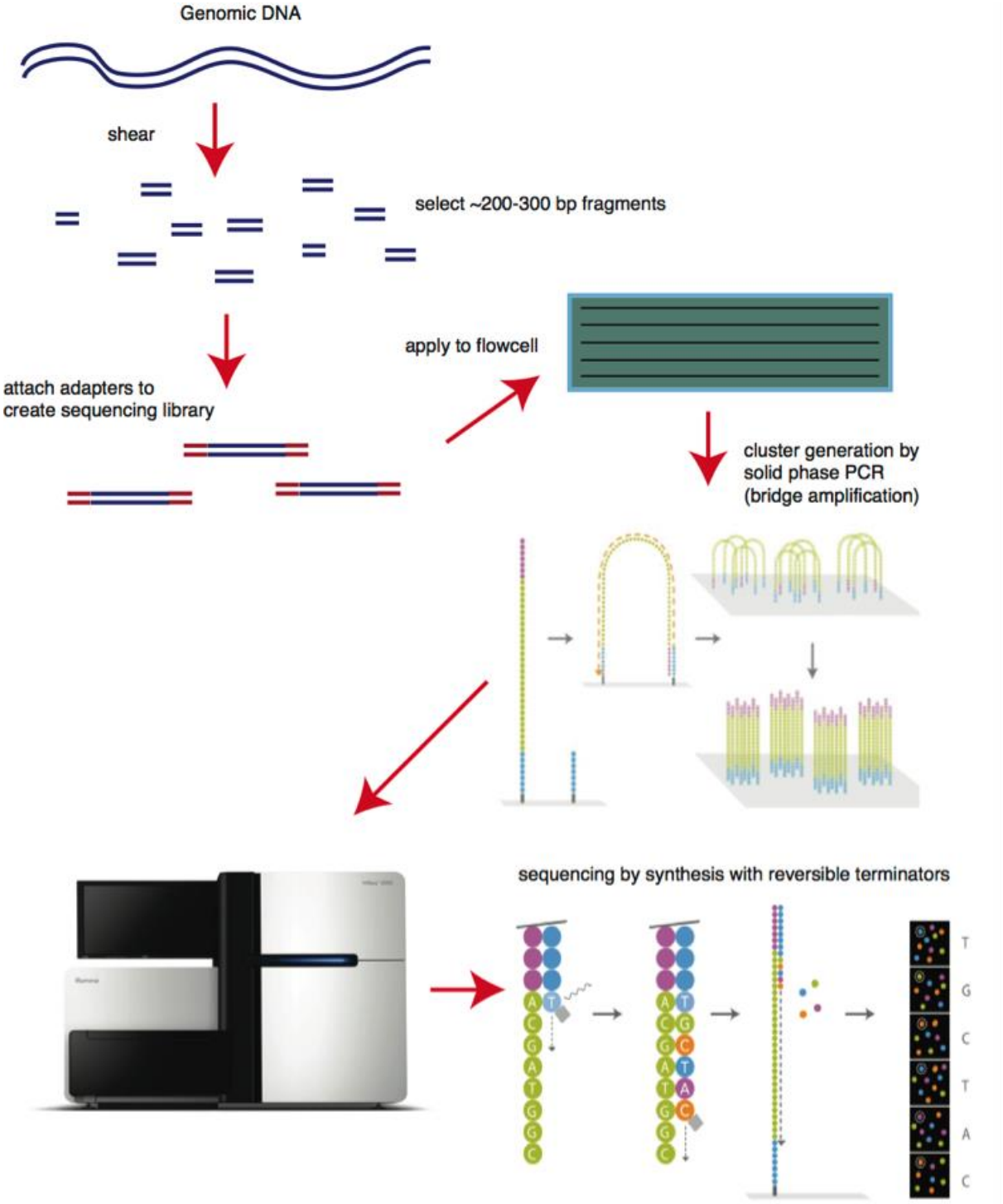

Figure 1.18 Illumina's sequencing-by-synthesis chemistry. Reproduced from (302).

Nanopore sequencing is a third-generation sequencing technology that has been commercialised by UK-based company Oxford Nanopore Technologies (ONT). It utilises a novel chemistry based on the use of protein pores (nanopores) embedded in a lipid bilayer, situated within a flow cell (Figure 1.19). DNA libraries are prepared by adding an adaptor molecule to the end of each DNA fragment. DNA libraries are applied to the flowcell where they are driven through a nanopore by means of an enzyme motor, which is part of the adapter (Figure 1.19). Electrical current passes through the nanopore and changes in conductivity occur as DNA is translocated, with each base producing a characteristic change. This is detected and converted to a trace that can be read and interpreted (Figure 1.19).

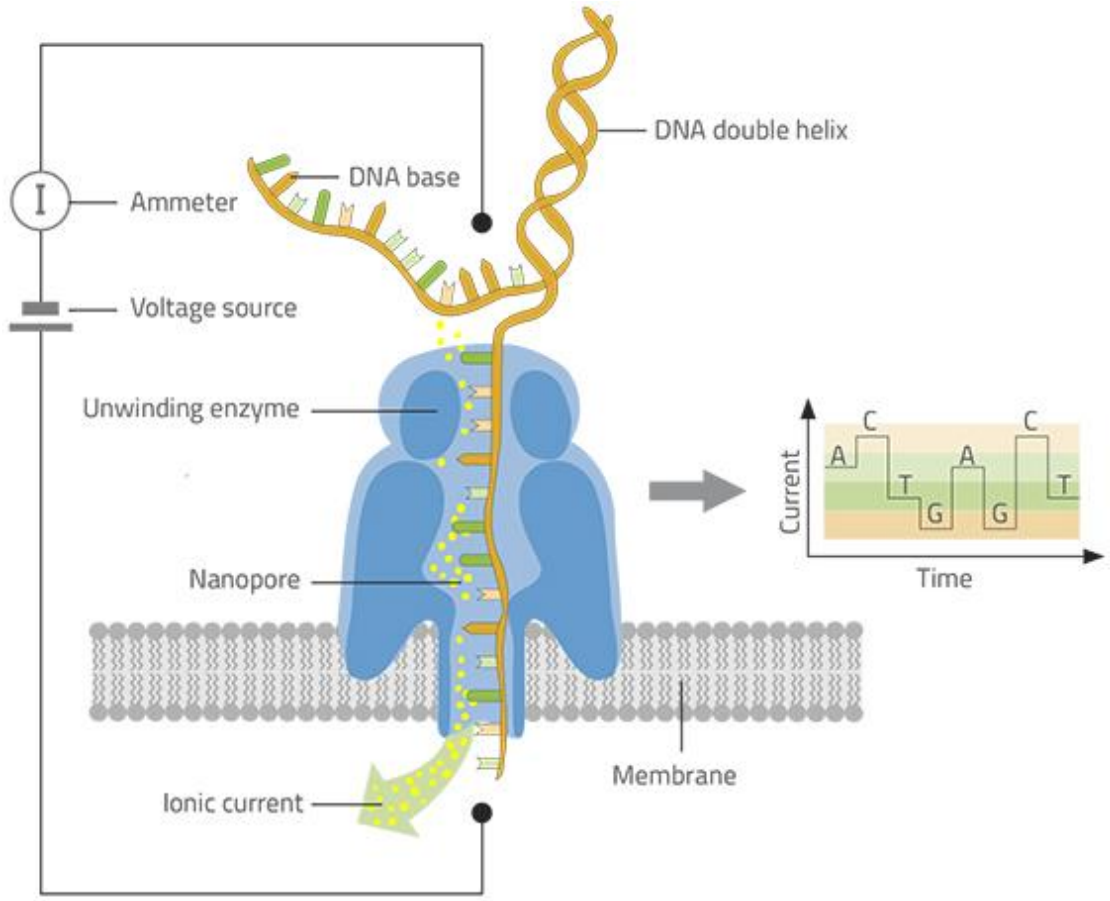

Figure 1.19 Nanopore sequencing chemistry. Reproduced from (303).

The most well-known ONT product is the MinION, a palm-sized DNA sequencer that is used in conjunction with a laptop computer, making it highly portable and therefore well suited to field-work. It has the capability to generate extremely long reads and produces data in real-time as the run progresses. The initial set-up costs are low, whilst reagents and flowcells come at a premium price. Compared with an Illumina benchtop sequencer, costs are much lower, especially as there is no service or maintenance contract costs. This makes nanopore sequencing a more realistic option for genome sequencing in low- and middle-income countries, or during EID outbreaks. The challenges of nanopore sequencing include a high DNA input requirement (meaning that although the

technology itself does not require a PCR amplification step, this is often practically necessary to get sufficient data), high error rates requiring high depth of coverage to compensate, and high cost consumables (Table 1.2) (14). However, whilst error rates are higher than that of Illumina, the errors generated tend to be random (resulting from a low signal-to-noise ratio) as opposed to the systematic biases observed in Illumina processes (304). Therefore, at high depth of coverage nanopore sequencing overcomes the high error rate, and the reduced systematic bias may even be preferable over Illumina sequencing for some applications.

Illumina error rates are the lowest of any current NGS technology, making it reliable and accurate for variant analysis (Table 1.2). Both Illumina and nanopore sequencing have the capability to multiplex samples using a barcoding system, meaning multiple samples can be sequenced in one run, the number of which is usually determined by the depth of coverage required for each sample. The initial set up costs of an Illumina sequencer are high compared to nanopore sequencing, with an instrument costing significantly more and the nature of the instrument meaning a molecular biology laboratory is required.

1.3.2 NGS OF PATHOGEN GENOMES

Prior to the advent of NGS technologies, virus genome sequencing was accomplished by generating multiple overlapping PCR amplicons followed by Sanger sequencing to obtain the complete genome sequence. This approach is costly in terms of time and effort, as primer pairs must be designed for each target, PCR reactions frequently require re-optimisation and errors can be introduced during amplification (305). NGS (particularly

metagenomic NGS, defined below) overcomes many of these drawbacks, and the increased depth of sequence data produced (hundreds or even thousands of reads at each nucleotide position) allows the heterogeneity of viral populations to be studied, providing important insights into viral evolution (40).

Sequencing requires DNA (although recent developments in nanopore technology have made possible direct sequencing of viral RNA (306,307)), however sequencing from RNA is easily achieved through the means of reverse transcription. Additional considerations are needed when performing metagenomic sequencing from RNA. RNA virus genomes are usually kilobases long, whereas host DNA genomes are often orders of magnitude larger. This means that a single contaminating host cell can form the equivalent of half a million virions in sequencing reads (308). To reduce this 'background', it is essential that DNA is removed from the sample prior to sequencing. Despite this, it is still possible (though not optimal) to detect the presence of DNA viruses, bacteria, fungi, and parasites, because ribosomal RNA and mRNAs produced by actively replicating DNA will be sequenced, allowing a broader range of pathogen detection (308).

1.3.3 TARGETED VERSUS METAGENOMIC SEQUENCING

Targeted NGS (Figure 1.20) uses target sequence capture/hybridisation techniques to enrich for target sequences, which is useful for viral genomes which usually make up a tiny proportion of the DNA or RNA present in a sample (305,309). These techniques allow more efficient viral genome sequencing and identification using NGS, which is useful when looking for several targets, when using poor quality samples, and when high sensitivity is a priority (310). Furthermore, the use of highly multiplexed target capture

with NGS, which utilises millions of pathogen-specific probes that can enrich for highly diverse sequences, is promising because of the high sensitivity and specificity of this method (311). However, targeted approaches require prior knowledge of the pathogen, meaning novel or genetically divergent pathogens are likely to be missed. In contrast, metagenomic sequencing (metagenomics) is the direct sequencing and characterisation of all genetic material present in a sample (312). This approach is an attractive alternative to conventional molecular diagnostic methods such as RT-PCR, or targeted NGS sequencing approaches, because novel or genetically divergent pathogens can be detected from clinical samples with no specific amplification and there is no requirement for prior knowledge of the pathogen genome sequence.

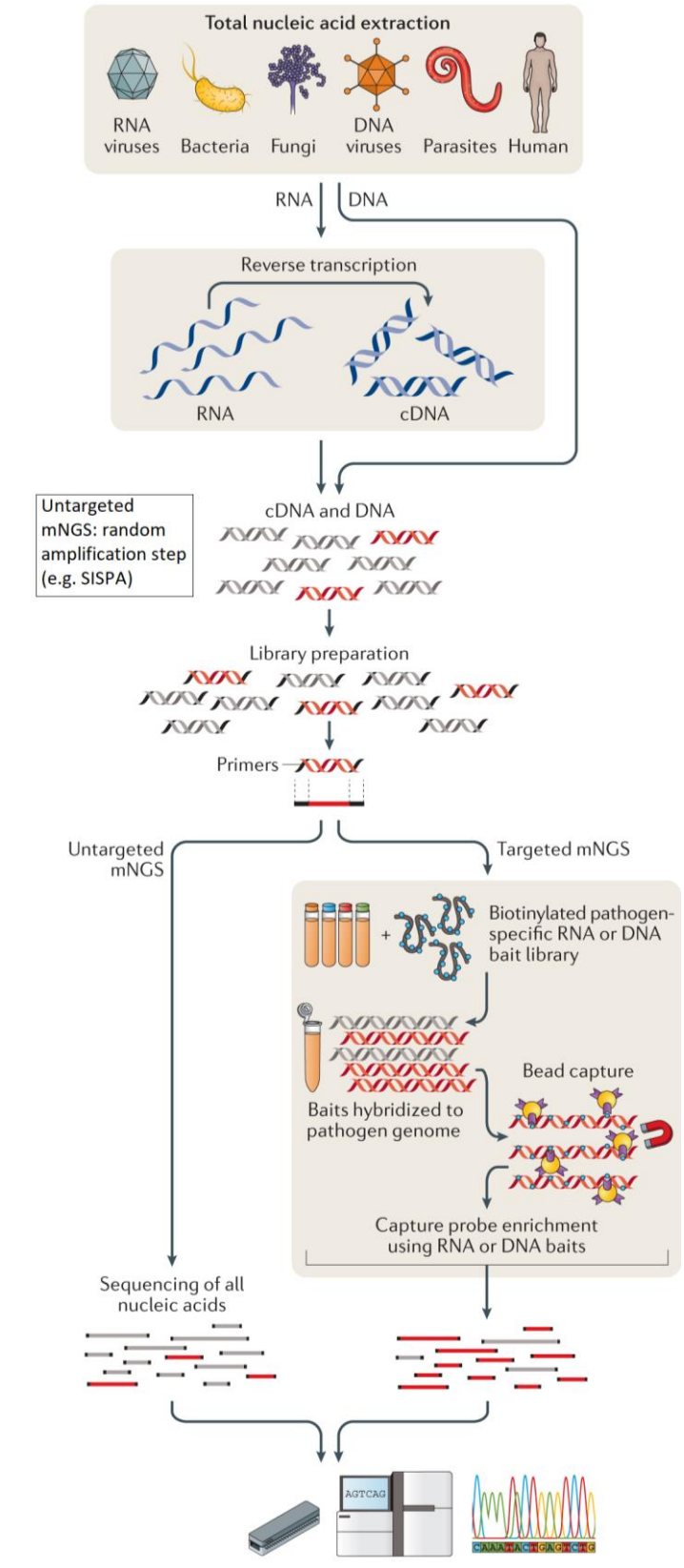

Figure 1.20 Workflows for targeted and non-targeted NGS approaches. Adapted from Chui and Miller (2019) (313).

1.3.4 METAGENOMICS WORKFLOW

A typical metagenomics workflow for identifying viral genomes begins with (if sequencing RNA) a DNAse treatment to remove contaminating DNA, followed by reverse transcription to generate complementary DNA (cDNA, Figure 1.20). These two initial steps are not required if sequencing is from DNA, and the former would be omitted if sequencing both RNA and DNA. Next, a random amplification may be performed (though not always) to increase the quantity of cDNA/DNA in the sample (Figure 1.20). Numerous methods have been described to achieve this, each of which carry their own potential source of bias (314). The SISPA (Sequence-Independent, Single-Primer Amplification) approach uses a primer with a defined sequence at the 5' end and a stretch of random nucleotides at the 3' end, to randomly amplify cDNA/DNA. Reported biases associated with the SISPA method are uneven distribution of sequencing reads across genomes, and poor representation of low abundance genomes (315). However, the method has been tested extensively on clinical samples and is well documented in recovering multiple pathogens: DNA and RNA viruses, bacteria, fungi, and parasites (316–323). Sequencing libraries, prepared from the randomly amplified cDNA/DNA, are then sequenced on the platform of choice (Figure 1.20).

A typical bioinformatics pipeline for analysing metagenomic data for the purpose of identifying microbial genomes uses the raw sequencing reads in a series of analysis steps (Figure 1.21). To start, data is optimised by filtering out poor-quality reads, trimming adaptor sequences, and removing host reads. Then identification of microbial genomes is achieved through a combination of taxonomic classification of individual reads, *de novo* read assembly, and alignment with reference genomes (Figure 1.21).

The metagenomic sequencing method chosen for this project focusses on identifying RNA viruses, which as previously explained, have a prominent role in EID. The method has previously been shown to be effective in identifying RNA viruses directly from clinical material (321,322,324,325), however as explained the detection of replicating DNA viruses and bacterial is still possible (though not optimal) because viral RNA intermediates and bacterial ribosomal RNA will be sequenced. An Illumina Miseq was chosen as the primary method of sequencing over the ONT MinION, because the lower error rate of the Illumina method is more desirable in the context of this project, and portability is not required.

The bioinformatics pipeline chosen starts with taxonomical classification of filtered and trimmed sequencing reads using Centrifuge (326). Virus classifications at species level exceeding 0.01% total reads were investigated further using mapping techniques. *De novo* assembly, an unbiased non-targeted analysis method, was performed using SPAdes (327). This generated contigs from which scaffolds were constructed. Scaffolds were analysed using Kaiju, which translates nucleotide sequence into amino acid sequence then compares this to a database of viral sequences using the Burrows-Wheeler transform, to assign a taxon to the query sequence (328). This assesses protein, not nucleotide homology, which is more sensitive for sequences that are divergent from the current known breadth of viral sequences. Mapping to relevant virus reference genomes was performed using BWA-MEM (329) to identify the number of reads mapping to a particular pathogen and determine genome coverage. Virus reference genomes were chosen to include: viruses previously tested for using RT-PCR assays (to identify any divergent strains that may not have been detected by the targeted assays),

viruses identified during taxonomic classification, *de novo* assembly and subsequent scaffold analysis.

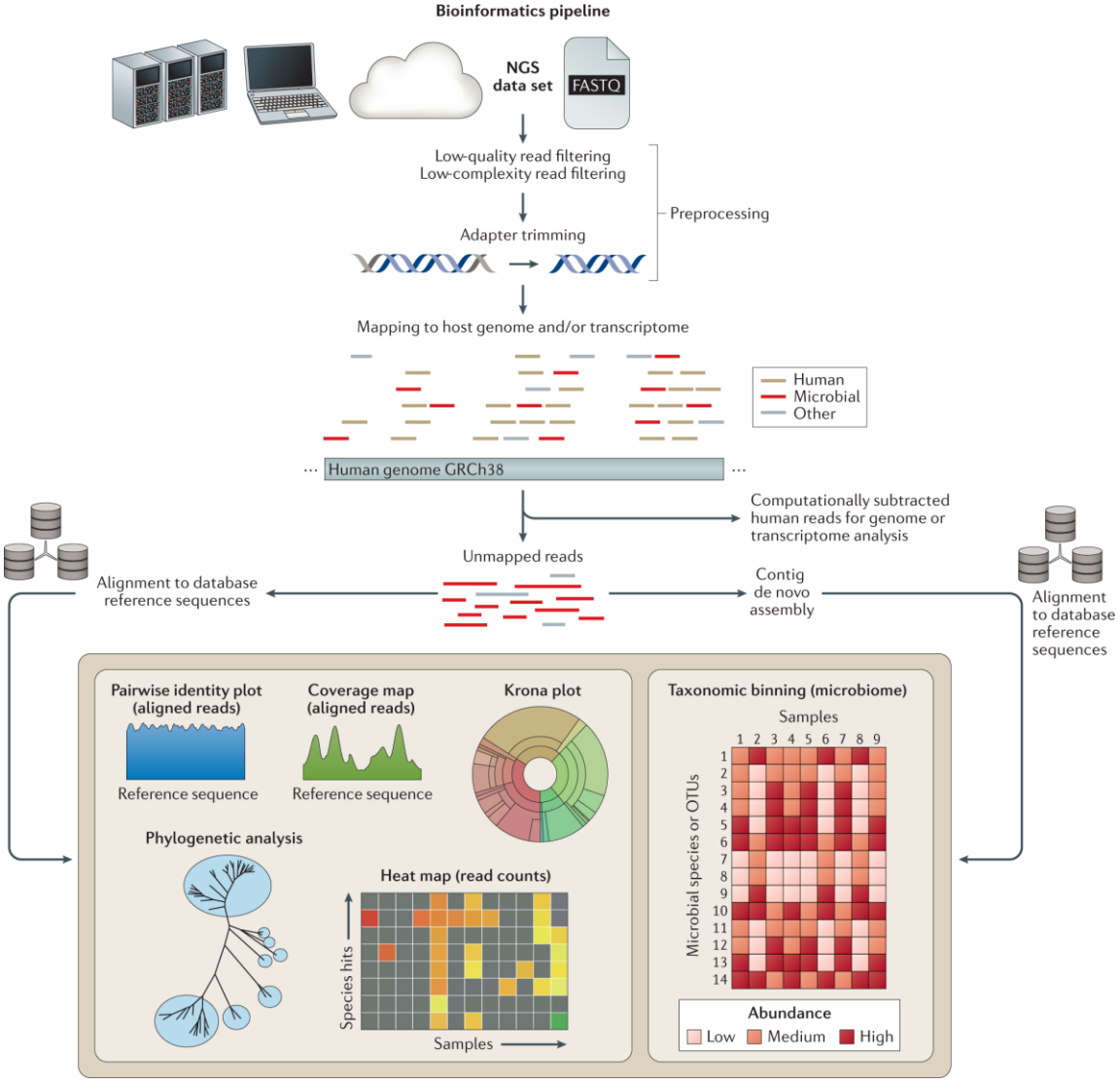

Figure 1.21 A typical NGS bioinformatics workflow. Reproduced from Chui and Miller (2019) (313).

1.3.5 APPLICATIONS OF METAGENOMIC SEQUENCING

1.3.5.1 CLINICAL DIAGNOSTICS

The application of metagenomic sequencing to the clinical diagnosis of infectious disease is an exciting prospect with many challenges. The first published clinical use of metagenomics was the detection of *Leptospira* in the CSF of a teenage boy with neurological symptoms, reported in 2014 (316). Leptospirosis was clinically suspected however PCR and culture tests were negative. The diagnostic PCR primers were found to poorly match the *Leptospira* genome (316). Since then, reports of using metagenomics to identify causative pathogens from patients with common presentations (330–332), as well as emerging viral infections (322), have demonstrated the potential of the approach. A recent study found that the majority of CHIKV and DENV-positive plasma samples contained quantities of viral RNA sufficient to generate significant portions of viral genomes using a metagenomic approach (321). Metagenomic pipelines for virus identification in AUFI patients have undergone development in recent years and show promise (322,333,334). Initial results from a study comparing conventional and metagenomic approaches to influenza virus detection in respiratory samples reported comparable specificity, but reduced sensitivity (335). This approach identified other viruses, demonstrating the potential of metagenomics for identifying co-infections, which could be missed using conventional approaches. Metagenomics has the added benefit of providing sequence information which can be used in epidemiology, transmission studies, vaccine efficacy studies and for informing public health advice (335). A validated metagenomic sequencing assay for

pathogen detection from clinical CSF samples was the first to successfully demonstrate proof-of-concept for diagnosis of infectious causes of meningitis and encephalitis (334).

Though results are promising, many challenges remain, including lower sensitivity than conventional tests and higher costs (14), which can make it less practical to use for large numbers of samples or in resource-limited settings. Although NGS is much more expensive than Sanger per sample, the potential for cost saving by using a single (metagenomic) test rather than multiple targeted diagnostic assays requiring separate reagents and instruments, coupled with decreasing sequencing costs, may make metagenomic sequencing attractive from a cost-perspective under the right circumstances.

The wide array of bioinformatics tools available means that reproducibility and standardisation can be difficult to achieve. Studies have demonstrated that the choice of bioinformatic algorithms can affect results when identifying the make-up of microbiota samples (336,337). The development of automatic 'user-friendly' bioinformatics pipelines are a step towards improving reproducibility and increasing suitability for clinical use (338). Metagenomic sequencing has traditionally taken more time than conventional molecular detection methods, however developments have led to sequencing library preparation and amplification methods which are easily completed in a matter of days or even hours (308).

1.3.5.2 VIRUS DISCOVERY

The pace at which novel viruses have been discovered has accelerated in recent years (Figure 1.22), thanks to the application of metagenomic sequencing. Unlike conventional

targeted PCR methods, *de novo* assembly of sequencing data enables identification of viruses that are novel or highly genetically divergent. This, in addition to the ability to sequence directly from a wide variety of clinical samples without requiring specific amplification, has proven to be invaluable in identifying causative agents in clinical cases. Furthermore, it has made large-scale studies of virus diversity within clinical, animal and environmental samples possible. Recent studies identified a staggering 184 novel vertebrate viruses (the majority of which belonged to the *Picobirnaviridae* family) from macaque faeces (339), and 1,445 from invertebrates (340). A novel bornavirus, originating from a squirrel, was identified as the cause of fatal encephalitis in three squirrel breeders (341), whilst a novel phlebovirus was identified in two men suffering from severe febrile illness after receiving tick bites in the state of Missouri, USA (342).

Whilst the discovery of such a large number of new viruses is exciting, further studies are required to understand the ecology of a novel virus, including its ability to cause disease in humans and to cross species barriers (14). In clinical cases, it is essential that findings are interpreted in a clinical context and confirmatory testing should be performed to demonstrate the causative role of the virus in the patient's illness.

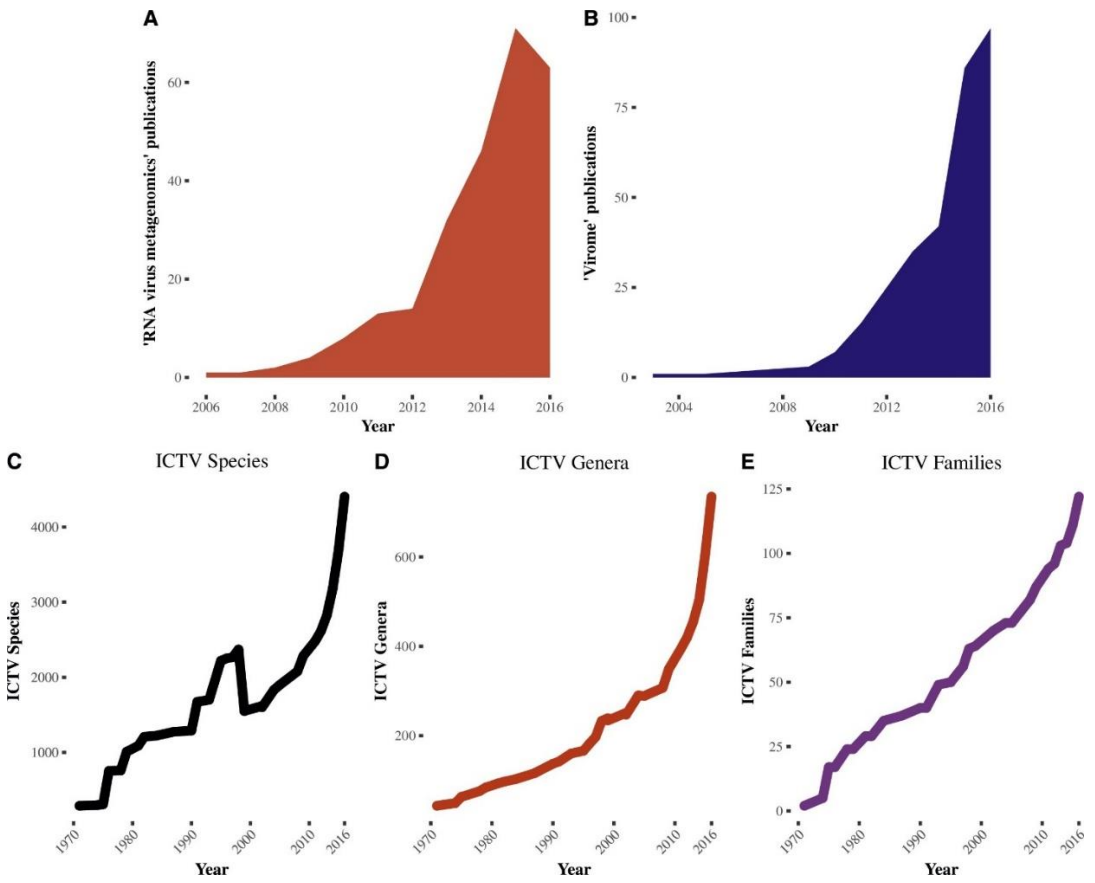

Figure 1.22 Publications by year for A) "RNA virus metagenomics" and B) "virome", from 2006-2016 using the "Results by Year" graph from Pubmed. C) number of viral species, D: genera, and E: families, assigned by the ICTV from 1970-2016. Reproduced from Greninger (2018) (308).

1.3.5.3 EID SURVEILLANCE AND OUTBREAK RESPONSE

NGS technology has recently reached a point at which rapid genomic surveillance can become part of the response to an outbreak of infectious disease. Conventionally, this response involves using epidemiological data gathered by interview-based contact tracing to understand transmission chains within an outbreak (311). Using pathogen genome sequencing to complement this approach overcomes limitations such as

incomplete case reporting, and provides data that can not only be used for epidemiological analyses and tracking the geographic and temporal spread of an outbreak, but also for monitoring virus evolution, identifying co-infections, and monitoring responses to vaccination or treatments (Figure 1.23) (311,343).

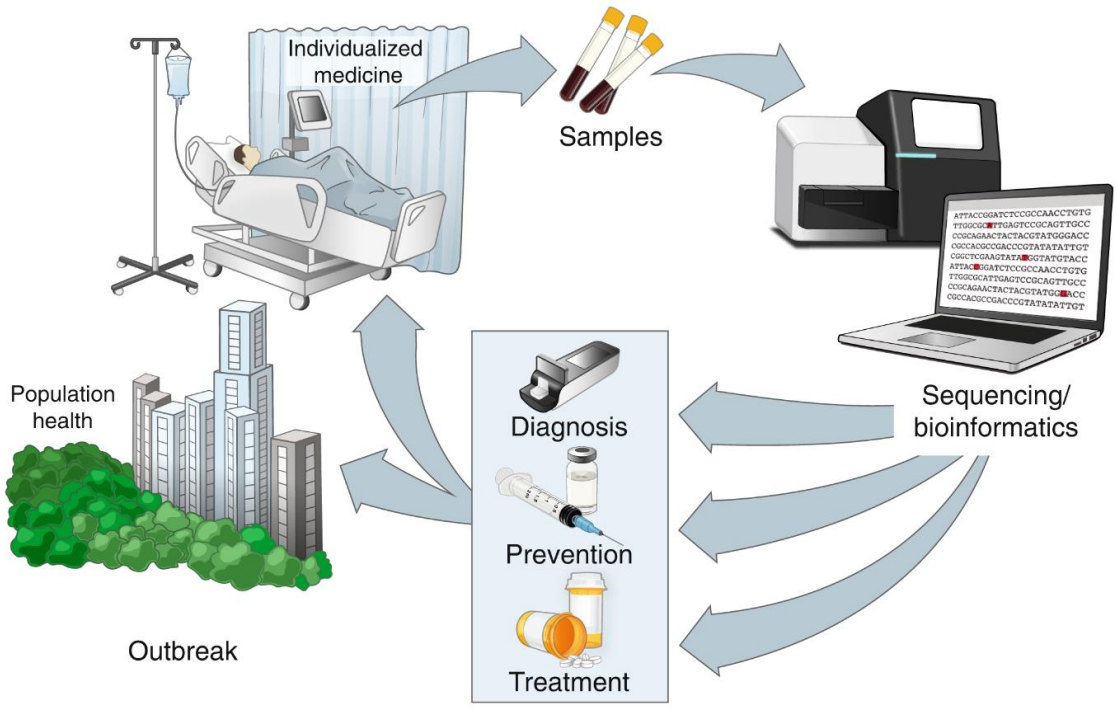

Figure 1.23 The application of pathogen genome sequencing for response to outbreaks of infectious disease. Reproduced from Ladner et al. 2019 (311).

The utility of this technology was exemplified during the West African EBOV outbreak, during which EBOV genome sequencing from Guinean patient samples, using an amplicon-based approach in conjunction with a MinION sequencer, mapped the genetic evolution of the virus from March 2014 to January 2015 and identified multiple virus lineages that had evolved from a single introduction in December 2013 (40). A similar

approach using samples from Sierra Leonean EBOV patients further demonstrated that real-time genome sequencing is possible during outbreaks in a resource-limited setting (343). Virus genome sequencing during the ZIKV outbreak in the Americas provided important data for epidemiological analyses. Two main ZIKV lineages exist, named 'African' and 'Asian'; the strain responsible for the outbreak in the Americas belonged to the Asian lineage, as did strains responsible for previous major ZIKV outbreaks in humans (344). Genome sequence analyses showed that during the Americas outbreak, the virus became more genetically diverse over time, due to the introduction into an immunologically naïve population (273). The implementation of cutting edge epidemiological and genomic surveillance during recent yellow fever outbreaks, including those in Angola and the DRC in 2015 and the largest Brazilian YFV outbreak for decades, detected late in 2016, has helped elucidate the demographic and ecological factors that contributed to the ongoing transmission of YFV (345,346). This real-time approach provides essential and timely information on virus transmission that can help public health authorities prioritise vaccination in relevant areas and demographics.

The unbiased nature of metagenomics is useful for monitoring viruses with high genetic diversity, such as LASV, which has previously proven difficult to detect using conventional targeted methods (347). Metagenomic sequencing of LASV genomes directly from clinical samples in Nigeria in 2018, during an unusually severe Lassa fever season with the largest upsurge of cases on record, allowed rapid phylogenetic analyses which informed the public health response whilst the outbreak was still ongoing (348). Analyses showed that the large number of cases were due to independent introductions from the rodent reservoir, rather than the evolution of a more virulent strain or increased human-to-human transmission (348).

Countries most at risk from EID events often have limited capability to respond to such events, frequently because of the financial and infrastructure constraints present in low- and middle-income countries (3). Laboratory capacity may be insufficient and using high-cost bench top sequencers is not an option. In this instance, the portability of the ONT MinION nanopore sequencing platform, in addition to the low start-up costs, makes it a very attractive option for sequencing under these circumstances. This makes the incorporation of metagenomic sequencing into diagnostic and surveillance protocols in countries at high risk of EID events much more realistic than it ever has been previously.

1.3.6 LIMITATIONS OF METAGENOMIC SEQUENCING

Sensitivity is the main limitation of metagenomics for virus detection. Viruses that typically show low viral loads in clinical samples are difficult to detect directly from clinical material with a high degree of confidence. These may require culturing prior to sequencing, or other confirmatory tests, if the virus is to be ruled out definitively (308). For example, genome sequencing was used extensively during the 2015 ZIKV outbreak in the Americas to better understand viral genetic diversity and transmission (42,349,350). Metagenomic sequencing was undertaken initially (349), however targeted approaches proved more useful due to the low amount of viral RNA present in clinical samples (42,349–351). For diagnostic purposes, RT-PCR assays frequently have a lower limit of detection than metagenomic sequencing, however, detection is reliant on the target site being well conserved throughout the viral population. In some cases, an effective strategy may be to use metagenomic sequencing to generate complete genomic sequence for a limited number of isolates, then design an RT-PCR based on the sequences for large scale screening.

The nature of the metagenomic sequencing method means that all nucleic acids present in a sample (RNA or DNA) are sequenced. This includes genetic material not just from the sample, but also any introduced during processing methods, for example contaminants within the laboratory, reagents, or sequencing instrument. Careful adherence to good practice in the molecular laboratory prior to sequencing is essential to minimise potential contaminants, and the addition of negative controls can help to minimise false-positive results (338). Data analysis and interpretation of results must be performed carefully and require a thorough understanding of the methodology and potential sources of contamination in order to accurately discriminate a pathogen from a contaminant.

1.4 PROJECT AIMS AND OBJECTIVES

1.4.1 RATIONALE AND ANTICIPATED OUTCOMES

As has been broadly introduced in this chapter, EIDs are an important cause of mortality and morbidity and place a large burden on global healthcare, despite medical and scientific advances in recent years (3). EIDs are most prevalent in areas that have drivers associated with disease emergence such as high biodiversity, and outbreaks are exacerbated by limited resources to respond (5,18). Numerous viruses have emerged to cause outbreaks in recent decades, including those transmitted by arthropod vectors including DENV, CHIKV and ZIKV, and rodent vectors including arenaviruses and hantaviruses. Zoonotic spillover events that lead to chains of human-to-human transmission, such as EBOV, are increasingly observed (5). Preventing and controlling outbreaks of viral disease is a complex and challenging task, requiring reliable infrastructure, sufficient and sustained funding, and co-ordination at both a national and international level.

At the time of the ZIKV outbreak in the Americas, the WHO made a number of recommendations for action as part of their 'Zika strategic response plan', in an effort to support national governments in controlling the outbreak (352). These recommendations are not exclusive to ZIKV and are relevant to many viral causes of EID. They include: 1) advancing research in prevention, surveillance and control of virus infection, 2) developing, strengthening and implementing integrated surveillance systems for virus infection, 3) strengthening the capacity of laboratories to test for virus infection, and 4) supporting global efforts to implement and monitor vector control strategies (352).

This project aims to support these actions by undertaking retrospective testing for viruses in two cohorts of patients from low and middle-income countries that have high biodiversity; Sierra Leone and Ecuador (353). The inclusion criteria for both cohorts were patients that presented voluntarily to a medical centre with fever. For Sierra Leonean patients, only those that tested negative for EBOV were included. Patients were sampled during the acute phase of their illness, during which many viruses are detectable in the blood due to viraemia, as discussed earlier in this chapter. This makes PCR/RT-PCR and sequencing appropriate methods to use with these samples, as opposed to serological detection of IgM antibodies, which are unlikely to have developed to a detectable level so early in the course of disease. Virus detection was carried out by combining a screening approach using a panel of PCR/RT-PCR assays for potential causative agents informed by geography, followed by metagenomic sequencing of a smaller subset of PCR/RT-PCR negative samples in an effort to detect novel, genetically divergent or unexpected viruses.

Additional anticipated outcomes from this project are:

- Support existing in-country laboratories by identifying circulating viruses and recommending additional assays to include in surveillance and diagnostic testing.
- Protect UK public health from imported infectious diseases by identifying pathogens that may be a risk to those returning from endemic countries.

- Enhance future surveillance efforts and collaborative research programmes by banking propagated, clinically significant viruses with national curated virus collections.

1.4.2 AIMS AND OBJECTIVES

The aims of the project are:

1. To establish if pathogenic viruses are present within the two study groups, focussing on RNA viruses.

2. To characterise viruses identified through whole genome sequencing and virus isolation.

3. To further investigate relevant virus(es) resulting from aims 1 and 2. Objectives will be based on the nature of the virus and relevant research questions stemming from it but will have a pathogenesis or immunological focus.

1.4.2.1 AIM 1 OBJECTIVES

- Perform testing for known pathogens on RNA extracted from patient plasma samples using a panel of RT-PCR and PCR assays (conventional and real-time).

- Use the RT-PCR/PCR results and sample metadata to identify a suitable subset of pathogen-negative samples for metagenomic sequencing, with the intention of detecting novel or unexpected pathogens.

- Perform unbiased metagenomic sequencing and subsequent data analysis to detect clinically important virus(es).

1.4.2.2 AIM 2 OBJECTIVES

- Isolate virus *in vitro* and generate stocks of purified, quantified virus.
- Generate complete, annotated viral genome sequences from cultured isolates using NGS, and make these publicly available via the online database GenBank.
- Compare viral genome sequences with other publicly available strains and perform relevant phylogenetic analyses.

1.4.2.3 AIM 3 OBJECTIVES

This set of objectives naturally evolved during the course of the project, based on the results from aims 1 and 2. The final objectives were:

- The focus of aim 3 became OROV pathogenesis, about which relatively little published literature exists and therefore performing fundamental research in this area would be valuable.
- Using cell lines from a range of different insects that may be relevant to OROV transmission, determine which insect-derived cell lines OROV replicates in.
- Identify human cell types that may be biologically relevant in natural infection and perform experiments to determine whether OROV is capable of replicating in these cells.

CHAPTER 2: MATERIALS AND METHODS

2.1 HUMAN PLASMA SAMPLES

2.1.1 SIERRA LEONEAN FEBRILE PATIENTS

Residual clinical samples and accompanying data were collected from patients following routine diagnostic testing in PHE-led laboratories during the EBOV outbreak in 2014-2015 in Sierra Leone. After the outbreak, samples and data were transferred to PHE laboratories in the UK for curation by PHE, forming the Sierra Leone Ministry of Health and Sanitation – PHE (MoHS-PHE) Ebola biobank (354). The MoHS in Sierra Leone retain ownership of the samples and data. The MoHS-PHE Ebola Biobank Governance Group is an independent group established to ensure the effective use of the biobank and co-ordinate access to samples and data for researchers.

One hundred and twenty plasma samples from the MoHS-PHE Ebola biobank were allocated for use in this project (Table 2.1) following ethical approval from the MoHS-PHE Ebola Biobank Governance Group, the Sierra Leone Ethics and Scientific Review Committee and the PHE Research Ethics and Governance Group (ref: R&D 270). Whole blood samples were obtained during 2014-2015 from patients presenting at an Ebola treatment centre (ETC) with a PHE-run EVD diagnostic laboratory on-site. All patients showed symptoms consistent with EVD. At the time of sampling, plasma was removed from centrifuged whole blood in ethylene diamine tetraacetic acid (EDTA), RNA was extracted and EBOV real-time reverse transcription PCR (qRT-PCR) performed using either the RealStar Zaire Ebolavirus qRT-PCR Kit 1.0 (Altona Diagnostics, UK) or a Zaire-specific qRT-PCR based on that published by Trombley *et al.* (355). Whole blood was also tested for *Plasmodium* using a rapid device test (RDT, BinaxNOW or SD Bioline Malaria Ag P.f. RDT, Abbott, UK). All patient samples included in this study tested negative for

EBOV at the time of sampling. Following testing, plasma was frozen and shipped to PHE for inclusion in the MoHS-PHE Ebola Biobank. Where available, the following metadata was provided with the samples (Appendix 1): Sierra Leone ID number, patient ID number (redacted from Appendix 1 to maintain patient confidentiality), laboratory of origin, sample type, specimen date, EBOV qRT-PCR result, *Plasmodium* RDT result, sample status (new/repeat/follow-up), patient age, patient district, patient chiefdom. Samples were allocated new ID numbers upon receipt ('PHE ID', Appendix 1).

Ebola treatment centre (ETC) location	Plasmodium negative	Plasmodium positive
Makeni	36	4
Port Loko	36	4
Kerry Town	36	4
Total:	108	12

Table 2.1 Laboratory origin and *Plasmodium* status of febrile patient samples from Sierra Leone. 90% of requested samples were *Plasmodium* negative to optimise the sample set for virus discovery, 10% were *Plasmodium* positive to identify co-infections.

2.1.2 ECUADORIAN FEBRILE PATIENTS

Plasma were obtained from whole blood samples taken from patients at Delphina Torres de Concha Hospital, Esmeraldas province, Ecuador in 2016 (*n*=196, Appendix 2) and 2017 (*n*=62, Appendix 3). These patients attended the hospital voluntarily and submitted their blood for routine DENV and ZIKV testing. Where possible, metadata was

collected with the samples: patient age, sex, patient location, number of days of fever, other clinical signs and symptoms. The use of patient samples in this project was approved by the bioethics committee of Universidad San Francisco de Quito (USFQ), Ecuador. This work was performed as part of a collaboration between PHE, USFQ and Delphina Torres de Concha Hospital.

2.2 CHEMICALS AND REAGENTS

Unless stated otherwise, all chemical/reagents were purchased from ThermoFisher Scientific, UK. Purification of PCR products was undertaken using a 2:1 ratio of Agencourt AMPure XP beads (Beckman Coulter, UK). RNA and DNA quantifications were performed using the Qubit RNA broad spectrum kit and Qubit dsDNA high sensitivity kit (Thermofisher Scientific, UK), respectively. Primers and probes were ordered from Integrated DNA Technologies, UK.

2.3 RNA EXTRACTION FROM PATIENT PLASMA SAMPLES

Plasma samples were inactivated using AVL buffer (Qiagen, UK) and ethanol and RNA was extracted using the QIAamp Viral RNA mini kit (Qiagen, UK). 140 µl plasma was added to 560 µl AVL buffer containing 5.6 µl linear polyacrylamide (LPA, Sigma-Aldrich, UK), and 24 µl MS2 bacteriophage (1.45e+5 plaque forming units) to act as an internal control. The mixture was incubated for 10 minutes at room temperature, then 560 µl of ethanol was added prior to a second 10-minute incubation at room temperature to complete the chemical virus inactivation process. Total sample was transferred to a spin column and wash steps performed in accordance with the manufacturer's instructions.

RNA was eluted from the spin column membrane in 175 µl nuclease-free water (Life Technologies, UK) and stored at -80°C. A negative extract control (nuclease-free water) was included in every batch of RNA extractions to act as a quality control for cross-contamination.

Plasma samples from Sierra Leone were stored and manipulated under containment level (CL) 4 conditions because of the risk of the presence of advisory committee on dangerous pathogens (ACDP) hazard group (HG) 4 pathogens. Due to the training and safety controls necessary to work in this environment, the initial chemical inactivation step was carried out by experienced CL4-trained staff. Once in AVL buffer, the samples were handled at CL3 for the subsequent ethanol inactivation step.

2.4 RT-PCR/PCR ASSAYS FOR PATHOGEN DETECTION

RNA was tested for pathogens known to cause acute fever, using real-time and conventional RT-PCR and PCR assays developed or optimised at PHE (Table 2.2). These assays form part of the PCR testing protocol used by the Rare and Imported Pathogen Laboratories (RIPL) to diagnose infection in returning UK travellers. As such, assay conditions and platforms were set to conform with those validated by RIPL.

RNA from Sierra Leonean patient samples was screened for CHIKV, DENV serotypes 1-4, EBOV, RVFV, YFV, ZIKV, *Leptospira*, *Rickettsia* and internal control MS2 bacteriophage using qRT-PCR assays. LASV and *Plasmodium* were tested for using conventional RT-PCR assays followed by agarose gel electrophoresis. For EBOV detection, two assays were used, the Zaire-specific assay adapted from Trombley *et al.* (2010) (355), used in the PHE-run field laboratories, and a pan-EBOV assay based on that described by Panning *et*

al. (2007) (356). This was because the Zaire-specific assay has better sensitivity for Zaire EBOV (the species responsible for the West Africa EBOV outbreak), and the pan-EBOV assay is capable of detecting non-Zaire EBOV species. RNA from Ecuadorian patient samples was tested using the same assays as described for Sierra Leone, except for EBOV, LASV and RVFV because they are not known to circulate in the Americas. MAYV was also tested for because it is known to circulate in South America. Details of each assay follow, grouped by the commercial kit used. For all assays, a standardised volume of RNA (5 µl) was used as template.

Pathogen	Target	Type of assay	Kit used	Positive control	Forward primer(s) sequence (5' – 3')	Reverse primer(s) sequence (5' – 3')	Probe(s) sequence (5' – 3')	Reference
CCHFV	NP gene	qRT-PCR	SSIII	pVHF array mix	CCTTTTTGAACTCTTCAAACC	TCTCAAAGAAACACGTGCC	FAM-ACTCAAGGKAACACTGTGGGCGTAAG-BHQ1 NFQ	PHE in-house assay
CHIKV	E1 gene	qRT-PCR	SSIII	NCPV CHIKV RNA	TCGACGCGCCCTCTTTAA	ATCGAATGCACCGCACACT	FAM-ACCAGCCTGCACCCATTCCTCAGAC-BHQ1	Edwards 2007 (357)
DENV serotypes 1-3	3' non-coding region	qRT-PCR	SSIII	pVHF array mix	GGATAGACCAGAGATCCTGCTGT	CATTCCATTTTCTGGCGTTC	FAM-CAGCATCATTCCAGGCACAG-BHQ1	Drosten 2002 (358)
DENV serotype 4	3' non-coding region	qRT-PCR	SSIII	NCPV DENV-4 RNA	GGATAGACCAGAGATCCTGCTGT	CAATCCATCTTGCGGCGCTC	FAM-CAGCATCATTCCAGGCACAG-BHQ1	Drosten 2002 (358)
LASV	GPC gene	RT-PCR	QOS	LASV RNA strain GA391 (S55/9)	ACCGGGGATCCTAGGCATTT	GTTCTTTGTGCAGGAMA	n/a	Oschläger 2010 (359)

						GGGGCATKG TCAT		
Leptospira spp.	16s rRNA	qPCR	Takyon	*Leptospira* DNA plasmid	GATCGGTAR CCGGCCT (F1) CGATCAGTA RCCGGCCT (F2)	CCATTGAGC AAGATTCTT AA	FAM-AGAGGGTGT TCGGCCACA ATG-BHQ1 (Path) JOE-AGAGGGTGT CCGGCCACA AT-BHQ1 (Inter) Cy5-AGAGGGTG AACGGCCAC AATG-BHQ2 (Enviro)	PHE in-house assay
MAYV	E1 gene	qRT-PCR	SSIII	NCPV MAYV RNA	CATGGCCTA CCTGTGGGA TAATA	GCACTCCCG ACGCTCACT G	FAM-TCGGGCGCA ACATGTAGT CAGGATAA-BHQ1	Powers 2010 (360)
OROV	N gene	qRT-PCR	SSIII	NCPV OROV RNA	CATTTGAAG CTAGATACG GACAA	CATCTTTGG CCTTCTTTTR G*	FAM-CAATGCTGG TGTTGTTAG	Weidmann 2003 (361)

							AGTCTTCTTC CT-BHQ1	
Pan-EBOV	L gene	qRT-PCR	Fast virus	pVHF array mix	AAGCMTTTC CHAGCAAYA TGATGGT	ATGHGGTG GATTATAAT AATCACTDA CATG	FAM-CCRAAATCA TCACTBGTRT GGTGCCA-MGB	Panning 2007 (356)
Plasmodium spp.	18s rRNA	RT-PCR	QOS	pVHF array mix	AGTTACGAT TAATAGGAG TAG	CCAAAGACT TTGATTTCTC AT	n/a	Ciceron 1999 (362)
Rickettsia spp.	Citrate synthase gene	qRT-PCR	SSIII	Rickettsia RNA with polyA carrier RNA	TCGCAAATG TTCACGGTA CTTT	TCGTGCATT TCTTTCCATT GTG	FAM TGCAATAGC AAGAACCGT AGGCTGGAT G BHQ1	Stenos 2005 (363), Paris 2008 (364)
RVFV	G2 gene	qRT-PCR	SSIII	RVFV RNA with polyA carrier RNA	GGATAGGCC GTCCATGGT AGT	GGACATGCC AGGCGYTGG T	FAM-CCAGTGACA GGAAGCCAC TCACTCAAG A-BHQ1	Drosten 2002 (358)
YFV	5’ non-coding region	qRT-PCR	SSIII	YFV RNA with polyA carrier RNA	AATCGAGTT GCTAGGCAA TAAACAC	TCCCTGAGC TTTACGACC AGA	FAM ATCGTTCGT TGAGCGATT AGCAG BHQ1	Drosten 2002 (358)

Zaire EBOV	NP gene	qRT-PCR	Fast virus	pVHF array mix	TCTGACATG GATTACCAC AAGATC	GGATGACTC TTTGCCGAA CAATC	FAM-AGGTCTGTC CGTTCAA-MGB	Trombley 2010 (355)
ZIKV	NS1 gene	qRT-PCR	Fast virus	NCPV ZIKV RNA	TGCACAATG CCCCCACTRT	TGGGCCTTA TCTCCATTCC A	FAM TTCCGGGCT AAAGATGGC TGTTGGT BHQ1 (Probe 1) FAM TTTCGAGCA AAAGACGGC TGCTGGT BHQ1 (Probe 2)	Pyke 2014 (365)

Table 2.2 Pathogen specific RT-PCR/PCR tests used in this study. SSIII = SuperScript III Platinum One-Step qRT-PCR kit (Invitrogen, UK). Takyon = Takyon Low ROX Probe 2X MasterMix dTTP blue (Eurogentec, Belgium), QOS = Qiagen One-Step RT-PCR kit (Qiagen, UK), Fast virus = TaqMan Fast virus 1-step master mix. FAM = 6-carboxyfluorescein, BHQ1 = Black Hole Quencher 1, MGB = Minor Groove Binder. *Primer designed during this study. NCPV = National Collection of Pathogenic Viruses. pVHF = pan-viral haemorrhagic fever.

2.4.1 SUPERSCRIPT III PLATINUM ONE-STEP QRT-PCR KIT

2.4.1.1 DROSTEN QRT-PCR ASSAY

Primer/probe mixes for each target were made in advance and frozen at -20^{o}C for subsequent use. Details of primer/probe mix formulations are provided in Table 2.3.

Assay target	Component	Final concentration	Volume for 100 reactions (µL)
CHIKV	Water	N/A	221.5
	2x reaction mix	1 x	1000
	$MgSO_4$ (50mM)	3.75 mM	150
	CHIK_E1 F (100µM)	900 nM	18
	CHIK_E1 R (100µM)	900 nM	18
	CHIK E1 P (100µM)	625 nM	12.5
DENV1-3	Water	N/A	104
	2x reaction mix	1 x	1000
	$MgSO_4$ (50mM)	6.25 mM	250
	Den Dros F (100µM)	300 nM	6
	Den Dros R1 (100µM)	900 nM	18
	Den Dros P (100µM)	500 nM	10
	MS2 F1 (10µM)	40 nM	8
	MS2 R1 (10µM)	40 nM	8
	MS2 Taq Cy5 (10µM)	80 nM	16
DENV4	Water	N/A	141
	2x reaction mix	1 x	1000

	$MgSO_4$ (50mM)	6.25 mM	250
	Den Dros F (10µM)	50 nM	10
	Den Dros R2 (100µM)	450 nM	9
	Den Dros P (100µM)	500 nM	10
MAYV	Water	N/A	344
	2x reaction mix	1 x	1000
	MAYARO 9666 (100µM)	900 nM	18
	MAYARO 9797 (100µM)	900 nM	18
	MAYARO 9734 FAM (10µM)	200 nM	40
Rickettsia	Water	N/A	381
	2x reaction mix	1 x	1000
	CS F (100µM)	900 nM	18
	CS R (100µM)	450 nM	9
	CS P (100µM)	600 nM	12
RVFV	Water	N/A	221.5
	2x reaction mix	1 x	1000
	$MgS0_4$ (50mM)	3.75 mM	150
	RVFNF (100µM)	900 nM	18
	RVFNR (100µM)	900 nM	18
	RVFNP (100µM)	625 nM	12.5
YFV	Water	N/A	170
	2x reaction mix	1 x	1000
	$MgSO_4$ (50mM)	5 mM	200

	TM YF FWD (100µM)	250 nM	5
	TM YF REV (100µM)	250 nM	5
	TM YF PRB (10µM)	200 nM	40

Table 2.3 Primer/probe mix formulations for Drosten qRT-PCR assay targets. $MgS0_4$ = magnesium sulphate.

Immediately prior to testing, primer/probe mixes were thawed and combined with platinum taq enzyme to make a mastermix for each target (Table 2.4).

Component	Volume for 1 reaction (µL)
Primer/probe mix	14.2
Platinum taq	0.8

Table 2.4 Mastermix formulation for Drosten qRT-PCR assay targets.

15 µl mastermix was aliquoted into each well in a 96-well PCR plate prior to the addition of 5 µl sample RNA, or positive/negative control per well. The reactions were performed on a LightCycler® 480 instrument (Roche, UK), using the 'Drosten with MS2' cycling conditions (Table 2.5).

Step	Analysis mode	Temp. (°C)	Time (M:S)	Acquisition mode	Cycles	Rate (°C/s)
Reverse Transcription	None	45	10:00	None	1	20
Denature	None	95	05:00	None	1	20
Amplify	Quantification	95	0:05	None	45	20
		57	0:35	Single		20
Cooling	None	40	0:30	None	1	20

Table 2.5 'Drosten with MS2' qRT-PCR cycling conditions.

2.4.2 TAQMAN FAST VIRUS 1-STEP MASTER MIX

Primer/probe mixes were made in advance and frozen at -20°C for subsequent use.

Details of primer/probe mix formulations are provided in Table 2.6.

Target	Component	Final concentration	Volume for 100 reactions (µL)
CCHFV	Water	n/a	59
	CCHF S122F	900	18
	CCHF S1R	900	18
	CCHF probe	250	5
Pan-EBOV	Water	n/a	59
	FiloA_Ebola	900	18

	FiloB_Ebola	900	18
	FAMEBO_DEGEN	250	5
Zaire EBOV + MS2	Water	n/a	27
	F565 Zaire	900	18
	R6405 Zaire	900	18
	P597S Zaire	250	5
	MS2 F1	40	8
	MS2 Rev	40	8
	MS2 Taq Cy5	80	16
ZIKV + MS2	Water	n/a	922
	Zika NS1 Fwd	900	18
	Zika NS1 Rev	900	18
	Zika NS1 Probe 1	250	5
	Zika NS1 Probe 2	250	5
	MS2 F1	40	8
	MS2 Rev	40	8
	MS2 TAQ Probe	80	16

Table 2.6 Primer/probe mix formulations for ABi fast-mix qRT-PCR assay targets.

Immediately prior to testing, primer/probe mixes were thawed and combined with 4x reaction mix to make a mastermix for each target (Table 2.7 and Table 2.8).

Component	Volume for 1 reaction (µL)
Water	9
4x reaction mix	5
Primer/probe mix	1

Table 2.7 Mastermix formulation for CCHFV and EBOV qRT-PCR assay targets.

Component	Volume for 1 reaction (µL)
4x reaction mix	5
Primer/probe mix	10

Table 2.8 Mastermix formulation for ZIKV qRT-PCR assay.

15 µl mastermix was aliquoted into each well in a 96-well PCR plate prior to the addition of 5 µl sample RNA, or positive/negative control per well. The reactions were performed on a 7500 or Viaa7 Real-Time PCR System (both Applied Biosciences, UK), using the 'Fast virus' cycling conditions (Table 2.9).

Step	Analysis mode	Temp (°C)	Time (M:S)	Acquisition mode	Cycles
Reverse Transcription	None	50	05:00	None	1
Denature	None	95	00:20	None	1
Amplify	Quantification	95	0:03	None	40
		60	0:30	Single	

Table 2.9 'Fast virus' qRT-PCR cycling conditions.

2.4.3 QIAGEN ONE-STEP RT-PCR KIT

2.4.3.1 PLASMODIUM RT-PCR

Plasmodium primer mix was made in advance and frozen at -20^{o}C for future use (Table 2.10).

Component	Final concentration	Volume for 100 reactions (µL)
Water	N/A	1270
5x RT-PCR Buffer	1x	500
dNTPS (10mM)	400 µM	100
Primer 'Mal F' (100 µM)	600 nM	15
Primer 'Mal R' (100 µM)	600 nM	15

Table 2.10 Primer mix formulation for *Plasmodium* RT-PCR assay.

Immediately prior to testing, primer mix was thawed and combined with the enzyme mix to make a mastermix (Table 2.11).

Component	Volume for 1 reaction (µL)
Primer mix	19
Enzyme mix	1

Table 2.11 Mastermix formulation for *Plasmodium* RT-PCR assay.

20 µl mastermix was aliquoted into 0.2 mL PCR tubes prior to the addition of 5 µl sample RNA, or positive/negative control per well. The reactions were performed on a GeneAmp 9700 thermocycler (Applied Biosystems, UK) using the '*Plasmodium*' cycling conditions (Table 2.12).

Step	Temp. (°C)	Time (M:S)	Cycles
Reverse Transcription	50	30:00	1
Denature	95	15:00	1
Amplify	95 54 72	0:30 0:30 1:00	40
Hold	72	5:00	1
Holding temp.	4	Indefinitely	n/a

Table 2.12 '*Plasmodium*' cycling conditions.

PCR products were visualised using gel electrophoresis (see section 2.5). The presence of a 291 bp product indicated a positive result.

2.4.3.2 LASV RT-PCR

LASV primer mix was made in advance and frozen at -20°C for subsequent use (Table 2.13)

Component	Final concentration	Volume for 100 reactions (µL)
Water	N/A	770
5x RT-PCR Buffer	1x	500
Q solution	1x	500
dNTPs (10mM)	400 µM	100
Primer Lassa 1 (36E2) (100 µM)	600 nM	15
Primer LVS-339-rev (100 µM)	600 nM	15

Table 2.13 Primer mix formulation for LASV RT-PCR assay.

Immediately prior to testing, primer mix was thawed and combined with the enzyme mix to make a mastermix (Table 2.14).

Component	Volume for 1 reaction (µL)
Primer mix	19
Enzyme mix	1

Table 2.14 Mastermix formulation for LASV RT-PCR assay.

20 µl mastermix was aliquoted into 0.2 mL PCR tubes prior to the addition of 5 µl sample RNA, or positive/negative control per well. The reactions were performed on a GeneAmp 9700 thermocycler (Applied Biosystems, UK) using the 'Lassa RT-PCR' cycling conditions (Table 2.15).

Step	Temp. (°C)	Time (M:S)	Cycles
Reverse Transcription	50	30:00	1 cycle
Denature	95	15:00	1 cycle
Amplify	95	00:30	45 cycles
	52	00:30	
	72	00:30	
Hold	4	Hold	1 cycle

Table 2.15 'Lassa RT-PCR' cycling conditions.

PCR products were visualised using gel electrophoresis (see section 2.5). The presence of a 340 bp product indicated a positive result.

2.4.4 TAKYON LOW ROX PROBE 2X MASTERMIX DTTP BLUE

Leptospira primer/probe mix was made in advance and frozen at -20^{o}C for subsequent use (Table 2.16).

Component	Volume for 100 reactions (µL)
LeptoF1 (forward) 100 µM	10
LeptoF2 (forward) 100 µM	10
LeptoR (reverse) 100 µM	10
Pathprobe (probe) 100 µM	2.5
Interprobe (probe) 100 µM	2.5
Enviroprobe (probe) 100 µM	2.5
Water	712.5

Table 2.16 Primer/probe mix formulation for *Leptospira* qRT-PCR assay.

Immediately prior to testing, primer/probe mix was thawed and combined with the enzyme mix to make a mastermix (Table 2.17).

Component	Volume for 1 reaction (µL)
Primer/probe mix	7.5
Takyon™ 2x master mix	12.5

Table 2.17 Mastermix formulation for *Leptospira* qRT-PCR assay.

20 µl mastermix was aliquoted into each well in a 96-well PCR plate prior to the addition of 5 µl sample RNA, or positive/negative control per well. The reactions were performed on a 7500 or Viaa7 Real-Time PCR System (both Applied Biosciences, UK), using the '*Leptospira*' cycling conditions (Table 2.18).

Step	Analysis mode	Temp. (°C)	Time (M:S)	Acquisition mode	Cycles	Rate (°C/s)
Denature	None	95	05:00	None	1	20
Amplify	Quantification	95	00:03	None	50	20
		60	00:30	Single		20
		72	00:10			20

Table 2.18 '*Leptospira*' qPCR cycling conditions.

2.4.5 INTERPRETATION OF QRT-PCR RESULTS

The qRT-PCR assays used in this study use a cut-off cycle quantification (Cq) value of 40, any value equal to or higher than this represents a negative result. A Cq value of <35 with an amplification plot showing a sigmoidal shaped amplification curve is considered positive. Cq values of 35 – 39.9 indicate a borderline result and are repeated in duplicate. The cut-off values were determined prior to this project using standardised validation protocols developed by RIPL at PHE Porton Down.

For samples with an initial borderline result, a repeat Cq of 35 – 39.9 (in duplicate) was considered positive, a repeat Cq of >40 was considered negative. The result was called inconclusive if, following the repeat test in duplicate, the sample showed a Cq value of

<40 for one replicate and no Cq for the other replicate. A sample was considered positive by conventional RT-PCR if a visible band of the correct size was present on the gel. Positive controls (Table 2.2) and negative controls (nuclease-free water) were included in every assay run. Negative extraction controls for each batch of RNA extractions were tested using all RT-PCR assays, to control for contamination at the extraction stage. A qRT-PCR assay targeting the internal control MS2 was performed to control for ineffective RNA extraction.

2.5 GEL ELECTROPHORESIS

PCR products were visualised on a 2% agarose gel stained with 1 µg/mL ethidium bromide (Sigma-Aldrich, UK), a DNA chelating agent that fluoresces under UV light. Amplicons were separated using 110 volts for 40 minutes and run alongside a 100 base pair (bp) DNA ladder (New England Biolabs, UK), then visualised under UV light using a transilluminator and GeneSys software (Syngene, UK).

2.6 ANTI-CHIKV, -DENV AND -ZIKV IGM ELISA

Plasma samples that had a CHIKV, DENV or ZIKV qRT-PCR Cq value of 35 – 40 were tested in triplicate for IgM antibodies against the virus in question, using commercial capture ELISAs to detect serological evidence of recent infection.

DENV IgM antibodies were detected using the dengue IgM capture ELISA (Abbott Rapid Diagnostics, UK), CHIKV and ZIKV IgM antibodies were detected using the anti-CHIKV and anti-ZIKV IgM ELISA (Euroimmun, UK), respectively. Assays were performed in accordance with manufacturer's instructions, except for the substrates which were

substituted for Super AquaBlue substrate. The kit substrates required an acidic stop solution which was incompatible with sodium hypochlorite, the decontamination agent used in the containment level 3 laboratory. Absorbance was measured at 405 nm using a Multiskan FC microplate photometer and interpretation carried out according to manufacturer's instructions.

2.7 OROV QRT-PCR DEVELOPMENT

2.7.1 PRIMER ALIGNMENTS

Primer and probe sequences were aligned with a set of 149 OROV N gene coding sequences from the Genbank nucleotide database (https://www.ncbi.nlm.nih.gov/genbank/), using the ClustalW algorithm in the MEGA7 software package. Sequences represented the geographic (Brazil, Panama, Peru and Trinidad and Tobago) and temporal diversity of OROV isolates from the 1950s to present day (363).

2.7.2 ASSAY OPTIMISATION AND VALIDATION

Primer concentrations were tested in multiple combinations at 1 µM, 3 µM, 9 µM and 18 µM. Probe concentrations were tested from 5 µM to 25 µM. Magnesium sulphate ($MgSO_4$) concentration was optimised by adding additional $MgSO_4$ to the reaction mix, from none added to a maximum concentration of 85 mM. Optimal concentrations were considered those that gave the lowest Cq value across the range of values tested, using RNA from strain OROV/EC/Esmeraldas/087/2016 as template.

Unless a substantial improvement in sensitivity was demonstrated (>2 Cq values), primer/probe/$MgSO_4$ conditions were set to comply with those standardised by RIPL. This ensured that the OROV assay could be easily incorporated into the RIPL test protocol for returning UK travellers. Cross-reactivity to 23 non-target virus species and a panel of negative human sera was also assessed. A cross-reaction was considered present if a Cq value of <40 was observed.

2.7.3 QRT-PCR LIMIT OF DETECTION ANALYSIS

Absolute quantitation of RNA copy number was calculated from a standard curve of serially diluted OROV S segment RNA, transcribed using the Megascript kit (Ambion, UK). A 711 bp region of the S segment, encompassing the N and Ns open reading frames (ORF), was amplified from strain OROV/EC/Esmeraldas/087/2016 cDNA using primers incorporating a T7 promoter sequence (forward primer sequence 5’ GTC AGA GTT CAT TTT CAA CGA TGT ACC ACA ACG G 3’, reverse primer sequence 5’ GAA ATT AAT ACG ACT CAC TAT AGG G CTC CAC TAT ATG TC 3’). RNA was quantified then purity confirmed using the RNA 6000 pico kit on a bioanalyzer (Agilent, UK). RNA copy number was calculated by first estimating the formula weight of the RNA standard using the product of the strand length (711 bases) and the average formula weight of RNA (assuming the average mass of an RNA nucleotide is 340 Daltons). The inverse of the formula weight is the number of moles of template present in one gram of material. The number of molecules of the RNA standard per gram was calculated using Avogadro's number (6.022e+23 molecules/mole) in the following equation:

$$\text{Number of copies} = \frac{\text{amount} * 6.022\text{x}10^{23}}{\text{length} * 1\text{x}10^{9} * 340}$$

The number of copies of RNA standard in the sample (Table 2.19) was estimated by multiplying by 1.0e+9 to convert to ng, then multiplying by the amount of RNA standard (in ng). A ten-fold serial dilution of RNA standard representing a range of concentrations from 1 copy to 1.0e+8 copies was tested using the optimised, validated qRT-PCR assay. Each data point on the standard curve was plotted using the mean Cq value from three separate experiments.

	OROV RNA standard
Strand length	711
M_r (g/mol)	228034.5
RNA conc. (ng/ul)	3240
Number of RNA copies/ul	8.1e+12

Table 2.19 RNA standard copy number, calculated from strand length, molecular weight and RNA concentration. M_r (molecular weight) was calculated using the formula: molecular weight of ssRNA = (# nucleotides x 320.5) + 159.

2.7.4 OROV QRT-PCR ASSAY CONDITIONS

The assay was modified from an assay developed by Weidmann *et al.* (2003) (361) that targets the OROV S segment (Table 2.20). The assay uses the Superscript III Platinum One-step quantitative RT-PCR kit (SSIII, Table 2.21) and was run on a 7500 Real-Time PCR System (Applied Biosystems, UK), using the cycling conditions detailed in Table 2.22.

Primer name	Reference	Sequence (5’ – 3’)
ORO F	Weidmann *et al.* (361)	CAT TTG AAG CTA GAT ACG GAC AA
OROV Ec2 R	This study	CAT CTT TGG CCT TCT TTT RG
ORO P	Weidmann *et al.* (361)	6FAM CAA TGC TGG TGT TGT TAG AGT CTT CTT CCT BHQ1

Table 2.20 Primers and probe used in the optimised OROV qRT-PCR assay (6FAM = 6-carboxyfluorescein, BHQ1 = black hole quencher 1).

Component Name	Stock concentration	Volume for 1 reaction (µl)
Water	n/a	1.7
2X Reaction mix	2x	10.0
ORO F	18µM	1.0
OROV EcR2	18µM	1.0
ORO P	25µM	0.5
SS III RT/Taq enzyme mix	n/a	0.8
Template	n/a	5.0

Table 2.21 Reaction formulation for the OROV qRT-PCR assay, using the Superscript III Platinum One-step quantitative RT-PCR kit.

Step name	Analysis mode	Temp. (°C)	Time (M:S)	Acquisition mode	Cycles	Rate (°C/sec)
RT	None	50	10:00	None	1	20
Denature	None	95	02:00	None	1	20
Amplify	Quantification	95	0:10	None	45	20
		60	0:40	Single		20
Cooling	None	40	0:30	None	1	20

Table 2.22 Cycling conditions used in the OROV qRT-PCR.

2.8 PREPARATION OF CDNA FOR METAGENOMIC SEQUENCING

RNA was treated with Turbo DNAse to remove DNA, then purified using the Zymo RNA clean & concentrator -5 kit (Cambridge Bioscience, UK). Sequence-independent single-primer amplification (SISPA) was performed as follows (321): first-strand cDNA was synthesised by annealing 1 µl Sol-primer A (40 pmol/µl, 5' GTT TCC CAC TGG AGG ATA NNN NNN NNN 3') to 4 µl template RNA at 65°C for 5 minutes. This was followed by a reverse transcription (RT) reaction using the total volume of the previous reaction plus 0.5 µl SuperScript™ III reverse transcriptase, 2 µl 5x first strand buffer, 1 µl dNTPs (10 µM) and 1 µl nuclease-free water at 42°C for 60 minutes. First-strand cDNA was converted to double stranded DNA by incubating the total volume of cDNA at 37°C for 8 minutes in a reaction with 0.15 µl Sequenase Version 2.0 DNA polymerase (Fisher Scientific, UK), 1 µl 5x reaction buffer and 3.85 µl nuclease-free water. This was followed by a further incubation at 37°C for 8 minutes after the addition of 0.15 µl Sequenase DNA polymerase and 0.45 µl dilution buffer.

5 µl of the cDNA product was used as template in a 50 µl PCR reaction containing 0.5 µl AccuTaq LA DNA polymerase (Sigma-Aldrich, UK), 5 µl 10x reaction mix, 1 µl Sol-Primer B (100 pmol/µl, 5' GTT TCC CAC TGG AGG ATA 3'), 1 µl DMSO, 2.5 µl dNTPs (10 µM) and 35 µl nuclease-free water. The thermal cycling conditions were: 98°C for 30 seconds (s), followed by 30 cycles at 94°C for 15 s, 50°C for 20 s, and 68°C for 5 minutes, with a final extension step at 68°C for 10 minutes. PCR product was purified and eluted in a final volume of 30 µl nuclease-free water, and DNA quantified to determine concentration (ng/µl).

2.9 ILLUMINA LIBRARY PREPARATION

Sequencing libraries were generated using the Nextera® XT DNA library prep kit (Illumina, UK), in accordance with the manufacturer's instructions. The Nextera transposome was used to fragment 1.5 ng of purified, quantified SISPA PCR product and add partial adapters in a process known as 'tagmentation' (366). The tagmented DNA was amplified using a limited-cycle PCR programme to add sequencing primer sequences and indices. Resulting DNA libraries were purified and normalised to ensure equal library representation prior to pooling in equal volumes. Sequencing libraries were run on an Illumina MiSeq in a 2 x 150 reads run.

2.10 NANOPORE LIBRARY PREPARATION

Library preparation for Ecuadorian febrile patient samples from 2017 was undertaken at USFQ using purified SISPA PCR products in accordance with the SQK-LSK108 1D Native

barcoding genomic DNA protocol (ONT, UK), followed by sequencing on a FLO-MIN106 MinION flow cell (ONT, UK).

2.11 NGS DATA ANALYSIS

Reads were trimmed to remove adaptors and low-quality bases using trimmomatic v0.3.0 (367) with default parameters, to achieve an average phred score of Q30 across the read. Analysis of NGS data was undertaken within a Linux environment and using a local instance of Galaxy, an open source web-based platform (368).

2.11.1 TAXONOMIC ANALYSIS USING CENTRIFUGE

Centrifuge is a classifier for metagenomic sequences that assigns taxonomic labels to short DNA sequences by querying a database of pathogen and human sequences for each *k*-mer in a sequence, classifying the query sequence based on the result. The system uses a novel indexing scheme based on the Burrows-Wheeler transform and the Ferragina-Manzini index (326). The database used was 'Bacteria, archaea, viruses, human' downloaded from https://ccb.jhu.edu/software/centrifuge/. For identification of viral sequences from patient RNA samples that tested RT-PCR-negative for target pathogens, Centrifuge was used to classify sequencing reads from fastq files prior to human read removal. The output datasets were analysed in Microsoft Excel to identify reads assigned as virus at the species level, using a threshold of ≥0.01% of total reads. Read classification statistics were generated using the Pavian web application (369).

2.11.2 HUMAN READ REMOVAL

Following taxonomic analysis, human reads were removed from the patient sequencing data to both improve the efficiency of data analysis by removing unnecessary reads and avoid ethical implications regarding human genome sequences. This was accomplished by mapping reads to the human genome (human_g1k_v37[1000 genomes]) using BWA-MEM v0.7.13 (329). Non-mapped reads were selected using SAMtools (370) fastq, with flag -F 2.

2.11.3 MAPPING READS TO VIRUS REFERENCE SEQUENCES

Reads were mapped to virus reference sequences using BWA-MEM v0.7.13 (329). The resulting SAM file was converted to a BAM file, which was sorted and indexed using SAMtools. Quasi bam (371), a tool developed in-house at PHE, was used to generate a consensus sequence and a heterogeneity report. Bamstat and SAMtools flagstat were used to provide general alignment statistics on mapping, including total reads, number and percentage of reads mapped.

2.11.4 MAPPING NON-HUMAN READS TO MULTIPLE VIRUS REFERENCE SEQUENCES

Non-human reads were mapped using BWA-MEM to a custom multifasta file containing genomes of interest, constructed following RT-PCR/PCR testing. Two separate files were constructed for analysing the Sierra Leone and Ecuadorian patient sample cohorts, comprised of: at least one representative genome from each viral RT-PCR target, any virus identified during the taxonomic analysis or BLAST analysis of *de novo* assembled scaffolds, and the internal control MS2 bacteriophage (Table 2.23 and Table 2.24).

Mapping was performed as described above. Detection of a virus was defined as the presence of ≥20% viral genome coverage (5x) when mapping to a reference genome.

Virus	Accession number	Reference(s)	Reason(s) for inclusion
CHIKV	HM045817.1	(372)	qRT-PCR target. Strain chosen for its geographical proximity (Senegal, 2005).
DENV-1	MF576311.1	This study	Positive control DENV-1 strain from NCPV. qRT-PCR target.
DENV-1 (partial envelope)	FJ502863.1	n/a	qRT-PCR target. Strain chosen for its geographical proximity (Nigeria, 2007).
DENV-2	LC121816.1	n/a	qRT-PCR target. Strain chosen for its geographical proximity (East Africa, 2016).
DENV-3 (partial envelope)	KT187282.1	n/a	qRT-PCR target. Strain chosen for its geographical proximity (Ivory Coast, 2008).
DENV-4	MF004387.1	n/a	qRT-PCR target. Strain chosen for its geographical proximity (Senegal, 1981).
EBOV	MF599508.1	n/a	Virus identified in patient sample(s) by Centrifuge. Strain is best BLASTn match to SL-096 EBOV consensus sequence.
GBV-C (human pegivirus)	KP710600.1	n/a	Virus identified in patient sample(s) by Centrifuge. Strain is best BLASTn match to patient GBV-C consensus.
HBV	GQ161781.1	(373)	Virus identified in patient sample(s) by Centrifuge. Strain is best BLASTn match to SL-024 HBV consensus.

HIV	AB485634.1	n/a	Virus identified in patient sample(s) by Centrifuge. Strain is best BLASTn match to SL-110 HIV consensus.
IAV (segment 1)	MK898494.1	n/a	Virus identified in patient sample(s) by Centrifuge. Strain is best BLAST match to SL0-63 IAV consensus sequence.
LASV (L segment)	KM821860.1	n/a	RT-PCR target. Strain chosen for its geographical proximity (Sierra Leone, 2012).
ONNV	KX771232.1	n/a	Virus identified by Centrifuge. Strain is 100% match to reads in SL-058 and has been previously handled in the sequencing laboratory.
RVFV	DQ380165.1, DQ380215.1, DQ375420.1	(374)	qRT-PCR target. Strain chosen for its geographical proximity (Guinea, 1981).
YFV	JX898868.1	(375)	qRT-PCR target. Strain chosen for its geographical proximity to Sierra Leone (Senegal, 1995).
ZIKV (partial envelope)	MF629798.1	(376)	qRT-PCR target. Strain chosen for its geographical proximity (Senegal, 2013).
MS2	V00642.1	(377)	Internal control.

Table 2.23 Reference sequences used for mapping non-human reads generated from Sierra Leonean patient samples using metagenomic sequencing.

Virus	Accession number	Reference(s)	Reason(s) for inclusion
HAV	X75216.1	n/a	*De novo* assembled scaffold(s) show homology to this accession.
CHIKV	MF503628.1, MF499120.1, LC259090.1	(378,379)	*De novo* assembled scaffold(s) show homology to MF503628.1 and MF499120.1. Colombian strain (LC259090.1) chosen for its proximity to Ecuador. qRT-PCR target.
OROV	MF926352.1, MF926353.1, MF926354.1	(380)	*De novo* assembled scaffold(s) show homology to these accessions; the complete genome sequence from the isolated OROV from patient D-087.
RVFV	KY366333.1	n/a	*De novo* assembled scaffold(s) show homology to this accession.
IAV	CY257968.1	n/a	*De novo* assembled scaffold(s) show homology to this accession (IAV matrix proteins 1 & 2).
DENV-1	MF797878.1	This study	qRT-PCR target. Strain chosen for its geographical and temporal proximity (Esmeraldas, Ecuador 2014).
DENV-2	KY474308.1	(381)	qRT-PCR target.
DENV-3	FJ898457.1	n/a	qRT-PCR target. Strain chosen for its geographical proximity (Ecuador).
DENV-4	KY474335.1	(381)	qRT-PCR target.

MAYV	KP842812.1, KP842815.1	(95)	qRT-PCR target. Strains chosen for their geographical proximity (Peru). Genotype N (KP842812.1) and genotype D (KP842815.1).
YFV	MF434851.1	(382)	qRT-PCR target. Strain chosen for its temporal proximity (Brazil, 2017).
ZIKV	MF794971.1	This study	qRT-PCR target. Strain chosen for its geographical and temporal proximity (Esmeraldas, 2016).
GBV-C (human pegivirus)	KR131788.1	n/a	Identified using taxonomic analysis of sequencing reads from Ecuadorian patient samples from 2017 (MinION). Reference sequence is from the NS5B protein gene, partial cds.
MS2	V00642.1	(377)	Internal control.

Table 2.24 Reference sequences used for mapping non-human reads generated from Ecuadorian patient samples using metagenomic sequencing.

HAV = Hepatovirus A, IAV = Influenza A virus, GBV-C = GB virus C (human pegivirus).

2.11.5 *DE NOVO* ASSEMBLY

De novo assembly of Illumina sequencing reads was performed using SPAdes v3.8.2 (327), using default options with the --meta flag. Kmers of 21, 33, 55, 77, 99, 127 were used. The resulting scaffolds were filtered on average coverage (≥2 reads depth) and length (≥300 bp) and analysed for homology to known protein sequences using Kaiju, a program for fast taxonomic classification based on sequence comparison to a reference database of microbial proteins (328). A viral subset of the nr NCBI RefSeq database ('kaiju_db_viruses.fmi', available at http://kaiju.binf.ku.dk/server) was used. Following filtering for non-human viruses and viruses shown to be potential contaminants (based on the negative control results, as described below), scaffolds with homology to pathogenic human viruses were identified.

De novo assembly of nanopore sequencing reads was performed following removal of human reads, assembled using Canu (383) and the resulting contigs were manually analysed using BLASTn to identify homology to viral sequences.

2.11.6 IDENTIFICATION AND REMOVAL OF CONTAMINANT SEQUENCES

Negative extraction controls from each batch of RNA extractions and a negative template control (water, included at the metagenomic sequencing RNA preparation stage) were sequenced and analysed using the same methods used with the patient samples (described above). This controlled for contaminants that may have been incorporated during the extraction and sequencing process. Virus-specific reads identified in the negative controls were considered potential contaminants if seen in the patient sample sequencing data.

2.12 RANDOM AMPLIFICATION OF CDNA ENDS (RACE)

Terminal sequences were confirmed by RACE analysis, undertaken using a modified version of a previously described protocol (186). DNAse treated RNA was polyadenylated using a Poly(A) tailing kit, then used in a RT reaction (ProtoScript II First Strand cDNA Synthesis Kit, New England Biolabs, UK) with an oligo-d(T) primer. Resulting cDNA was amplified by PCR (Q5 High-Fidelity 2X Master Mix, New England Biolabs, UK) using a 3' PCR anchor primer and a primer specific to each terminal sequence. Amplified products were Sanger sequenced and data analysed using the DNASTAR Lasergene package to assemble contigs and confirm nucleotide sequences. For OROV, it was possible to generate both the 5' and 3' terminal sequences using 3' RACE analysis as viral RNA from cell culture contains both genomic and anti-genomic sequences.

2.13 MULTIPLEX TILING PCR PRIMER 'PRIMAL' SCHEME

An amplicon-based approach using the algorithmic design method described by Quick *et al.* (2017) (351) was implemented for OROV. The Ecuadorian strain OROV/EC/Esmeraldas/087/2016 (MF926352.1 - MF926354.1) was used as a reference sequence to generate a set of primers using the 'Primal Scheme' webtool (http://primal.zibraproject.org/). To avoid generating three separate schemes for each segment, which may be incompatible, the S, M and L genomic segments were concatenated and input to the webtool using the default settings (400 bp amplicons, 50 bp overlap). The designed primer scheme was subsequently modified manually to account for segment ends, incorporating 5' and 3' end primers.

RNA extracted from OROV-positive Ecuadorian patient plasma samples and the cell-cultured prototype strain were reverse transcribed using the ProtoScript II First Strand

cDNA Synthesis Kit (New England Biolabs, UK) and random hexamers. The resulting cDNA was used as a template in two multiplex PCR reactions using the Ecuador OROV primers designed as described above with Q5 High-Fidelity 2X Master Mix (New England Biolabs, UK), to generate multiple overlapping amplicons that spanned the viral genome. PCR products were purified, quantified and visualised on a 1.5% agarose gel stained with 1:10,000 ethidium bromide, run alongside a 1 kb DNA ladder (New England Biolabs, UK). The expected DNA concentration was 5-50 ng/µl DNA, negative control values should be ≤1 ng/µl. Purified DNA was prepared for NGS using a modified version of the 1D Native barcoding genomic DNA protocol (ONT, UK) developed as part of the Zibra project (http://www.zibraproject.org/blog/protocol-low-input-native-barcoding-protocol/), followed by sequencing using a MinION flowcell (ONT, UK). The resulting reads were mapped to the relevant OROV reference sequences using BWA-MEM.

2.14 COMPARATIVE VIRAL GENOME ANALYSES

2.14.1 OROV

For analysis of Ecuadorian OROV strains against publicly available OROV sequences, OROV/EC/Esmeraldas/087/2016 was selected as a representative Ecuadorian strain. Alignments and maximum-likelihood phylogenetic trees were generated in MEGA7 for S, M and L segments, using all complete OROV coding sequences (*n*=112 S, *n*=24 M, *n*=23 L) in the GenBank nucleotide database, with 100 bootstrap replicates. Alignment and analysis of Ecuadorian OROV strains was performed in MegAlign v14 using ClustalW. The final S segment tree was produced in FigTree 1.4.2.

2.14.2 HEPATITIS B VIRUS (HBV)

The patient hepatitis B virus (HBV) genome sequence was analysed using BLASTn to identify the most closely related sequence from the nucleotide collection (nr/nt) database. Representative HBV genomes were aligned with the patient sequence using ClustalW in MEGA7. These were full-length genome sequences from alignments made publicly available by Bell *et al.* (384), the number of sequences included from each genotype was proportionate to the total number sequences available for that genotype (A=25, B=50, C=77, D=36, E=12, F=9, G H and I = 1). A phylogenetic tree was constructed from the alignment using the maximum-likelihood method based on the Tamura-Nei model in MEGA7.

2.14.3 HIV

Patient HIV genome sequences were analysed using BLASTn to identify the most closely related sequence from the nucleotide collection (nr/nt) database. For patient genomes that had complete coverage of the pol gene, the Recombinant Identification Programme (RIP) (385) available at https://www.hiv.lanl.gov/content/sequence/RIP/RIP.html) was used to identify viral subtypes by comparing sequences with HIV-1 M subtypes previously identified in Sierra Leone (A1, A2, A6, B, C, G, CRF02_AG, CRF09_cpx and CRF06_cpx (386)).

2.15 VIRUS ISOLATION, PROPAGATION AND QUANTIFICATION

2.15.1 CELL LINES

Cell lines were kindly provided free of charge by the European Collection of Authenticated Cell Cultures (ECACC, Table 2.25).

Cell line	Species	Cell type	Source
C6/36	Aedes albopictus	Embryonic	ECACC (89051705)
Vero	African green monkey	Kidney, epithelial	ECACC (84113001)

Table 2.25 Cell lines used to propagate virus from febrile patient plasma samples.

2.15.2 VIRUS PROPAGATION

Virus isolation from suspected positive (CHIKV, DENV, OROV, ZIKV) patient plasma samples was undertaken by inoculating Vero (70% confluent) and C6/36 (50% confluent) cell monolayers in T25 flasks (Nunc, UK) with 250 µl patient plasma diluted 1:10 in the relevant cell culture medium. Cultures were incubated at 37°C, 5% (v/v) CO_2 (Vero) or 28°C (C6/36) for 14 days or until signs of cytopathic effect (CPE) were observed. Supernatants were sampled at days 5, 7, 11 and 14 post-infection, RNA was extracted as described above (see section 2.3), then viral RNA was measured using pathogen-specific qRT-PCR to determine relative quantity over time. Supernatants from virus positive cultures were harvested as described in section 2.15.3.

Subsequent passaging of viral supernatant was undertaken to increase volume and virus titre using the same method described above but using 80-90% confluent Vero cell (OROV) or 50% confluent C6/36 cell (ZIKV) monolayers. Cells were inoculated with virus supernatant from the previous passage, diluted 1:10 in the relevant cell culture medium.

Cultures were harvested (see section 2.15.3) 3-4 days (OROV) or 14 days (ZIKV) post-infection.

Isolation of OROV from qRT-PCR-positive patient plasma samples was undertaken by inoculating 80% confluent Vero cell monolayers with patient plasma diluted 1:10 in minimum essential medium (MEM, Life Technologies Ltd., UK) to a volume of 1 mL, then incubating at 37°C with 5% (v/v) CO_2 for 96 hours. Supernatants were sampled at 24-hour intervals for 96 hours, replication was determined by measuring OROV RNA using qRT-PCR.

2.15.3 VIRUS HARVEST

Virus cultures were frozen at -80°C for at least 30 minutes to disrupt cellular membranes for maximum viral yield. Upon thawing, supernatant and dislodged cells were centrifuged at 3000 revolutions per minute (rpm) for 10 minutes to pellet cellular debris. Viral supernatants were filtered through a 0.2 µm pore filter (Sartorius, UK) to remove cellular debris, then aliquoted and stored at -80°C.

2.15.4 VIRUS QUANTIFICATION BY PLAQUE ASSAY

Ten-fold serial dilutions of virus supernatant were made in MEM. 80 -90% confluent Vero cells in 6- or 24-well plates (Corning, UK) were washed with Dulbecco's phosphate-buffered saline (D-PBS, Fisher Scientific, UK), 250 µl (6-well plate) or 100 µl (24-well plate) virus dilutions were inoculated in triplicate. Plates were incubated at 37°C, 5% (v/v) CO_2 for 60 minutes. Inoculum was removed then 3 mL (6-well plate) or 0.5 mL (24-well plate) overlay medium (2x MEM, (Life Technologies, UK), 5% foetal bovine serum

(FBS, Sigma-Aldrich, UK), 1% non-essential amino acids (NEAA, Invitrogen, UK), 1% antibiotic-antimycotic (Invitrogen, UK), 2 mM L-glutamine (Fisher Scientific, UK), 1.5% Seaplaque agarose (Scientific Laboratory Supplies, UK)) was added. Plates were incubated at 37°C, 5% (v/v) CO_2 for 3 days, then fixed with 20% formaldehyde for a minimum of 5 hours to inactivate virus and fix cell monolayers. Agarose plugs were removed and monolayers stained with 2.3% crystal violet for 60 minutes. Plates were rinsed with water before air drying, plaques were counted by eye. Virus titre was calculated using the number of visible plaques from the lowest dilution showing >10 plaques, using the equation: *average number of plaques* ***x*** *dilution factor* ***x*** *volume factor = plaque forming unit (pfu)/mL.*

2.15.5 POSITIVE CONTROL VIRUS STRAINS

Viruses were kindly provided free of charge by the National Collection of Pathogenic Viruses (NCPV) for use as positive control material (Table 2.26). They were propagated at the same time as patient plasma samples to ensure that culture conditions were suitable for viral growth. To check for cross-contamination, RNA extracted from positive control cultures underwent metagenomic sequencing, from which complete genome sequences were generated and compared with patient sequencing data.

Virus species	Strain name	NCPV catalogue number
DENV-1	TC861[HA]	0106037v
CHIKV	S27 Petersfield	0006254v
ZIKV	PRVABC59	1604131v
OROV	NCPV: 1409261v	1409261v

Table 2.26 Viruses used as positive controls during virus propagation, provided by NCPV.

2.16 OROV REPLICATION IN BIOLOGICALLY RELEVANT CELL TYPES

2.16.1 CELL LINES

Cell lines and animal models capable of supporting OROV replication (from published studies) are summarised in Table 2.27. Cell lines used in OROV replication experiments in this study were kindly provided free of charge by the ECACC, Plymouth University, and the Pirbright Institute (Table 2.28).

Cell name	Cell type	Species	Study type	Study reference(s)
Vero	Kidney cells	African green monkey	In vitro	(185,387–389)
MDCK	Kidney epithelial cells	Canine	In vitro	(185)
DF-1	Embryonic fibroblasts	Chicken	In vitro	(185)
MRK101	Kidney cells	Gray red-backed vole	In vitro	(185)
BHK-21	Kidney fibroblasts	Hamster	In vitro	(185)
A549	Epithelial alveolar adenocarcinoma cells	Human	In vitro	(185)
HeLa	Epithelial cervical adenocarcinoma cells	Human	In vitro	(185,388)
2fTGH	Epithelial fibrosarcoma cells	Human	In vitro	(185)
HuH-7	Hepatocarcinoma cells	Human	In vitro	(390)
THP-1	Monocytes with a macrophage-like phenotype	Human	In vitro	(390)
Jurkat	Transformed T lymphocytes	Human	In vitro	(390)
Primary fibroblasts	Skin cells	Human	In vitro	(391)

QT-35	Fibrosarcoma cells	Quail	In vitro	(185)
LLC-MK2	Kidney epithelial cells	Rhesus macaque	In vitro	(185)
CPT-Tert	Choroid plexus cells	Sheep	In vitro	(185)
Hepatocytes	Liver cells	Hamster	In vivo	(392,393)
Kuppfer cells	Liver macrophages	Hamster	In vivo	(392)
Neurons	Brain cells	Hamster	In vivo	(393)
Brain cells	Brain cells	Neonatal BALB/c mice	In vivo	(188)

Table 2.27 Cell types in which OROV replication has been demonstrated.

Cell line	Species	Cell type	Source
1BR3	Human	Skin fibroblast	ECACC (90011801)
Aag-2	Aedes aegypti	Embryonic	Pirbright Institute
AE	Aedes aegypti	Unknown	Pirbright Institute
AF319	Aedes aegypti	Embryonic	Pirbright Institute
BHK-21	Hamster	Kidney, fibroblast	Pirbright Institute
C6/36	Aedes albopictus	Embryonic	ECACC (89051705), Pirbright Institute
HEKn	Human (neonatal)	Primary epidermal keratinocyte	Plymouth University
HepG2	Human	Liver, hepatoma	ECACC (85011430)
HPEKp	Human (juvenile)	Primary epidermal keratinocyte	Plymouth University
HSU	Culex quinquefasciatus	Ovary	Pirbright Institute
KC	Culicoides variipennis	Embryonic	Pirbright Institute
PBMC	Human	Mononuclear blood cells	This study
Sua4a-2	Anopheles gambiae	Larvae	Pirbright Institute
U4.4	Aedes albopictus	Embryonic	Pirbright Institute
Vero	African green monkey	Kidney, epithelial	ECACC (84113001), Pirbright Institute

Table 2.28 Cell lines used in OROV replication experiments. ECACC catalogue numbers are given in parentheses.

2.16.1.1 ISOLATION OF PERIPHERAL BLOOD MONONUCLEAR CELLS (PBMCS)

Twenty healthy volunteers were recruited from PHE Porton Down through a request for participants. Volunteers were given information on the study and provided informed consent. Ethical approval for taking these samples was given by the PHE Research Ethics and Governance Group.

Forty mL of blood was taken from each volunteer into sodium heparin vacutainers (Scientific Laboratory Supplies, UK). Whole blood was processed immediately to isolate peripheral blood mononuclear cells (PBMCs). Blood was mixed 1:1 with Roswell Park Memorial Institute 1640 medium (RPMI, Invitrogen, UK), then transferred to Greiner 50 mL LeucoSep tubes (Scientific Laboratory Supplies, UK) and centrifuged for 20 minutes at 2000 rpm. PBMCs were aspirated into a fresh conical tube filled with RPMI and centrifuged for 10 minutes at 1700 rpm. The cell pellet was resuspended in 15 mL RPMI and centrifuged for a further 10 minutes at 1700 rpm. The cell pellet was resuspended in 5 mL RPMI and cells were stained with 0.5% Trypan Blue (Invitrogen, UK) using a 1:10 ratio. Live cells were counted using a Neubauer improved haemocytometer (VWR International, UK), using the mean of three counts. Following counting, PBMCs were centrifuged for 10 minutes at 1700 rpm then resuspended in a volume of freezing medium (Dimethyl sulfoxide (DMSO):FBS in a ratio of 1:9) that gave 5e+6 cells/mL. 1 mL aliquots were transferred to a Mr. Frosty freezing container (Life Technologies, UK) and frozen at -80°C overnight, before being transferred to liquid nitrogen for long term storage.

2.16.2 OROV REPLICATION TIMECOURSE EXPERIMENTS

2.16.2.1 OROV REPLICATION IN HUMAN CELL TYPES

For adherent cells (HepG2, 1BR3, HEKn and HPEKp), 24-well plates were seeded with the appropriate density of cells (Table 2.29) one day prior to infection (day -1). On day 0, cells were observed for confluency then washed with D-PBS prior to infection. Virus (OROV strain OROV/EC/Esmeraldas/087/2016 passage (P)2 or P3 Vero, cultured and harvested as per sections 2.15.2 and 2.15.3) was diluted in culture medium to obtain inoculum of the desired multiplicity of infection (MOI). Cells were inoculated with 200 µl virus inoculum, or mock-infected with the same volume of uninfected Vero cell culture supernatant. Cells were incubated at 37^{o}C, 5% (v/v) CO_2 for 60 minutes, inoculum was removed and cells washed with D-PBS prior to the addition of 600 µl culture medium (Table 2.29). At designated timepoints, the total volume of supernatant was removed from the cell monolayer and frozen at -80^{o}C. The monolayer was washed with D-PBS, then 350 µl of RLT buffer (Qiagen, UK) with 1:100 β-mercaptoethanol (VWR International Ltd., UK), 1:100 LPA and 1.45e+5 pfu internal control MS2 bacteriophage was added to the monolayer and incubated for 10 minutes at room temperature. Cells in RLT buffer were physically removed from the plate and aspirated to a microtube, then frozen at -80^{o}C.

During the time-course experiments, cell viability was assessed at each timepoint to control for lack of virus replication due to suboptimal cell health. This was achieved using mock-infected cells (for biosafety reasons it was not possible to assess infected cell viability or the presence of CPE at CL3). Cell monolayers were dissociated using 0.25% Trypsin-EDTA (hepatocytes and fibroblasts) or TryPLE (keratinocytes), then stained 1:1 with 0.4% Trypan Blue prior to counting under a light microscope using a

haemocytometer. Percentage viability was determined using the mean of three counts in the equation:

Viability = total viable cells/total cells x 100

For the PBMC time-course experiment, the following adjustments were made to accommodate the non-adherent cell type: cells were plated on the day of infection and incubated for at least one hour prior to infection following plating. At each timepoint, supernatants and cells were harvested by low speed centrifugation to pellet the cells, followed by aspiration of supernatant to a microtube. Each well was rinsed with 350 µl buffer RLT (+ LPA + MS2), which was then added to the cell pellet and incubated for 10 minutes at room temperature. Supernatants and cells in buffer RLT were stored at -80^{o}C. Pilot time-course experiments were performed using single replicates, subsequent time-courses were performed using biological triplicates.

Cell line	Cell seeding density	Culture medium
HepG2	6.8e+5	EMEM + 10% FBS + 2mM L-glutamine + 1% NEAA + 1% Pen-Strep.
1BR3	2.5e+5	EMEM + 15% FBS + 2 mM L-glutamine + 1% NEAA + 1% Pen-Strep.
HEKn	2.6e+4	EpiLife + HKGS + 1% Anti/Anti.
HPEKp	2.6e+4	EpiLife + HKGS + 1% Anti/Anti.
PBMCs	5.00e+5	RPMI-1640 + 10% FBS + 2 mM L-glutamine + 1% Pen-Strep.

Table 2.29 Cell seeding densities and culture medium used in human cell timecourse experiments. EMEM = Eagle's minimum essential medium (Scientific Laboratory Supplies Ltd., UK). FBS = Foetal bovine serum. NEAA = Non-essential amino acids. Pen-strep = penicillin-streptomycin (Sigma-Aldrich, UK). HKGF = Human keratinocyte growth supplement. Anti/Anti – antibiotic/antimycotic.

2.16.2.2 OROV REPLICATION IN INSECT AND MAMMALIAN CELL TYPES

This experiment was performed in collaboration with Dr. Barry Atkinson at the Pirbright Institute, Surrey. On day -1, insect and mammalian cell lines were seeded into T25 flasks (Nunc, UK) at a density of 1.0e+6 and 5.0+e5 cells/flask, respectively. Cells were observed prior to infection on day 0 and all were 40-70% confluent. Two flasks per cell line were seeded; one for OROV infection and one for mock-infection using PBS with 1% bovine albumin (PBS-A, Sigma-Aldrich, UK).

On day 0, all cell lines were infected with OROV strain OROV/EC/Esmeraldas/087/2016 (P1 Vero, cultured and harvested as per sections 2.15.2 and 2.15.3), at a MOI of 0.1. Virus was diluted in PBS-A to obtain 1 mL inoculum per T25 flask. This was added to the cell monolayer following one wash with PBS-A. 1 mL PBS-A was added to all mock-infected flasks. Following a 60-minute incubation at 33^{o}C with 5% (v/v) CO_2 (mammalian cell lines) or 28^{o}C (insect cell lines), 10 mL of the respective culture medium (Table 2.30) was added to each flask. Following the removal of the day 0 timepoint supernatants, flasks were returned to the incubators at the aforementioned conditions for 7 days. Supernatants were sampled at 0, 1, 2, 3, 4, 5 and 7 days post-infection and stored at -80^{o}C.

Cell line	Culture medium
***Aedes agypti* cell lines**	L-15 + 2% FBS + 10% TPB + 1% Pen-Strep.
Other insect cell lines	Schneider's Drosophila Medium + 2% FBS + 10% TPB + 1% Pen-Strep.
Vero	DMEM + 2% FBS.
BHK-21	GMEM + 2% NBCS + 10% TPB + 1% Pen-Strep.

Table 2.30 Cell culture media used in insect and mammalian cell timecourse experiments. TPB = Tryptose phosphate broth (Sigma-Aldrich, UK). FBS = Foetal bovine serum. DMEM = Dulbecco's modified eagle medium. GMEM = Glasgow minimum essential medium. Pen-strep = penicillin-streptomycin. NBCS = New born calf serum.

2.16.2.3 RNA EXTRACTION AND OROV QRT-PCR

RNA was extracted manually from infected cells harvested from human cell time-course experiments using the RNeasy mini kit (Qiagen, UK). At CL3, one volume of 70% ethanol was added to thawed cells in buffer RLT (with 1:100 β-mercaptoethanol, 1:100 LPA and 1.45e+5 pfu internal control MS2 bacteriophage) that had previously undergone a 10-minute incubation in the RLT buffer to inactivate virus. This subsequent 10-minute incubation with the ethanol completed the chemical inactivation procedure. At CL2, RNA was extracted in accordance with manufacturer's instructions and eluted in 30 µl of nuclease-free water.

RNA was extracted from infected cells harvested from human cell time-course experiments and from supernatants harvested from mammalian and insect cell time-course experiments using the BioSprint 96 One-For-All Vet Kit (Indical Bioscience, Germany) with the automated Kingfisher Flex System. Thawed cells in 350 µl buffer RLT (with additions as described above) or 100 µl supernatant in 300 µl buffer RLT (with additions as described above), were inactivated at CL3 for 10 minutes at room temperature, then one volume of isopropanol was added and incubated for a further 10 minutes to complete the chemical inactivation procedure. At CL2, 40 µl proteinase K was added to samples originating from cellular material to aid the complete lysis of cells. RNA extracted was carried out in accordance with manufacturer's instructions, using the 'BS96 Vet 100' protocol on the Kingfisher Flex System. RNA was eluted in 75 µl AVE buffer (Indical Bioscience, Germany).

OROV and MS2 RNA was measured semi-quantitatively from experimental RNA samples using the OROV qRT-PCR previously described in section 2.7.4, with the following changes: the TaqMan Fast virus 1-step master mix was used instead of the SSIII kit, and

the assay was multiplexed to detect MS2 (Table 2.31) under standardised RIPL conditions (mastermix volumes identical to those given in Table 2.8, cycling conditions given in Table 2.9). These changes were made by RIPL prior to incorporating the assay into their qRT-PCR portfolio and was used in this instance to save resources via the MS2 multiplex capability.

Component	Final concentration (nM)	Volume for 100 reactions (µL)
ORO_F	900	18
OROV Ec2R	900	18
ORO_P	250	5
MS2 F1	40	8
MS2 Rev	40	8
MS2 Taq Cy5	80	16
Water	n/a	927

Table 2.31 Primer/probe mix formulations for OROV/MS2 multiplex qRT-PCR assay.

CHAPTER 3: PATHOGEN DETECTION IN FEBRILE SIERRA LEONEAN PATIENTS

3.1 INTRODUCTION

3.1.1 INFECTIOUS DISEASE IN SIERRA LEONE

Sierra Leone is situated on the coast of West Africa and shares borders with Liberia and Guinea. The population totals just over 7 million people (census 2016) in an area of approximately 70,000km^2 (394), with clusters of population in the lower elevations of the south and west, and the northern third of the country more sparsely populated (395). Sierra Leone is classified as a low-income country, as defined by having a gross national income per capita of 995 United States Dollars (USD) or less (396). Following many decades of colonialism, it became independent from Britain in 1961. Political instability resulted in a long-standing civil war from 1991-2002; consequentially over 2 million people were displaced and tens of thousands died (395). Since peace was achieved in 2002, democracy has slowly been re-established and in the present day, Sierra Leone functions as a republic (395). The country is divided into 14 districts that sit within four provinces (Eastern, Northern, North Western and Southern) and one area (Western) (395). The climate is tropical with a wet season (May to December) and dry season (December to April). The terrain is made up of a coastal belt of mangrove swamps, wooded hill country, upland plateau and mountains to the east (395).

Life expectancy in Sierra Leone in 2016 was 52 for men and 54 for women. Childhood mortality is high, with 105 deaths per 1000 live births (397). Six of the ten leading causes of death in Sierra Leone have infectious causes, with malaria the leading cause, estimated to contribute to 20% of all deaths of those under five years old (398,399). Malaria is a serious public health problem in Sierra Leone, responsible for 38% of hospital consultations, with 17.6% of patients admitted with malaria dying of the disease

(400). Malaria prevalence has decreased in recent decades and the Sierra Leone MoSH aim to reduce malaria morbidity and mortality by 40% by 2020 (400).

HIV infection/acquired immunodeficiency syndrome (AIDS) is the 9th leading cause of death in Sierra Leone (401). In 2016, 67,000 people were living with HIV infection, 5,300 new infections were acquired and 2,800 AIDS-related deaths occurred (402). An estimated 26% of HIV-positive people accessed antiretroviral therapy (402). HIV infections and deaths have increased since 2010 (402) and it is likely that the weakening of the public health system following the EBOV outbreak contributed to this. However, to combat this the MoHS launched a National HIV Strategic Plan 2016-2020 (400) that targets interventions at groups at higher risk of HIV transmission, including female sex workers, men who have sex with men, and prisoners (402,403).

Cholera and tuberculosis (TB) are important bacterial diseases endemic to Sierra Leone. Major outbreaks of Cholera (caused by *Vibrio cholerae*) occurred in the 1980s and 1990s, with the most recent in 2012, detected via an increase in diarrhoea and vomiting cases reported in weekly surveillance (400). TB (caused by *Mycobacterium tuberculosis*) burden is high in Sierra Leone and was detrimentally affected by the West African EBOV outbreak due to a reduction in care-seeking and impacts on the health system (400). TB is a priority for the MoHS which aims to improve surveillance, community engagement, address co-infection with HIV, and combat drug-resistance (400).

Haemorrhagic fevers caused by LASV and EBOV sporadically cause disease in Sierra Leone. LASV is endemic, with the highest proportion of cases recorded from the south-eastern districts of Kenema, Bo and Kailahun (404). The MoSH have collaborated with the WHO and other international partners to establish a network that supports the

development of national prevention strategies, enhances laboratory diagnostics and provides training in laboratory diagnosis, clinical management and environmental control (400). The emergence of EBOV in West Africa resulted in the worst outbreak on record, affecting mainly Sierra Leone, Guinea and Liberia. This outbreak is outlined later in this thesis. EBOV transmission from virus persisting in the bodily fluids of EVD survivors, as well as zoonotic introductions, remains a risk. A study investigating the cause of illness in febrile LASV negative patients in Sierra Leone identified antibodies against EBOV, DENV, CHIKV, WNV, *Leptospira*, and typhus, as well as widespread infection with *Plasmodium falciparum* (405). Other viral diseases of public health importance in Sierra Leone include viral hepatitis, measles, polio, rabies and yellow fever (400).

3.1.2 PUBLIC HEALTH IN SIERRA LEONE

Sierra Leone's healthcare system functions within three tiers of service delivery: peripheral health units, district hospitals, and referral hospitals. There are approximately 19,000 healthcare workers (Figure 3.1) and almost 1,300 healthcare facilities in total, including 40 hospitals, around half of which are government owned and the other half privately-owned (400). The impact of the West African EBOV outbreak (2014-2016) on the Sierra Leonean public health system was significant, both directly in terms of the death of hundreds of healthcare workers following nosocomial transmission, and indirectly by paralysing the healthcare system so that it could not effectively respond to other, non-EVD related public health issues. Since the end of the outbreak, the WHO has worked with the MoSH to help strengthen the public health

service via health workforce planning and management, health information systems, policy and planning, district and hospital management and health financing (400).

Figure 3.1 Healthcare workforce statistics for Sierra Leone in 2017. Reproduced from WHO (400).

3.1.3 EBOLA VIRUS OUTBREAK IN WEST AFRICA, 2014-2016

The EBOV outbreak that occurred in West Africa from 2014-2016 was the worst on record in terms of the number of recorded cases and deaths (194). The index case was retrospectively identified as a two-year-old child who became ill in the village of Meliandou in December 2013 and subsequently died in the forested district of Guéckédou in south-eastern Guinea (Figure 3.2), bordering Liberia and Sierra Leone (41). Members of the child's family became infected, resulting in nosocomial transmission within a healthcare centre which is thought to have enabled the spread of the virus into a town setting (41). In March 2014, cases of EBOV were reported from two other rural locations in Guinea (Macenta and Kissidougou, Figure 3.2) by the WHO African regional office (406).

Figure 3.2 Map of Guinea showing the initial locations of the EBOV outbreak. Reproduced from (407).

By the end of March and May 2014, cases had been confirmed in Liberia and Sierra Leone, respectively. The WHO provided support to national healthcare services during the early phase of the outbreak in an attempt to control the spread of the virus, however, in August 2014 rapidly increasing case numbers led the WHO to issue a statement declaring the EBOV outbreak a public health emergency of international concern. The international community responded by providing support in all three countries, working with national healthcare workers to run ETCs and provide EBOV diagnostic capability. Despite best intentions, much of this was done following the peaks of the outbreak that occurred in September 2014 in Liberia and November 2014 in Sierra Leone (cases numbers in Guinea remained relatively stable throughout the duration of the outbreak), leading to criticism that the WHO moved too slowly (41). By the end of the outbreak, 24/34 districts in Guinea and every district in Liberia and Sierra Leone had reported EBOV transmission. In addition, Nigeria, Mali, Senegal, the USA, the UK, Spain and Italy reported imported cases during the outbreak, with Spain experiencing the first case of autochthonous EBOV transmission outside of Africa (194).

Towards the end of the outbreak, the major challenge was identifying and isolating the few remaining cases. EBOV-free status was defined as a 42-day period with no new cases. Guinea was initially declared EBOV-free in December 2015, however additional cases were identified in March 2016 and final EBOV-free status was granted in June that year (41). Similar situations occurred in Liberia and Sierra Leone, with Liberia initially declared EBOV-free in May 2015, then for the final time in June 2016 following a small number of cases identified in the intervening period (41). Sierra Leone was declared EBOV-free in November 2015, but another case was identified in January 2016. Final EBOV-free status was achieved two months later in March (41).

In response to the call from WHO, the UK government pledged £427 million to help control the outbreak (408). This included building ETCs in Sierra Leone and deploying medical and scientific experts to staff them alongside national healthcare workers. Three ETCs had a PHE-run diagnostic laboratory integrated on-site, voluntarily staffed by scientists from PHE, other government bodies and academic institutions. These ETCs were located in: Kerry Town, 19 miles from the capital Freetown and run by non-governmental organisation (NGO) Save the Children; Port Loko district, run by NGO GOAL; and Makeni, Bombali district, run by NGO International Medical Corps (Figure 3.3) (408). Together, these laboratories were the largest provider of field pathology services in Sierra Leone during the outbreak (207).

Figure 3.3 Locations of PHE-run EBOV diagnostic laboratories in districts within Sierra Leone, indicated by stars. Blue = Kerry Town ETC, green = Port Loko ETC, yellow = Makeni ETC. Map adapted from https://commons.wikimedia.org/wiki/File:Districts_in_Sierra_Leone_2018.svg

The EBOV positivity rate from samples tested has been published from a number of laboratories that functioned during the outbreak (409,410), including the European Mobile Laboratory in Guéckédou, Guinea, which was operational from 2014-2015 and tested 2,178 samples from hospitalised patients. Of these, 43% were negative for EBOV, despite showing clinical signs consistent with the local case definition (409). Due to resource limitations during the outbreak, it was not possible to test EBOV-negative patients for differential diagnoses, except for *Plasmodium* in some laboratories (including the three PHE-run laboratories). O'Shea *et al.* (2015) investigated the cause of illness in 51 EBOV-negative patients that presented at a British-run ETC in Kerry Town, located in the Western Area, between November 2014 and February 2015. Whilst a substantial proportion of patients were infected with *Plasmodium* (25.5%); influenza A virus, coronavirus and astrovirus infections were also identified in addition to bacterial infections including *E.coli*, *Shigella* and *Vibrio* spp. (411). This project attempts to address the alternative causes of illness experienced by EBOV-negative patients by investigating the presence of other viral agents in the blood of patients from the Kerry Town, Port Loko and Makeni ETCs.

3.1.4 PHE-RUN DIAGNOSTIC FIELD-LABORATORIES

The three PHE-run EBOV diagnostic field laboratories opened in October (Kerry Town) and December (Port Loko and Makeni) 2014, for the purpose of providing molecular testing for EBOV and rapid device testing (RDT) for *Plasmodium* (410). The laboratories processed blood samples from patients at the ETCs and local holding centres, and blood

and buccal swab samples from the wider community (410). The EBOV molecular assay was a qRT-PCR in which the Cq value for a given sample indicated the relative quantity of EBOV RNA present. In the field laboratories, patient sample Cq values were interpreted as positive (<40) or negative (≥40) and reported to the medical team to inform patient management and to the Sierra Leone MoHS for surveillance and epidemiological purposes.

Following sample inactivation using AVL buffer and ethanol, RNA extraction was carried out in the field laboratories either using an automated EZ1 nucleic acid extraction machine (Qiagen, UK), or manually, using the same column-based kit used in this project; the QIAamp viral RNA mini kit (Qiagen, UK). Purified RNA (including internal control MS2 bacteriophage) was eluted in 60 µl of AVE elution buffer (410). Initially, the RealStar Filovirus Screen qRT-PCR Kit 1,0 (Altona Diagnostics, UK), targeting the EBOV L gene, was used for laboratory confirmation of EBOV infection. Due to operational requirements and some performance issues, all three laboratories transitioned from this assay to a modified version of the EBOV Zaire-specific 'Trombley' qRT-PCR assay (355), targeting the NP gene, around the time of January 2015 (410). The Trombley assay is used in this project alongside a pan-EBOV assay, for molecular detection of EBOV RNA in patient samples. The BinaxNOW RDT (Abbott, UK) was initially used for *Plasmodium* diagnosis in the field due to its successful use in a previous field-based setting and its broad detection of *Plasmodium* species, however, in line with efforts to standardise testing across diagnostic laboratories in Sierra Leone, it was replaced with the SD Bioline Malaria Ag P.f. RDT (Abbott, UK), which showed improved specificity for the major *Plasmodium* species in the country, *P. falciparum* (410).

Whilst the field laboratories were operational, the Kerry Town laboratory tested 6,148 samples, of which 19.7% (*n*=1,209) were EBOV-positive, 77% (*n*=4,738) EBOV-negative and 3.3% (*n*=201) were indeterminate or needed a repeat test (due to poor sample condition) (410). The Port Loko laboratory tested 18,458 samples of which 5.1% (*n*=936) were EBOV-positive, 90.1% (*n*=16,626) EBOV-negative and 4.8% (*n*=896) indeterminate or needed a repeat test (410). The Makeni laboratory tested 26,117 samples (including the samples it tested in its subsequent role as a 'legacy laboratory', following decommissioning of the ETC), of which 1.2% (*n*=325) were EBOV-positive, 95.9% (*n*=25,045) EBOV-negative and 2.9% (*n*=747) indeterminate or requiring a repeat test (410). The laboratories ceased testing when the ETCs they were embedded in were decommissioned in November (Kerry Town) and December 2015 (Port Loko and Makeni) (410). The large proportion of samples that tested negative for EBOV begs the question of what caused the symptoms these patients experienced. This formed a major aim of this project; to identify viral causes of disease in this group of patients in order to better understand the causes of febrile illness in Sierra Leone, and subsequently provide information to strengthen the disease surveillance and response system.

3.2 METHODOLOGY: SAMPLE SELECTION FOR METAGENOMIC SEQUENCING

From the samples that had no positive RT-PCR/PCR result for any pathogen, 33 were selected for metagenomic sequencing based on the following criteria:

Samples excluded:

- Samples with an EBOV-positive or inconclusive qRT-PCR result
- Samples with a *Plasmodium* positive PCR result
- Samples designated 'follow-up' in the associated metadata
- Samples from patients aged ≤13 years old (in accordance with a request from the PHE-MOHS biobank committee)
- A single *Leptospira* qRT-PCR positive sample (because the project focus is RNA viruses)

Samples selected:

- Samples initially qRT-PCR inconclusive for CCHFV (*n*=2)
- Samples initially RT-PCR inconclusive for LASV (*n*=1)

A subset of samples that met the above criteria were chosen to include a similar number of samples per ETC, over the complete breadth of dates, with as much metadata as possible. In addition, three samples that were EBOV-positive by qRT-PCR were sequenced. A full list of the samples sequenced is given in Appendix 4.

3.3 RESULTS

3.3.1 RT-PCR/PCR TESTING OF FEBRILE PATIENT PLASMA

RT-PCR/PCR results for CCHFV, CHIKV, DENV, LASV, RVFV, YFV, ZIKV and *Rickettsia* were negative for all of the 120 patient samples tested (Table 3.1). One patient was positive for *Leptospira*. 22 patients were positive for *Plasmodium* and two were inconclusive (Table 3.1). A comparison of *Plasmodium* RDT results from the field with RT-PCR results obtained in the laboratory during this project shows that there is a disparity in 10.9% of the samples tested (Table 3.2). Of this, 6.7% are samples that tested positive by RT-PCR but negative by RDT and 4.2% are samples that tested negative by RT-PCR but positive by RDT. Unexpectedly, eight patients tested positive for EBOV by qRT-PCR, with a further ten samples yielding an inconclusive result (Table 3.1). EBOV and *Plasmodium* results, with associated metadata, are summarised for EBOV-positive/inconclusive samples in Table 3.3. All patient samples were positive for internal control MS2. A complete list of RT-PCR/PCR results, including Cq values, are provided in Appendix 4.

	Positive	Negative	Inconclusive
EBOV	8	102	10
Plasmodium	22	98	2
Leptospira	1	119	0
LASV	0	120	0
CCHFV	0	120	0
CHIKV	0	120	0
DENV	0	120	0
RVFV	0	120	0
YFV	0	120	0
ZIKV	0	120	0
Rickettsia	0	120	0

Table 3.1 Pathogen detection results from qRT-PCR, RT-PCR and PCR assays.

	PCR positive	PCR negative	PCR inconc.	Total
RDT positive	7.5	4.2	1.7	13.3
RDT negative	6.7	63.3	0.0	70.0
RDT n/t	4.2	12.5	0.0	16.7
Total	18.3	80.0	1.7	

Table 3.2 A comparison of test results for *Plasmodium* performed in the field (RDT) or retrospectively during this project (RT-PCR). Values given are percentages of the total number of samples (*n*=120). Inconc. = inconclusive, n/t = not tested.

Sample ID	Overall EBOV result	Pan-EBOV PCR Cq value	Zaire EBOV PCR Cq value	Date sample taken	Sample type	Lab	District	Chiefdom	Field EBOV test result	Field malaria rapid test result	Patient age	Original /follow up sample
SL-040	Positive	33.55	32.24	25/12/2014	Blood	Port Loko	Port Loko	Maforki	Negative	n/a	35	Follow-up
SL-043	Positive	33.16	32.64	26/11/2014	Blood	Kerry Town	WA	nd	Negative	n/a	56	Original
SL-053	Positive	34.43	34.01	22/12/2014	Blood	Kerry Town	Western Area Urb	nd	Negative	Negative	36	Original
SL-055	Positive	No Cq	35.93	20/02/2015	Blood	Kerry Town	nd	nd	Negative	Negative	23	Original
SL-090	Positive	34.76	33.31	01/01/2015	Blood	Makeni	Port Loko	Koya	Negative	Negative	30	Original
SL-094	Positive	38.14	33.38	15/12/2014	Blood	Makeni	Bombali	Makari Gbanti	Negative	Negative	9	Original
SL-096	Positive	32.21	30.85	16/12/2014	Blood	Makeni	Bombali	Bombali Sebora	Negative	Negative	17	Original

SL-111	Positive	No Cq	34.42	14/01/2015	Blood	Makeni	nd	nd	Negative	n/a	43	Follow-up
SL-005	Inconc.	No Cq	34.02*	02/04/2015	Blood	Port Loko	Kambia	Masungbala	Negative	Positive	20	Original
SL-006	Inconc.	No Cq	36.04*	03/04/2015	Blood	Port Loko	Port Loko	Maforki	Negative	Negative	35	Follow-up
SL-010	Inconc.	No Cq	35.99*	04/01/2015	Blood	Port Loko	Port Loko	Marampa	Negative	Negative	16	Original
SL-050	Inconc.	No Cq	36.14*	03/01/2015	Blood	Kerry Town	Western Area Urb	nd	Negative	Negative	18	Original
SL-051	Inconc.	No Cq	35.96*	03/01/2015	Blood	Kerry Town	nd	369	Negative	n/a	25	Original
SL-070[†]	Inconc.	No Cq	35.82*	11/01/2015	Blood	Kerry Town	Western Area Urb	nd	Negative	Negative	38	Original
SL-076	Inconc.	No Cq	36.54*	20/01/2015	Blood	Kerry Town	Western Area Urb	nd	Negative	Positive	16	Original
SL-077	Inconc.	No Cq	34.83*	19/03/2015	Blood	Kerry Town	Western Area Urb	nd	Negative	n/a	48	Follow-up

SL-079	Inconc.	No Cq	35.34*	21/03/2015	Blood	Kerry Town	Western Area Urb	nd	Negative	n/a	15	Follow-up
SL-112	Inconc.	No Cq	35.38*	14/01/2015	Blood	Makeni	nd	nd	Negative	n/a	15	Follow-up

Table 3.3 Details of the samples with a qRT-PCR EBOV-positive or inconclusive result. Inconc. = inconclusive. nd = no data. n/a = not applicable because a malaria test was not performed on this sample. [†]Note that the MS2 Cq value for this sample was abnormally high, progressing to negative in subsequent tests. *Denotes that the sample was repeated in duplicate. The Cq value shown is from one replicate only, the other showed no Cq value.

3.3.2 VIRUS DETECTION BY METAGENOMIC SEQUENCING

The total number of reads generated per patient sample ranged from 598,037 to 3,047,881 (mean = 1,139,132, Table 3.4). On average, 59% of reads were of human origin (minimum 11.1%, maximum 92.0%), and 6% were of microbial origin (minimum 0.01%, maximum 75.6%). The mean number of viral reads per sample was 0.55% (minimum 0.0002%, maximum 4.96%). The number of reads specific to internal control bacteriophage MS2 ranged from 0 to 159 (Table 3.4).

Sample ID	Origin laboratory	Total reads	Chordate reads (%)	Microbial reads (%)	Bacterial reads (%)	Viral reads (%)	MS2 reads
SL-007	Port Loko	878,690	54.2	0.3	0.3	0.005	7
SL-009	Port Loko	888,242	51.9	0.8	0.8	0.025	3
SL-013	Port Loko	1,050,824	69.0	1.8	1.7	0.041	159
SL-014	Port Loko	907,837	49.8	10.3	5.3	4.960	8
SL-017	Port Loko	742,779	67.4	2.8	0.9	1.860	3
SL-018	Port Loko	624,260	92.0	0.9	0.9	0.068	2
SL-023	Port Loko	872,056	57.6	0.7	0.6	0.090	4
SL-024	Port Loko	822,202	61.0	3.3	0.4	2.920	24
SL-029	Port Loko	903,912	53.5	3.2	3.1	0.011	1
SL-041	Kerry Town	829,718	57.5	0.3	0.3	0.010	1
SL-043	Kerry Town	1,222,021	52.4	0.2	0.2	0.002	2
SL-044	Kerry Town	1,119,205	51.9	0.1	0.1	0.011	1
SL-046	Kerry Town	638,196	73.2	0.4	0.3	0.059	0
SL-058	Kerry Town	906,338	91.3	2.9	2.8	0.107	0
SL-063	Kerry Town	695,572	86.0	2.1	1.9	0.142	63
SL-065	Kerry Town	1,244,050	54.8	1.2	1.2	0.006	1
SL-071	Kerry Town	934,890	91.2	1.1	1.1	0.025	0
SL-073	Kerry Town	1,329,914	11.1	75.6	75.6	0.002	1
SL-074	Kerry Town	1,762,774	59.3	0.0	0.0	0.000	1
SL-078	Kerry Town	3,047,881	57.3	0.8	0.8	0.011	17
SL-080	Kerry Town	598,037	59.2	0.6	0.2	0.323	1

SL-082	Makeni	832,223	58.6	2.4	2.3	0.060	31
SL-086	Makeni	1,402,458	54.0	0.0	0.0	0.001	0
SL-090	Makeni	1,754,839	61.2	0.4	0.4	0.009	61
SL-091	Makeni	1,095,595	51.2	0.1	0.1	0.000	0
SL-093	Makeni	1,337,792	57.9	6.0	2.1	3.880	84
SL-095	Makeni	1,380,305	48.8	0.3	0.3	0.006	14
SL-096	Makeni	2,062,315	36.0	42.2	42.0	0.110	13
SL-097	Makeni	767,545	48.5	3.1	2.4	0.710	7
SL-098	Makeni	1,138,384	43.1	14.4	14.4	0.028	8
SL-104	Makeni	1,307,147	73.3	1.4	1.4	0.010	0
SL-108	Makeni	1,017,142	46.1	18.8	18.5	0.229	74
SL-110	Makeni	887,413	47.1	4.7	0.8	3.910	4
SL-113	Makeni	1,475,595	48.9	13.6	13.5	0.014	1
SL-116	Makeni	1,332,504	77.9	0.9	0.9	0.015	4
SL-117	Makeni	1,198,098	62.3	0.5	0.5	0.008	2
Mean	n/a	1,139,132	58.79	6.06	5.50	0.546	17

Table 3.4 Descriptive statistics for Sierra Leone patient sample sequencing data, classified using Centrifuge. Read classification statistics were generated using the Pavian web application (369).

3.3.2.1 IDENTIFICATION AND REMOVAL OF CONTAMINANT SEQUENCES

Reads matching pathogen sequences present in the negative extraction controls (NXC) and no template control (NTC) were identified as potential contaminants and removed from further analyses. These were O'nyong-nyong virus (ONNV), influenza A virus (IAV) and CHIKV (Table 3.5). Reads from patient samples that mapped to known strains handled in the laboratory were also removed from further analyses (DENV-1 strain TC861HA).

Contaminant	Reason(s) for exclusion	Number of samples showing contaminant reads	Number of contaminant reads in samples (min – max)
CHIKV	Present in NTC. Frequently handled in the laboratory.	10	2 - 316
DENV-1 strain TC861HA	Control strain handled in the laboratory.	3	2 - 410
ONNV	Present in NTC. Sequence matches known lab strain.	12	2 - 176
IAV	Reads map to only one of 8 viral genome segments. Frequently handled in the laboratory.	3	2 - 272

Table 3.5 Contaminants identified in metagenomic sequencing data.

3.3.2.2 TAXONOMIC IDENTIFICATION USING CENTRIFUGE

Taxonomic assingment of reads was performed using Centrifuge (326) with the 'Bacteria, archaea, viruses, human' database, detailed in section 2.11.1. Centrifuge outputs were filtered using a threshold of ≥0.01% of total reads. Viruses exceeding this were investigated further using mapping and assembly methods (detailed in section 2.11). Centrifuge identified four viruses known to infect humans that exceeded the threshold (Figure 3.4). These were: EBOV (*n*=1), GB virus C (GBV-C, commonly known as human pegivirus, *n*=5), hepatitis B virus (HBV, *n*=1), and human immunodeficiency virus (HIV, *n*=5). A HBV and HIV co-infection was identified in patient SL-024. At least one virus was identified by Centrifuge in eleven of the 36 patient samples sequenced. Of the three patients that were EBOV positive by qRT-PCR, only one patient had ≥0.01% total reads classified as EBOV by Centrifuge (SL-096). The other patients, SL-044 and SL-090, had eight and one EBOV-specific read(s), respectively. In the remaining 25 patients, no viruses known to infect humans were identified by Centrifuge.

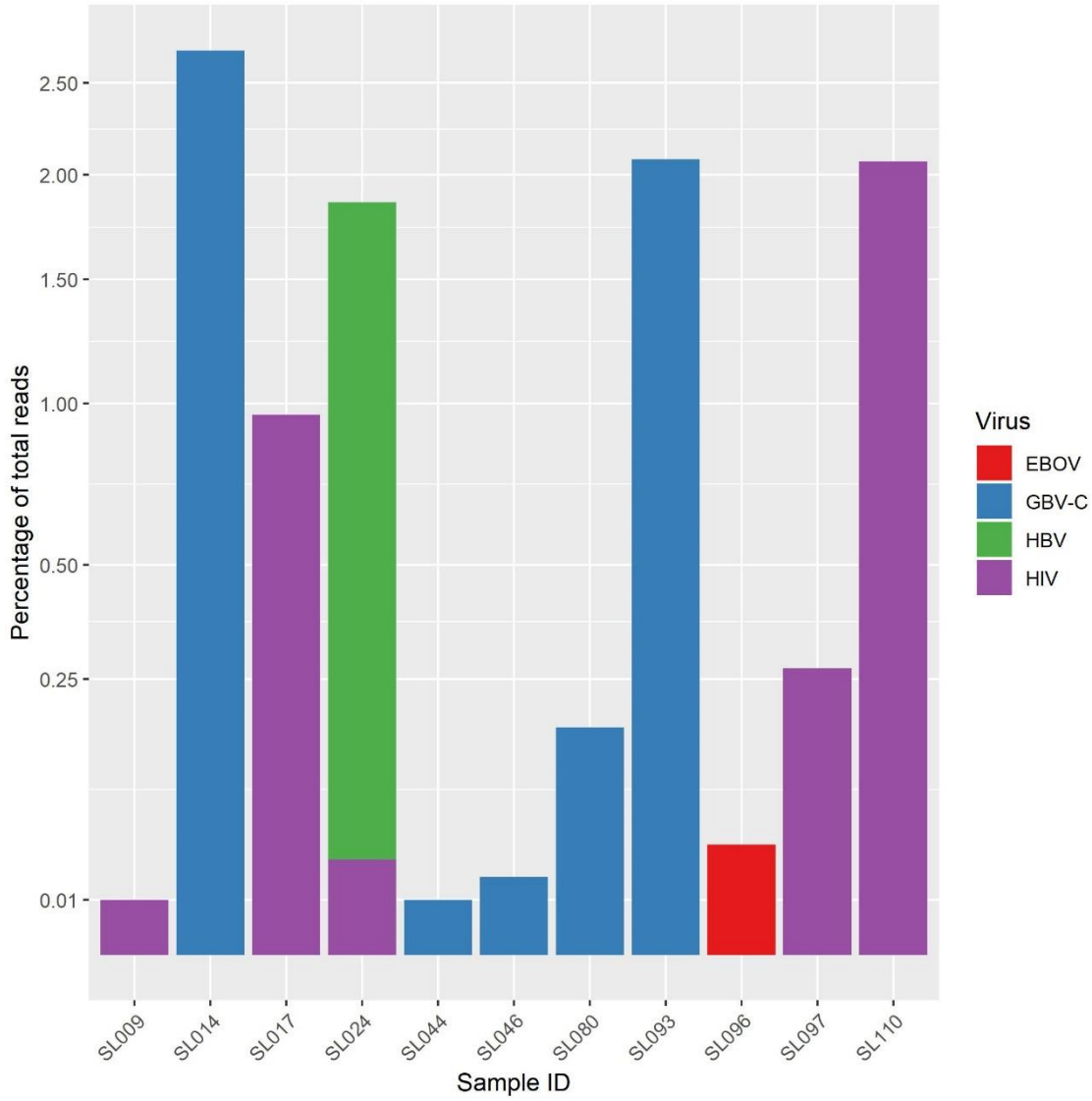

Figure 3.4 Viruses identified in the Sierra Leone cohort using Centrifuge, shown as a percentage of the total sequencing reads from each patient sample. The threshold used was ≥0.01% of total reads.

3.3.2.3 IDENTIFICATION OF VIRUS-SPECIFIC SCAFFOLDS FROM *DE NOVO* ASSEMBLY

Following removal of human reads, *de novo* assembly and subsequent data analysis were performed as described in section 2.11. 10/36 samples contained scaffolds with homology to a pathogenic human virus, the remaining 26 samples did not contain any such scaffolds. Scaffolds with protein sequence homology to GBV-C, HBV, human herpesvirus-8 (HHV-8), HIV-1 and EBOV Zaire were identified (Table 3.6). A complete list of scaffold details including length, coverage and matching accessions is provided in Appendix 5.

Sample ID	GBV- C	HBV	HHV-8	HIV-1	EBOV Zaire
SL-014	2	-	-	-	-
SL-017	-	-	-	23	-
SL-024	-	3	-	2	-
SL-071	3	-	-	-	-
SL-080	6	-	-	-	-
SL-093	4	-	-	-	-
SL-096	-	-	-	-	8
SL-097	-	-	-	14	-
SL-110	-	-	-	92	-
SL-117	-	-	1	-	-

Table 3.6 A summary of the number of *de novo* assembled scaffolds with protein sequence homology to human viruses, for each sample, identified using Kaiju.

3.3.2.4 IDENTIFICATION OF VIRUS-SPECIFIC READS BY MAPPING TO REFERENCE GENOMES

Mapping to multiple reference genomes identified reads specific to DENV-4, EBOV, GBV-C, HBV, HIV, RVFV, YFV and ZIKV (Table 3.7). In some cases, very few internal control (MS2) reads were present but other virus-specific reads were present in relatively large numbers, for example sample SL-110 which contained 135,835 reads mapping to HIV, despite none mapping to MS2.

Sample ID	DENV-4	EBOV	GBV-C	HBV	HIV	RVFV	YFV	ZIKV	MS2
SL-007									8
SL-009			6		532	2			4
SL-013		2			4				180
SL-014			101,234	2	2				6
SL-017			9	2	35,686				6
SL-018					2				
SL-023		2	2					284	8
SL-024			14	25,604	1,127				12
SL-029		4							
SL-041									
SL-043		8							
SL-044			313		12				
SL-046			624	4	6				
SL-058	2		32	4			8		2
SL-063			10						12
SL-065									2
SL-071			250			8			
SL-073								2	
SL-074									
SL-078					8				18
SL-080			4,396						20
SL-082									
SL-086			18						
SL-090		6			14		2		54
SL-091					6				
SL-093			129,663						103
SL-095									18
SL-096		3128							12
SL-097					7,048				12
SL-098									10
SL-104									
SL-108									91
SL-110			6		135,835				
SL-113									
SL-116									4
SL-117					12				2

Table 3.7 Virus-specific sequencing reads from Sierra Leonean metagenomic sequencing of febrile patient plasma, identified by mapping to virus reference sequences. MS2 is the internal control.

For samples containing virus-specific reads, genome coverage was assessed at 1x and 5x coverage, and read coverage across the genome was plotted for samples containing a virus with ≥20% genome coverage at 5x coverage (Figure 3.5). GBV-C was present in five samples (SL-014, SL-044, SL-046, SL-080 and SL-093, 34.0 – 99.7% genome coverage, Figure 3.5A), HIV in 5 samples (SL-009, SL-017, SL-024, SL-097 and SL-110, 71.6 – 91.8% genome coverage, Figure 3.5B), HBV in one sample (SL-024, 100.0% genome coverage, Figure 3.5C) and EBOV in one sample (SL-096, 45.5% genome coverage, average coverage depth at each base was 55 reads, Figure 3.5C). To investigate the presence of the HHV-8 scaffold from sample SL-117, non-human reads were mapped to reference genome HHV-8 GK18 (NC_009333.1), however no reads mapped.

A)

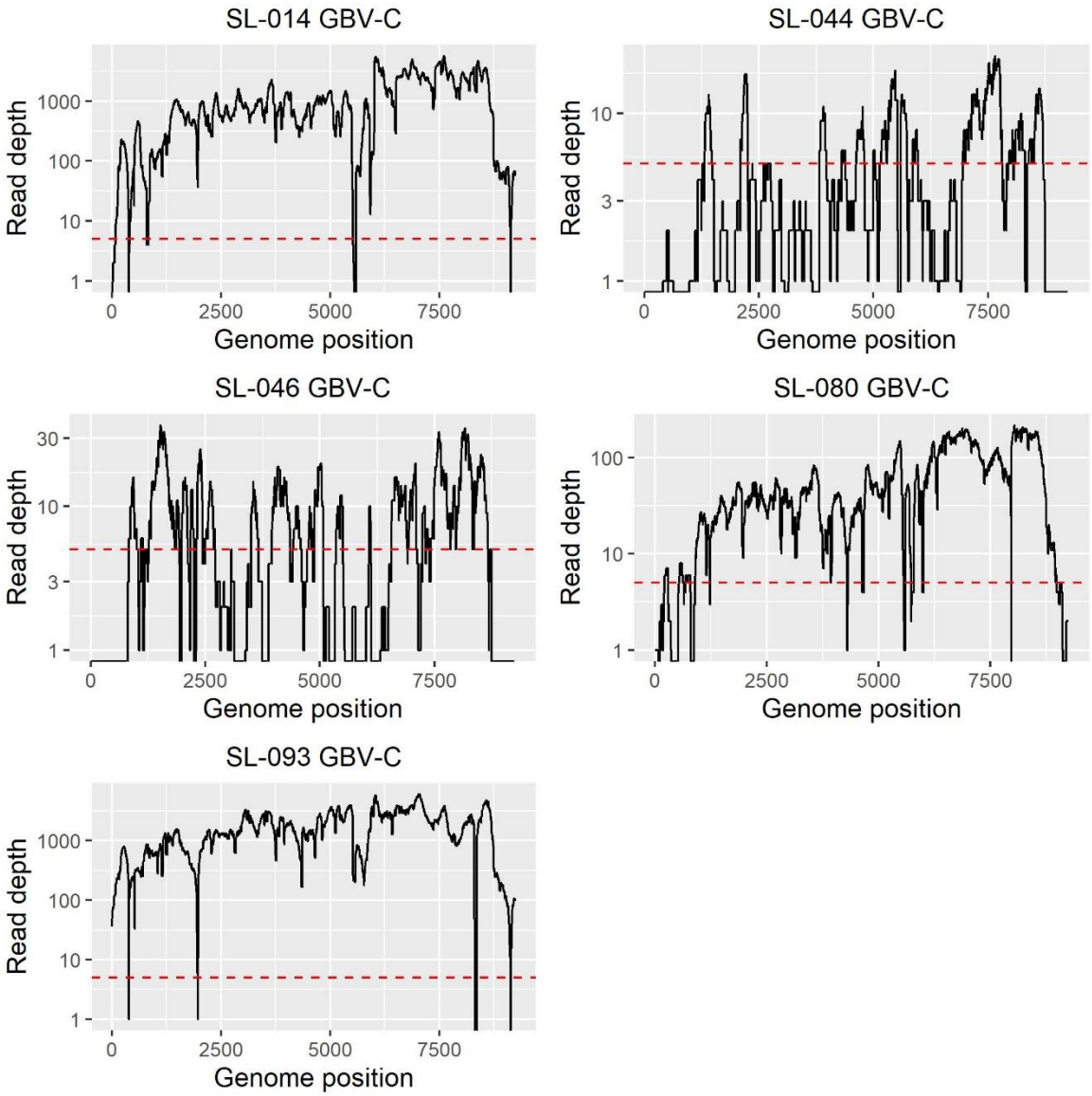
SL-014 GBV-C
Read depth
1000
100
10
1
0
2500
5000
7500
Genome position
SL-044 GBV-C
Read depth
10
3
1
0
2500
5000
7500
Genome position
SL-046 GBV-C
Read depth
30
10
3
1
0
2500
5000
7500
Genome position
SL-080 GBV-C
Read depth
100
10
1
0
2500
5000
7500
Genome position
SL-093 GBV-C
Read depth
1000
100
10
1
0
2500
5000
7500
Genome position

B)

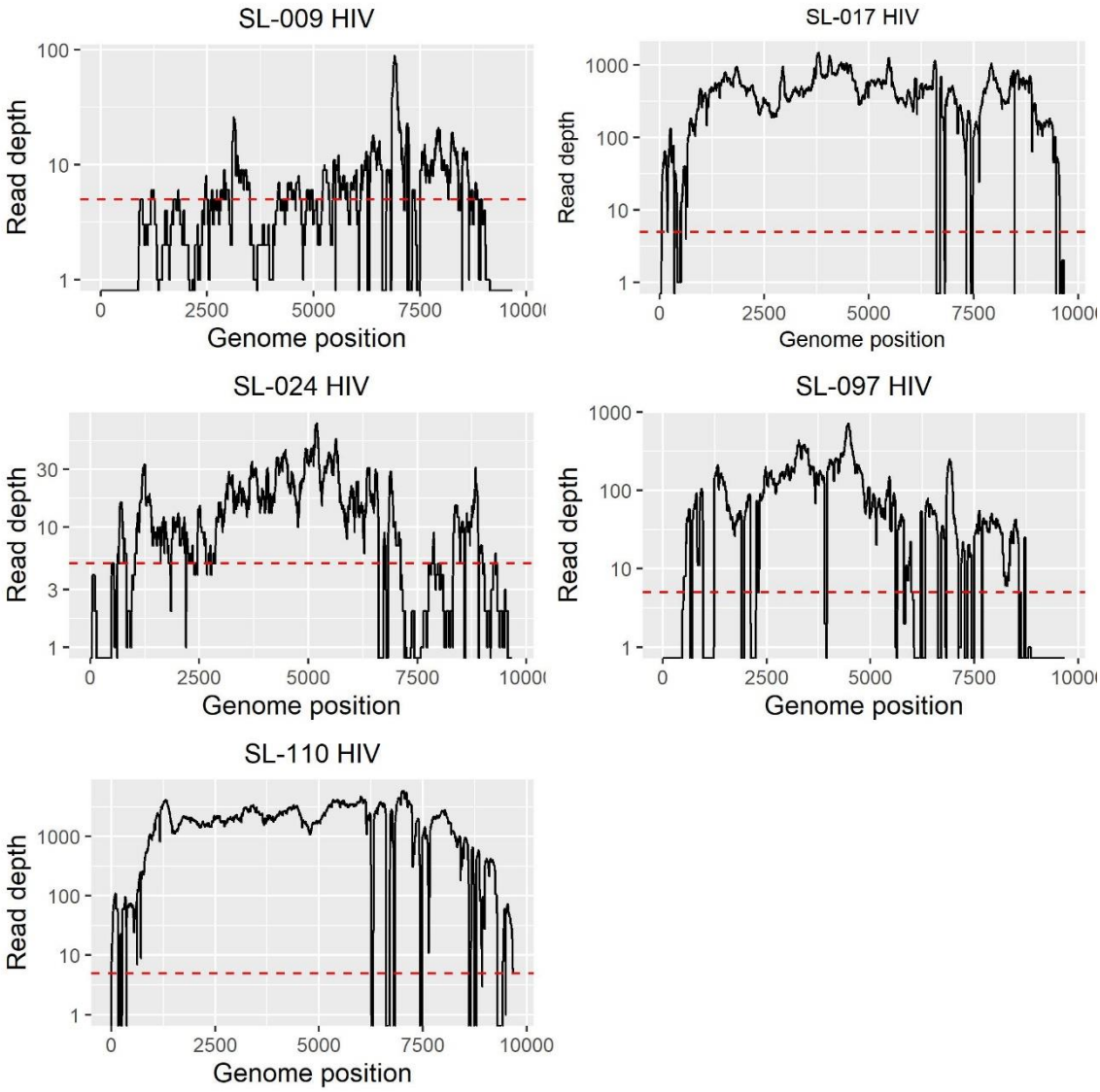
SL-009 HIV
Read depth
100
10
1
0
2500
5000
7500
10000
Genome position
SL-017 HIV
Read depth
1000
100
10
1
0
2500
5000
7500
Genome position
SL-024 HIV
Read depth
30
10
3
1
0
2500
5000
7500
Genome position
SL-097 HIV
Read depth
1000
100
10
1
0
2500
5000
7500
Genome position
SL-110 HIV
Read depth
1000
100
10
1
0
2500
5000
7500
10000
Genome position

C)

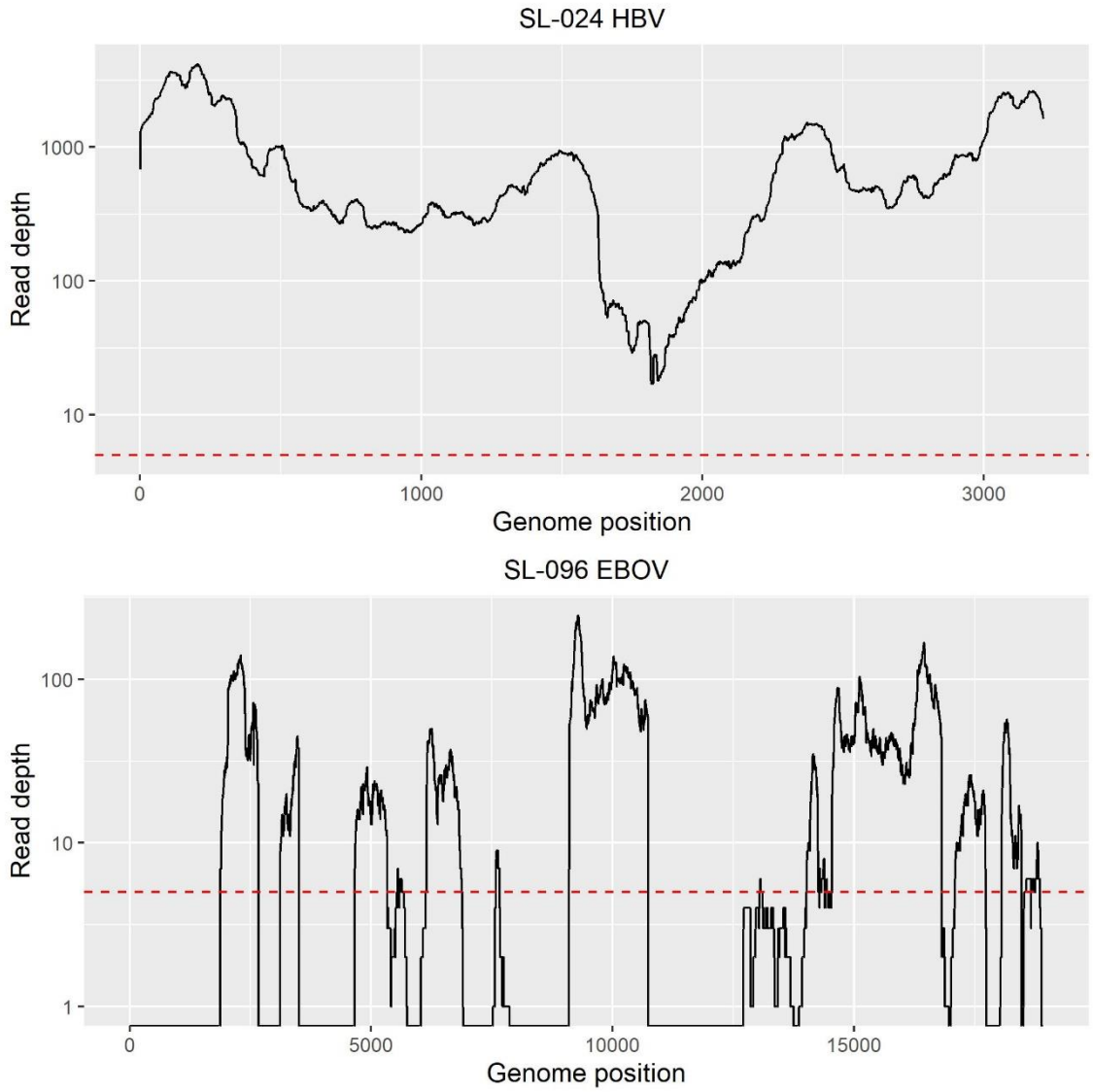

Figure 3.5 Coverage of viral genomes from metagenomic sequencing from patient plasma samples, generated by mapping reads to a reference genome. The red dotted line indicates 5x coverage. **A)** GBV-C genome coverage from five patient plasma samples. **B)** HIV genome coverage from five patient plasma samples. **C)** HBV (above) and EBOV (below) genome coverage from two separate patient plasma samples.

3.3.2.5 SUMMARY OF VIRUSES DETECTED BY METAGENOMIC SEQUENCING

In summary, through a combination of taxonomic classification, *de novo* assembly and mapping to reference genomes, EBOV (*n*=1), GBV-C (*n*=5), HBV (*n*=1) and HIV (*n*=5) were detected in patient plasma samples using metagenomic sequencing (Table 3.8).

Sample	Virus	Reads assigned by Centrifuge†	% of total reads assigned by Centrifuge	Reads mapped	Genome coverage 1x (%)	Genome coverage 5x (%)	Virus-specific assembled scaffolds	Scaffold length (bp, min-max)
SL009	HIV	168	0.01	532	81.4	48.6	0	na
SL014	GBV-C	44,261	2.69	101,234	99.3	97.7	2	342-8949
SL017	HIV	13,194	0.96	35,686	97.4	95.8	23	306-2022
SL024	HBV	22,023	1.42	25,604	100.0	100.0	3	558-2530
	HIV	88	0.01	1,127	90.7	71.6	2	767-1426
SL044	GBV-C	118	0.01	313	80.1	34.0	0	na
SL046	GBV-C	258	0.02	624	72.5	52.4	0	na
SL080	GBV-C	1,913	0.17	4,396	96.6	89.3	6	323-3249
SL093	GBV-C	51,303	2.08	129,663	99.7	99.7	4	314-5861
SL096	EBOV	1,479	0.04	3,128	57.4	45.8	8	536-2974
SL097	HIV	3,992	0.27	7,048	74.9	71.6	14	322-1446
SL110	HIV	34,320	2.07	135,835	95.2	94.8	92	307-1258

Table 3.8 Summary of viral reads identified from Sierra Leonean patient plasma samples by metagenomic sequencing. The threshold used for detection was ≥20% 5x genome coverage. Only virus-specific scaffolds of specified quality were counted (≥2 mean coverage, ≥300 bp). na = not applicable.

3.3.3 COMPARATIVE ANALYSES OF GBV-C, HBV AND HIV SEQUENCES

3.3.3.1 GB VIRUS C

Patient GBV-C consensus sequences were analysed using BLASTn to identify the most closely related genome sequences from the NCBI nr/nt database. All five genomes were most closely related to genomes from Sierra Leonean patients with EBOV and GBV-C co-infections, June 2014, sequenced by Gire *et al.* (412) and analysed by Lauck *et al.* (413) (Table 3.9).

Patient sequence ID	Best BLASTn match (accession)	Description	Query cover (%)	Identity (%)	Country of origin	Date sampled	Reference
SL-014	KM670099.1	GB virus C isolate G3765.2 polyprotein	97.00	92.79	Sierra Leone	14/06/14	(413)
SL-044	KM670101.1	GB virus C isolate G3850 polyprotein gene, complete cds	26.00	94.29	Sierra Leone	18/06/14	(413)
SL-046	KM670107.1	GB virus C isolate G3826 polyprotein gene, complete cds	46.00	92.34	Sierra Leone	16/06/14	(413)
SL-080	KM670102.1	GB virus C isolate G3825 polyprotein	82.00	94.63	Sierra Leone	16/06/14	(413)
SL-093	KM670109.1	GB virus C isolate G3808 polyprotein	99.00	92.36	Sierra Leone	15/06/14	(413)

Table 3.9 GBV-C genomes from the NCBI nt database identified as most closely related to each patient genome, using BLASTn.

3.3.3.2 HEPATITIS B VIRUS

The single HBV genome originated from a 38-year-old patient from Port Loko district, who also had an HIV infection. The full-length HBV consensus sequence was most similar to a genotype E strain originating from a patient in Guinea in 2006 (100% query coverage, 98.7% sequence identity, BLASTn). To confirm the genotype and put the sequence in the context of the wider picture of HBV phylogeny, the patient sequence was aligned with representative HBV genomes and the resulting phylogenetic tree confirmed that the HBV genome from patient SL-024 clusters with sequences from the genotype E group (Figure 3.6). Poor resolution within the genotype E group precluded further comment on the relationship between individual sequences and geographical origin.

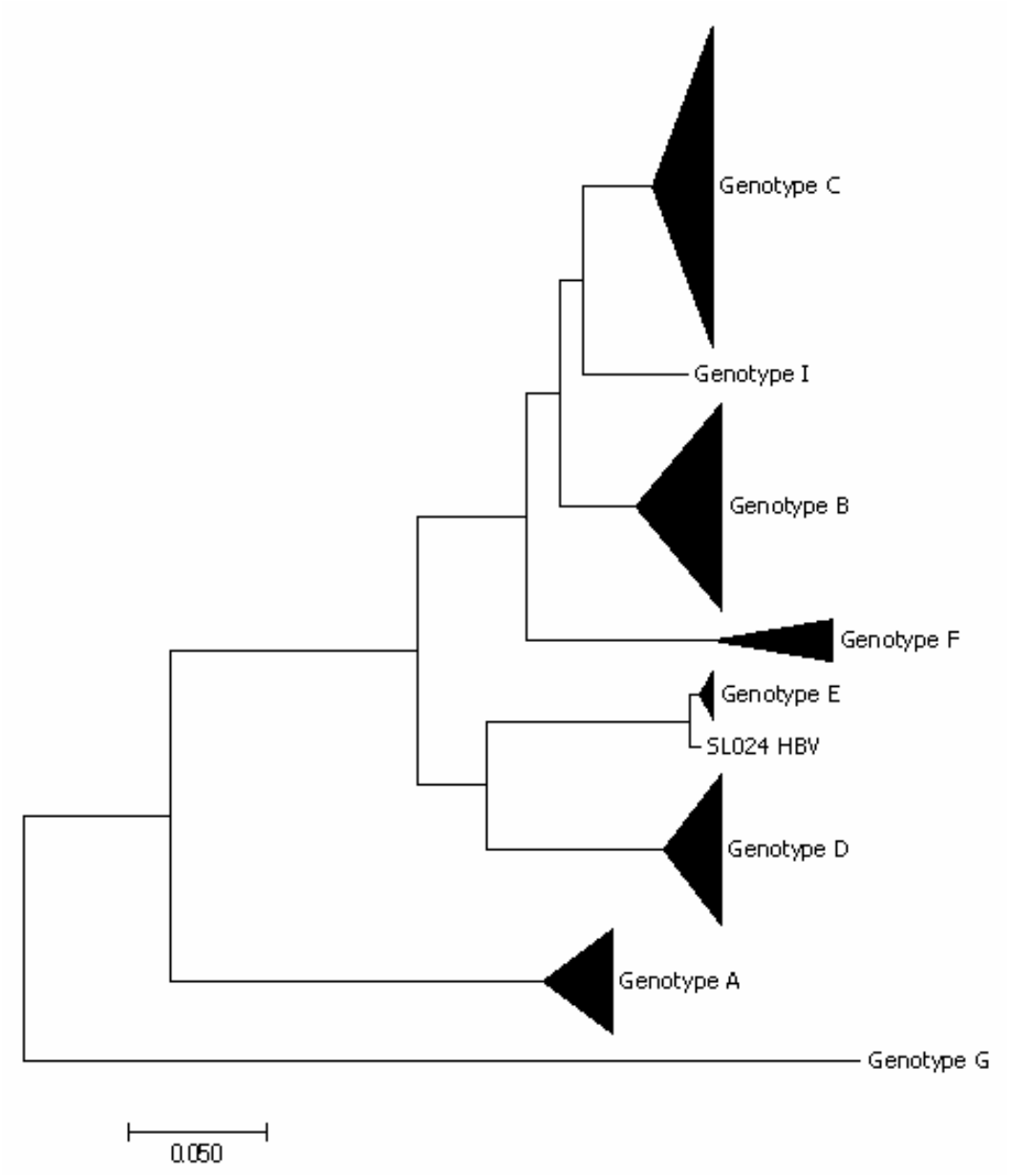

Figure 3.6 Molecular phylogenetic analysis of 213 complete HBV genomes. The evolutionary history was inferred by using the Maximum-Likelihood method based on the Tamura-Nei model (414) in MEGA7 (415). The single sequence generated from this study is labelled SL024 HBV.

3.3.3.3 HUMAN IMMUNODEFICIENCY VIRUS

The five HIV-positive patients identified in this study originated from two districts; Port Loko (*n*=3) and Bombali (*n*=2). All five were adults aged 21-39 years old (Table 3.10). The HIV genome sequences generated ranged from 75-99% coverage. All genomes showed high similarity to sequences belonging to HIV-1 group M, strongly suggesting that the patient strains also belong to this group (Table 3.10). Sequence similarity in the pol gene was assessed in an effort to determine viral subtypes for HIV genomes SL-017 and SL-110. Genomes SL-014, SL-024 and SL-097 were excluded from this analysis because the pol gene was not present with sufficient depth of coverage (5x coverage at all positions). SL-017 was most similar to subtype CRF02_AG across the pol gene, SL-110 was most similar to CRF02_AG throughout the majority of the gene however a small region showed higher similarity to subtype A1 (Figure 3.7).

Patient sequence ID	Patient district	Patient age	Best BLASTn match (accession number)	Nucleotide identity (%)	Query coverage (%)	Country of origin	Year sampled	HIV-1 group
SL-009	Port Loko	21	EU786671.1	92.55	33.00	Spain	2006	M
SL-017	Port Loko	28	AB485635.1	93.5	92.00	Djibouti	nd	M
SL-024	Port Loko	38	AB485634.1	92.24	67.00	Djibouti	nd	M
SL-097	Bombali	38	KM050646.1	93.86	28.00	Zambia	2000	M
SL-110	Bombali	39	AB485634.1	92.58	94.00	Djibouti	nd	M

Table 3.10 HIV genomes from the NCBI nt database identified as most closely related to each patient genome, using BLASTn. nd = no data.

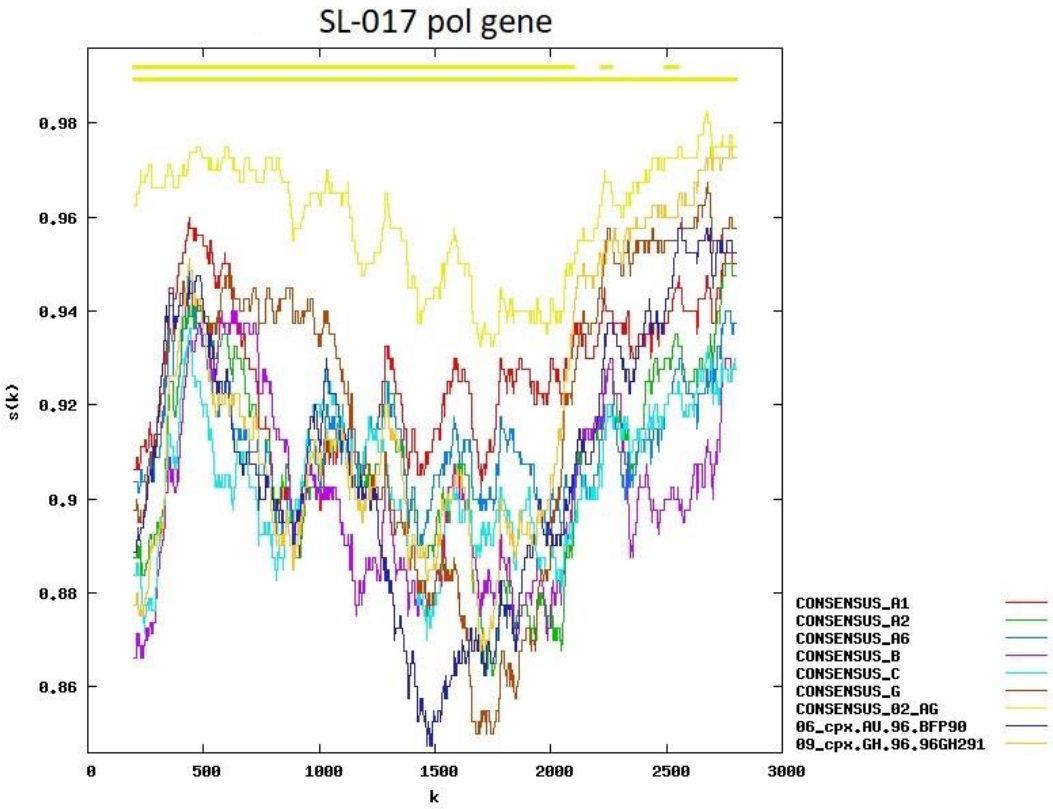
SL-017 pol gene
s(k)
k
0.98
0.96
0.94
0.92
0.9
0.88
0.86
0
500
1000
1500
2000
2500
3000
CONSENSUS_A1
CONSENSUS_A2
CONSENSUS_A6
CONSENSUS_B
CONSENSUS_C
CONSENSUS_G
CONSENSUS_02_AG
06_cpx.AU.96.BFP90
09_cpx.GH.96.96GH291

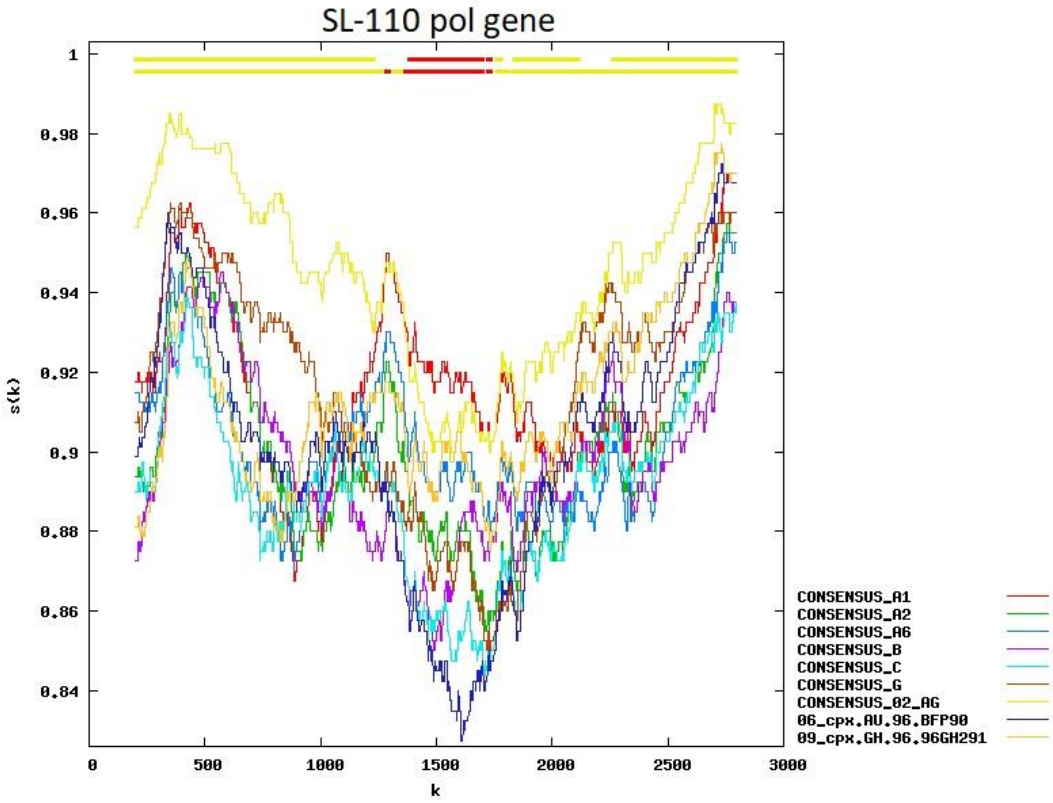
SL-110 pol gene
s(k)
k
1
0.98
0.96
0.94
0.92
0.9
0.88
0.86
0.84
0
500
1000
1500
2000
2500
3000
CONSENSUS_A1
CONSENSUS_A2
CONSENSUS_A6
CONSENSUS_B
CONSENSUS_C
CONSENSUS_G
CONSENSUS_02_AG
06_cpx.AU.96.BFP90
09_cpx.GH.96.96GH291

Figure 3.7 Plots showing the similarity of a number of HIV-1 subtypes to two HIV-1 sequences generated from Sierra Leone patient samples SL-017 and SL-110. Plots were generated using the Recombinant Identification Program (RIP) (385). Each patient sequence was aligned against a custom RIP background, consisting of representative sequences for HIV subtypes A1, A2, A6, B, C, G, CRF02_AG, CRF06_cpx and CRF09_cpx (colours indicated in legend). The x-axis (k) represents the query sequence position at the centre of the moving window (400 bp). The y-axis, s(k), shows the similarity between that window of sequence and each of the background sequences. The two bars across the top of the graph represent the 'best match' (lower bar, the background sequence with the highest similarity to the query) and the significance of this match (upper bar). The upper bar shows colour at positions where the best match is significantly better than the second match.

3.3.4 INVESTIGATION OF EBOLA VIRUS POSITIVE RESULTS

The detection of EBOV RNA in eight patient samples using qRT-PCR is concerning, because (to the best of the author's knowledge) these patients would have been treated as EBOV negative following a negative qRT-PCR result in the field. To investigate whether the discrepancy in qRT-PCR results could have occurred due to assay sensitivity issues stemming from primer/probe mismatches, the SL-096 EBOV genome sequence was analysed to look for primer/probe mismatches in the relevant assays.

Primer/probe sequences for the RealStar Filovirus Screen RT-PCR Kit 1,0 (Altona Diagnostics, UK), targeting the L gene, are not publicly available. Primer/probe sequences for the Zaire-specific Trombley and pan-EBOV assays are (Table 3.11).

Primer/probe sequences were aligned with the SL-096 EBOV genome sequence and a closely related reference sequence (Zaire_Makona_2014, accession KM233070.1), which was used to map patient reads and generate the SL-096 consensus sequence. The Trombley primer/probe sites were missing from the SL-096 sequence as no reads covered this area of the genome, however, the reference genome sequence was identical to the Trombley primer/probe sequences (Table 3.11). The pan-EBOV primer/probe sites were present in the patient genome; no mis-matches were detected with the SL-096 genome or the reference genome (Table 3.11).

Assay name	Target gene	Oligo type	Oligo name	Sequence (5'-3')	Position	Match to refseq	Match to SL-096
Trombley (Zaire-specific)	NP	Primer	F565 Zaire	TCTGACATGGATTACCACAAGATC	518-541	Yes	Site not present
	NP	Primer	R6405 Zaire	GATTGTTCGGCAAAGAGTCATCC	594-571	Yes	Site not present
	NP	Probe	P597S Zaire	FAM-AGGTCTGTCCGTTCAA-MGB	550-565	Yes	Site not present
Panning (Pan-EBOV)	L	Primer	FiloA_Ebola	AAGCMTTTCCHAGCAAYATGATGGT	13,340-13,364	Yes	Yes*
	L	Primer	FiloB_Ebola	ATGHGGTGGATTATAATAATCACTDACATG	13,632-13,603	Yes	Yes
	L	Probe	FAMEBO_DEGEN	FAM-CCRAAATCATCACTBGTRTGGTGCCA-MGB	13,411-13,436	Yes	Yes

Table 3.11 Primer and probe details for two EBOV qRT-PCR assays. Altona (no primer/probe details available) and Trombley assays were used in the field laboratories, Trombley and Panning assays were used in this project. Refseq = reference sequence KM233070. *Site only partially covered at 5x coverage (8 bases have 5x coverage or less. The minimum coverage is 4x. At each position, all reads show the same base, this base matches the reference and therefore also matches the primer sequence).

To investigate whether the change from the Altona assay to the Trombley assay could be related to these potentially missed EBOV cases, the dates the samples were taken were looked at. Seven of the eight EBOV-positive samples were collected and tested before the date the laboratories changed from the Altona to the Trombley assay, suggesting they were tested using the Altona assay (Figure 3.8). The sample that was collected and tested in February (SL-055), following the assay change, has the highest Cq value of all EBOV-positive samples (Cq 35.9) and is close to the limit of detection of the Trombley assay. In contrast to the retrospective EBOV-positive/field EBOV-negative samples, the ten samples that tested EBOV-inconclusive by qRT-PCR (Table 3.3) show no obvious pattern with regard to the date they were collected and tested.

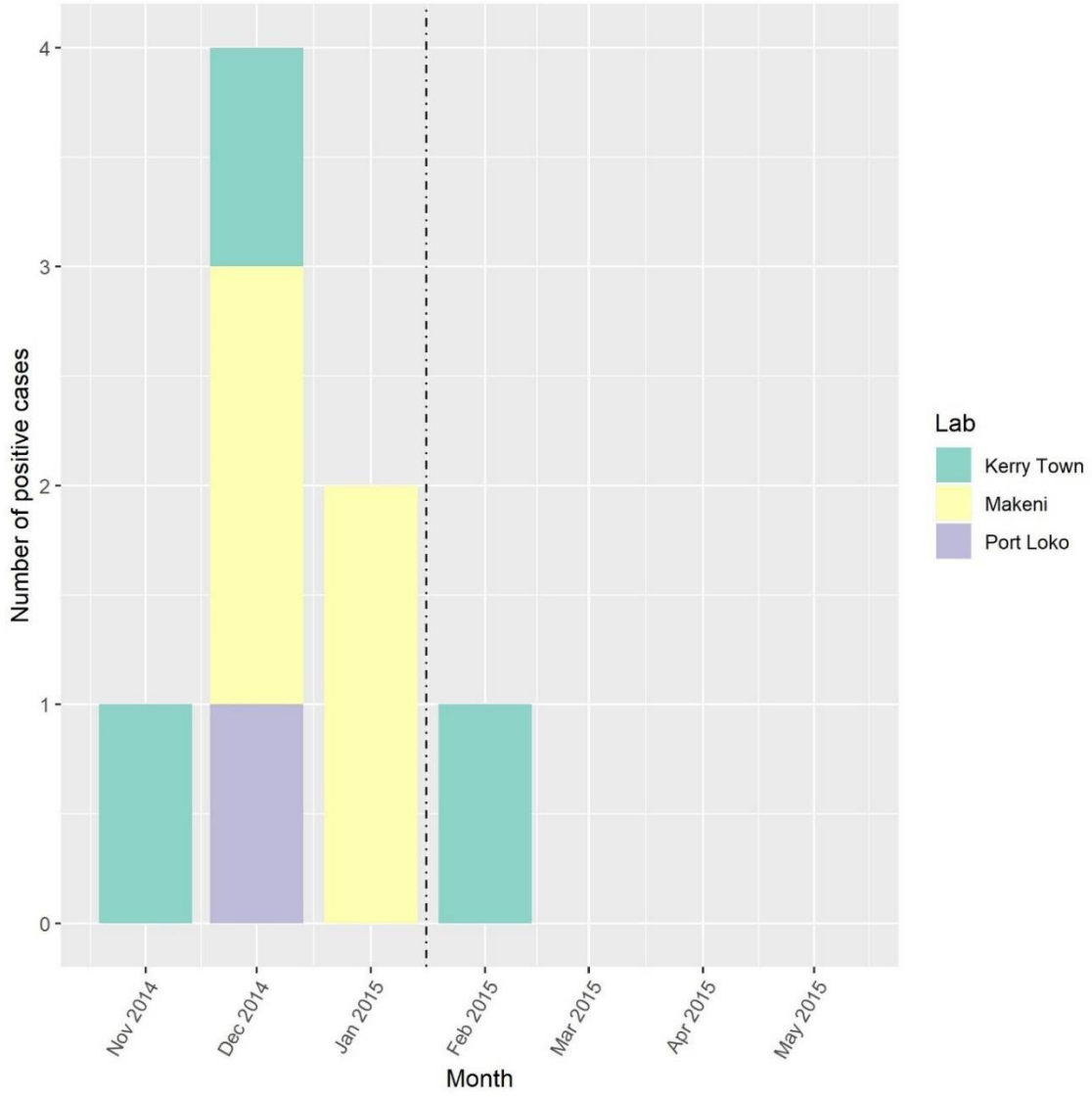

Figure 3.8 Timeline showing the date of collection and qRT-PCR testing for the eight patient samples that tested negative upon initial testing in the field, then positive upon subsequent testing during this project. Colour indicates the field laboratory samples were tested in. Black dashed line indicates the time at which laboratories switched from the Altona qRT-PCR to the Trombley qRT-PCR.

3.4 DISCUSSION

3.4.1 RT-PCR/PCR TESTS DETECTED PLASMODIUM, EBOLA VIRUS AND LEPTOSPIRA IN FEBRILE PATIENTS

Pathogen detection in a cohort of 120 Sierra Leonean febrile patient plasma samples began with an effort to detect eleven pathogens known to circulate in Africa at present or in the past, using RT-PCR/PCR assays. Prior to discussing results, some anomalies require attention with regard to the patient samples. Sample SL-072 is labelled in the metadata as an 'unknown swab', however, it has a *Plasmodium* RDT result, which is only possible from a blood sample. It seems likely that there was an error when recording metadata and that this sample is in fact blood, however it is not possible to know this for certain therefore results for this sample should be treated with caution. Sample SL-070 showed an abnormally high MS2 qRT-PCR Cq value, subsequently progressing to become MS2 negative in repeat tests, therefore RT-PCR/PCR results for this sample cannot be relied upon as there could be inhibiting substances present in the sample.

RNA from patient samples was tested using qRT-PCR, RT-PCR and PCR assays targeting individual pathogens and *Leptospira* (*n*=1), *Plasmodium* (*n*=22) and EBOV (*n*=8) was detected. Leptospirosis is a relatively common bacterial infection with a worldwide distribution, transmitted through contact with urine from infected animals. Despite its common occurrence, little is known about the true incidence in affected areas (289). The detection of *Plasmodium* in 22 patients is consistent with the wider incidence of malaria in Sierra Leone. Malaria was the cause of the highest proportion of disability-adjusted life years (DALYs) in Sierra Leone in 2014, 2015 and 2017 (45). Malaria prevalence in this study cohort is 18%, markedly lower than the national average of 36% in 2014-2015 (45). The reasons for this are likely to be multi-factorial and it's possible that individuals suspecting they have malaria would not present at an ETC for fear of

exposure to EBOV. In just over 1 in 10 samples tested, there is a difference between the field RDT *Plasmodium* result and the RT-PCR result from this project. 6.7% of the samples positive by RT-PCR were negative by RDT. Conversely, 4.2% of RDT-positive sample were RT-PCR-negative.

Abbott manufactures both RDTs used in the field laboratories. The sensitivity of the BinaxNOW RDT for *P. falciparum* is stated by the manufacturer as 99.7% and specificity is 94.2% (for parasitaemia levels >5,000 parasites/µl) (416). The manufacturer states that the SD Bioline Malaria Ag P.f. RDT sensitivity is 99.7% for *P. falciparum* and 95.5% for non-*P. falciparum* species. The specificity is 99.5% (417), however, it is not clear what detection method the RDTs were compared against. A study comparing sensitivity and specificity of three RDTs (including both Abbott devices) with PCR for *Plasmodium* detection determined the sensitivity and specificity of the RDTs to be lower; 71-75% and 80-84%, respectively (418).

The RT-PCR used in this study is based on an assay capable of detecting all four plasmodium species (362). The assay is reported to detect to a limit of one parasite in 50 ml of whole blood and in comparative studies was shown to be more sensitive than a microscopy-based method (362). Without a direct comparison of the RDT method with the RT-PCR using a panel of known Plasmodium positive/negative samples, it is not possible to meaningfully compare the sensitivity and specificity of the two methods. Furthermore, data on which RDT was used to test each patient sample in the field was not available.

The lack of detection of CCHFV, RVFV and ZIKV is consistent with current information on virus distributions. Though considered endemic in Africa, no evidence of CCHFV has

been reported from Sierra Leone to date (419). Similarly, no outbreaks of RVFV have been reported, although the WHO classifies the country as at risk based on virological and/or serological evidence (420). Although the ZIKV vector is present, no cases of infection have been reported to date (421).

Cases of yellow fever have been reported from Sierra Leone, most recently in 2011, however vaccination campaigns have helped keep incidence low (422). Rickettsial disease is described throughout Africa, resulting from infection with a variety of bacterial species (423). Published information on the distribution and frequency of rickettsial infections in Sierra Leone specifically is not available, with the exception of a single paper from 1986 showing that 5.3% of the cohort tested were seropositive for antibodies to spotted fever-group *Rickettsiae* (424).

LASV is endemic in Sierra Leone and much of surrounding West Africa. Transmission is usually by contact with infected rodents or rodent excrement, infections are known to follow a seasonal pattern in which outbreaks typically occur between December and March (104). Given that the samples were taken during LASV season and the clinical signs of disease overlap considerably with EBOV, it seemed likely that LASV would be detected in some patients in this study, however, no cases of infection were identified.

CHIKV has been identified in nearly 40 countries to date, including those in sub-Saharan Africa (425). The virus caused outbreaks during the 1950s-1970s (426), then seemingly disappeared during the 1980s before re-emerging in the early 2000s (427,428). CHIKV was detected by serosurveillance in Sierra Leone in 1972 (429), then again in 2012 in the town of Bo where anti-CHIKV IgM antibodies were detected in 400 people (430). Despite not being detected in this study, it is well known that DENV infection occurs in Sierra

Leone and dengue fever is ubiquitous throughout the tropics (22). The samples in this study were collected during the dry season, during which the risk of transmission viruses with mosquito vectors are lower (22). This could explain the lack of detection of arboviruses such as CHIKV and DENV in this study.

3.4.2 EBOV RNA WAS DETECTED IN PATIENTS DEEMED EBOV-NEGATIVE IN THE FIELD

Despite all samples testing EBOV-negative using qRT-PCR in the field, eight patient samples tested retrospectively positive for EBOV by qRT-PCR and a further ten samples gave an inconclusive result. The high Cq values of the EBOV-positive samples indicate a low level of viral RNA, which could be the reason they were not detected in the field during initial testing. A field study by Broadhurst *et al.* (431) assessed the utility of an EBOV RDT by comparing sensitivity and specificity with the Altona qRT-PCR, which at the time was established in the two field laboratories involved in the study. The authors explain that during the study, they became aware that the Altona assay had imperfect sensitivity. This was discovered when the Trombley assay was used in conjunction with the Altona assay to test 16 samples that showed discordant results between the RDT and the Altona assay. Six samples tested positive by the Trombley assay (Cq value range 29.1–39.8), one of the six also tested newly positive by the Altona assay (Cq value 28.4) (431). The authors suggest that there is a drop-off in sensitivity in the Altona assay above a Cq value of approximately 30. This fits with the results from the EBOV-positive samples in this project, from which a Cq value range of 30.9-35.9 is observed using the Trombley assay. This, coupled with the timescale of the change from Altona to Trombley in the field laboratories, suggests that these samples may have been tested using the less sensitive Altona assay in the field and interpreted as negative.

It is worth noting that a number of the EBOV-positive (2/8) and inconclusive (4/10) samples are labelled as 'follow-up (treatment centre)' in the 'sample status' field of the metadata. An 'original' sample means that the blood sample was drawn from the patient on first admission to the ETC. Despite enquiries, it has not been possible to determine the exact meaning of 'follow-up (treatment centre)'. One possibility is that the patient was referred from another medical facility or 'holding centre', in which case the sample is akin to an 'original' sample. Another possibility is that the patient previously had a EBOV-positive qRT-PCR result and this sample is a follow up blood sample from the convalescing patient. In the latter case, the implications of a positive test result differ from the former, as the patient would have been a known EBOV positive and treated as such.

Three EBOV-positive patient samples were sequenced using the metagenomic approach. Of the three, one sample (SL-096) produced sufficient EBOV-specific reads to generate a partial consensus sequence, covering 46% of the genome at an average depth of 55 reads per base. This depth of coverage is consistent with data from a previous study that compared qRT-PCR Cq values with the average sequence depth in 179 clinical samples (40).

The pan-EBOV qRT-PCR primer/probe sequences were compared with the patient SL-096 EBOV sequence, confirming that there were no mismatches in either the patient sequence or a closely related reference sequence and confirming that this assay is suitable for use with this patient cohort. For the assays used in the field (Altona and Trombley) it was not possible to assess primer/probe suitability effectively. For the Altona assay this was because the primer/probe sequences are unavailable due to its commercial nature. For the Trombley assay the primer binding sites were not present in

the SL-096 sequence. Although the closely related reference sequence showed 100% match to the primer/probe set, it is not possible to know if there were polymorphisms present in the patient sequence which could have had a negative impact on assay sensitivity.

It is difficult to improve the coverage of the patient EBOV genome using metagenomic sequencing because the amount of viral RNA in this particular set of patient samples is low. Of the EBOV-positive samples identified by qRT-PCR, sample SL-096 had the lowest Cq value and therefore should contain the highest amount of RNA. Metagenomic sequencing generated 46% of the EBOV genome at 5x coverage and 57% at 1x coverage and it is unlikely that sequencing additional samples with higher Cq values would result in improved coverage, furthermore, this is not a cost-effective way of generating this data. Another approach, such sequencing amplicons from a multiplex tiling PCR primer scheme (343), would be a better way forward.

3.4.3 METAGENOMIC SEQUENCING DETECTED HIV, HBV AND HUMAN PEGIVIRUS IN FEBRILE PATIENTS

Metagenomic sequencing of 36 febrile patient plasma samples produced viral genome sequences for GBV-C (*n*=5), HIV (*n*=5), HBV (*n*=1) and EBOV (*n*=1). A complete HBV genome was generated from patient SL-024; a 38-year-old from Port Loko who was co-infected with HIV. Sierra Leone is considered a high-endemic area for HBV; the estimated prevalence in Africa as a whole is 6.1% (432). Previous studies of different groups in Sierra Leone identified antibodies in 18% of primary school children (433), 6% of pregnant women of middle and high socio-economic class (434), and 13-15% of blood donor candidates in Tonkolili district (435). The patient genome sequence from this

study shows high similarity to HBV genotype E. This is consistent with results of a meta-analysis of >900 publications of HBV genotyping data which showed that genotype E is predominant in West Africa and is responsible for 17.6% of HBV infections globally, 97% of which occurred in sub-Saharan Africa (436).

HIV prevalence during 2018 in Sierra Leone was 1.5% in adults aged 15-49, with an estimated 63,000 adults and 6,600 children living with HIV infection (402). A study investigating HIV prevalence in suspected EVD patients from 2015 observed a high prevalence (17.6%) among 678 EVD-negative patients tested using antibody detection methods (437). HIV prevalence in the present study cohort is considerably lower at 4.2%. It's possible that some HIV-positive patients were not detected in the present study, for example in cases where patients were on an effective antiretroviral therapy regimen and viral load was very low. This is a limitation of using a nucleic acid-based method to detect infection, and further confirmatory testing would be required to produce an accurate prevalence figure. It is also possible that variation in prevalence exists through the country, and/or that the relatively small sample size does not accurately reflect the true prevalence in the population.

HIV as a species has very high genetic diversity (438), therefore an agnostic metagenomic approach is an advantage for detecting this virus. Prior knowledge of the viral sequence is not required, and the sequence data generated can be used to identify viral group, subtype and recombinants. This information is useful for tracking viral evolution and epidemiology (439). Both HIV and HBV were identified in patient SL-024, demonstrating the utility of the metagenomic sequencing method for detecting co-infections. It is possible that the presence of one virus would have been missed if targeted testing had revealed the presence of the other, as clinical symptoms may be

attributed solely to the detected virus, potentially resulting in sub-optimal patient management. Data on HIV-1 subtype prevalence in Sierra Leone is relatively sparse, however one study looking at 2015 HIV-positive patients from Freetown determined that the majority (83%) were infected with HIV-1 subtype CRF02_AG (386). In this study, for patient sequences that had sufficient coverage, HIV-1 subtype was identified by comparing the pol gene sequence to known subtypes using RIP. This revealed that both patient sequences were most similar to CRF02_AG across the majority of the gene, with one strain showing greater homology to subtype A1 across a small portion of the gene.

GBV-C, also known as human pegivirus C (genus *Pegivirus*, family *Flaviviridae*), is a human virus with a worldwide distribution and is considered to be non-pathogenic (440). Previous studies have estimated the global prevalence of GBV-C between 1-13% (441–444) with higher prevalence in developing countries, approaching 20% in some areas (445,446). A study looking at GBV-C EBOV co-infection in patients during the West Africa EBOV outbreak (412,413) identified 13/49 patients with such a co-infection. Of the GBV-C-positive patients, 53% survived EBOV infection in contrast with only 22% of GBV-C-negative patients (413). This association between survival and GBV-C infection was confounded by an association with age, however, it warrants further investigation. Interestingly, a similar association between co-infection and improved outcome has been made between HIV and GBV-C co-infection in AIDS patients (446,447), potentially due to reduced T-cell and B-cell activation in HIV-infected individuals (447,448). Despite evidence for an increased prevalence of GBV-C in HIV-positive people (440), the present study did not identify any such co-infections. Perhaps unsurprisingly, the GBV-C sequences most closely related to the patient GBV-C consensus sequences were

sampled in Sierra Leone in June 2014, from patients co-infected with EBOV and GBV-C (412,413).

3.4.4 LIMITATIONS

The nature of the metagenomic sequencing method is such that contaminants are commonly sequenced; introduced during sampling, in the laboratory or present in reagents (308). It is important to control for these in order to rule out false positive results. Determining whether reads are contaminants can be challenging, particularly in instances where the number of reads is very low. This is a challenge that must be overcome if metagenomic sequencing is to successfully transition into routine use within a clinical diagnostic setting (313).

In the present study contaminants were controlled for by sequencing a NTC that underwent the same random amplification, library preparation, sequencing and data analysis protocols. This method has previously shown to be effective, for example, a metagenomic virus discovery workflow was used in an attempt to identify a viral cause of disease in cattle exhibiting symptoms of unknown aetiology (449). Parvovirus-like sequences were identified in multiple samples, however, these were confirmed to be contaminants following the detection of an identical sequence in the negative extraction control and confirmatory testing using qRT-PCR (449).

To date, no standardised threshold values exist for the analysis of metagenomic sequencing data. Establishing thresholds can be achieved in individual laboratories by carrying out receiver-operator curve analysis using a panel of known clinical samples

(313), which is necessary when establishing a workflow for diagnostic purposes. For the purposes of this research project, threshold values were informed by the NTC results.

Bacteriophage MS2 was used as an internal control for the metagenomic sequencing assay, from the point of extraction through to sequencing. The presence of MS2-specific reads confirmed that the assay performed as expected, and conversely a lack of MS2-specific reads suggested sub-optimal assay performance. Compared with other samples using this control previously processed in the same laboratory (including the Ecuadorian plasma samples described in chapter 4), very low numbers of MS2-specific reads were generated by sequencing. However, it is clear from the results from individual samples that sequencing did successfully produce viral reads, but no/very few MS2-specific reads. For example, sample SL-110 produced 135,835 HIV-specific reads, but only four MS2-specific reads. This could be because of the high levels of HIV RNA diluting the MS2 signal. This can also happen in samples that have high levels of background sequence, for example because of variability in cell lysis prior to plasma separation, or variability in sample storage and handling conditions (450). MS2 input concentration (1.45e+5 pfu) was optimised as an internal control for qRT-PCR rather than metagenomic sequencing. It is likely that this concentration was simply too close to the limit of detection of the sequencing assay, and therefore future optimisation of the MS2 control specifically for metagenomic sequencing would be beneficial.

In instances where no MS2-specific reads or viral reads are present, the assay must be considered to have failed; this occurred in one of the 36 samples sequenced (SL-104). One possible explanation for the low numbers of MS2-specific reads observed in general is the longer processing time compared to that of the Ecuadorian samples. The Sierra Leonean samples were handled and inactivated in a CL4 laboratory, before being

transferred to a CL3 laboratory for the remainder of the procedure. This meant that these samples spent longer in AVL buffer than the Ecuadorian samples, and AVL buffer has been shown to have a detrimental effect on RNA integrity, which deteriorates quickly at room temperature (450). Another possibility is the presence of inhibiting substances in some plasma samples that were not removed during the RNA extraction process (451). However, RNA sequences were present at some level in all samples, as demonstrated by the amplification of MS2 RNA using qRT-PCR.

CHAPTER 4: PATHOGEN DETECTION IN FEBRILE ECUADORIAN PATIENTS

4.1 INTRODUCTION

4.1.1 ECUADOR

Ecuador is situated on the coast of north-western South America, bordering Peru on the east and south, and Colombia on the north, on a similar latitude to Sierra Leone and Guinea. Its land area is almost 250,000km^2 and the population is estimated at 16.3 million people (census 2016) (394). Ecuador is an upper middle-income country, defined by a gross national income per capita of 3,896-12,055 USD, but has a wide range of socio-economic groups including indigenous populations (396). Ecuador is a republic and is split into 24 provinces (Figure 4.1), which are divided into cantons (452). Quito is the capital city, however, provinces are 'zoned' together (452). This chapter focusses on the detection and characterisation of pathogens in a cohort of 196 febrile patients with acute undifferentiated febrile illness, from Esmeraldas province in Ecuador, 2016. The province is located in the north-west of the country on the coast (Figure 4.1) and belongs to zone 1, along with Carchi, Imbabura and Sucumbios provinces. The climate and terrain in Ecuador varies throughout the country; with a tropical climate along the coastal plain, tropical climate with flat to rolling eastern jungle in the Amazonian lowlands, and a cooler climate inland at higher elevation in the inter-Andean central highlands (452). Almost half the Ecuadorian population is located in the Andean basins and valleys; the western coastal area is well populated and the rainforest areas are sparsely populated (452).

Figure 4.1 Map showing the 24 provinces of Ecuador. The orange star shows the location of the medical centre in Esmeraldas province, at which febrile patient plasma was collected. Map adapted from free media repository (453).

4.1.2 PUBLIC HEALTHCARE AND INFECTIOUS DISEASE

Ecuador's national healthcare system was established in 1967 and historically struggled to provide adequate care, ranked by the WHO for healthcare efficiency as 111th out of 221 countries in the year 2000 (454), with government instability, corruption, funding and legal restrictions all contributing factors (455). Healthcare reform occurred in 2008, following the implementation of a new constitution that aimed to provide free-of-charge, high quality healthcare by allowing the government better control and oversight of public health, with increased budget and system reform (455). As a result, Ecuador was ranked 20th for healthcare efficiency in 2014 (455). The healthcare system functions as three major sectors: 1) public, which provides free services for everyone, 2) social security, which is available to working-class people and their families via tax paid by employers, and 3) a private system, which is used by the 3% of Ecuadorian citizens classified as upper- and middle-class (456). The Ecuadorian Ministry of Health (MoH) is responsible for the services provided by both public and private entities (456).

Life expectancy in Ecuador was 74 and 79 years for men and women, respectively, in 2016 and the mortality rate under the age of five years old was 14/1000 live births (457). Over the past decade, mortality from communicable diseases in Ecuador decreased, with an incidence of 96.1 deaths per 100,000 people in 2008, falling to 74.5 per 100,000 in 2016 (458). HIV infection and AIDS-related illness were the leading causes of communicable disease-related death in Ecuador in 20-44 years olds in 2014 (459). In 2018, 44,000 people were living with HIV infection, 2,200 new infections occurred and <1000 people died because of AIDS (460). The incidence of TB in Ecuador was 44 infections per 100,000 people in 2018, which has remained fairly stable since 2005,

preceded by a decline in incidence from the year 2000 (461). Drug resistant TB is a problem, with Ecuador showing the fourth highest percentage of rifampicin-resistant or multidrug-resistant TB cases in the Americas (462).

Successful control campaigns have been implemented against a number of endemic tropical diseases of clinical and economic importance in Ecuador, including the parasitic infections Chagas disease and Onchocerciasis, for which no cases have been reported since 2010 (463). Human rabies cases resulting from dog bites are well controlled, however transmission from vampire bats has been reported more recently and poses an ongoing risk (464,465). Cases of leptospirosis have risen in recent years, which fits with the trend seen globally. Reasons for this include an increase in intensive farming, poor sanitation and effluent management, as well as El Niño events that lead to increased temperature and number of static water sites (463).

Historically, malaria was a major cause of infection but between 1990 and 2011 incidence reduced by >75% thanks to a nationwide elimination programme which is still active (466), and by 2018, reports of malaria were restricted to the Amazon region (467). During a similar time period, cases of dengue fever increased, expanding from urban areas into previously unaffected rural areas (221). Re-emergence of DENV in Ecuador occurred in 1998, with cases peaking in 2000 then fluctuating over subsequent years. Trends of both malaria and dengue fever incidence in Esmeraldas province match those seen at the country-level (468). DENV serotypes 1, 2, 3 and 4 have circulated in Ecuador (469), with DENV-1 and DENV-4 detected in Esmeraldas. Furthermore, an introduction of DENV-4 to Esmeraldas from Colombia in 2004 led to the spread of this serotype into the rest of the country (468). It has been postulated that Esmeraldas might be a key point of introduction for pathogens because of the road system connecting Colombia to

the rest of Ecuador (468,470,471). DENV infection in southern coastal Ecuador is highly seasonal (472). Disease incidence correlates with vector density and is highest during the hot rainy season of February to May (472,473), and epidemics of disease occur as a result of the increased air temperature associated with El Niño events (472).

DENV, CHIKV and ZIKV are all transmitted via the mosquito vector *Aedes aegypti* which is endemic in Ecuador and much of South America (474), and circulation of all three arboviruses have been documented in Ecuador (381,472,474–476). Following the introduction of CHIKV into the Americas in 2013, three reports of autochthonous CHIKV transmission in Ecuador were made at the end of 2014 (381,477), which preceded almost 30,000 infections in 2015 (477). Since then cases have decreased dramatically, but the potential for transmission still exists due to the wide distribution of the vector.

Malaria awareness is high due to the country's previous history of infection, and fever is often still assumed to be a result of *Plasmodium* infection (468). However, the downward trend of malaria and the emergence of other infections with similar symptoms, including DENV, CHIKV and ZIKV, mean that a change in awareness is needed. It is important that resources and facilities are available, in terms of laboratories and assays, to be able to accurately determine infectious causes of fever and therefore inform an effective patient treatment plan. It is also necessary to consider that the incursion and spread of emerging pathogens not previously seen in the country can cause infections without detection.

Multiple pathogens have been detected in Ecuadorian febrile patients through direct detection (pathogen antigen or nucleic-acid) or indirect detection (antibodies), including DENV, ZIKV, CHIKV, YFV, hantavirus, Venezuelan equine encephalitis virus, OROV, Ilheus

virus, St. Louis encephalitis virus, *Leptospira*, *Rickettsia*, *Brucella, Coxiella* and *Plasmodium* (381,468,476,478–481).

4.1.3 ZIKA VIRUS OUTBREAK IN THE AMERICAS

The detection of ZIKV in Ecuador in 2016 was part of a larger outbreak that spread across the Americas following the introduction of the virus to Brazil in March 2015 (482), demonstrating the potential for extensive spread of an emerging virus through a naïve population. Data provided by affected countries showed that in South America, the worst-affected region, the number of cases peaked early in 2016, with over 30,000 cases reported in one week (272). Central America experienced a peak of cases around the same time, but at a much lower level (around 4,000 cases a week) (272). Compared with South America, the Caribbean reported fewer but more stable numbers of cases weekly, with a peak in mid-2016 (272). North America reported cases from 2015-2018, the majority of which were returning travellers, however, presumed local transmission was reported from the states of Florida and Texas, in addition to a small number of sexually transmitted cases (483). The USA territories of Virgin Islands, Puerto Rico and Samoa were also affected (273). Although a low level of local transmission is still possible, the ZIKV outbreak is now widely considered to be over, with a decline in reported cases in 2017 which was attributed mainly to acquired immunity within the affected populations (484).

Ecuador reported its first laboratory-confirmed ZIKV cases in epidemiological week (EW) 2 of 2016, from the provinces of Guayas and Manabi (475), the latter of which borders Esmeraldas province. Laboratory confirmation was performed by the National Institute

of Public Health and Research at the Ecuador Ministry of Public Health, using a combination of serology (IgM ELISA) and molecular detection (qRT-PCR) methods (475). Cases continued to increase weekly from EW 16, culminating in a peak of 320 cases during EW 25 in mid-June 2016 (Figure 4.2) (475). Following this there was a decline in the number of cases. Interestingly, during the early part of 2017 when the majority of countries in South America were reporting a decline in cases, Ecuador reported an increase between EWs 4 and 20 (272). As of September 2017, Ecuador reported autochthonous transmission of ZIKV in 17 of the 24 provinces in the country. During the last 8 weeks for which data is available (EW 24 to 31 of 2017), on average 68 cases were reported weekly (475). During the outbreak, Esmeraldas province showed one of the highest incidences of ZIKV infection in the country (23.9 – 201.8 cases per 100,000 population) (475).

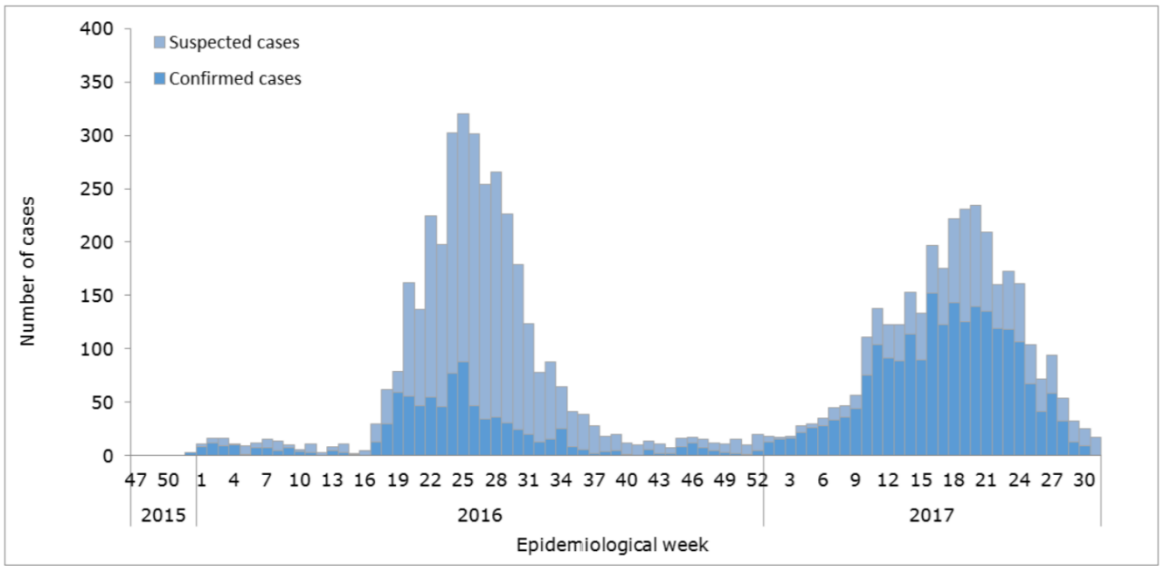

Figure 4.2 ZIKV cases (suspected and confirmed) reported to the Ecuador Ministry of Public Health, EW 47 of 2015 to EW 31 of 2017. Figure reproduced from (475).

On April 16th 2016 a major earthquake took place in Ecuador, occurring between the Nazca and South American plates and measured at a magnitude of 7.8 (485). The disaster resulted in approximately 30,000 injuries and 700 deaths, with coastal Esmeraldas and Manabi the worst affected provinces (486). Natural disasters can influence the incidence of infectious diseases in the affected population due to a combination of factors, including the rapid movement of people from one area to another, and poor hygiene conditions due to the breakdown of sanitation infrastructure (485). Vector-borne diseases in particular may increase because of changes in conditions that increase the density or number of the vector or bring people into closer contact with it. For example, increased mosquito populations were seen in Haiti following the 2010 earthquake, because debris increased the number of available vector breeding sites (stagnant water reservoirs), which led to a rise in malaria incidence (487,488). A study investigating ZIKV incidence following the earthquake in Ecuador in 2016 demonstrated that there was a significant increase in autochthonous ZIKV cases following the earthquake (controlled for socioeconomic and climatic variables), particularly in severely affected cantons (485). This natural disaster is likely to have contributed to the incidence of ZIKV in Ecuador during the outbreak and highlights the importance of natural disasters and increased incidence of infectious disease. This project aims to identify other causative agents of illness in febrile patients from Esmeraldas, Ecuador, during the time of the ZIKV outbreak.

4.1.4 AIMS

The plasma samples used in this study were taken during the time of the ZIKV outbreak in 2016 and were routinely tested at the time of sampling for ZIKV, DENV and CHIKV using qRT-PCR. The majority of patients were negative for all three viruses. The aim of this chapter was to detect causative pathogens in these patients using a combination of targeted RT-PCR/PCR testing, followed by metagenomic sequencing of RT-PCR/PCR-negative patients. Used in conjunction with one another, these methods can detect both known and as of yet unknown causes of fever, with a focus on RNA viruses. The characterisation of identified viruses using whole genome sequencing and virus isolation provides essential information on viral genetics that can be used for further analyses. Genome sequences were made publicly available online, and isolated viruses were deposited in national virus collections with the aim of enhancing future surveillance efforts and collaborative research programmes relevant to Ecuador.

4.2 METHODOLOGY: SAMPLE SELECTION FOR METAGENOMIC SEQUENCING

Total RNA from 196 febrile Ecuadorian patient plasma samples collected in 2016 were tested for CHIKV, DENV (serotypes 1-4), MAYV, YFV, ZIKV, *Leptospira*, *Plasmodium, Rickettsia* and internal control MS2 using a panel of RT-PCR/PCR-based assays. Following testing, 18 samples from the patient cohort were selected for metagenomic sequencing. Two samples were selected based on their inconclusive RT-PCR/PCR test results; sample D-087 (Cq values 35-39.9 for DENV and CHIKV) and sample D-124 (Cq values 35-39.9 for ZIKV and CHIKV). These samples were selected with the intention of identifying virus specific reads for the pathogens in question and generating virus genome sequences. The additional sixteen samples were selected from the group of patients for which no infectious agent had been identified by RT-PCR/PCR testing, using the following criteria:

1. Minimum number of days of fever; to maximise the chance of detecting pathogen RNA.

2. Maximum fields of metadata available.

3. Maximum number of symptoms recorded; headache, joint pain, muscle pain and/or nausea.

4.3 RESULTS

4.3.1 RT-PCR/PCR TESTING OF FEBRILE PATIENT PLASMA

Positive cases (Cq value <35) were identified for ZIKV (prevalence 11.2%, *n*=22), DENV (prevalence 2.0%, *n*=4) and *Leptospira* (prevalence 0.5%, *n*=1) (Figure 4.3). In addition, several potentially positive cases (Cq value 35-39.9) were identified (ZIKV *n*=15, DENV *n*=3, CHIKV *n*=2 and *Leptospira* spp. *n*=1, Figure 4.3). Two potential co-infections were observed; patient D-087 (DENV and CHIKV) and D-124 (ZIKV and CHIKV), although high Cq values (34-36) were observed for all three pathogens. No cases of MAYV, YFV, *Plasmodium* or *Rickettsia* were identified. 152 samples were negative for all the pathogens that were tested for. All samples were positive for internal control MS2. A table of PCR/RT-PCR results including Cq values are provided in Appendix 6.

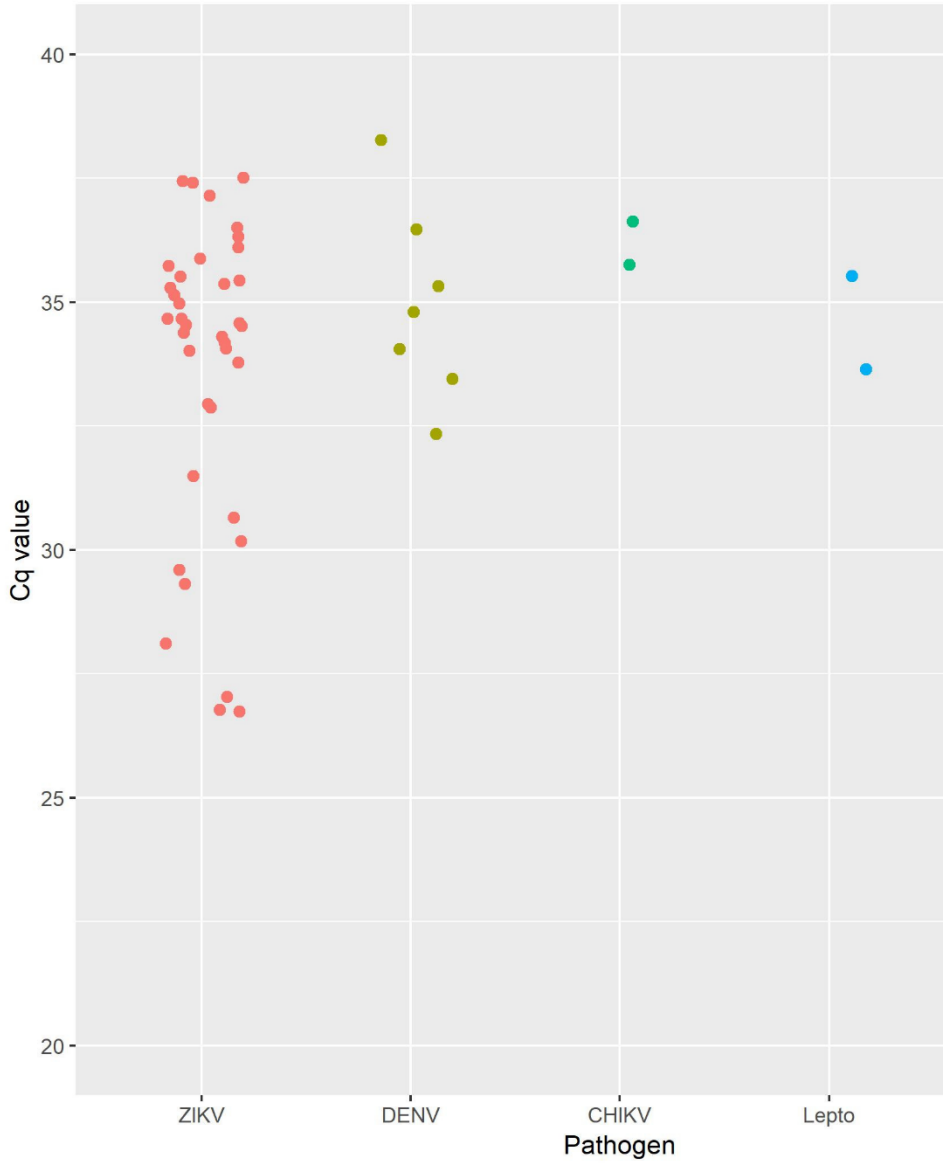

Figure 4.3 RT-PCR/PCR assay test results. Cq values from pathogen positive (Cq <35) and potentially-positive (Cq 35-39.9) patient samples tested by qRT-PCR. 152/196 samples were negative for all pathogens (not shown). DENV = serotypes 1-3. Lepto = *Leptospira* spp.

Plasma samples that had a Cq value of 35-39.9 for CHIKV, DENV or ZIKV were tested for IgM antibodies against the virus in question using qualitative commercial IgM capture ELISA assays (see section 2.6). Detection of IgM antibodies indicates a recent infection and can help clarify high Cq qRT-PCR results. Two samples were tested for anti-CHIKV IgM; one was borderline and one was negative (Table 4.1). Two out of three samples tested for anti-DENV IgM were positive, and only two of 12 samples tested for anti-ZIKV IgM were positive (Table 4.1). Taking the qRT-PCR and IgM antibodies results together, the prevalence of *Leptospira*, ZIKV and DENV in the tested samples was 0.5%, 12.2% and 3.1%, respectively.

Sample ID	IgM test	Result	qRT-PCR Cq value
D-087	CHIKV	Negative	36.6
D-124	CHIKV	Borderline	35.8
D-009	DENV	Positive	36.5
D-087	DENV	Positive	35.3
D-099	DENV	Negative	38.3
D-041	ZIKV	Positive	36.5
D-055	ZIKV	Negative	36.1
D-080	ZIKV	Negative	37.1
D-095	ZIKV	Negative	36.3
D-109	ZIKV	Negative	37.4
D-118	ZIKV	Negative	35.1
D-136	ZIKV	Negative	37.5
D-139	ZIKV	Negative	35.7
D-149	ZIKV	Negative	35.4
D-156	ZIKV	Positive	35.5
D-186	ZIKV	Negative	35.3
D-209	ZIKV	Negative	37.4

Table 4.1 Anti-CHIKV, -DENV and ZIKV- IgM antibody results from Ecuadorian patient plasma samples with qRT-PCR Cq values of 35-39.9 for the virus in question. Tests were performed using commercial IgM capture ELISAs (see section 2.6).

4.3.2 VIRUS DETECTION BY METAGENOMIC SEQUENCING

Eighteen patient RNA samples were sequenced in total. Two of these; D-087 and D-124, showed putative co-infections as determined by RT-PCR/PCR and were sequenced metagenomically with the aim of confirming or refuting this by looking for reads specific to the pathogens implicated, in addition to screening for other viruses. The remaining 16 samples were RT-PCR/PCR-negative for all pathogens tested for.

The total number of reads generated per patient sample ranged from 45,190 to 2,176,382 (mean = 1,097,957, Table 4.2). On average, 56% of reads were of human origin (minimum 8.75%, maximum 91.90%), and 17% were of microbial origin (minimum 0.43%, maximum 79.70%). The mean number of viral reads per sample was 1.07% (minimum 0.01%, maximum 4.13%). All samples contained reads belonging to internal control bacteriophage MS2, ranging from 4 to 56,771 reads (Table 4.2).

Sample ID	Total reads (number)	Chordate reads (%)	Microbial reads (%)	Bacterial reads (%)	Viral reads (%)	MS2 reads (number)	MS2 reads (%)
D-001	2,176,382	60.50	1.13	1.09	0.04	944	0.02
D-002	1,442,421	71.70	6.39	6.20	0.19	2,526	0.10
D-005	1,695,587	91.90	4.74	4.62	0.12	1,438	0.07
D-010	1,665,762	50.10	5.48	5.29	0.18	2,893	0.09
D-014	1,412,807	48.60	0.43	0.42	0.01	180	0.01
D-018	752,271	50.40	19.00	18.10	0.90	6,428	0.47
D-020	1,377,949	33.40	50.30	46.10	4.13	56,771	2.40
D-029	1,606,349	85.20	3.54	3.49	0.05	4	0.00
D-030	1,376,838	52.50	3.89	3.19	0.64	8,790	0.33
D-035	1,065,425	57.00	4.62	4.04	0.53	5,613	0.28
D-040	1,516,950	52.80	1.66	1.62	0.04	598	0.02
D-047	1,244,665	68.40	4.51	4.04	0.47	5,805	0.25
D-074	1,397,452	69.00	14.20	12.40	1.75	24,293	0.98
D-075	45,190	65.70	4.86	4.26	0.59	246	0.30
D-087	462,977	38.8	46.30	43.4	2.95	7,031	0.98
D-091	109,193	49.30	34.80	31.40	3.33	3,514	2.04
D-124	356,780	8.75	79.70	77.9	1.62	63	0.01
D-131	58,227	55.00	19.20	17.30	1.77	954	0.96
Mean	1,097,957	56.06	16.93	15.83	1.07	7,116	0.52

Table 4.2 Sequencing read statistics for Ecuadorian 2016 patient sequencing data, classified using Centrifuge. The percentage read data was generated using the Pavian web application (369).

4.3.2.1 IDENTIFICATION AND REMOVAL OF CONTAMINANT SEQUENCES

Reads matching pathogen sequences that were present in the negative extraction controls (*n*=5) and/or the no template control (*n*=1) were identified as potential contaminants and excluded from further analyses (Table 4.3). These were CHIKV and IAV.

Contaminant	Reason(s) for exclusion	Number of samples showing contaminant reads
CHIKV	Present in NXCs and NTC. Frequently handled in the laboratory.	12
IAV	Present in NXCs. Frequently handled in the laboratory.	13

Table 4.3 Contaminants identified in metagenomic sequencing data.

4.3.2.2 TAXONOMIC IDENTIFICATION USING CENTRIFUGE

Centrifuge identified three pathogenic human viruses present at a level exceeding 0.01% of the total reads; OROV, DENV-1 and hepatovirus A virus (HAV, previously named Hepatitis A virus). 5,076 OROV-specific reads (0.63% of total reads) and 473 DENV-1-specific reads (0.06% of total reads) were identified from sample D-087. Prior qRT-PCR testing did not include an OROV assay. 478 HAV-specific reads were identified from sample D-005 (0.02% of total reads). No viruses known to infect humans were identified in the remaining 16 patients.

4.3.2.3 IDENTIFICATION OF VIRUS-SPECIFIC SCAFFOLDS FROM *DE NOVO* ASSEMBLY

Following the removal of human reads, reads were *de novo* assembled and analysed as described in section 2.11.5. 16/18 samples did not contain any scaffolds with homology to a pathogenic human virus. The exceptions were D-005, from which two scaffolds showed homology to HAV, and D-087, from which scaffolds showed homology to OROV and DENV-1 (Table 4.4), in agreement with the Centrifuge results. 13/18 samples contained at least one scaffold matching internal control MS2, the exceptions were samples D-014, D-029 and D-075.

Sample ID	Scaffold ID	Scaffold length (bp)	Mean scaffold coverage	Matching accessions	Family	Genus	Species
D-005	38	1410	3.55	NP_041007.1, NP_041008.1	*Picornaviridae*	*Hepatovirus*	Hepatovirus A
D-005	107	1126	5.51	NP_041007.1, NP_041008.1	*Picornaviridae*	*Hepatovirus*	Hepatovirus A
D-087	2	3433	31.07	NP_982304.1	*Peribunyaviridae*	*Orthobunyavirus*	Oropouche virus
D-087	5	2873	14.61	NP_982303.1	*Peribunyaviridae*	*Orthobunyavirus*	Oropouche virus
D-087	22	1521	20.43	NP_982304.1	*Peribunyaviridae*	*Orthobunyavirus*	Oropouche virus
D-087	185	610	8.89	NP_982305.1	*Peribunyaviridae*	*Orthobunyavirus*	Oropouche virus
D-087	418	386	16.52	NP_982303.1	*Peribunyaviridae*	*Orthobunyavirus*	Oropouche virus
D-087	6	2867	39.52	NP_059433.1	*Flaviviridae*	*Flavivirus*	Dengue virus-1

Table 4.4 *De novo* assembled scaffolds with protein sequence homology to pathogenic human viruses, as identified by Kaiju.

4.3.2.4 IDENTIFICATION OF VIRUS-SPECIFIC READS BY MAPPING TO REFERENCE GENOMES

Non-human reads from the 18 patient samples were mapped to multiple reference genomes, selected for their relevance to the patient cohort (see section 2.11.4). Of the 13 viruses included, reads from six were identified (DENV-1, DENV-2, DENV-3, DENV-4, HAV, OROV, Table 4.5). Viral reads were identified in six patient samples; D-005 (HAV, OROV, DENV-2), D-010 (DENV-2, OROV, DENV-3), D-020 (DENV-2, OROV, DENV-3, DENV-4), D-029 (DENV-2, OROV), D-087 (DENV-1, OROV) and D-124 (DENV-2, Table 4.5). Most virus-specific reads were present at a very low frequency (<150 reads) except for HAV from D-005, for which 1,550 reads were identified, covering 39% of the genome at 5x depth (Figure 4.4), and OROV and DENV-1 in D-087. The remaining patient samples contained reads that mapped to internal control MS2, but no other viruses (Table 4.5).

Sample ID	DENV1	DENV2	DENV3	DENV4	HAV	OROV	RVFV	MS2
D-001								1012
D-002								3282
D-005		66			1550	76		2922
D-010		120	2			34		3104
D-014								251
D-018								8110
D-020		134	2	2		26		67171
D-029		42				28		4
D-030								11573
D-035								6050
D-040								758
D-047								6846
D-074								32462
D-075								254
D-087	486	2				9942		8292
D-091								4282
D-124		2						76
D-131								1208

Table 4.5 Virus-specific sequencing reads identified by mapping metagenomic sequencing reads from 18 Ecuadorian febrile patient plasma samples to a panel of virus reference sequences. MS2 reads act as an internal control. Colour indicates relative number of reads; green = least, red = most.

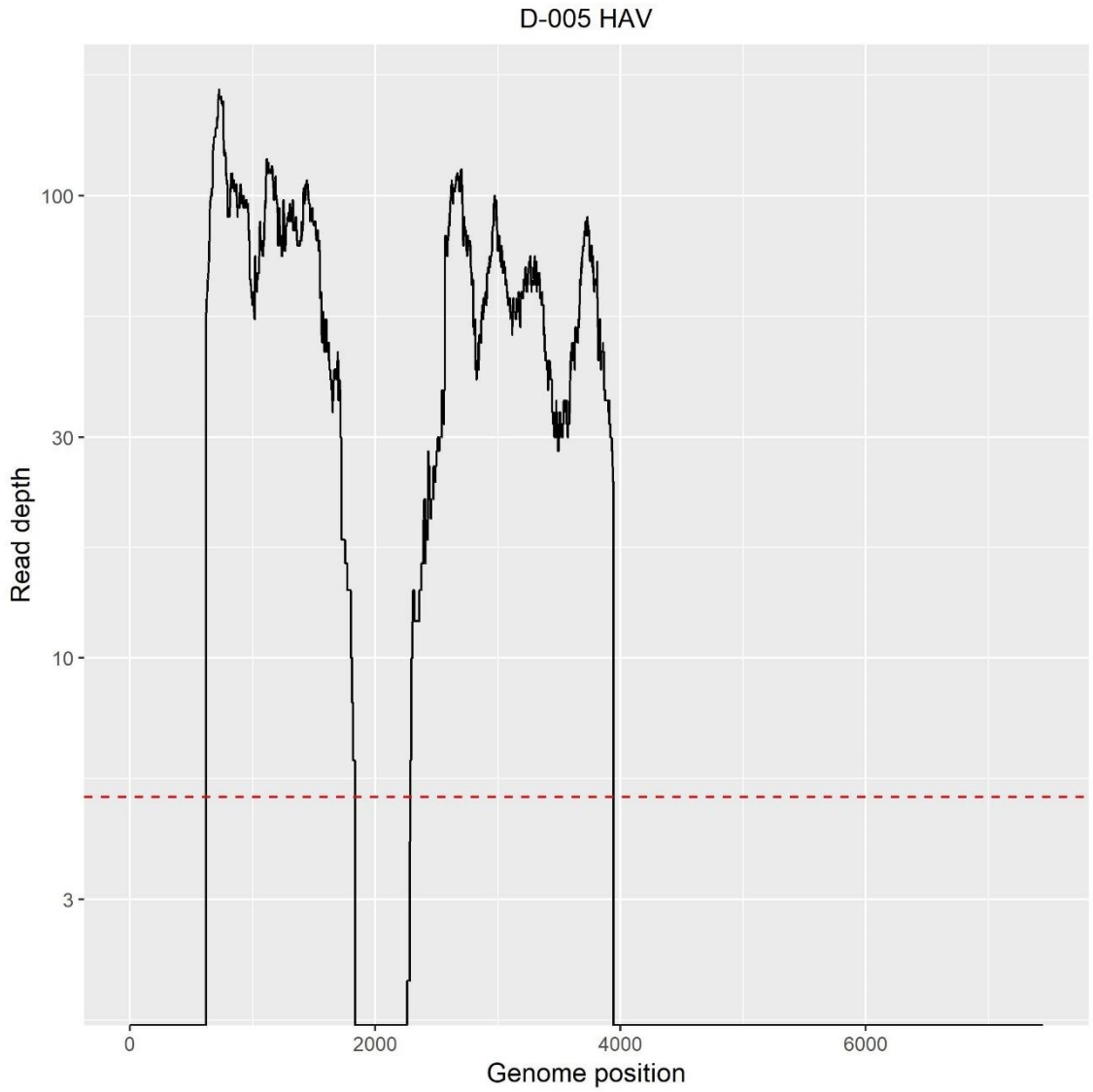

Figure 4.4 Coverage of the HAV genome (7,446 nt), generated by mapping sequencing reads from sample D-005 to a HAV reference sequence (X75216.1). Red dotted line indicates depth of 5 reads.

Mapping reads from sample D-087 to a DENV-1 reference genome (NC_001477.1) resulted in 1123 reads mapping, the majority of which were located within a single 732 nucleotide (nt) region spanning a region of the polyprotein gene coding for non-structural protein NS4B and NS5 RNA-dependent RNA polymerase (Figure 4.5). An OROV consensus sequence was generated by mapping reads from the patient sample to reference sequences for each of the three genomic segments (S: KP691632.1, M: KP052851.1, L: KP691612.1), which resulted in coverage of 69%, 76%, and 79% of S, M, and L OROV segments, respectively (Figure 4.6).

During the mapping process, a BLASTn analysis revealed that the OROV S segment sequence from patient D-087 was very similar to Iquitos virus (IQTV), a reassortant orthobunyavirus that contains S and L segments similar to OROV and a novel M segment belonging to the Simbu virus serogroup (489). To confirm that the genome from the patient belonged to OROV not IQTV, mapping to an IQTV genome (strain MIS-0397; KJ866386.1, KJ866387.1 and KJ86638.1) was performed. Reads mapped to the S and L segments with similar coverage to that seen in the OROV mapping, however only two reads mapped to the IQTV M segment, confirming that the origin of the reads is OROV.

Despite the CHIKV qRT-PCR result for D-087, no CHIKV-specific reads were identified by any bioinformatic method. No reads were detected by taxonomic assignment and none mapped to any of the five CHIKV genomes chosen from varying geographical locations, including a Colombian CHIKV sequence from 2016 (KX496989.1). The CHIKV primer and probe sequences from the screening qRT-PCR assay were assessed for homology to the scaffolds from the SPAdes assembly using BLASTn but no similarities were found. Analysis of reads from patient sample D-124 did not identify reads specific to ZIKV or

CHIKV (suggested to be present by qRT-PCR), nor did it identify any other pathogenic viruses.

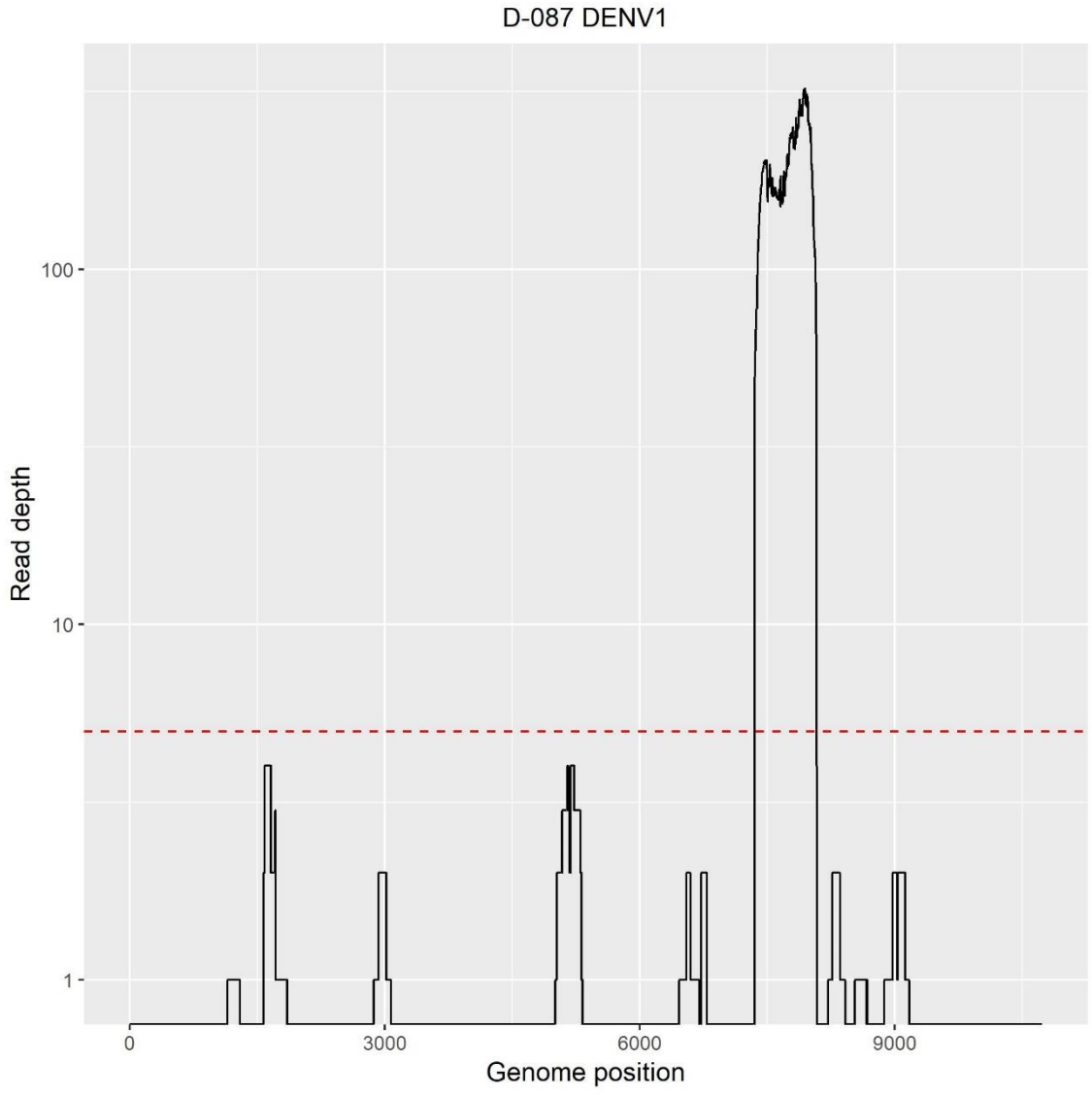

Figure 4.5 Coverage of the DENV-1 genome, generated by mapping sequencing reads from sample D-087 to a reference sequence (NC_001477.1). Red dotted line indicates depth of 5 reads.

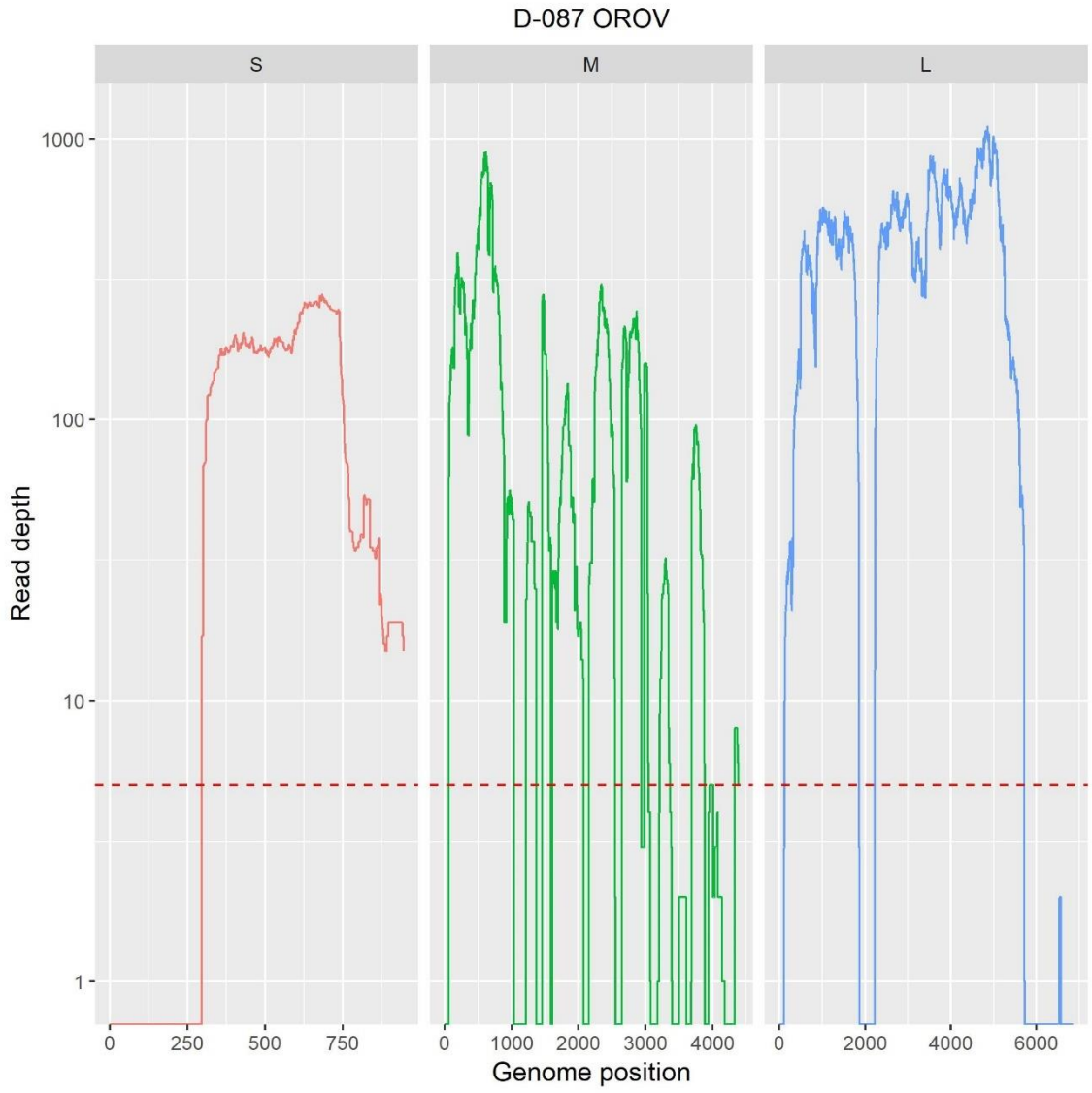

Figure 4.6 Coverage of OROV genomic segments (S, M, L), generated by mapping sequencing reads from sample D-087 to reference sequences (S: KP691632.1, M: KP052851.1, L: KP691612.1). Red dotted line indicates depth of 5 reads.

4.3.2.5 SUMMARY OF VIRUSES DETECTED BY METAGENOMIC SEQUENCING

In summary, two viruses; HAV and OROV, were detected in two separate patients from the 18 patient RNA samples sequenced (Table 4.6). Their presence was determined using a combination of taxonomic classification, mapping to viral reference sequences and *de novo* assembly of reads. A small fragment of DENV-1 was also identified in the OROV-positive patient, and although coverage of the genome was very low, the positive anti-DENV IgM result for this patient (Table 4.1) in combination with the sequence data suggests the patient had a recent DENV infection. There was no evidence of other human viruses within the patients sequenced.

Sample	Virus	Reads assigned by Centrifuge	% of reads assigned by Centrifuge	Reads mapped	Genome coverage 1x (%)	Genome coverage 5x (%)	Virus-specific scaffolds	Scaffold length (bp, min-max)
D-005	HAV	478	0.02	1550	39.0	38.6	2	1126-1410
D-087	OROV S	5052†	0.7†	296	68.9	60.5	1	610
D-087	OROV M	5052†	0.7†	2646	93.1	84.7	2	386- 2873
D-087	OROV L	5052†	0.7†	7000	76.9	75.4	2	1521-2422

Table 4.6 A summary of viruses identified from Ecuadorian patient plasma samples using metagenomic sequencing. The mapping and assembly figures are based on data stripped of human reads. OROV mapping was performed to the OROV/EC/Esmeraldas/087/2016 genome, HAV mapping was performed using genome X75216.1. The threshold used for detection was ≥20% 5x genome coverage. †Centrifuge does not discriminate between viral genome segments, therefore read numbers and percentages for OROV as a whole are given.

4.3.3 ISOLATION OF VIRUS FROM PATIENT PLASMA

Virus isolation was attempted from five samples containing viral RNA, identified by RT-PCR/PCR assays or metagenomic sequencing. Sample D-087 was selected because OROV was detected, D-124 was selected because of a potential co-infection (ZIKV and CHIKV), D-004 was DENV qRT-PCR-positive, and three ZIKV qRT-PCR-positive samples (D-121, D-124, D-194) showing the lowest ZIKV Cq values in the cohort were chosen. Isolation was undertaken in Vero and C6/36 cells (see section 2.15.2). Positive control viruses and negative control cells (media only) were cultured at the same time (see section 2.15.5). At days 5, 7, 11 and 14 post-infection, supernatants were sampled and cell monolayers were observed for CPE. RNA extracted from supernatants was tested using qRT-PCR for the expected virus, to detect changes in quantity of viral RNA over time.

OROV RNA increased over time in the D-087 culture, measured by a decrease in qRT-PCR Cq value between days 5 and 7 (no Cq value at day 0), suggesting viral replication (Figure 4.7A). CPE was observed at 5 days post-infection (dpi) (Figure 4.7B), the severity of which increased by 7 dpi, at which point the culture was frozen to lyse cells and subsequently harvested (see section 2.15.3). Virus titre was determined by plaque assay (see section 2.15.4). Plaques were observed (Figure 4.7C) and titre calculated as 1.56e+7 pfu/mL.

ZIKV RNA increased over time in the D-121 and D-124 cultures, measured by a decrease in qRT-PCR Cq values (Figure 4.8A). CPE was observed in both cultures, progressing in severity from 5 dpi to 14 dpi (Figure 4.8B). To increase the titre and volume of the virus stocks, ZIKV strains D-121 and D-124 were passaged a second time in C6/36 cells (see section 2.15.2). Plaques were observed (Figure 4.8C) and titres calculated as 3.3e+5 pfu/mL for D-121 ZIKV C6/36 P2, and 5.00e+2 pfu/mL for D-124 ZIKV C6/36 P2.

No meaningful change in Cq value was seen in the D-004 and D-194 cultures (DENV and ZIKV qRT-PCR positive, respectively), suggesting that viable virus was not present. All control viruses demonstrated RNA replication as expected and no evidence of viral RNA replication was observed in the negative controls. Table 4.7 summarises the isolation of OROV and ZIKV isolation from patient samples; no other viruses were isolated.

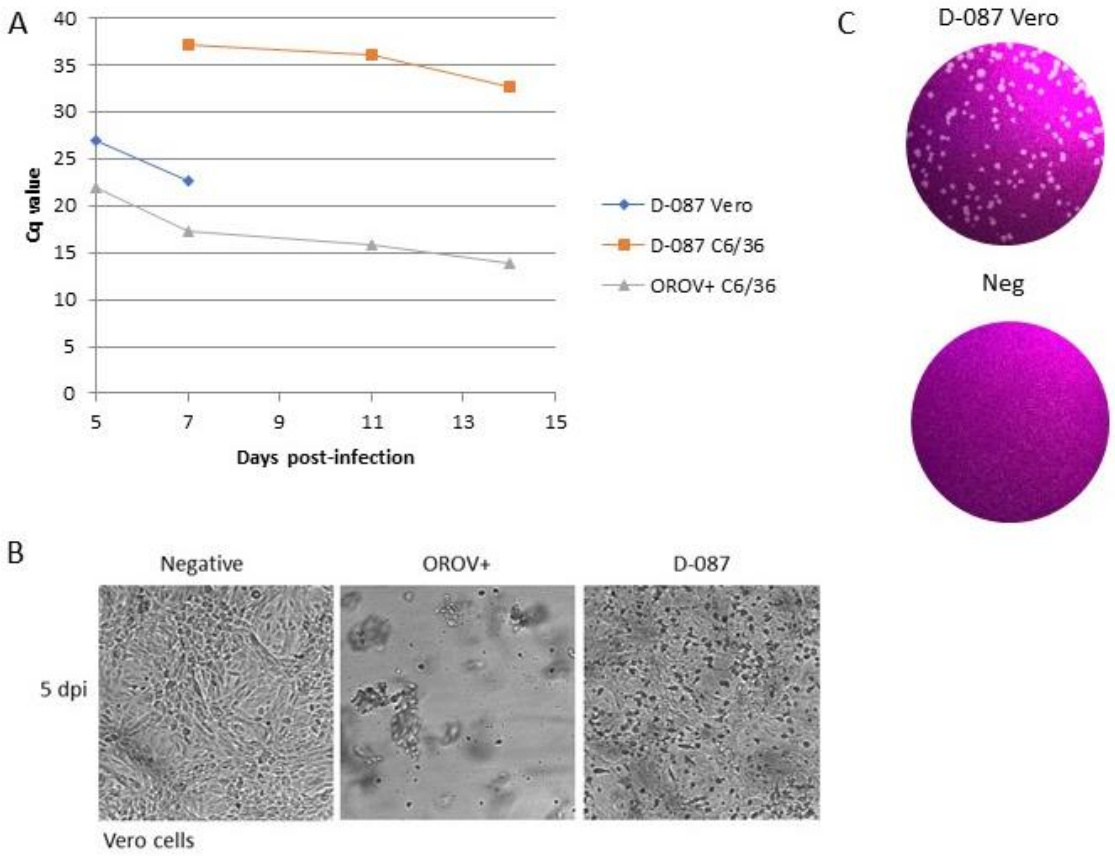

Figure 4.7 Isolation of OROV from patient sample D-087. A) OROV RNA replication in P1 cultures over 14 days. Cq values from D-087 cultures and the positive control are shown. Vero culture was terminated upon the observation of severe CPE at 7 dpi. **B)** Observation of CPE at 5 dpi in Vero cells. OROV+ denotes the positive control. **C)** Plaques formed by D-087 OROV in a Vero cell monolayer, compared with the negative control.

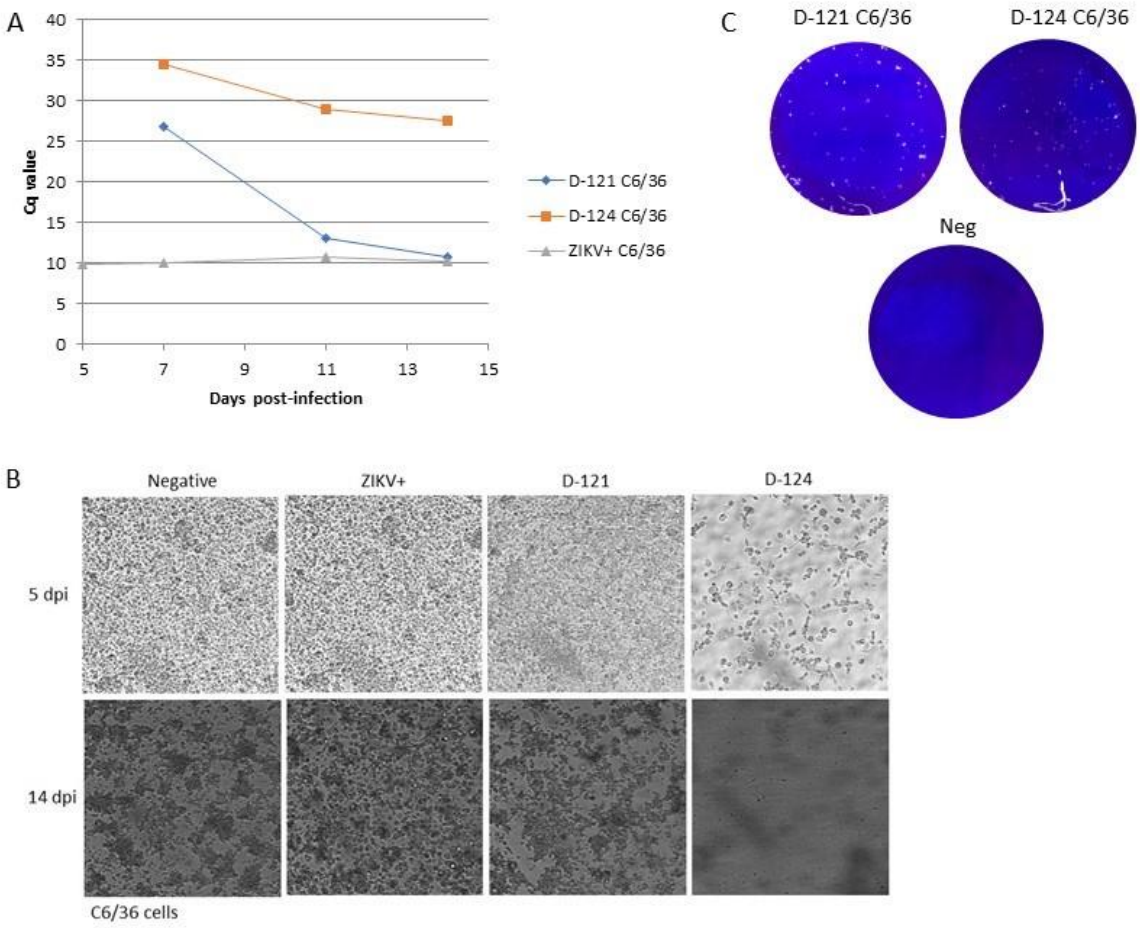

Figure 4.8 Isolation of ZIKV from patient samples D-121 and D-124. A) ZIKV RNA replication in P1 cultures over 14 days. Cq values from D-121 and D-124 cultures and the positive control are shown. **B)** Observation of CPE in C6/36 cells. ZIKV+ denotes the positive control. **C)** Plaques formed by D-121 and D-124 ZIKV in a Vero cell monolayer, compared with the negative control.

Sample ID	Suspected virus	qRT-PCR Cq value from patient sample	RNA replication?	CPE observed?	Plaque formation observed?
D-004	DENV-1	33.45	No	No	n/a
D-087	CHIKV	36.63	No	No	n/a
D-087	DENV-1	35.33	No	No	n/a
D-087	OROV	n/a	Yes*†	Yes*	Yes
D-121	ZIKV	26.74	Yes†	Yes†	Yes
D-124	CHIKV	35.76	No	No	n/a
D-124	ZIKV	34.54	Yes†	Yes†	Yes
D-194	ZIKV	28.11	No	No	n/a

Table 4.7 Virus isolation results from five febrile patients, measured by viral RNA replication, observation of CPE, and plaque assay. *Replication in Vero cells. †Replication in C6/36 cells. n/a = not applicable.

4.3.4 COMPLETE GENOME SEQUENCING OF VIRUS ISOLATES

4.3.4.1 OROV/EC/ESMERALDAS/087/2016

Following the isolation of OROV from patient D-087 in Vero cells, the complete genome sequence was generated from RNA extracted from P1 supernatant, using the metagenomic approach described earlier. Mapping to reference sequences resulted in 28.0%, 12.2% and 21.1% of the total 1.6 million reads mapping to segments S, M and L, respectively. Average depths of coverage were 55,532; 4,954 and 5,674 for S, M, and L segments, respectively. Terminal untranslated region (UTR) sequences were confirmed by RACE and Sanger sequencing (see section 2.12). The strain was named OROV/EC/Esmeraldas/087/2016, consensus sequences were annotated and submitted to GenBank (MF926352.1, MF926353.1, MF926354.1). The S segment (952 bp) contains 2 overlapping open reading frames (ORFs) encoding the nucleoprotein and non-structural protein. The M segment (4,387 bp) contains a single ORF encoding a polyprotein. The L segment (6,852 bp) contains a single ORF encoding the RNA-dependant RNA polymerase. The final sequences were used as references to map the sequencing reads from the patient sample, which increased coverage of the M segment from 76% to 98.7% (Figure 4.9). The S and L segment coverage remained the same.

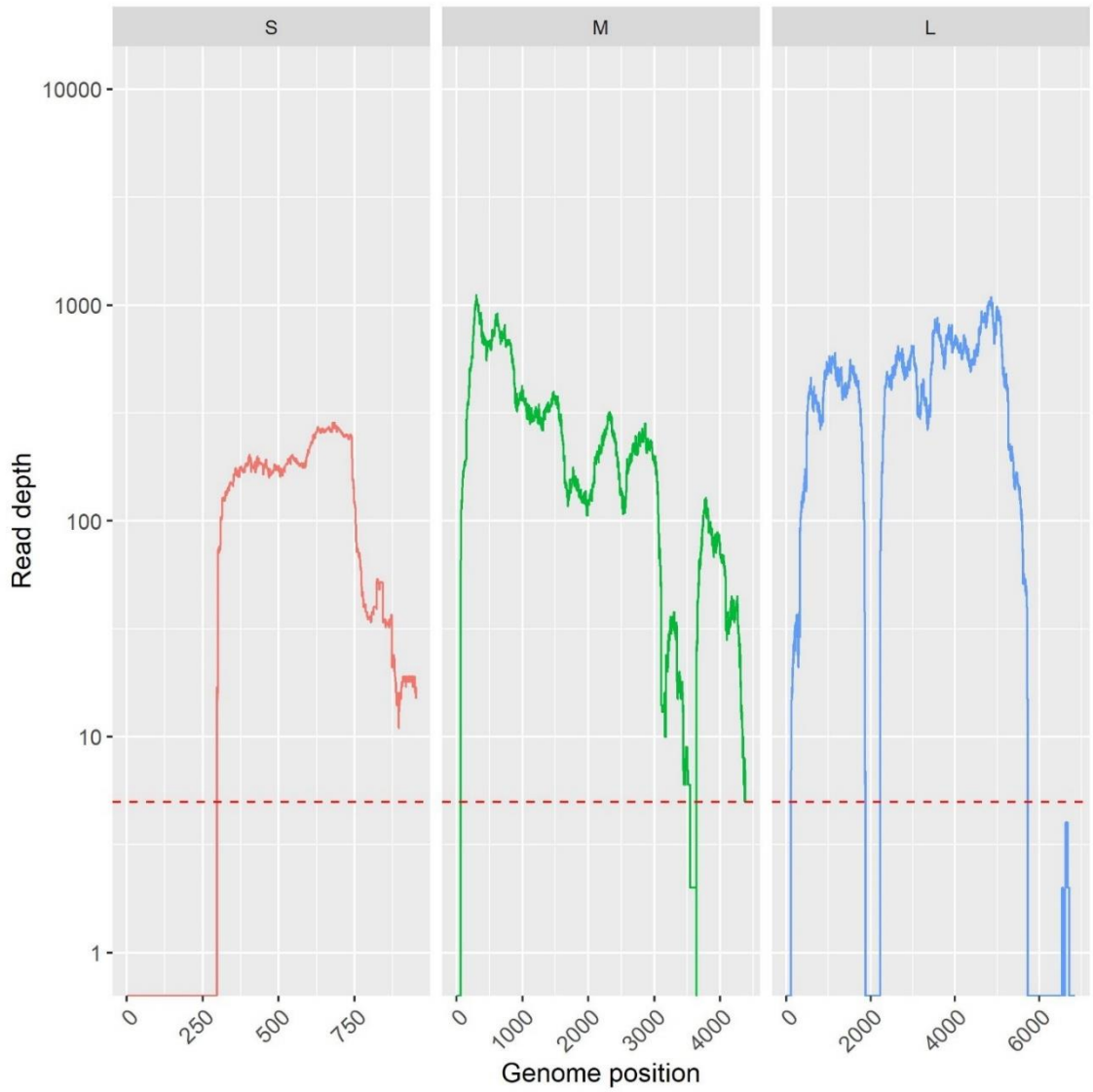

Figure 4.9 Coverage of OROV genomic segments (S, M, L) from patient sample D-087, generated by mapping sequencing reads to the complete genome sequence from cultured isolate OROV/EC/Esmeraldas/087/2016 (S: MF926352.1, M: MF926353.1, L: MF926354.1). Red dotted line indicates depth of 5 reads.

4.3.4.2 ZIKV/EC/ESMERALDAS/121/2016

RNA extracted from ZIKV D-121 P1 C6/36 supernatant was sequenced using the same metagenomic approach. An almost complete genome sequence was generated, with 27% of the total 1.5 million reads mapping to ZIKV reference sequence KX879603.1. The sequence covers the entire coding region and the majority of the 5' and 3' UTRs, however, their lengths were not confirmed. The strain was named ZIKV/EC/Esmeraldas/121/2016 and the annotated consensus sequence submitted to GenBank (Table 4.8). An attempt was made to generate genome sequence from cultured ZIKV D-124, however almost no ZIKV-specific reads were present, most likely because the titre of the virus was so low (5.00e+2 pfu/mL).

4.3.4.3 POSITIVE CONTROL ISOLATES

Genomes from the positive control viruses DENV-1 TC861(HA), CHIKV S27 Petersfield and OROV NCPV: 1409261v were sequenced for comparison with patient sequences to detect cross-contamination. In addition, DENV/EC/Esmeraldas/210/2014, isolated from a febrile Ecuadorian patient from 2014, was sequenced to provide a relevant strain to use as a reference sequence for mapping. These genomes were made publicly available via GenBank (Table 4.8).

Strain name	Virus and region	Accession number
TC861(HA)	DENV-1, complete genome	MF576311.1
S27 Petersfield	CHIKV, complete genome	MF580946.1
NCPV: 1409261v	OROV, complete S segment	MF620127.1
NCPV: 1409261v	OROV, complete M segment	MF620128.1
NCPV: 1409261v	OROV, complete L segment	MF620129.1
ZIKV/EC/Esmeraldas/121/2016	ZIKV, complete genome	MF794971.1
DENV/EC/Esmeraldas/210/2014	DENV-1, complete genome	MF797878.1
OROV/EC/Esmeraldas/087/2016	OROV, complete S segment	MF926352.1
OROV/EC/Esmeraldas/087/2016	OROV, complete M segment	MF926353.1
OROV/EC/Esmeraldas/087/2016	OROV, complete L segment	MF926354.1

Table 4.8 Genome sequences generated from virus isolates using the metagenomic approach and deposited into GenBank.

4.4 DISCUSSION

4.4.1 RT-PCR/PCR TESTING DETECTED DENV, ZIKV AND *LEPTOSPIRA* IN FEBRILE PATIENTS

Pathogen detection in 196 Ecuadorian febrile patient plasma samples was initiated by testing extracted RNA for eight pathogens known to circulate in Ecuador or South America at present or in the past. Nucleic acid from *Leptospira* (*n*=1), ZIKV (*n*=22) and DENV (*n*=4) was unequivocally detected (Cq <35), in addition to several potentially positive cases (Cq 35-39.9). Plasma samples with CHIKV, DENV and ZIKV qRT-PCR Cq values of 35-39.9 were tested for IgM antibodies. The presence of IgM confirms a recent infection, however, the absence of IgM does not preclude an infection, because it's possible that sampling occurred at a time where viraemia had declined to an almost undetectable level, and IgM antibodies had yet to rise to a detectable level. Recent infection was confirmed by detection of IgM in 2/3 and 2/12 patients for DENV and ZIKV, respectively, but no positive IgM results were obtained for either of the two CHIKV query patients. Taking these results into account, the prevalence of *Leptospira*, ZIKV and DENV was 0.5%, 12.2% and 3.1%, respectively.

Leptospira has a wide global distribution (289) that includes Ecuador. A previous study of AUFI in the Amazon basin region of the country identified leptospirosis as the most commonly diagnosed infection (alongside malaria), with 40/272 patients testing positive (480). Risk factors associated with leptospirosis are inadequate sewage disposal and water treatment (289). Esmeraldas city is located on the coast, has relatively good infrastructure, and the majority of the canton is urban, with only 18.7% of the land classed as rural (490). This makes it likely that fewer leptospirosis risk factors are present in Esmeraldas compared with other areas of the country, reflected in the low number of cases. Another explanation could be that serological testing for anti-*Leptospira*

antibodies was not performed, which would identify previous leptospirosis infections rather than solely the current ones detectable by PCR.

The detection of ZIKV RNA in 12% of the patient samples in this study reflects the wider picture of ZIKV in Ecuador, where a high incidence was observed in Esmeraldas province during a time at which ZIKV had only recently been detected in the country. The relatively large number of cases detected is not unexpected because the febrile patients presented to the medical centre in the months leading up to the peak of ZIKV cases observed in mid-June 2016 (272).

The relatively low prevalence of DENV cases in the cohort is interesting. Over previous decades, a change in the major infectious causes of fever has been observed in north-western Ecuador, with prevalence of malaria falling and dengue fever rising (468). Seasonality of DENV infection in coastal Ecuador involves annual and two-yearly peaks in incidence, which can be influenced by El Niño events (472,491). DENV seasonality in rural Ecuador involves an annual peak in mid-March (21), correlating with the rainy season occurring from February to May (472,473). In 2015, the year preceding the sampling for this study, a large spike in DENV cases was observed with 42.5 thousand cases reported (492), coinciding with a very strong el Niño event (493). It's possible that population immunity following 2015 was high and this is reflected in the low number of cases identified in the present study. Similar reasoning may explain the lack of CHIKV cases detected. The number of infections reported from Ecuador as a whole in 2016 was 1,195 (477), approximately a 30-fold decrease from the previous year.

Differences in prevalence between the study cohort and Ecuador as a whole could be explained by a number of factors including differences in geography, population density,

or vector abundance, to name just a few. Although the prevalence of pathogen RNA detected in febrile patients is interesting, the underlying causes are multi-factorial and difficult to identify definitively, therefore the observations made above must be viewed as speculative. Furthermore, interpretation of the RT-PCR/PCR results in a wider context is constrained by practical factors such as the relatively small sample size and the lack of information on the residence of most patients. However, the primary aim of the RT-PCR/PCR testing was to identify known agents and rule out samples for metagenomic sequencing, which was performed for the most part on samples with negative RT-PCR/PCR results with a view to detecting novel or unexpected viruses.

4.4.2 OROPOUCHE VIRUS WAS DETECTED IN A FEBRILE PATIENT FROM ECUADOR

Two potential co-infections, observed in patients D-087 (DENV and CHIKV) and D-124 (ZIKV and CHIKV), were investigated using metagenomic sequencing. OROV was unexpectedly detected in patient D-087, identified initially from taxonomic assignment, then by mapping to reference sequences, resulting in approximately 75% coverage of the genome across all three genomic segments. This was further corroborated by the identification of OROV-specific scaffolds generated from *de novo* assembly of reads. In addition to OROV and in agreement with the qRT-PCR result, a small fragment of DENV-1 sequence was detected from D-087, however isolation of DENV *in vitro* was unsuccessful. Anti-DENV IgM antibodies were detected using ELISA, suggesting a recent DENV infection in this patient. No CHIKV reads or anti-CHIKV IgM antibodies were identified, suggesting that the high Cq qRT-PCR result was non-specific, although the possibility of an infection that was below the limit of detection of metagenomic sequencing, and from which IgM antibodies had yet to reach a sufficient level for

detection, cannot be ruled out. Despite extensive efforts to identify a pathogenic agent using taxonomic assignment, mapping to reference genomes and *de novo* assembly, no viral sequence was identified from sample D-124.

Oropouche orthobunyavirus is an enveloped, single-stranded, negative-sense RNA virus belonging to the *Orthobunyavirus* genus within the *Peribunyaviridae* family. The OROV genome is segmented; the small (S) segment contains two overlapping ORFs coding for the viral nucleocapsid protein (N) and a second non-structural protein (NSs), the medium (M) segment encodes two glycoproteins (Gn and Gc) and a nonstructural protein (NSm), and the large (L) segment encodes the viral RNA-dependent RNA polymerase (176). Due to the segmented nature of the genome, reassortment is well-documented. In nature this can result in the occurrence of reassortant viruses, a number of which have been previously identified and characterised (494), including OROV-like reassortants (489,495). One such reassortant is IQTV, isolated from a febrile patient in the Peruvian city of Iquitos in 1999 (489). OROV and IQTV share S and L segments but have a different M segment (489). To check the genome sequence from the patient belonged to OROV and not IQTV, reads were mapped to an IQTV reference genome. No coverage of the M segment was achieved using the IQTV reference genome, which confirmed the virus species as OROV, highlighting an additional advantage of using metagenomics over qRT-PCR alone.

In humans, OROV causes a self-limiting febrile illness known as Oropouche fever. Cases of infection have been documented in Brazil, Peru, Panama, and Trinidad and Tobago, but prior to this study evidence of OROV in Ecuador had not been demonstrated either by detection of viral RNA or virus isolation. Two studies have demonstrated the presence of anti-OROV IgM antibodies in small numbers of people in Ecuador (479,480). Manock

et al. (2009) detected antibodies in 1/304 febrile patients sampled between 2001-2004 in the Pastaza province in the Amazon basin of Ecuador. Although virus isolation in Vero cells was unsuccessful (no CPE was observed), an OROV immunofluorescent assay subsequently performed on the cells did detect OROV (480). Forshey *et al.* (2010) detected antibodies in 2/350 febrile patients from Guayaquil, sampled between 2003-2007, although the result for one patient was considered presumptive because less than a 4-fold difference was measured between acute and convalescent serum samples (479).

The detection of OROV sequence in patient sample D-087 was confirmed by isolation of OROV in Vero and C6/36 cells, measured by an increase in viral RNA over a period of 7 days (Vero) and 14 days (C6/36). The presence of high titre infectious virus, quantified by plaque assay on Vero cells, was confirmed in the P1 Vero cell supernatant. Sequencing RNA extracted from supernatant resulted in the complete virus genome sequence, named OROV/EC/Esmeraldas/087/2016. Terminal sequences were confirmed by RACE to complete the genome. The genetic organisation of this strain is similar to that previously described for OROV (28). The sequence was submitted to the GenBank database and the isolated virus was banked with the NCPV, making it available for use by the wider scientific research community.

The complete OROV/EC/Esmeraldas/087/2016 genome sequence was used to re-map reads from the clinical sequencing data, which improved coverage of the M segment, but not the S or L segments. Interestingly, the OROV M segment was recently shown to have two distinct lineages within South America; lineage 1 representing central-eastern strains, and lineage 2 representing western strains (363). These were thought to diverge more than 200 years before the most recent common ancestors of the S or L segments

(363). The original mapping M segment reference sequence (strain BeAn19991, KP052851.1) belongs to lineage 1, whereas the Ecuadorian M segment belongs to lineage 2. The divergence in M segment sequences probably explains the lower M segment coverage from the original mapping.

Patient D-087 was a 41-year-old male patient who experienced fever, headache, joint pain, muscle pain and nausea in April 2016, when he presented at the medical centre in Esmeraldas and gave a blood sample for routine testing. The patient confirmed to collaborating researchers at the Universidad San Francisco de Quito (USFQ), in Ecuador, that he had been in Esmeraldas for more than three months. Furthermore, he had not travelled outside the province during that time, making it extremely likely that this infection was acquired in Esmeraldas. Interestingly, personal communications with Dr. Sonia Zapata, an entomologist at USFQ, suggest that the *Culicoides paraensis* midge; the primary vector of OROV transmission in urban outbreaks, is absent from the Pacific Coast region in which Esmeraldas is situated. This raises the question of the role of other insect vectors in this region, such as *Culex* species mosquitoes, which have been implicated in urban OROV transmission (180). The detection and isolation of OROV from patient sample D-087 constitutes the first direct detection of OROV in Ecuador (380). The utility of metagenomic sequencing for virus identification from febrile patients has been demonstrated by several studies (316,496–498). This approach is becoming more practicable as costs decrease, the major benefit being the ability to detect unexpected or novel viral sequences, as evidenced by this detection of OROV.

4.4.3 METAGENOMIC SEQUENCING DETECTED HEPATITIS A VIRUS IN A FEBRILE PATIENT

Metagenomic sequencing of RNA from 16 febrile patients with negative RT-PCR/PCR results was undertaken with the aim of detecting causative viruses. Despite applying multiple methods of data analysis encompassing taxonomic identification of reads, mapping to reference sequences and *de novo* assembly of reads, no evidence of causative viruses was present in 15/16 patient samples. The exception was sample D-005, from which 39% of the HAV genome was generated, strongly suggesting an infection in this patient.

The presence of internal control MS2 reads in patient samples was more consistent within the Ecuadorian cohort compared with the Sierra Leone cohort. As stated in chapter 3, this could be due to differences in sample processing, resulting from constraints related to containment level (the Ecuadorian samples could be processed at CL3, whereas the Sierra Leone samples had to be processed at CL4). All Ecuadorian patient samples contained MS2 reads, although the number per sample was highly variable.

HAV is a non-enveloped, single-stranded, positive-sense RNA virus belonging to the genus *Hepatovirus*, family *Picornaviridae* (49). Transmission is by the faecal-oral route via contaminated food or water, infection can be asymptomatic or show symptoms 2-6 weeks after infection, including fever, nausea, vomiting, diahorrea and jaundice (499). More serious cases result in acute liver failure and HAV infection is the most common cause of acute liver disease worldwide, with prevalence highly dependent on sanitary conditions (499). Ecuador is considered to have an intermediate level of endemicity for HAV (500) and as such there is no HAV vaccination campaign implemented in Ecuador (501). Prevalence rates in 2015 were reported to be 3.5 infections per 100,000 people

(502), although it is likely that incidence varies within Ecuador depending on sanitary conditions. A study investigating viral diversity in urban streams in the capital city of Quito detected HAV sequence in a single water sample (501), whereas a study on exposure of indigenous communities to waterborne pathogens in the Amazon region of Ecuador detected high seroprevalence rates (503).

4.4.4 ZIKV WAS ISOLATED FROM A FEBRILE PATIENT AND THE COMPLETE GENOME SEQUENCE ELUCIDATED

ZIKV was isolated from patient D-121 following one passage in C6/36 cells, measured by an increase in viral RNA over 14 days. One further passage was undertaken to increase titre and volume and virus supernatant was quantified using plaque assay. Isolation of ZIKV from D-124 was also achieved in C6/36 cells, however, the virus grew to a very low titre. Nonetheless, these isolations confirm the presence of infectious virus in the plasma of these febrile patients.

The ZIKV strain isolated from patient sample D-121 was named ZIKV/EC/Esmeraldas/121/2016 and was taken forward as a representative Ecuadorian ZIKV isolate for whole genome sequencing. The complete coding sequence was generated, annotated and is available on GenBank. This strain provides an important contribution to the bank of publicly available ZIKV sequences, of which only five of the 2,953 ZIKV entries in GenBank originate from Ecuador. This addition improves the diversity of available sequences, allowing better resolution in analyses of ZIKV ecology and genetic relationships.

Sequencing from cultured ZIKV D-124 was attempted but failed to produce genome sequence. This is unsurprising as previous experience of metagenomic sequencing ZIKV

(351) has shown that sequencing from samples with relatively high Cq values produces very low numbers of viral reads.

4.4.5 COMPLETE GENOME SEQUENCES OF CONTROL STRAIN VIRUSES DETERMINED

In addition to sequencing patient-derived viruses, a number of control viruses were also sequenced; CHIKV, DENV-1 and OROV strains held by the NCPV, and one DENV-1 strain isolated from a febrile Ecuadorian patient in 2014. The addition of these complete genomes to GenBank provides added value for NCPV customers as well as other researchers, as the sequences are now freely available. The sequence information has contributed to the improved characterisation of the NCPV catalogue. The inclusion of these sequences as reference sequences during the metagenomic sequencing data analysis was helpful in identifying any potential contaminant sequences, as well as providing a contemporary Ecuadorian DENV-1 strain for mapping purposes.

4.4.6 LIMITATIONS

Although metadata was collected with the patient samples, some valuable fields of information are missing for many samples. Most notably, a location of residence and the precise date of sampling is missing for the majority of samples. Despite continued efforts of collaborating researchers in Ecuador to obtain these details, it has not been possible. This makes it difficult to further investigate potential geographical or temporal foci of infection.

RT-PCR/PCR testing was carried out primarily to aid sample selection for metagenomic sequencing by identifying samples infected with pathogens commonly seen in Ecuador

and surrounding areas. A positive result indicates the presence of pathogen nucleic acid but does not necessarily confirm an infection, particularly when high Cq values are observed. To confirm, undertaking complementary testing such as virus isolation or detection of virus-specific IgM antibodies is desirable. Virus isolation and ELISA were undertaken on a small number of selected samples, but widescale virus isolation and antibody detection did not align with the focus of the project; namely detection and investigation of novel or unexpected viruses.

The limitations relating to metagenomic sequencing and data analysis, outlined in section 3.4.4, also apply to pathogen detection in the Ecuadorian cohort. Contaminant sequences were controlled for in the same way; by sequencing NXCs from each batch of RNA extractions along with a NTC, then analysing the resulting data in the same way as the patient samples. This is a good way of ruling out reads that may result from laboratory or reagents, however it is possible that pathogen-specific reads originating from the patient may be discarded. Differentiating between 'real' and 'contaminant' reads in this instance is very challenging. This study took a conservative approach by ruling out all potential contaminant reads in order to avoid misinterpreting or over-interpreting data of unclear origin.

CHAPTER 5: DEVELOPMENT OF MOLECULAR DETECTION METHODS FOR OROPOUCHE VIRUS AND SUBSEQUENT DETECTION OF MULTIPLE CASES FROM ECUADOR

5.1 INTRODUCTION

OROV was first isolated from a febrile forest worker in Trinidad and Tobago in 1955 (177). In subsequent decades the virus has been responsible for over 30 epidemics of Oropouche fever in Central and South America, totalling approximately 500,000 infections (182). Most outbreaks have occurred in Brazil; epidemics occurred in a number of municipalities in the state of Pará during the 1960s and 70s (504). In the 1980s and 90s, outbreaks were reported from other Brazilian states; Amazonas, Amapá, Acre, Rondônia, Maranhão and Tocantins (505–510). Since the 2000s, outbreaks in regions of Pará and Amazonas states have continued, including the re-emergence of the virus in the north-eastern area of Pará state after 26 years without detection (511,512). Outbreaks have also been reported in Panama and Peru. A single outbreak was reported from a village 50 km from Panama City in 1989 (28). In Peru, OROV was first reported from Iquitos City in 1992 (513), then from the Amazon region in 1994 (514). More recently, outbreaks were reported from Cusco and the western region of the Peruvian Amazon (515,516).

The molecular detection and isolation of OROV from a febrile Ecuadorian patient using metagenomic sequencing, described in chapter 4, was the first time this emerging virus was directly detected in Ecuador (380). Although the metagenomic sequencing approach is becoming more practicable as costs decrease (44), in most cases the cost per sample is still substantially higher than that incurred by conventional detection methods such as RT-PCR or ELISA. This is of particular importance considering that drivers of EID emergence are more prevalent in low-and-middle income countries (5),

where public health capacity is often already overstretched. An aim of this chapter was to develop a sensitive, relatively low-cost method capable of detecting OROV RNA that could be used to test the Ecuadorian patient sample cohort and would be relatively straightforward to implement in-country.

A number of RT-PCR assays capable of detecting OROV are described in the literature (361,517–522). The real-time RT-PCR format provides benefits over the conventional approach in speed, specificity (particularly when using hydrolysis probes), the ability to observe results in real-time, and the ability to relatively quantitate RNA. At the time this work was performed, only two of the published assays were in real-time format (361,517). Preliminary work had been done at PHE prior to this project to adapt the OROV-specific real-time RT-PCR assay targeting the S segment, developed and published by Weidmann *et al.* (2003) (361). The adapted assay successfully amplified OROV RNA from the prototype strain TRVL 9760. Following the detection of OROV in patient sample D-087 using metagenomic sequencing, the patient RNA was tested using the adapted Weidmann assay, however detection of OROV RNA was unsuccessful. This led to the qRT-PCR adaptation and development work described in this chapter.

The objectives of this chapter were to establish whether OROV was present within other patient samples from Esmeraldas, Ecuador in 2016, and to characterise any detected OROV using whole genome sequencing and virus isolation. Genome sequences were used in phylogenetic analyses in an attempt to shed light on the dynamics of OROV in Ecuador and neighbouring areas. Complementary to these objectives was the development of a nucleic acid amplification assay that has utility both in this project and in supporting in-country laboratories in OROV surveillance and diagnostic testing.

5.2 RESULTS

5.2.1 DEVELOPMENT OF AN OROV QRT-PCR

5.2.1.1 PRIMER DESIGN AND TESTING

Primer and probe sequences from the Weidmann OROV qRT-PCR assay (361) were compared with the OROV/EC/Esmeraldas/087/2016 consensus sequence. Two mismatches were identified in the reverse primer (the forward primer and probe were identical to the consensus sequence). Two new reverse primers were designed. Primer 'EcR' binds to the same region of the S segment, but the mismatched bases were altered to match the Ecuadorian sequence (Table 5.1). Primer 'Ec2R' is located at an alternative region of the S segment, genome position 179-198 (Table 5.1). This region was identified as well conserved from an alignment of known OROV nucleoprotein (N) gene sequences (Appendix 7), representing OROV sequences sampled from the 1950s to the late 2000s, covering genetic diversity from outbreaks in Trinidad & Tobago, Panama, Peru and Brazil.

Sensitivity of the two newly designed primers was compared to the original using two OROV strains from genetically distinct lineages: the OROV/EC/Esmeraldas/087/2016 strain and the 1955 prototype Trinidad and Tobago strain TRVL 9760 (KP026179.1 - KP026181.1). Ten-fold dilution series of RNA from both strains were tested using the adapted qRT-PCR (conditions in section 2.7.4). The original reverse primer (OROV R) was less sensitive to the Ecuadorian strain (detected to 10^{-4} dilution) compared with the prototype strain (detected to 10^{-6} dilution, Figure 5.1). Primer EcR detected the Ecuadorian strain with higher sensitivity compared with the original primer (detected to 10^{-7} dilution and 10^{-4} dilution, respectively) but was less sensitive to the prototype strain (detected to 10^{-3} dilution, Figure 5.1). Ec2R improved sensitivity compared to the original

primer by three logs for the Ecuadorian strain and by one log for the prototype strain (Figure 5.1).

Oligo name	Sequence (5' - 3')	Start position	End position	Length (bp)	Tm (°C)	GC content (%)	Reference
OROV F	CATTTGAAGCTAGATACGGACAA	118	140	23	59	39	(361)
OROV R	CCATGGGCCTCGATG	225	211	15	52	67	(361)
EcR	CCATGGGCCGCGACG	225	211	15	57	80	This study
Ec2R	CATCTTTGGCCTTCTTTTRG	198	179	20	54-56	40-45	This study
OROV P	CAATGCTGGTGTTGTTAGAGTCTTCTTCCT	146	175	30	69	43	(361)

Table 5.1 Oligonucleotides used in the development of the OROV qRT-PCR.

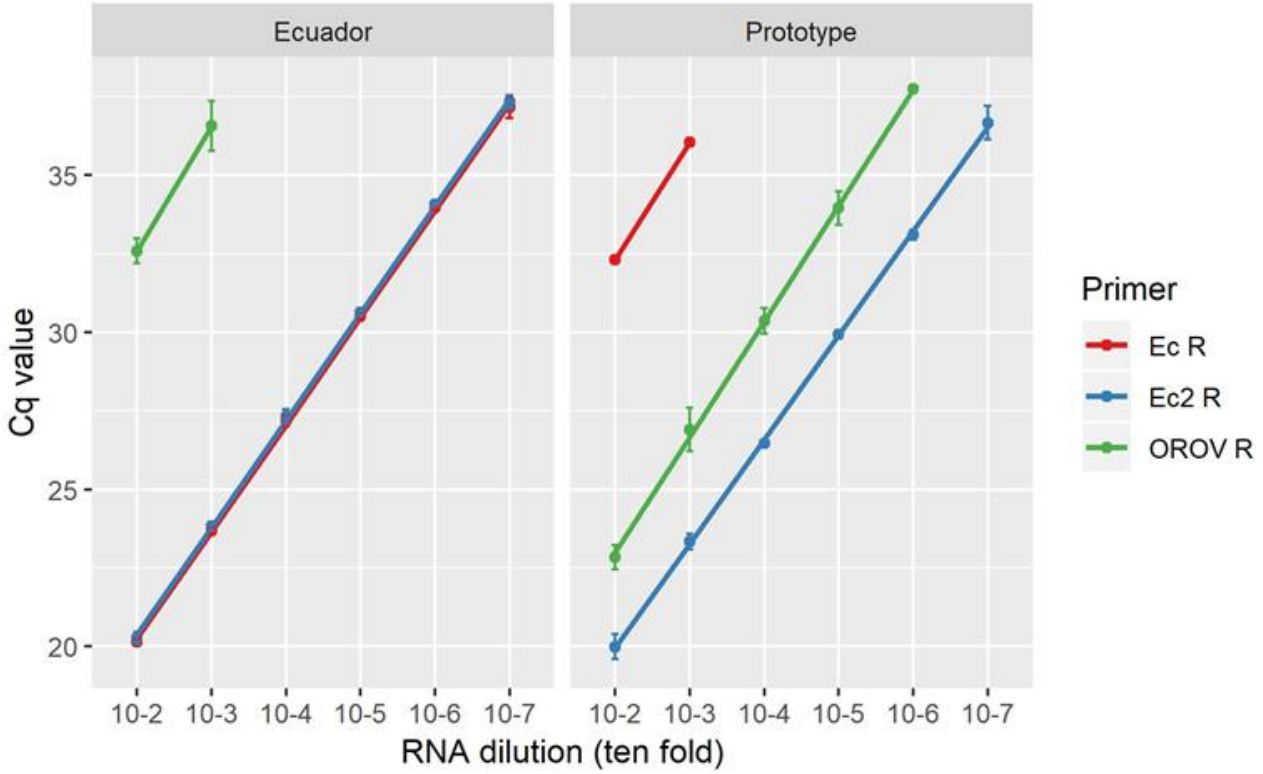

Figure 5.1 Sensitivity analysis of three reverse primers as part of the OROV qRT-PCR assay development. Cq values are shown for ten-fold serial dilutions of OROV RNA, from the prototype strain (KP026181.1), and the Ecuadorian strain OROV/EC/Esmeraldas/087/2016 (MF926352.1). Three separate experiments were performed, from which the means (data points) and standard deviations (error bars) were calculated.

In the absence of an extensive panel of OROV strains to test against, primer Ec2R and the original OROV R primer were aligned with all publicly available (*n*=149) existing OROV N gene sequences to identify mismatches that may indicate reduced sensitivity for certain strains (Appendix 7). 19 strains had mismatch(es) to the forward primer (17 strains with a single mismatch, 2 strains with two mismatches), 21 strains had a single mismatch to the probe, and 26 strains had mismatch(es) to the original OROV R primer (20 strains = one mismatch, 6 strains = two mismatches, Table 5.2). In contrast, no strain had more than one mismatch to reverse primer Ec2R; however, the number of strains with a single mismatch was higher (*n*=41, Table 5.2). Reverse primer Ec2R was selected for use in the qRT-PCR assay because of the improved sensitivity observed for both the Ecuadorian and prototype OROV strains.

Number of mismatches	Forward primer	Reverse primer (OROV R)	Reverse primer (Ec2R)	Probe
1	17	20	41	21
2	2	6	0	0
>2	0	0	0	0

Table 5.2 Mismatches to oligonucleotide sequences observed from an alignment of 149 OROV N gene sequences. Values are the number of sequences with mismatches to the primer/probe sequence.

5.2.1.2 ASSAY OPTIMISATION AND VALIDATION

As explained in section 2.7.3, unless a substantial improvement in sensitivity was demonstrated (>2 Cq), primer/probe/$MgSO_4$ conditions were set to comply with those standardised by the Rare and Imported Pathogens Laboratory (RIPL). This ensured that the assay could be easily incorporated into the RIPL test protocol for returning UK travellers.

Optimal primer, probe and $MgSO_4$ concentrations were determined using RNA from strain OROV/EC/Esmeraldas/087/2016. Optimal conditions were defined as those giving the lowest Cq value across the range tested. From the primer concentrations tested (multiple combinations at 1 µM, 3 µM, 9 µM and 18 µM), the optimal concentration for the forward and reverse primer was 18 µM (Cq 26.20), identical to the RIPL standard concentration Table 5.3). The probe concentration was tested from 5 µM to 25 µM and the optimal concentration was 5 µM (Cq 24.59). However, the RIPL standard of 12.5 µM gave a relatively similar result (Cq 26.15) and was therefore adopted (Table 5.3). The optimal condition of $MgSO_4$ was 85 mM (Cq 27.30), however the RIPL standard (no added $MgSO_4$) gave a similar result (Cq 28.20) and again was adopted (Table 5.3). Cross-reactivity to RNA from 23 virus species (Table 5.4) and a panel of negative human sera was assessed, no cross-reactions were observed.

	Optimal		RIPL standard	
Parameter	Concentration	Test result (Cq)	Concentration	Test result (Cq)
Primers	18 µM	26.20	18 µM	26.20
Probe	5 µM	24.59	12.5 µM	26.15
$MgSO_4$	85 mM	27.30	None added	28.20

Table 5.3 Cq values from optimal and RIPL standardised qRT-PCR conditions.

Virus family	Virus genus	Virus species
Arenaviridae	Mammarenavirus	Tamiami mammarenavirus
Flaviviridae	Flavivirus	Powassan virus
Flaviviridae	Flavivirus	West Nile virus
Flaviviridae	Flavivirus	Yellow fever virus
Flaviviridae	Flavivirus	Karshi virus
Flaviviridae	Flavivirus	Usutu virus
Flaviviridae	Flavivirus	Dengue virus serotype 1
Flaviviridae	Flavivirus	Dengue virus serotype 2
Flaviviridae	Flavivirus	Dengue virus serotype 3
Flaviviridae	Flavivirus	Dengue virus serotype 4
Flaviviridae	Flavivirus	Zika virus
Nairoviridae	Orthonairovirus	Crimean-Congo hemorrhagic fever orthonairovirus
Nairoviridae	Orthonairovirus	Issyk-Kul virus
Peribunyaviridae	Orthobunyavirus	Batai orthobunyavirus
Peribunyaviridae	Orthobunyavirus	La Crosse orthobunyavirus
Peribunyaviridae	Orthobunyavirus	Inkoo virus
Peribunyaviridae	Orthobunyavirus	Tahyna virus
Phenuiviridae	Phlebovirus	Bhanja virus
Phenuiviridae	Phlebovirus	Severe fever with thrombocytopenia syndrome virus
Phenuiviridae	Phlebovirus	Rift Valley fever phlebovirus
Togaviridae	Alphavirus	Chikungunya virus
Togaviridae	Alphavirus	Mayaro virus
Togaviridae	Alphavirus	O'nyong-nyong virus

Table 5.4 Viruses tested for cross-reactivity with the OROV qRT-PCR.

5.2.1.3 DETERMINING THE OROV QRT-PCR LIMIT OF DETECTION

To determine the absolute detection limit of the optimised qRT-PCR assay, a ten-fold dilution series of synthetically generated OROV RNA (711 bp region of the OROV/EC/Esmeraldas/087/2016 S segment encompassing the N and Ns ORFs, see section 2.7.3); was tested in triplicate. Mean Cq values were used to construct a standard curve (Figure 5.2). A linear relationship between mean Cq value and log RNA copy number was observed and the absolute limit of detection of the assay was 10 copies of OROV RNA at a mean Cq value of 38.25 (95% confidence interval 37.8 to 38.7).

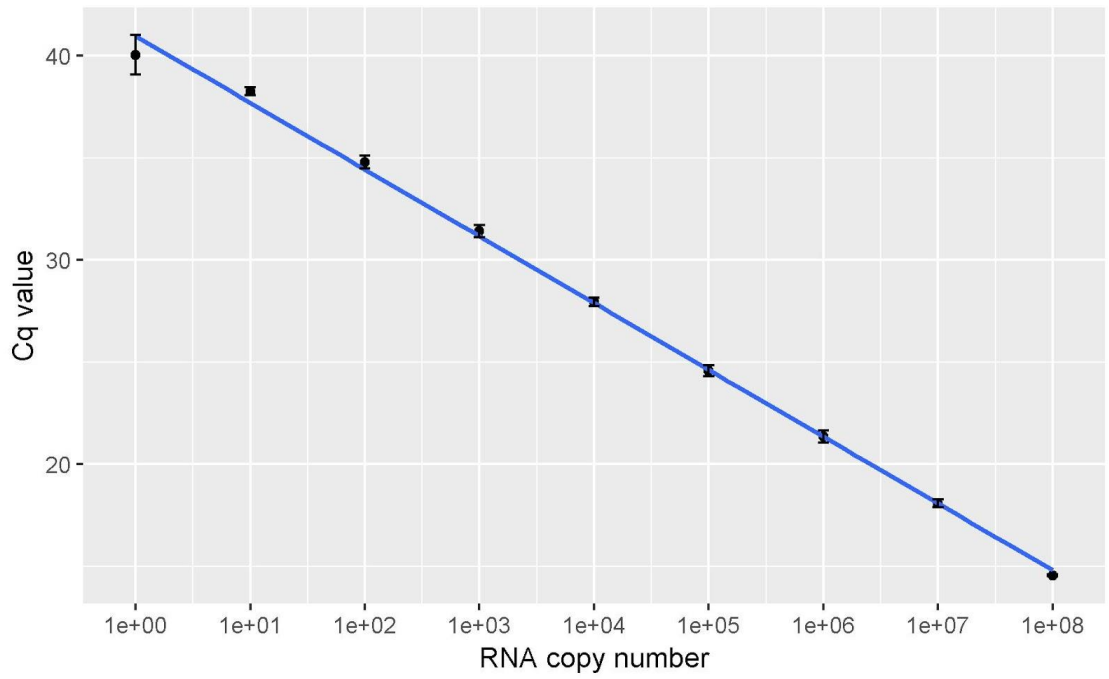

Figure 5.2 Absolute quantitation was performed from a standard curve generated from a ten-fold serial dilution of a synthetic OROV RNA standard. Each data point is the mean Cq value from three separate experiments. Error bars indicate standard deviation from the mean. R^2 = 0.9978.

5.2.2 RETROSPECTIVE QRT-PCR TESTING FOR OROV IN THE ECUADOR 2016 PATIENT COHORT

The optimised, validated qRT-PCR was shown to be sensitive for the Ecuadorian OROV strain to a limit of 10 RNA copies. The assay was used to screen the entire febrile patient Ecuador 2016 cohort (*n*=196) which identified a total of six patient samples (3.1% prevalence) positive for OROV, including the original sample D-087 (Table 5.5). 5/6 patients were male, age data was only available for 2/6 patients (Table 5.5). The length of time patients reported experiencing fever prior to blood sampling (2-7 days) inversely correlated with OROV genome copies/mL plasma (Figure 5.3).

Sample ID	Sex (M/F)	Age	Days of Fever	OROV qRT-PCR (Cq value)	Estimated genome copies/mL plasma
D-057	M	35	3	25.66	1.3e+9
D-087	M	41	7	36.26	9.6e+3
D-155	M	nd	2	25.75	1.2e+9
D-171	F	nd	2	26.75	6.0e+8
D-206	M	nd	4	30.87	2.0e+7
D-210	M	nd	3	29.18	9.2e+7

Table 5.5 Ecuadorian OROV-positive patient samples, determined by OROV S segment qRT-PCR. Genome copies/mL plasma are estimated based on the absolute quantitation standard curve. nd = no data.

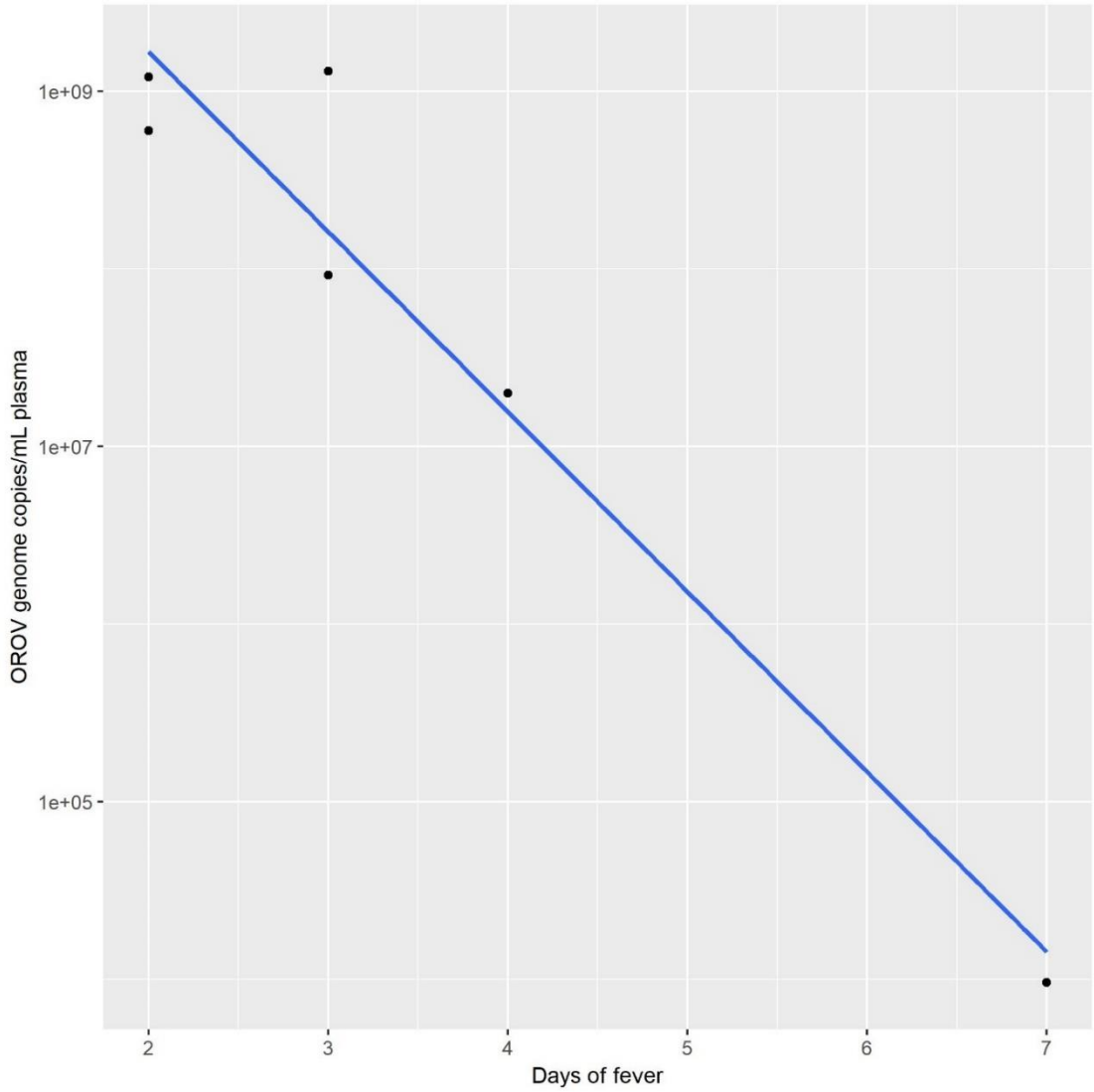

Figure 5.3 The inverse correlation between the number of days of fever experienced by OROV-positive patients prior to blood sampling, and OROV genome copies/mL plasma. $R^2 = 0.9405$.

5.2.3 WHOLE GENOME SEQUENCING OF OROV PATIENT GENOMES

To confirm the OROV qRT-PCR results and generate genome sequences from the five additional OROV-positive patients, metagenomic sequencing was undertaken as described in sections 2.8 and 2.9. The reads from each patient were mapped to the complete OROV/EC/Esmeraldas/087/2016 genome sequence. Sequencing resulted in coverage ranging from 63.5 – 99.4% of the OROV genome for all five samples (Table 5.6, Figure 5.4), however, only two reads from D-206 mapped to the S segment sequence. The proportion of reads mapping to the OROV reference sequence varied between samples but loosely correlated with the number of OROV genome copies/mL (Figure 5.5).

To detect co-infections with other viruses in the additional five OROV-positive samples, sequencing data was analysed as previously described in Chapter 4, using a combination of taxonomic assignment of reads (Centrifuge), mapping to a range of relevant virus reference genomes, and *de novo* assembly of reads (see section 2.11). No other viruses were identified.

Sample ID	Reads mapped to OROV genome (number)	Proportion of total reads mapped to OROV genome (%)	OROV genome coverage (%)	S segment coverage (%)	M segment coverage (%)	L segment coverage (%)
D-057	870,960	33.95	99.41	100.00	98.68	99.80
D-155	24,274	5.29	84.61	82.14	86.30	83.87
D-171	145,146	15.63	94.79	95.80	94.73	94.69
D-206	277,019	5.60	63.50	0.00	78.62	62.64
D-210	733,986	26.12	87.40	88.76	97.54	80.72

Table 5.6 Mapping statistics for the five additional OROV-positive patient plasma samples. Coverage cut off was a minimum of five reads. Reads mapped refers to all three genome segments combined. Mapping was to strain OROV/EC/Esmeraldas/087/2016.

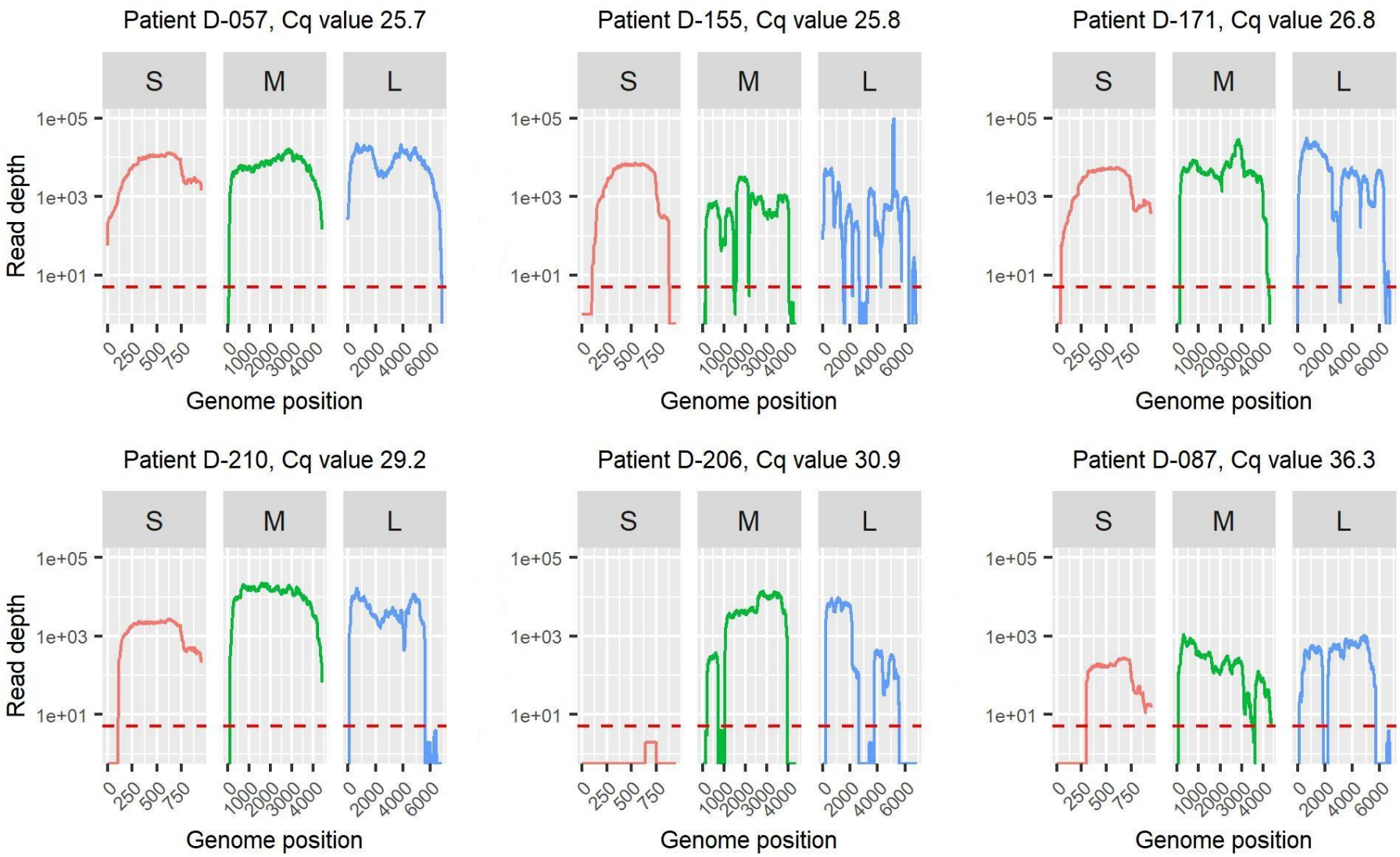
Patient D-057, Cq value 25.7
Patient D-155, Cq value 25.8
Patient D-171, Cq value 26.8
Patient D-210, Cq value 29.2
Patient D-206, Cq value 30.9
Patient D-087, Cq value 36.3
S
M
L
Read depth
1e+05
1e+03
1e+01
0
250
500
750
1000
2000
3000
4000
6000
Genome position

A)

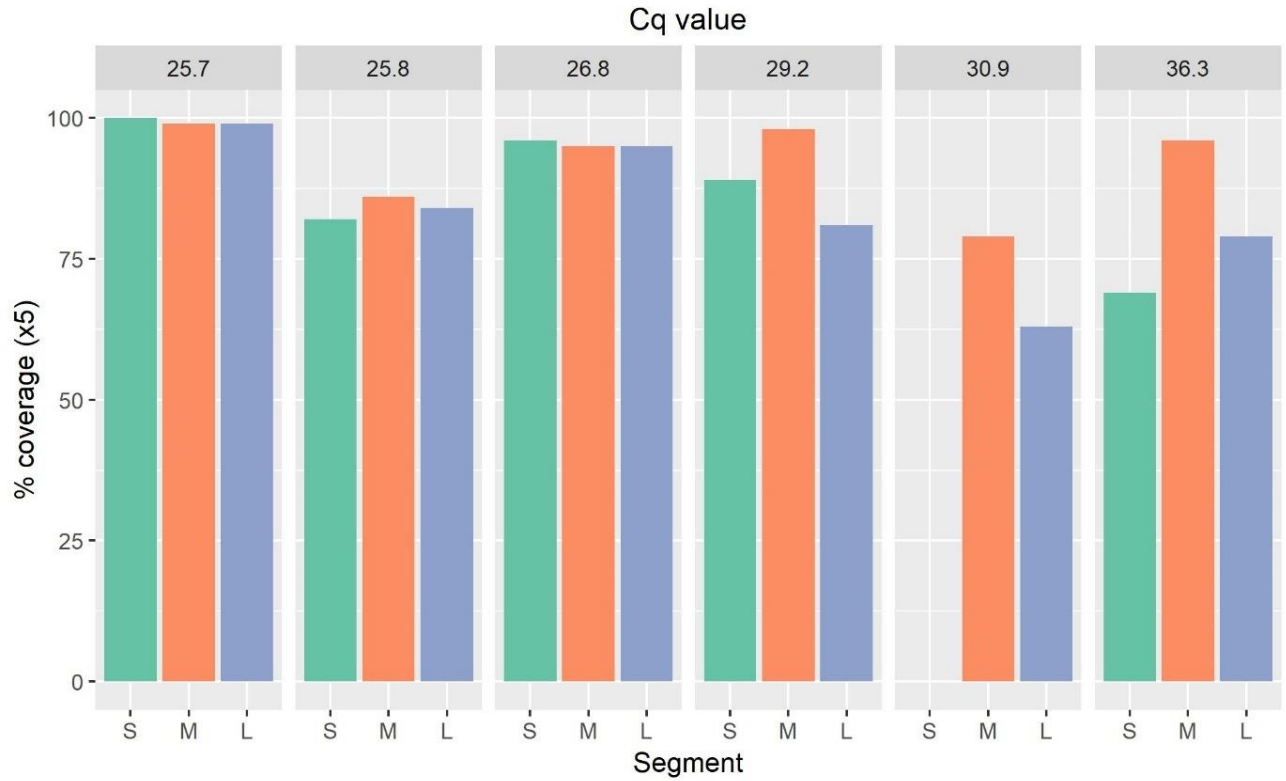

B)

Figure 5.4 OROV genome coverage generated from six OROV positive patient plasma samples, using a metagenomic sequencing approach. Reads were mapped to reference sequences OROV/EC/Esmeraldas/087/2016 (MF926352.1- MF926354.1). **A)** OROV genome coverage shown as the number of reads at each genomic position. Plots are separated by genome segment (S, M, L). Red dashed line indicates 5x coverage. **B)** OROV genome segment (S, M, L) coverage (%). qRT-PCR Cq value is given at the top of each plot. Coverage is defined as a minimum of 5 reads at any given position.

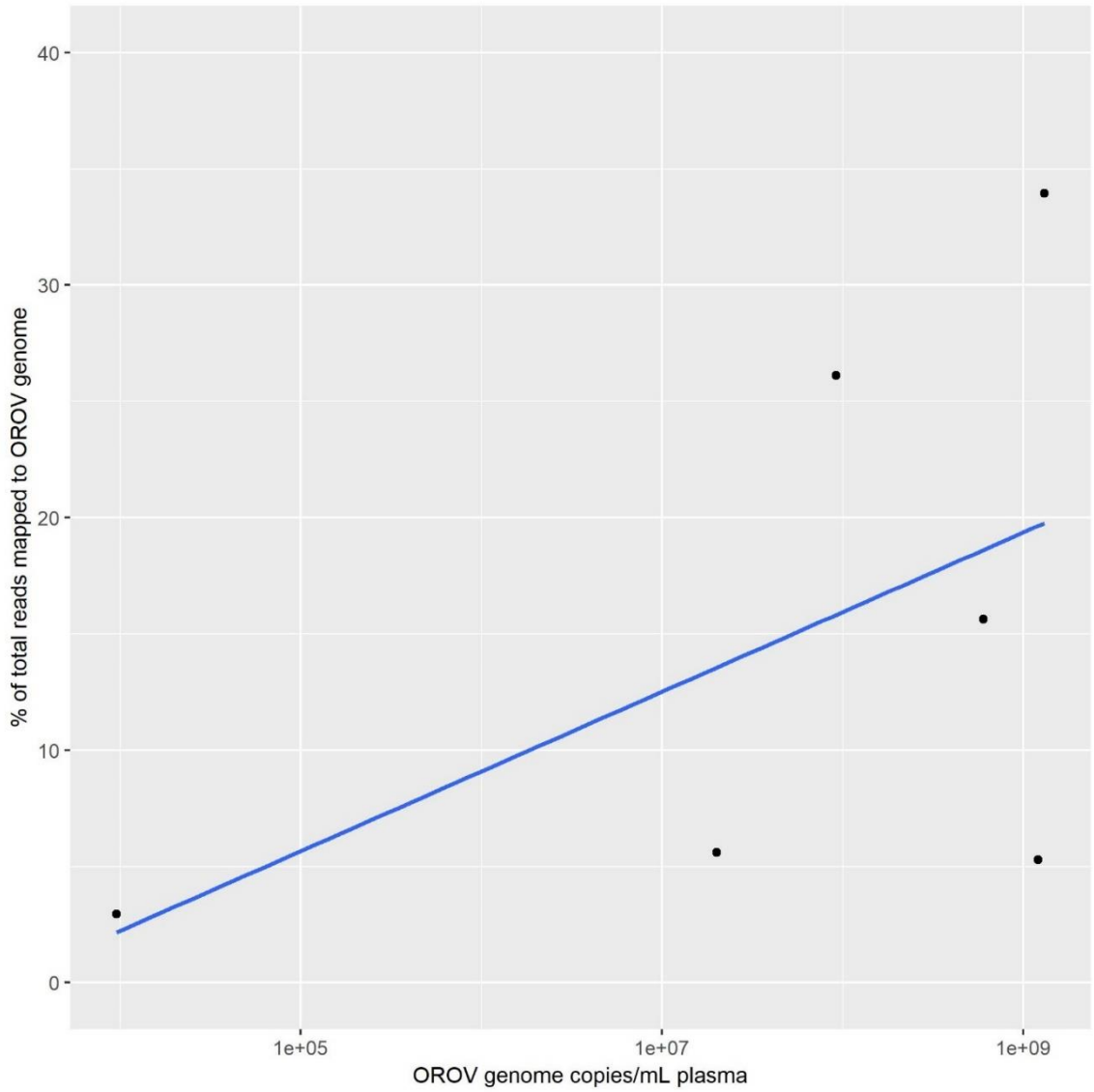

Figure 5.5 The correlation between the proportion of sequencing reads mapped to an OROV reference genome, and the number of OROV genome copies/mL in the patient's plasma. R2 = 0.1319

5.2.4 ISOLATION OF OROV AND ANALYSIS OF VIRUS GENOME SEQUENCES

OROV was successfully isolated from all five OROV positive patient plasma samples following one passage in Vero cells. S segment copy numbers for all samples increased by at least 5 logs, to approximately 1.0e+12 copies/mL at 72 hours post-infection (Figure 5.6), demonstrating OROV genome replication.

RNA was extracted from the isolated viruses and metagenomic sequencing was performed. Reads were mapped to the OROV/EC/Esmeraldas/087/2016 genome sequence and consensus sequences were generated from the mapped reads using Quasi bam (see section 2.11.3). Complete OROV genomes were generated for all five isolates. Sequences were annotated and made available on GenBank under accession numbers MK506818.1 - MK506832.1.

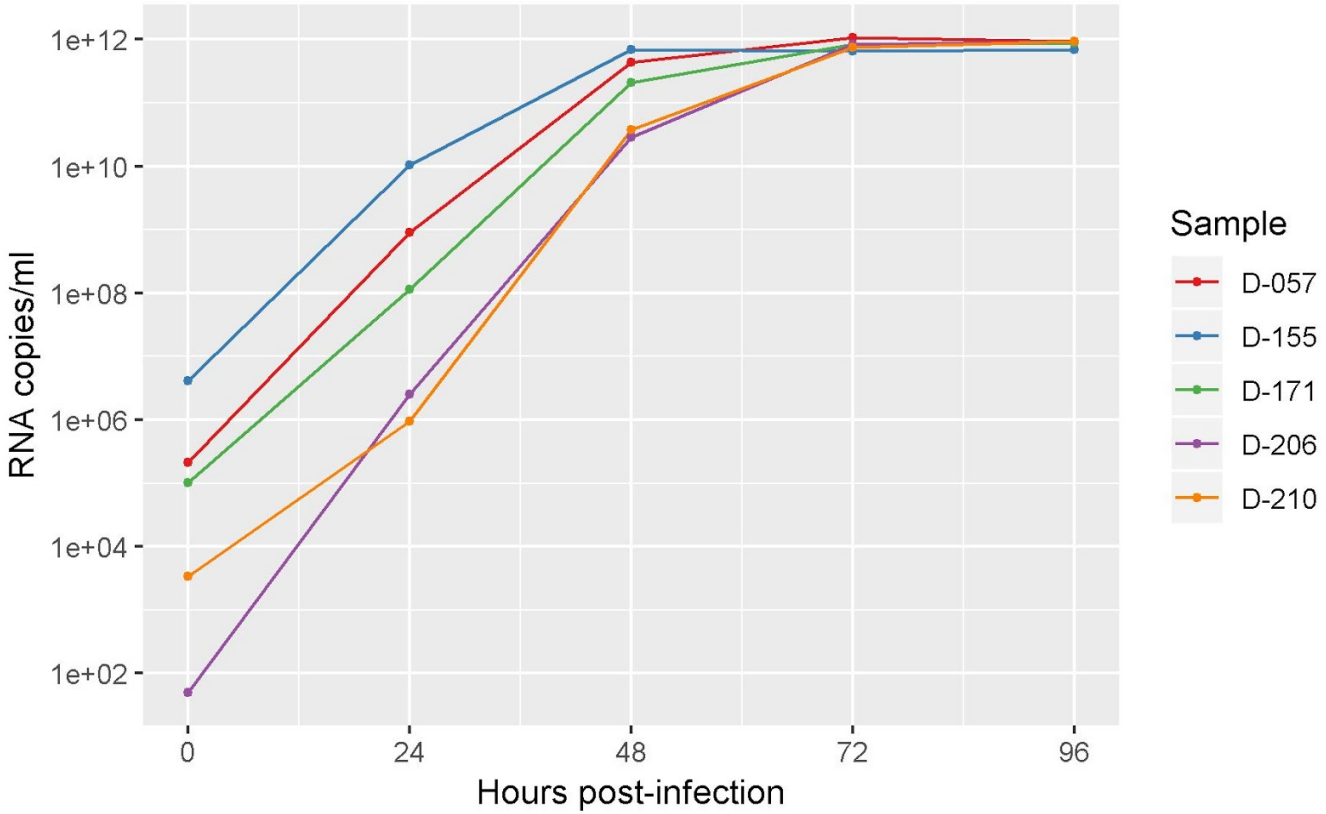

Figure 5.6 OROV genome copies increased over 96 hours in Vero cells, demonstrating OROV genome replication in five independent OROV cultures from OROV-positive patient plasma samples.

The six Ecuadorian OROV genomes were aligned to compare nucleotide identity. The genomes were 99.7-100% identical to one another in the S segment and 99.9-100% identical in the M and L segments. Single nucleotide polymorphisms (SNPs) were observed at 33 positions throughout the genome, all of which occurred in coding regions (Table 5.7). Protein sequences were aligned to compare amino acid identity. The N protein was identical between isolates, whilst isolate D-206 showed a single amino acid substitution in the NSs protein (Table 5.8). Isolate D-210 showed two amino acid substitutions in the M protein, and three other isolates (D-057, D-155 and D-206) showed one substitution in this protein (Table 5.8). Two isolates (D-155 and D-210) showed a single amino acid substitution in the L protein (Table 5.8). A total of eight substitutions were observed, five of which constituted a reactive (R) group change (three in the M segment and two in the L segment, Table 5.8).

Genome position	Genome segment	D-057 base	D-087 base	D-155 base	D-171 base	D-206 base	D-210 base
329	S	G	G	G	G	A	G
551	S	T	C	C	C	C	C
689	S	A	G	G	G	G	G
1501	M	A	A	T	A	A	A
1751	M	T	T	T	T	C	T
2038	M	C	C	C	C	T	C
2230	M	A	A	A	A	A	G
2363	M	T	C	T	T	T	T
2403	M	A	G	G	G	G	G
2810	M	G	R*	G	G	G	G
2859	M	A	A	A	A	A	G
3290	M	T	T	C	T	T	T
4028	M	C	C	C	C	C	A
4124	M	G	G	A	G	G	G
4313	M	T	T	T	T	C	T
4340	M	G	A	A	A	A	A
4490	M	T	C	C	C	C	C
6129	L	T	C	T	T	T	T
6174	L	A	A	A	A	G	A
6200	L	A	A	A	A	A	G
6579	L	G	G	G	G	A	G
7599	L	T	C	C	C	C	C
8865	L	G	A	A	A	A	A

9235	L	T	T	T	T	T	C
9336	L	G	G	A	G	G	G
9571	L	A	A	G	A	A	A
9591	L	G	A	G	G	G	G
10039	L	A	G	G	G	G	G
10737	L	A	A	A	G	A	A
10791	L	C	C	C	C	C	T
11133	L	C	T	C	C	C	C
11208	L	C	C	C	C	A	C
11733	L	C	C	C	C	T	C

Table 5.7 SNPs identified between six Ecuadorian OROV genomes (sequenced from P1 Vero cell supernatant). Variant base is shaded grey. *R position = 79% T, 21% C.

Protein	Isolate	Codon	Consensus AA	SNP AA	R group change
NSs	D-206	88	C	Y	None
M (Gn)	D-155	173	Q	L	Polar / non-polar
M (NSm)	D-206	352	A	V	None
M (NSm)	D-210	416	K	R	None
M (NSm)	D-057	464	A	T	Non-polar / polar
M (Gc)	D-210	626	T	A	Polar / non-polar
L	D-210	273	D	G	Acidic / non-polar
L	D-155	1397	T	A	Polar / non-polar

Table 5.8 Amino acid variation between six Ecuadorian OROV genomes. AA = amino acid. Gn = glycoprotein Gn. NSm = non-structural protein NSm. Gc = glycoprotein Gc. Bunyavirus Gn, NSm and Gc protein positions are taken from GenPept entry AGH07923.1. R group = reactive group.

OROV genome sequences from patient and cultured material were compared to identify SNPs incurred during passage. The number of SNPs ranged from one (D-057) to 15 (sample D-155, Table 5.9). The majority of changes were from a base where there was a mixed population in the patient (defined as no one base occupying >80% of reads), to either a different mixed population, or a majority population (majority defined at a base occupying >80% reads at a position) in the cultured isolate. The complete list of SNPs is given in Appendix 8. Changes from a majority population in the patient were less common, seen at two (D-171 and D-210) to five (D-087) positions, with sample D-057 showing no changes of this type (Appendix 8). Only one of the 49 positions showing

polymorphisms between patient and cultured sequences was conserved between isolates (M segment position 59, Appendix 8).

OROV strain	S SNPs	M SNPs	L SNPs	Total SNPs
D-057	1	0	0	1
D-087	1	6	5	12
D-155	2	6	7	15
D-171	1	2	3	6
D-206	nd	2	7	9
D-210	0	2	5	7

Table 5.9 A summary of the number of SNPs present in each OROV genome segment (S, M and L), between patient and cultured genome sequences. nd = no patient genome data available.

5.2.5 PHYLOGENETIC ANALYSIS OF ECUADORIAN OROV GENOMES

Phylogenetic analysis of the Ecuadorian OROV genome sequences in the wider context of OROV sequence diversity was investigated by aligning a representative Ecuadorian OROV sequence (OROV/EC/Esmeraldas/087/2016) with OROV complete coding sequences from Genbank (*n*=112 S segments, *n*=24 M segments, *n*=23 L segments. These include two IQTV isolates). Maximum Likelihood phylogenetic trees revealed that all three Ecuadorian segment sequences cluster with Peruvian sequences. The most closely related strain was IQE-7894, isolated from Peru in 2008 (KP795084.1-KP795086.1, Figure 5.7 and Figure 5.8). The Ecuadorian OROV N gene is also closely related to that of two IQTV strains isolated in Peru (Figure 5.7), however, the genetic divergence from IQTV seen in the M and L segments (Figure 5.8) confirms that the Ecuadorian strains are OROV, not IQTV. The Ecuadorian and closely related Peruvian N gene sequences do not cluster with a pre-defined genotype (Figure 5.7).

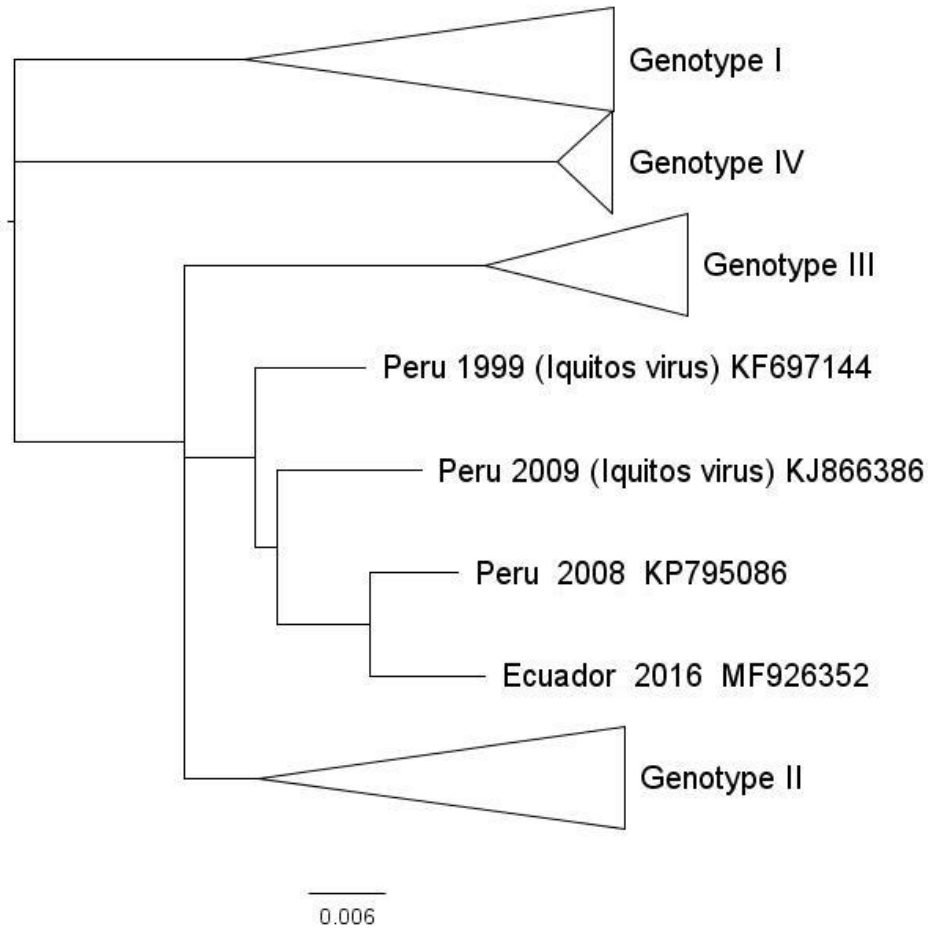

Figure 5.7 Maximum Likelihood tree for the OROV N gene (S segment). Roman numerals indicate genotypes as previously described for OROV (28). FigTree 1.4.2 (http://tree.bio.ed.ac.uk/software/figtree) was used to produce the final tree.

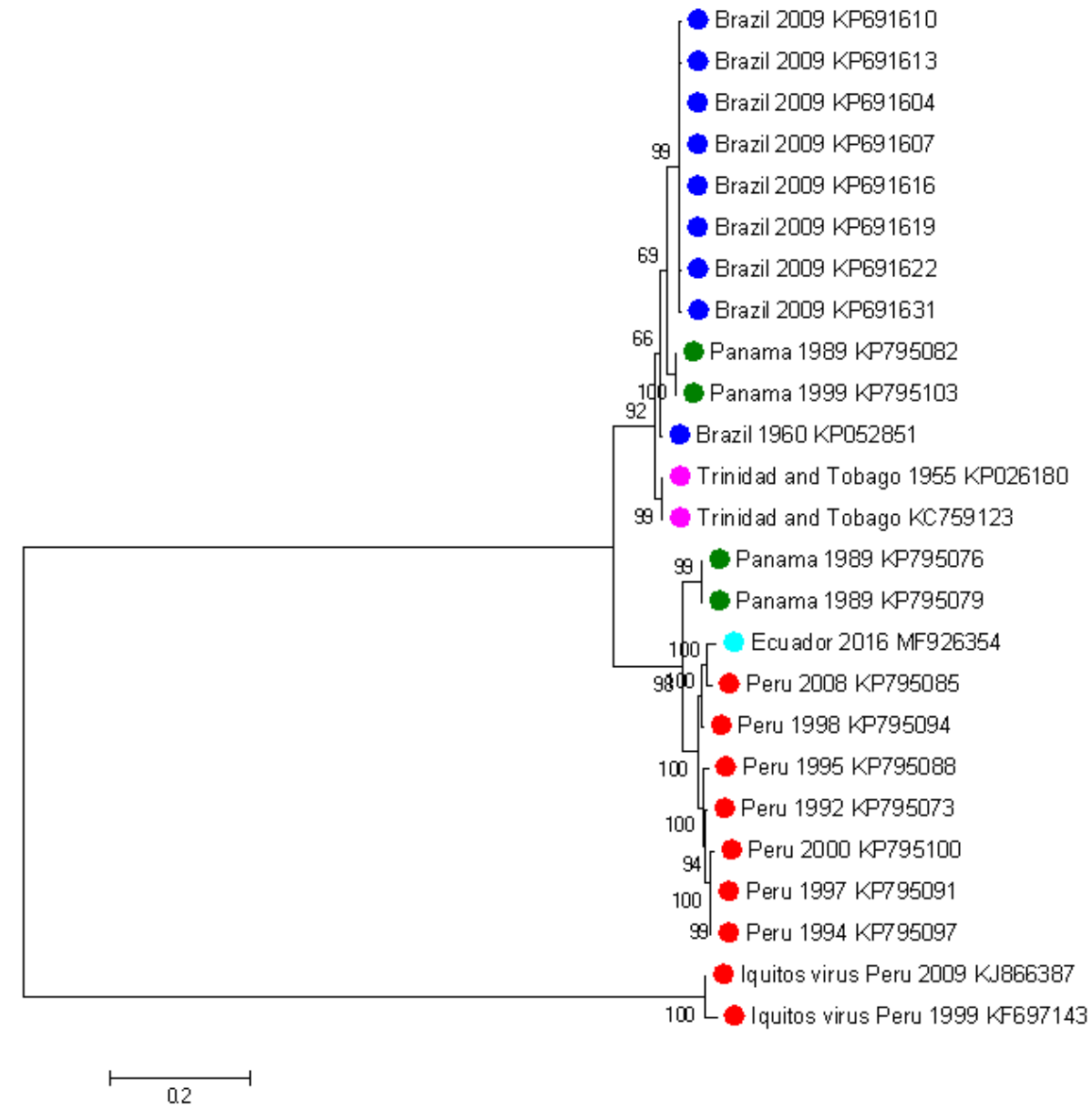
Brazil 2009 KP691610
Brazil 2009 KP691613
Brazil 2009 KP691604
Brazil 2009 KP691607
Brazil 2009 KP691616
Brazil 2009 KP691619
Brazil 2009 KP691622
Brazil 2009 KP691631
Panama 1989 KP795082
Panama 1999 KP795103
Brazil 1960 KP052851
Trinidad and Tobago 1955 KP026180
Trinidad and Tobago KC759123
Panama 1989 KP795076
Panama 1989 KP795079
Ecuador 2016 MF926354
Peru 2008 KP795085
Peru 1998 KP795094
Peru 1995 KP795088
Peru 1992 KP795073
Peru 2000 KP795100
Peru 1997 KP795091
Peru 1994 KP795097
Iquitos virus Peru 2009 KJ866387
Iquitos virus Peru 1999 KF697143
99
69
66
100
92
99
99
100
98
100
94
100
99
100
0.2

A)

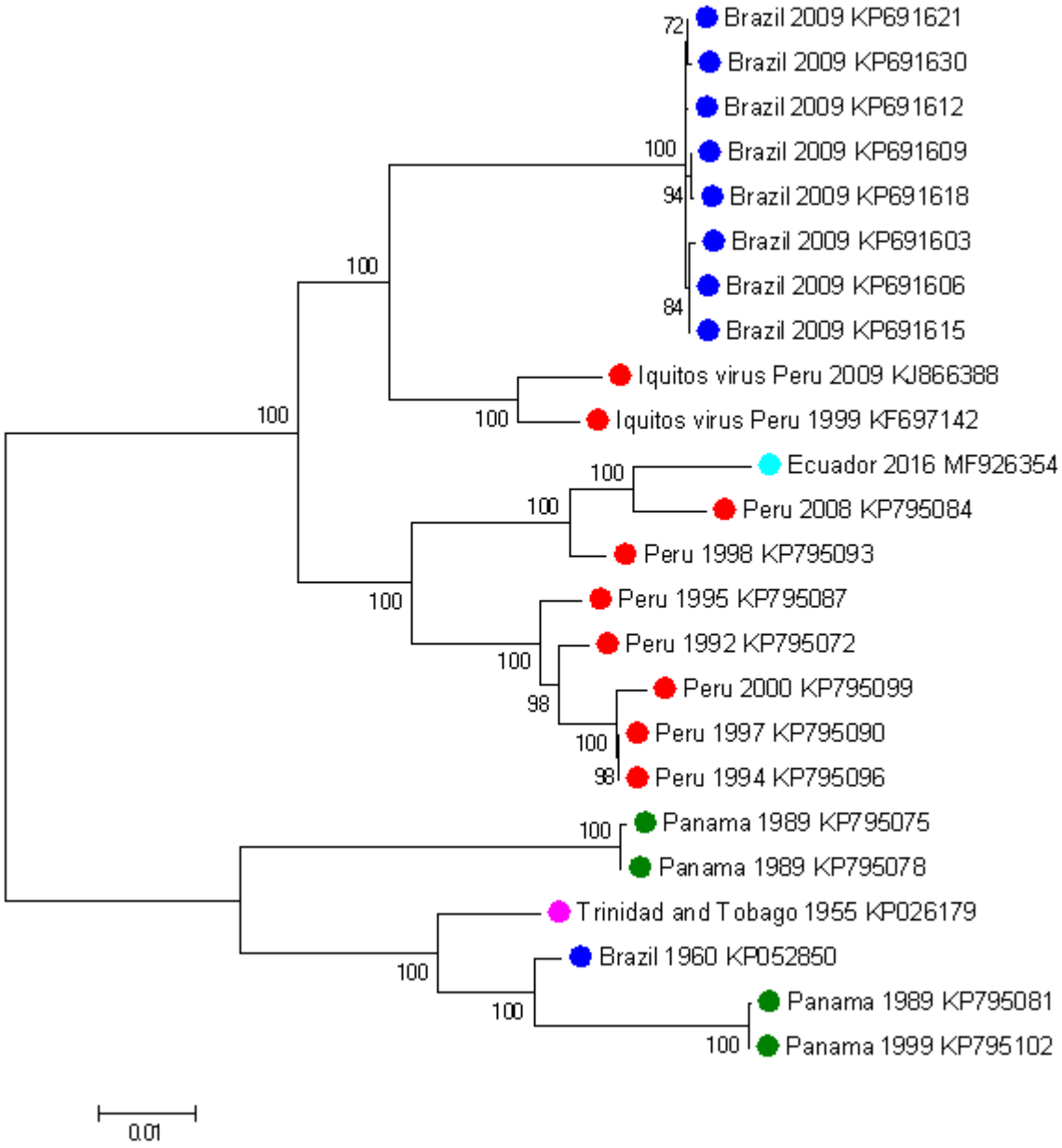

B)

Figure 5.8 Maximum Likelihood trees showing genetic relationships between complete coding sequences of A) OROV M segments and B) L segments. Sequences are coloured by country of origin. Dark blue = Brazil, red = Peru, light blue = Ecuador, green = Panama, pink = Trinidad and Tobago. The tree is drawn to scale, with branch lengths measured in the number of substitutions per site. Node support from 100 bootstrap replicates is shown for the basal internal nodes of each tree.

5.2.6 DEVELOPMENT OF AN OROV MULTIPLEX TILING PCR PRIMER SCHEME

Clinical samples with lower levels of viral RNA can present challenges in generating complete genome sequences using a metagenomic sequencing approach (Table 5.5, Figure 5.4). To address this, a set of primers capable of amplifying the entire OROV genome was designed using the 'Primal Scheme' algorithmic method described by Quick *et al.* (351) (see section 2.13).

The OROV multiplex tiling PCR primer scheme was tested using two Ecuadorian OROV strains (RNA from clinical sample D-057 and RNA from cultured strain OROV/EC/Esmeraldas/087/2016) and the prototype strain, which has considerable sequence divergence from the former strains. A negative control (nuclease-free water) was included. Primer pools were tested at concentrations of 10 µM and 100 µM to determine which generated the highest concentration of DNA. Amplified products were quantified using Qubit dsDNA HS assay (ThermoFisher Scientific, UK, Table 5.10) and visualised via agarose gel electrophoresis (Figure 5.10).

Bands of approximately 400 bp were observed for all samples except the NTC. The Ecuadorian strains produced more concentrated DNA products (Table 5.10), which was expected as the scheme was designed based on the D-087 genome sequence. The prototype OROV genome was amplified but not as efficiently. The 100 µM primer pools produced more concentrated products than the 10 µM pools (Figure 5.10). cDNA libraries were prepared for NGS from the D-057 and prototype strain OROV amplicons (100 µM primer pools) and sequenced using a MinION as described in section 2.13.

	DNA (ng/µl) (10µM primer)		DNA (ng/µl) (100µM primer)	
Sample ID	Pool 1	Pool 2	Pool 1	Pool 2
D-057	28.0	21.2	39.4	25.2
D-087	23.6	17.5	56.8	37.4
Prototype	1.6	1.4	8.1	4.6
NTC	0.2	Too low	1.5	1.1

Table 5.10 DNA concentration (ng/µl) of OROV primer scheme PCR amplicons, determined by Qubit fluorometric quantitation.

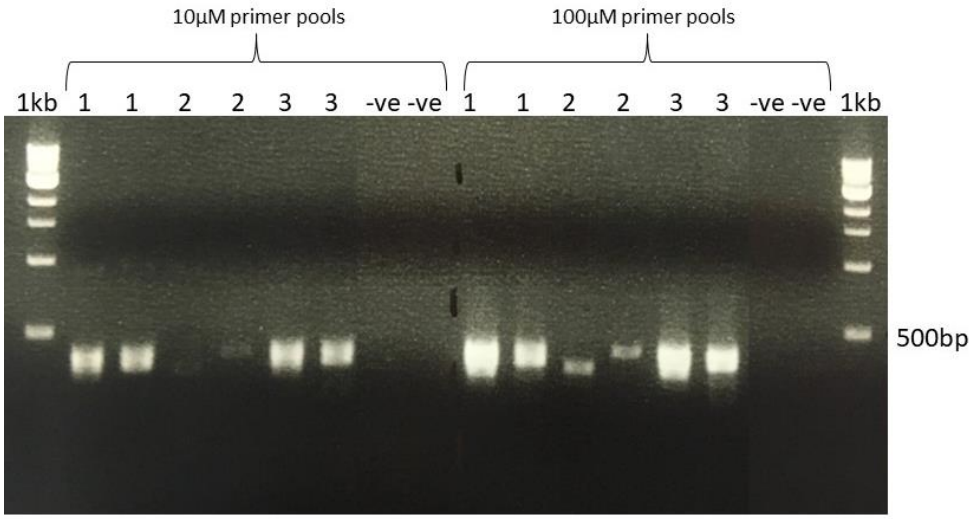

Figure 5.9 Agarose gel electrophoresis showing OROV primer scheme PCR amplicons. 1kb = DNA ladder. 1 = D-057, 2 = prototype strain, 3 = D-087 strain, -ve = NTC. For each sample, products from both primer pool 1 and pool 2 are shown. The expected amplicon size is approximately 400 bp.

>99% of all three Ecuadorian OROV genome segment sequences were generated directly from clinical sample D-057 (a cut-off value of 20x read depth was used), with average depth of coverage of 7,075, 9,894 and 7,381 for the S, M and L segments, respectively (Figure 5.11). For the OROV prototype strain, 98% of the S segment (average depth of coverage 126,860), 93% of the M segment (average depth of coverage 119) and 92% of the L segment (average depth of coverage 189) were obtained, despite the considerable sequence divergence from the Ecuadorian strains. Multiplex tiling PCR primer details are given in Appendix 9.

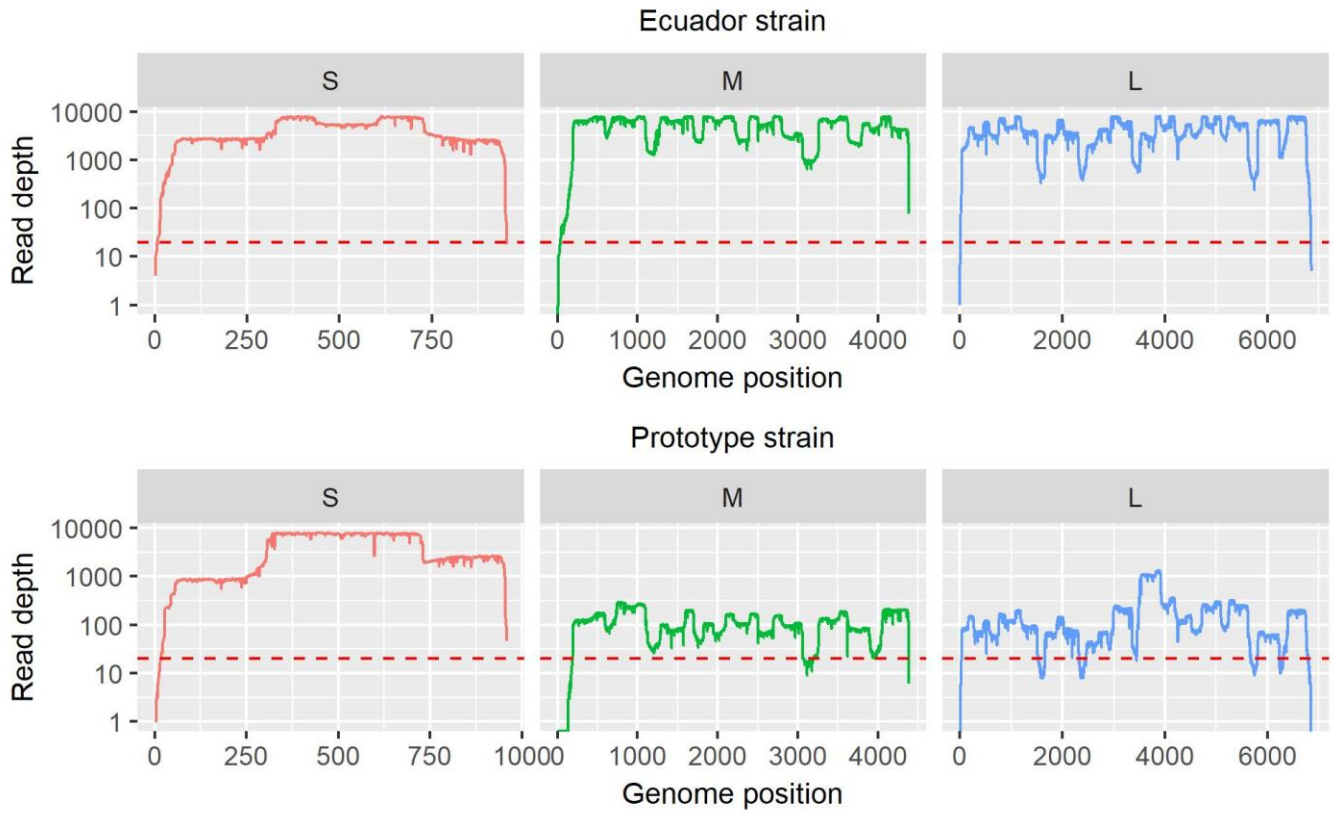

Figure 5.10 Genome coverage of two OROV strains (Ecuadorian strain OROV/EC/Esmeraldas/087/2016 MF926352.1 - MF926354.1, and prototype strain KP026179.1 - KP026181.1), sequenced using a MinION (Oxford Nanopore), from multiplex tiling PCR amplicons. Plots are separated by genome segment (S, M, L). Red dashed line indicates 20x coverage.

5.2.7 FOLLOW-UP TESTING OF FEBRILE PATIENTS FROM 2017

Following the identification of OROV in multiple patients from Esmeraldas in 2016, RNA extracted from plasma samples collected from febrile patients from Esmeraldas in 2017 (*n*=62) were tested for OROV, CHIKV, DENV serotypes 1-4, MAYV, YFV, ZIKV and *Rickettsia* using the qRT-PCR assays described previously (see section 2.4). Internal control MS2 was added prior to RNA extraction, the efficiency of which was checked using qRT-PCR to detect MS2 RNA. No sample was positive (Cq <35) for any of the pathogens tested for and all were positive for the internal control.

Six samples were selected for metagenomic sequencing with the aim of detecting a virus not targeted by a qRT-PCR assay. Selection was based on the observation of a late (Cq >35) or abnormal amplification in a qRT-PCR assay, or a short period of fever prior to blood sampling (Table 5.11), which may suggest a more recent infection thereby increasing the chances of detecting a causative pathogen. Sequencing was undertaken using the metagenomic approach described in section 2.8, followed by sequencing using a MinION (see section 2.10).

The number of sequencing reads per patient sample ranged from 35,870 to 117,109 (mean = 59,769). On average, 56% of reads were of human origin (minimum 36.3%, maximum 68.5%), and 17.3% were of microbial origin (minimum 4.6%, maximum 35.3%). The mean number of viral reads per sample was 10.4% (minimum 3.2, maximum 22.5%). All samples contained reads belonging to internal control bacteriophage MS2 (Table 5.11). Reads were analysed using Centrifuge which identified GBV-C in 2/6 samples and MS2 internal control in all samples (Table 5.11). Human reads were mapped and removed from the data prior to *de novo* assembly (see section 2.11.5), which produced scaffolds with sequence homology to GBV-C and MS2 (Table 5.11). Mapping

to relevant virus reference genomes (see section 2.11.3) identified reads mapping to GBV-C and MS2 reference sequences (Table 5.11), no other viruses were identified.

Reads from patient samples D-245 and D-271 were mapped to the most closely related GBV-C sequences (identified using BLASTn), resulting in 88% 1x genome coverage from D-245 (53% 5x coverage) and 70% 1x genome coverage from D-271 (38% 5x coverage, Figure 5.11).

			Centrifuge		*De novo* assembly			Mapping	
Sample ID	Reason for inclusion	Virus detected	Reads (%)	Number of reads	Number of scaffolds	Scaffold length(s)	Accession	Number of reads	Accession
D-222	?DENV1-3	MS2	3.7	2315	2	1661 & 2674	MK213795.1	2950	V00642.1
D-229	?CHIKV	MS2	5.8	3759	1	3448	MK213795.1	4884	V00642.1
D-237	?OROV	MS2	6.1	8748	0	n/a	n/a	11283	V00642.1
D-245	2-day fever	GBV-C	3.3	2705	1	7152	U45966.1	475	KR131788.1
		MS2	1.7	1379	0	n/a	n/a	1832	V00642.1
D-215	3-day fever	MS2	14.9	7961	1	2160	MK213795.1	10203	V00642.1
D-271	?OROV	GBV-C	1.5	3042	1	8457	D90601.1	692	KR131788.1
		MS2	0.3	617	0	n/a	n/a	763	V00642.1

Table 5.11 Ecuadorian patient samples from 2017 selected for metagenomic sequencing. GBV-C was identified in 2/6 samples from a combination of taxonomic assignment, do novo assembly and mapping to reference genomes. MS2 is the internal control.

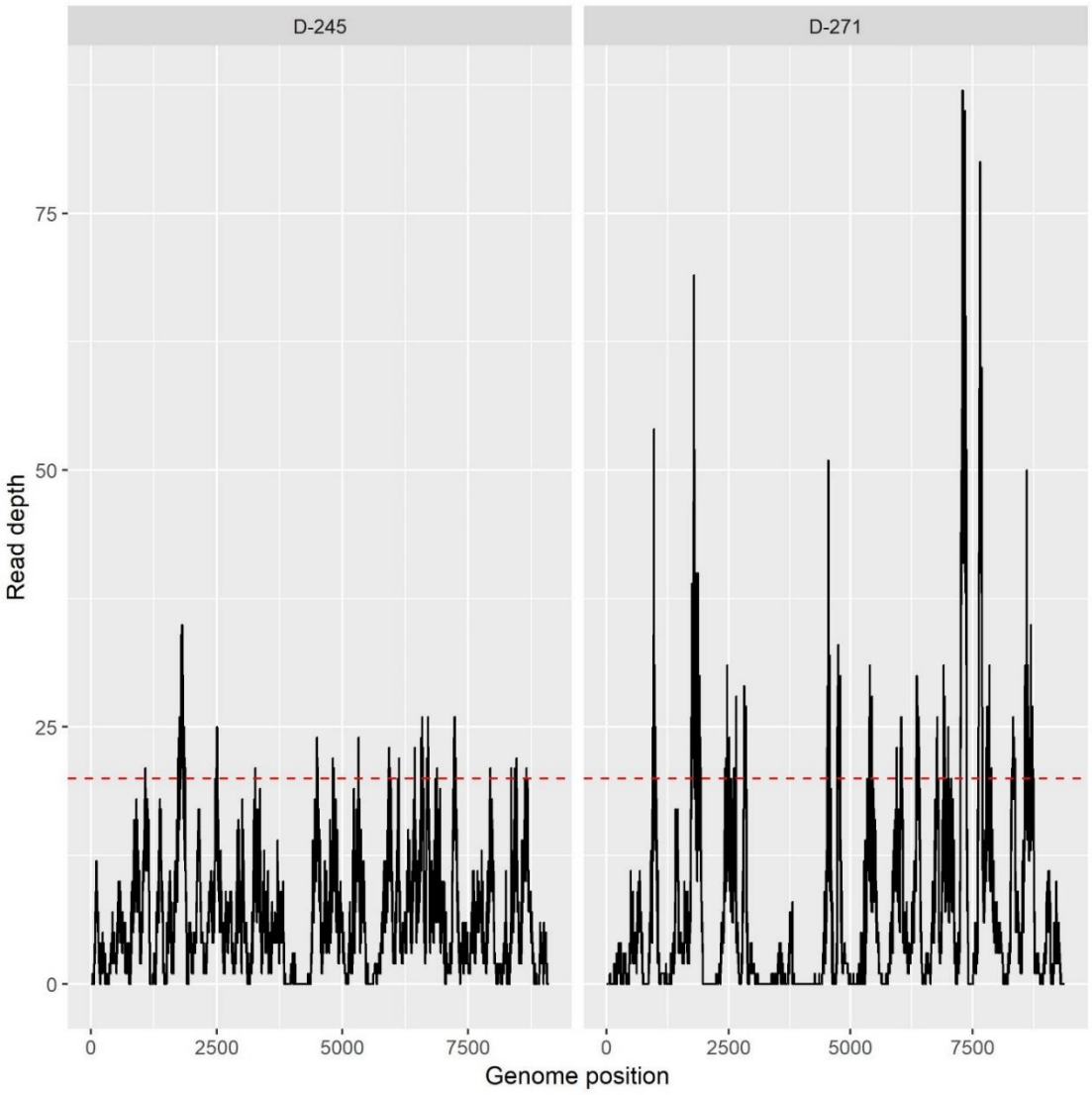

Figure 5.11 Coverage of GBV-C genomes from patient samples D-245 and D-271, generated by mapping sequencing reads to reference sequences (U45966.1 and D9060.1, respectively). Red dotted line indicates depth of 20 reads.

5.3 DISCUSSION

5.3.1 A MODIFIED OROV QRT-PCR IDENTIFIED MULTIPLE CASES OF INFECTION IN FEBRILE ECUADORIAN PATIENTS

Following the detection of OROV in a febrile Ecuadorian patient described in chapter 4, there was a requirement for a qRT-PCR assay with good sensitivity for existing strains including the Ecuadorian strain. A previously published assay (361), capable of detecting the OROV prototype strain, could not detect OROV RNA in patient sample D-087 despite the identification of a substantial portion of the genome using metagenomic sequencing and virus isolation *in vitro*. To address this, the primer/probe sequences were compared to the OROV/EC/Esmeraldas/087/2016 S segment sequence and two mismatches to the reverse primer were detected. It was hypothesised that these mismatches resulted in poor sensitivity for the Ecuadorian strain. Subsequent design and testing of two alternative reverse primers demonstrated that reverse primer Ec2R (which bound to an alternative conserved region of the S segment) was more sensitive for both the Ecuadorian strain and the prototype strain than the original reverse primer.

As part of the optimisation and validation of the qRT-PCR assay, the absolute limit of detection for Ecuadorian strain OROV RNA was assessed and the assay was determined to be highly sensitive, with a limit of detection conservatively stated at 10 copies of RNA. Detection below this threshold was achieved, but less reliably, probably because of the stochastic nature of nucleic acid present in dilutions below 1e+1. The OROV S segment is shared by a number of reassortant orthobunyaviruses including IQTV, which circulates in neighbouring Peru and can cause Oropouche fever (489). The modified assay has the potential to detect reassortant orthobunyaviruses that contain the OROV S segment.

RNA from 196 Ecuadorian febrile patient plasma samples from 2016 were tested for OROV using the modified qRT-PCR and a total of six samples (including the original sample D-087) were OROV-positive. Estimations of the number of genome copies/mL of plasma, based on the absolute quantitation, revealed a range of RNA plasma concentrations from 9.6e+3 to 1.3e+9 copies/mL, inversely correlated with the number of days of fever experienced by the patient prior to blood sampling. This fits the clinical picture of OROV infection in which the onset of symptoms is accompanied by a high level of viraemia (182), following which viral titres in the blood reduce significantly. Observations from OROV-infected Brazilian patients showed a reduction of 72% on the third day, and 44% and 23% on the fourth and fifth days following onset of symptoms (180). One patient in the present study was sampled after a reported 7 days of fever, with 9.6e+3 OROV genome copies/mL plasma; still easily within the detection range of the optimised assay.

5.3.2 SUBSTANTIAL PORTIONS OF OROV GENOME ARE DETECTABLE DIRECTLY FROM CLINICAL MATERIAL USING METAGENOMIC SEQUENCING

The initial identification of OROV from patient sample D-087 using metagenomic sequencing, from which OROV RNA was not detectable using a published OROV qRT-PCR, highlights the challenges in developing amplification-based detection assays for pathogens with limited genome sequence data, and the benefits offered by unbiased sequencing technologies. Sequencing directly from OROV-positive patient plasma resulted in coverage of 63.5-99.4% of the OROV genome, demonstrating that metagenomic detection of OROV is possible from patient plasma samples with viral RNA concentrations as low as 9.6e+3 genome copies/mL, and suggesting that this method is

effective for both detection and characterisation of OROV genomes from clinical samples. Genome copies/mL loosely correlated with the proportion of sequencing reads that mapped to the OROV genome, however large variability in the latter metric was observed, which has been reported for other arboviruses sequenced from clinical material (321). This likely reflects variation in the level of host background RNA present in samples. The absence of S segment sequence from sample D-206 is likely due to the stochastic nature of the metagenomic sequencing method, which is exacerbated for smaller fragments (S segment 952 bp). The S segment is detected by qRT-PCR and is present in the sequencing of the virus directly cultured from this sample.

5.3.3 SIX COMPLETE ECUADORIAN GENOME SEQUENCES WERE GENERATED FROM ISOLATED VIRUS

Following one passage in Vero cells, which was necessary to isolate and amplify OROV, complete OROV genome sequences were obtained from cell culture supernatants. It is well-documented that mutations occur during passaging *in vitro* (8) and passaging was limited to minimise the number of mutations between patient and cultured virus genomes. Analysis of intra-sample variation revealed a number of positions with a mixed population of variants present in the patient genome, which progressed to a majority population in the cultured genome. Majority-to-majority changes were rare, and only one of the 49 SNPs observed between patient and cultured genomes was seen in two individual strains, suggesting that these changes are due to random selection during propagation rather than a reflection of a shared selective pressure within the cultures.

An alignment of the Ecuadorian consensus sequences revealed that 33 SNPs were present in coding regions throughout the genome. These nucleotide changes

corresponded to just eight non-synonymous amino acid substitutions, five of which constitute a reactive group change (three in the M segment and two in the L segment) and therefore may influence the structure or function of the protein. Two of these occur in the OROV glycoproteins, which play important roles in virus adaptation because of their interaction with the host immune system (523). The collaborative work performed on the evolutionary analysis of OROV demonstrated an increased number of sites under positive selection on the OROV Gc protein compared to other OROV proteins (363), however further studies are required to investigate any selective pressure at this site.

5.3.4 OROV GENOME ANALYSES SUGGEST OROV HAS BEEN CIRCULATING UNDETECTED IN ECUADOR

Analysis of the Ecuadorian OROV S, M and L genomic segment sequences revealed that all three are most closely related to isolates from Peru from the 1990s and 2000s. Strain IQE-7894 is particularly closely related, isolated from a patient close to Iquitos city, Peru, in 2008. OROV was previously classified into four genotypes based on N gene nucleotide sequences (28,521), representing distinct genetic linages circulating in the Americas (521). As of 2017, genotype I was detected in Trinidad and Tobago and Brazil; genotype II in Panama, Peru, and Brazil; genotype III in Brazil and Peru, and genotype IV exclusively in Brazil (Figure 5.12) (28). This classification can be useful for looking at OROV epidemiology, however it is based on a small region of the genome. Furthermore, the Ecuadorian N gene sequences and the closely related Peruvian sequences do not cluster with any of the pre-defined genotypes. The generation of complete viral genomes using metagenomic sequencing or a multiplex tiling PCR, as opposed to the small fragments generated using conventional RT-PCR, enables more detailed and accurate molecular

epidemiological analyses (524). The utility of this approach was exemplified in the present study by making it possible to rule out the Ecuadorian sequences as belonging to reassortant OROV-like virus IQTV. Despite having a closely related N gene sequence, the genetic divergence observed in the L and particularly the M segment demonstrated that the Ecuadorian strains belong to OROV. However, the S segment similarity to IQTV and OROV isolates originating nearby to Iquitos city raises the possibility that OROV was introduced to Ecuador across the Peru–Ecuador border. Further studies are needed to investigate this.

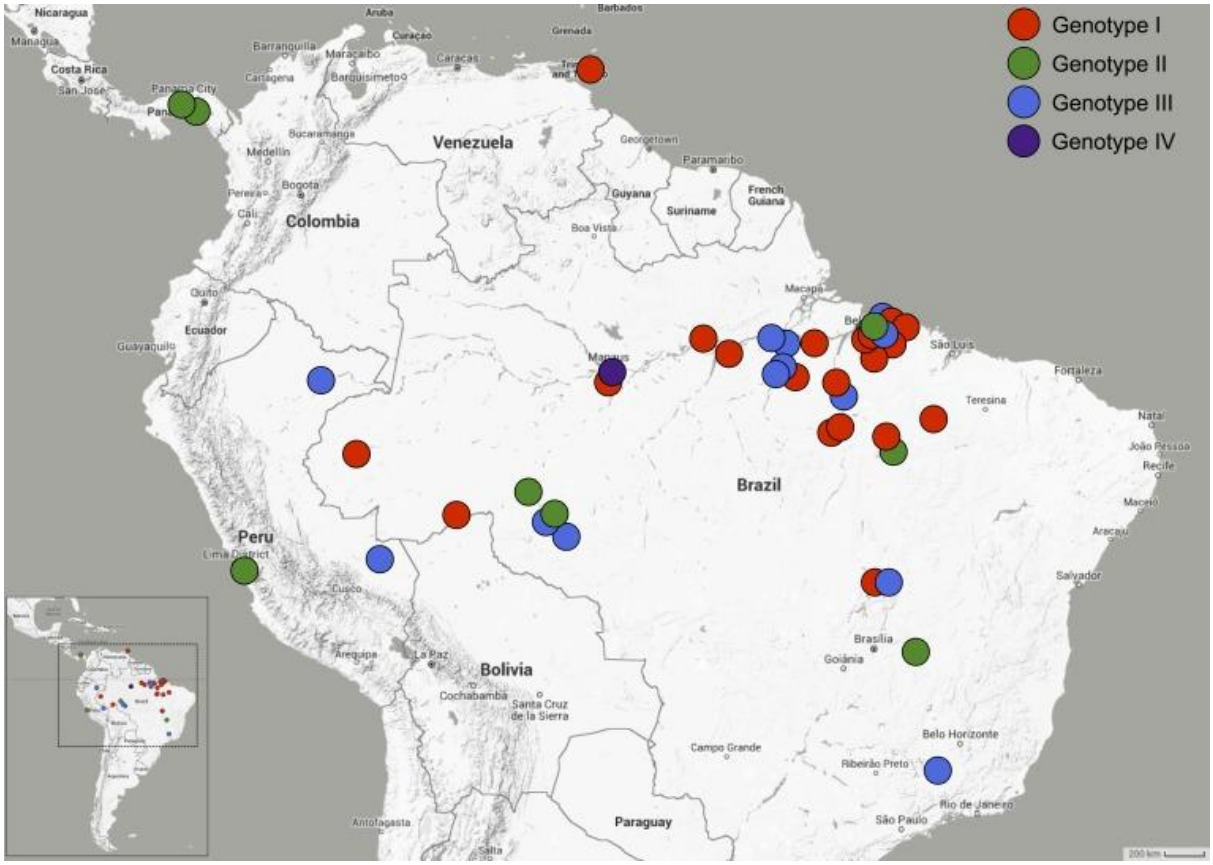

Figure 5.12 The distribution of OROV genotypes in the Americas, based on 114 N gene sequences. Reproduced from Travassos da Rosa *et al.* (2017) (28).

The six Ecuadorian sequences were incorporated into a comprehensive analysis of the evolution of OROV in South America, as part of a collaboration with Oxford University (363). Phylogenetic analyses were performed using all available S, M and L OROV sequences, representing OROV cases and outbreaks from Trinidad & Tobago, Panama, Peru and Brazil. The addition of the Ecuadorian sequences meant that this dataset covered the complete sampled history of the virus from the mid-1950s to the present day (*n*=149 S, *n*=64 M, *n*=64 L). Maximum Likelihood trees demonstrated that the Ecuadorian sequences cluster in a well-supported monophyletic group (363), separate from other genomes but most closely related to Peruvian isolates, confirming the previous observations (Figure 5.7 and Figure 5.8).

Evolutionary timescale analyses of the OROV genome segments suggested that OROV first emerged in the early-to-mid 20th century (363). Furthermore, the M segment has an older common ancestor than the S and L segments; two M segment lineages diverged in the 17th century then diversified in the early to mid-1900s (Figure 5.13A). The differences in time to most recent common ancestor (TMRCA) between genome segments is a result of genetic reassortment that occurs when different orthobunyavirus strains or species infect the same cell and produce progeny virions with reassorted genome segments. Topological differences in the evolutionary rate trees for the different segments suggested multiple reassortment events occurred during the evolution of OROV in South America, however, no reassortment events related to the Ecuadorian sequences were observed (363). The TMRCA of the Ecuadorian OROV sequences was estimated to be late-2011 (95% credible intervals: 2009-2015), mid-2011 (95% credible intervals: 2008-2015) and early 2014 (95% credible intervals: 2011-2016) for the S, M and L segments, respectively (Figure 5.13B) (363).

The WHO define an outbreak as the occurrence of disease cases in excess of what is normally expected in a particular time and place (525). The monophyletic clustering of the Ecuadorian genomes suggests an outbreak of Oropouche fever occurred in Esmeraldas in 2016. Urban outbreaks usually result from a human infection that occurs via a bite from an infected insect in a forested area where the sylvatic OROV transmission cycle is present (28). Movement of the infected person into an urban setting in which a competent vector species (thought to be *Culicoides paraensis*) is present facilitates onwards transmission from person-to-person, resulting in explosive outbreaks (183). The majority of Esmeraldas canton is urban, but 18.7% is rural (490), providing potential opportunities for sylvatic circulation of OROV and interactions between infected insects and humans.

The OROV cases from Esmeraldas could have occurred via multiple introductions from an animal reservoir, or in a transmission chain from person-to-person (facilitated by a vector in both scenarios). The former seems most feasible because there is approximately five years' worth of genetic diversity between the two most distantly related Ecuadorian S sequences (Figure 5.13B). Some sequences are more closely related than others, but given that patients typically show levels of viraemia sufficient to infect *C. paraensis* for only 3-4 days from the onset of symptoms (28), and the timescale of genetic differences between the Ecuadorian sequences is months to years, there is no clear evidence of a human-to-human transmission chain.

The Ecuadorian sequences share a MRCA somewhere between 2008 and 2016. This ancestor could have existed in Ecuador or elsewhere, possibly Peru based on the genetic similarity to the 2008 Peruvian genome. The collection of OROV sequences used in this analysis was the most complete available, but it is almost certain that there is much

unsampled diversity, meaning the picture of OROV in South America (and most-likely Ecuador) is under-sampled and incomplete. The fact that anti-OROV IgM antibodies were detected in patient samples from Pastaza province (480) and Guayaquil (479), which are approximately 350 km apart and both approximately 450 km from Esmeraldas, suggests OROV circulation within Ecuador is not restricted to Esmeraldas. Furthermore, the time of these detections (2001-2007) predates the earliest credible TMRCA of the Ecuadorian sequences discovered in this study. This points to the existence of other, unsampled lineages of OROV that may have been circulating in Ecuador prior to the lineage identified from patient samples from Esmeraldas. However, it is important to note that antibody-based detection methods are less specific than molecular detection assays, and antibodies to viruses in the Simbu serogroup to which OROV belongs frequently cross-react with multiple other members of the group (526,527). It is possible that antibody cross-reactivity with other orthobunyavirus species or OROV reassortants could have been responsible for the detections from Pastaza province and Guayaquil. The availability of more OROV genomes, particularly from Ecuador, would help further elucidate the relationships between the Ecuadorian genomes.

Where OROV circulates in nature is not well understood, it is possible that transmission to a person occurred in Esmeraldas or elsewhere in Ecuador, where OROV is circulating undetected. Another possibility is that infection of the human index case occurred in Peru, with subsequent travel of the infected person to Ecuador where transmission was established and has continued undetected. Without the exact locations of the patient's residences in Esmeraldas, and their travel histories, it is difficult to speculate as to the geographical range of OROV in Ecuador.

A further uncertainty is the mode of transmission from person-to-person in Esmeraldas, if this did occur. As first discussed in chapter 4, the primary vector in urban transmission, *C. paraensis,* is reported to be absent there (S. Zapata, personal communication, 31st August 2017). Certain mosquito species may play a role in transmission, but studies show inefficient transmission (180,528). An investigation of potential OROV vector species in Esmeraldas would be highly informative.

Transmission of viruses within the *Peribunyaviridae* family is documented to occur by insect vector (mosquitoes and culicoid flies (529)) and there is no evidence of other routes of transmission from person-to-person, however, this does not rule out the existence of other modes of transmission. Many orthobunyaviruses have a wide range of vertebrate hosts, including rodents (530), but it is not known whether direct contact with contaminated rodents or other host species leads to human infection. However, hantaviruses, which also belong to the order *Bunyavirales*, primarily infect humans via direct contact with their rodent reservoirs (146). Furthermore, secondary routes of transmission may be masked by the higher numbers of cases resulting from the dominant transmission route. For example, sexual transmission of ZIKV was only discovered in 2008, decades after the virus was first discovered, following infection of a woman in the USA via sexual transmission from her husband who had recently contracted ZIKV in Senegal. Despite a large outbreak of ZIKV in Yap island the previous year (2007), during which 70% of the islands' inhabitants were infected (270), this route of transmission was only discovered from this unusual case of ZIKV infection in Colorado, highlighting the challenge of unpicking transmission routes in large outbreaks within low-income settings.

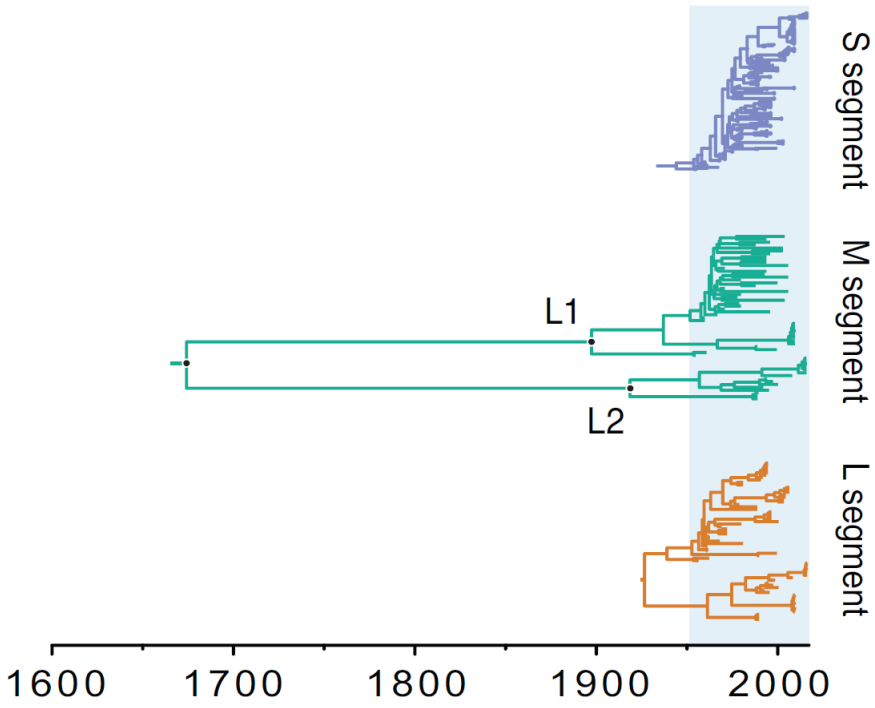

A)

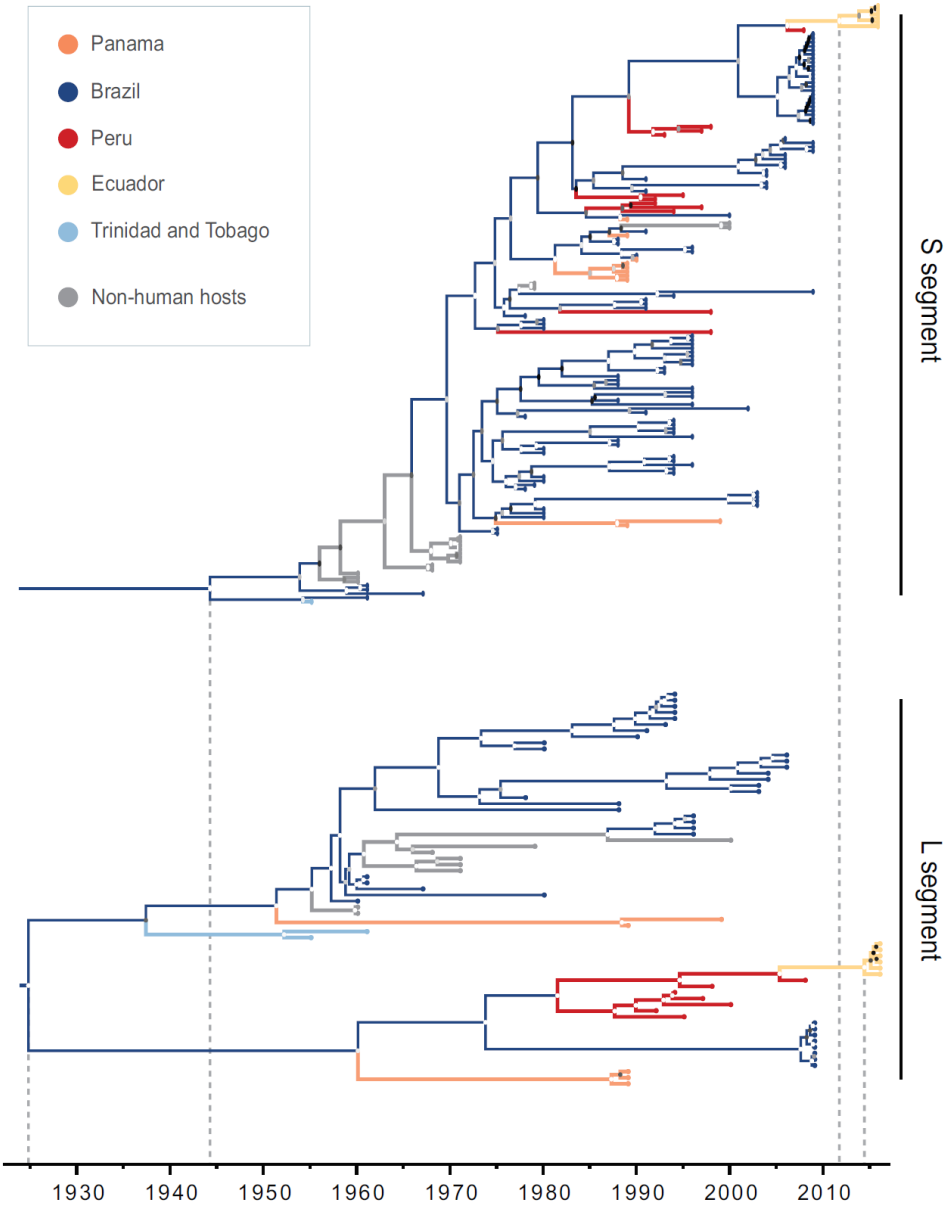

B)

Figure 5.13 Time-calibrated and evolutionary rate analysis of the OROV genome. A) Comparison of the OROV genome segments showed that the M segment has an older common ancestor than the S and L segments (L1 and L2 = Lineage 1 and Lineage 2, respectively) **B)** Evolutionary timescale analysis of the S and L segments. The posterior probabilities (PP) of each node is shown based on a greyscale colour scheme (0.0 PP = black to 1.0 PP = white). Reproduced from Gutierrez *et al.* (2019) (363).

5.3.5 FOLLOW-UP TESTING OF FEBRILE PATIENTS FROM 2017 DID NOT DETECT OROV

No cases of OROV or any other virus tested for by qRT-PCR were detected during follow-up testing of 62 febrile patient samples from Esmeraldas in 2017. Previous outbreaks of Oropouche fever have been episodic and self-limited in nature (28); the six cases identified from 2016 could represent an outbreak or outbreaks that ended that year. Alternatively, if OROV transmission did occur in Esmeraldas in 2017, the lack of detection could be related to the limited sample size of the 2017 cohort. Furthermore, the majority of samples tested from 2017 were taken in June/July, whereas the OROV positive samples from 2016 (that dates are available for) were taken in April. If there is a seasonal component to OROV outbreaks in Ecuador, as is seen in Brazil where outbreaks are usually reported in the wet season (28), this difference could be relevant as the wet season in Ecuador ends in May. Outbreaks in Brazil have been shown to exhibit an epidemic dispersal process involving transmission of OROV to multiple locations close to the region in which the virus was first detected (28,511,531). This is proposed to result from the movement of viraemic people into areas where the vector is present, facilitating onward transmission (28). A larger-scale study is necessary to determine whether a similar process exists in Ecuador, and the prevalence and distribution of OROV in the Ecuadorian population.

Metagenomic sequencing of six patient samples from 2017 did not identify any pathogenic viruses, but did identify GBV-C in two patients, from which 70% and 88% coverage of the genome was generated. Previously introduced in chapter 3, where it was detected in multiple Sierra Leonean patients, the human pegivirus GBV-C has a worldwide distribution and is more prevalent in developing countries (445,446), however is it not thought to be pathogenic (440).

5.3.6 DEVELOPMENT OF OROV DETECTION ASSAYS AND IMPLEMENTATION IN ECUADOR BUILDS CAPACITY FOR THE DETECTION OF EMERGING VIRUSES

In addition to the OROV qRT-PCR developed in this study, a multiplex tiling PCR primer scheme was designed that amplifies the entire genome of OROV using RT-PCR. This scheme produced genome sequence from both Ecuadorian OROV and the genetically divergent prototype strain with good depth of coverage. It is a useful tool for generating genome sequence from clinical material with very low amounts of viral RNA. In the present study, the resulting amplicons were sequenced using the ONT MinION, which (as previously discussed) is highly portable and requires relatively low start-up costs, making it suitable for use in resource-limited settings.

A key outcome of this project was to support existing in-country laboratories by identifying circulating viruses and additional assays to include in surveillance and diagnostic testing. In line with this, training was provided to researchers at USFQ, both in-country and during a visit to PHE Porton Down, initiating the implementation of the OROV qRT-PCR assay alongside a number of other relevant qRT-PCR assays. Furthermore, training in the metagenomic sequencing approach using a portable MinION sequencer was provided. Although the cost associated with metagenomic sequencing may be prohibitive for frontline diagnosis in developing countries, it can be used in prospective screening studies to identify potential issues with qRT-PCR assays, as demonstrated here, providing essential genome information that allows for assay adaptation. These activities fall in line with the actions promoted by WHO for effective response to the threat of emerging viruses, including advancing research in prevention, surveillance and control of virus infection; developing, strengthening and implementing integrated surveillance systems for virus infection; and strengthening the capacity of laboratories to test for virus infection (352). It is hoped that the OROV molecular assays

developed as part of this project will be valuable tools for laboratories performing viral diagnostics and surveillance in the Americas.

5.3.7 LIMITATIONS

RNA from two strains of OROV were available for use in assay optimisation and validation. Despite best efforts, no other strains could be accessed for inclusion in the validation process, therefore it cannot be definitively stated that the molecular assays detect the full range of OROV strains present in nature. However, for the qRT-PCR, an alignment of all publicly available strains showed that the majority of sequences are homologous to the primer/probe sequences, suggesting that based on sequence similarity the assay is likely to be suitable. Further validation using a wider range of strains would improve the qRT-PCR and multiplex tiling primer scheme.

The identification of OROV-positive febrile patients in this study was based on nucleic-acid detection methods, which provide useful information in the form of viral genome sequence. Future studies incorporating OROV antibody detection would be useful for understanding the prevalence of OROV in the Ecuadorian population. Although a number of anti-OROV IgM and IgG ELISA assays are described in the literature (479,509,513,514,532), these are produced 'in-house' by individual laboratories and are therefore difficult to standardise. At present no OROV ELISA assays are commercially available, however this would be useful and allow comparison of results between studies.

The OROV genomes sequenced directly from patients are incomplete, therefore the complete sequences derived from cell culture supernatant were used in the

phylogenetic analyses. It's possible that differences between the patient and cultured sequences could have a limited confounding effect at the very smallest scale of analysis; when looking at the relationships between the Ecuadorian genomes themselves. The missing regions of the OROV patient genomes (1-36% of the genome), could include further SNPs between the patient and cultured genomes that it is not possible to know about. Conversely, approximately half of the SNPs identified between the patient and cultured genomes are 'mixed population' to 'majority population' changes (26/49). For certain positions this may simply reflect the low depth of coverage of the patient genome; meaning the few reads present do not represent the true proportion of variation in base at that position. Or, for positions with high coverage, the data truly represents the more diverse viral population within the patient which is subsequently lost in culture because of selective pressure to adapt to the new environment. Differences between patient and cultured genomes is a further reason to sequence directly from patient samples using metagenomic sequencing where possible. As stated in results, SNPs between patient and cultured genomes appear to be randomly distributed and therefore should not affect the analysis significantly. Nonetheless, no firm conclusions are drawn about the relationships between the Ecuadorian genomes, in part for this reason.

5.3.8 SUMMARY

The detection of six OROV cases from patients local to Esmeraldas, Ecuador, in 2016, provides further evidence that OROV is responsible for an unrecognised burden of human disease in previously unreported areas. It is likely that cases of Oropouche fever have gone unreported or misdiagnosed in Ecuador, as the clinical picture is very similar

to that of other viral, protozoan, and bacterial diseases previously reported to circulate in the country (28,476,480,481). This work highlights the need for increased surveillance for OROV in Ecuador; the virus should be considered when diagnosing Ecuadorian patients with febrile illness. Effective diagnostic assays are needed that can differentiate between emerging pathogens sharing common clinical descriptions and circulating in the same area. Very little is known about the dynamics of OROV in Ecuador or its endemicity in neighbouring regions; this detection of OROV in multiple Ecuadorian febrile patients warrants further investigation into the prevalence, associated vectors, and transmission of this emerging virus.

CHAPTER 6: OROV REPLICATION IN BIOLOGICALLY RELEVANT CELL TYPES

6.1 INTRODUCTION

Despite causing more than half a million cases of Oropouche fever in the Americas since its discovery in the 1950s, OROV transmission and pathogenesis is poorly understood compared to that of other arboviruses. A search for “Oropouche virus” in the PubMed database yielded 84 articles, compared with 13,903, 6,329 and 4,161 articles for “dengue virus”, “Zika virus” and “chikungunya virus”, respectively.

Two OROV transmission cycles are known to exist, based on field studies and laboratory experiments. The sylvatic cycle is maintained in the forest between vertebrate reservoir hosts and vectors (181) (Figure 6.1). Reservoir hosts include the pale-throated sloth (*Bradypus tridactylus*), non-human primates (*Callithrix* spp. and *Alouatta caraya*), rodents (*Proechimys* spp.) and possibly some wild bird species (387,504,505,508,533). Which insect vectors are involved in sylvatic transmission is not clear, although OROV was isolated from mosquito species *Aedes (Ochlerotatus) serratus* in Brazil and *Coquilletidia venezuelensis* in Trinidad (28,505).

The urban, or epidemic, cycle occurs between human hosts and insect vectors (Figure 6.1). The biting midge *Culicoides paraensis* is the primary vector in these cycles, based on evidence that *C. paraensis* can transmit OROV from infected to susceptible hamsters (534), and from viraemic patients to hamsters (181,505). However, a low isolation rate (1:12,500) has been reported from the field during epidemics (505) which is at odds with the number of human cases observed. Entomological surveys from the outbreak locality of Iquitos, Peru, showed that *C. paraensis* was present but no infected midges were detected (516). This raises the question of whether there are other insect vectors participating in OROV epidemics. *Culex quinquefasciatus* may play a role; OROV RNA was

detected in small numbers of these mosquitoes in the 1960s (180), then again in febrile patients and *Cx. quinquefasciatus* from the same location in Brazil in 2011-2012 (534). However, in the laboratory the efficiency of OROV transmission by *Cx. quinquefasciatus* is low (528).

The dynamics of OROV in Ecuador are completely unknown. The detection of six OROV-positive patients from Esmeraldas in 2016, the genomes from which cluster together phylogenetically, suggests that an outbreak occurred in Esmeraldas. However, *C. paraensis* is thought to be absent from the Pacific Coast region in which Esmeraldas is situated. This is based on entomological collections performed since 2009 which identified *C. paraensis* in the Amazon region of the country only (S. Zapata, personal communication, 17th October 2017). This fits with the previously described distribution of *C. paraensis* in South America (535), in which the midge is present in the south and Amazon areas of Ecuador. Further studies into alternative OROV vectors, perhaps through a combination of screening field collections and performing vector competence laboratory experiments, would be highly informative.

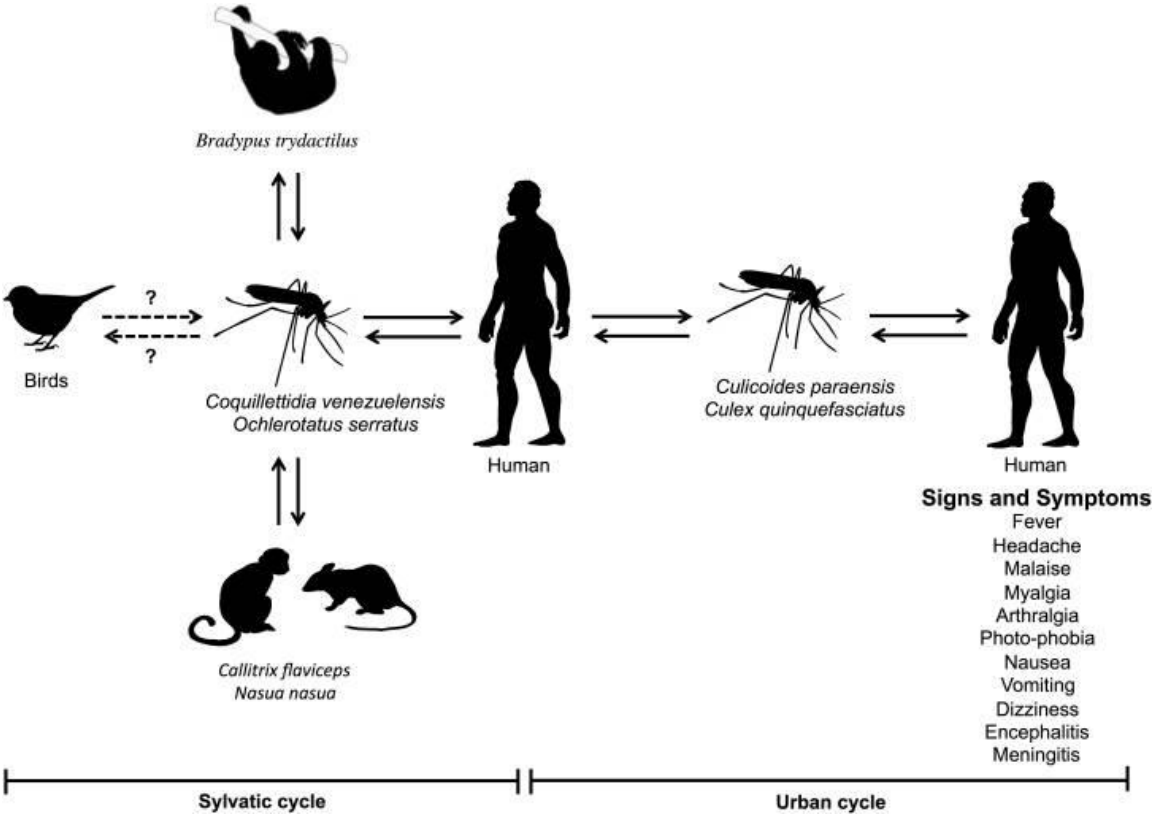

Figure 6.1 OROV transmission cycles. Reproduced from Travassos da Rosa *et al.* (2017) (28).

OROV pathogenesis is also not well understood and it is not known which cell types the virus replicates in during human infection. Viraemia is detected during the acute phase of infection (28) and virus has been detected in peripheral blood leukocytes from patients (536). Less frequently, OROV has been recovered from cerebrospinal fluid from patients experiencing a less typical, more severe form of disease involving encephalitis (183,537). Most recently, OROV RNA was detected in the urine and saliva of febrile patients (538,539).

Some aspects of OROV pathogenesis have been studied using small animal models; hamsters and mice (28). Early experiments in hamsters intra-cerebrally inoculated with OROV showed infection resulted in liver lesions, hepatocyte necrosis and Kuppfer cell hypoplasia, suggesting that OROV is able to travel from the brain to the liver via the blood (392). A more recent study in the hamster model detected high titres of virus in the liver and brain following subcutaneous inoculation (393). *In vitro* studies have demonstrated OROV replication in a handful of human derived cell types; as well as cell types from other species (Table 2.27).

A recent study of OROV morphogenesis provided novel insights into the assembly pathway of OROV in HeLa-I cells and identified host components essential for viral replication (388), demonstrating that OROV recruited host endosomal sorting complex required for transport (ESCRT) machinery to the site of Oropouche viral factory units at the Golgi cisternae. This machinery was required for membrane remodelling, essential for efficient viral assembly and budding. These kinds of studies are important for understanding the OROV replication cycle, however, they are constrained by the requirement for cell lines and viruses that are easily manipulated in the laboratory and are often not representative of a natural infection. Studies using low-passage, wildtype virus and biologically relevant cell types may provide insights that are more relevant to a natural infection.

BST-2 (also known as tetherin) is an interferon stimulated gene that has broad inhibitory activity against enveloped viruses. Orthobunyaviruses with human tropism (including OROV) are restricted by sheep BST-2, but not by human BST-2, whilst for orthobunyaviruses with ruminant tropism the opposite is true (391). The mechanism underlying this is the ability of BST-2 to block virus replication by reducing the quantity

of envelope glycoprotein that is incorporated into virions egressing from infected cells (391). This was the first identification of a host determinant of species susceptibility to bunyavirus infection and provides insight into adaptations required for these viruses to cross species barriers.

This chapter aims to identify cell types that are susceptible and permissive for OROV replication. As a step towards understanding what other insect species may transmit OROV, a study was performed to identify insect-derived cell lines that support OROV replication *in vitro.* These cell lines were from mosquito species *Ae. agypti*, *Ae. albopictus*, *Anopheles gambiae* and *Cx. quinquefasciatus*, and the biting midge *Culicoides v. sonorensis*. Mammalian cell lines Vero and BHK-21 were also included, as these have previously been shown to support OROV replication (185,387,388). To understand which human cell types may be involved in the natural course of OROV infection, an attempt to identify human primary cell types and cell lines permissive for OROV replication was made. Skin fibroblasts and keratinocytes, peripheral blood mononuclear cells (PBMCs), and hepatocytes were assessed on the basis that these cell types are likely to be biologically relevant based on the OROV route of transmission and on previous observations of pathogenesis.

6.2 RESULTS

6.2.1 OROV REPLICATION IN INSECT AND MAMMALIAN CELL LINES

OROV replication in insect and mammalian cell lines was assessed over seven days using a multiplicity of infection (MOI) of 0.1, determined as suitable for OROV growth curve experiments based on pilot experiments in human cells and on published work (185). OROV genome replication was assessed using qRT-PCR to measure changes in the relative quantity of viral RNA present in the supernatant (see section 2.16.2.3). The production of infectious virions was assessed by measuring viral titres in the supernatant using a plaque assay (see section 2.15.4).

6.2.1.1 ASSESSMENT OF OROV GENOME REPLICATION

OROV genome replication was observed in all three *Ae. aegypti* cell lines by 1 dpi, followed by a substantial increase by 2 days post-infection (dpi, Figure 6.2). After 2 dpi, OROV RNA continued to increase but at a slower rate. In the AE cell line, a plateau in OROV RNA was reached between 4 and 7 dpi (Figure 6.2). A similar trend in OROV genome replication to that seen in the *Ae. aegypti* cell lines was observed in both *Ae. albopictus* cell lines over the 7-day period. Substantial genome replication was observed by 1 dpi, which continued whilst tapering off over the remainder of the time-course (Figure 6.2). The quantity of OROV RNA was higher in supernatants from U4.4 cells compared to C6/36 cells, first observed at 1 dpi then increased at 2 dpi and maintained through days 3 and 4 post-infection (Figure 6.2).

Substantial OROV genome replication, represented by a decrease of approximately 10 Cq values, was observed 2 dpi in both mammalian cell lines, although this was delayed in Vero cells compared to BHK-21 (Figure 6.2). Similar levels of genome replication were

observed after 2 dpi, corroborated by the similar virus titres measured at 4 dpi (Figure 6.3). No OROV genome replication was observed in cell lines from *Cx. quinquefasciatus* (HSU), *Anopheles gambiae* (Sua) or *Culicoides v. sonorensis* (KC, Figure 6.2).

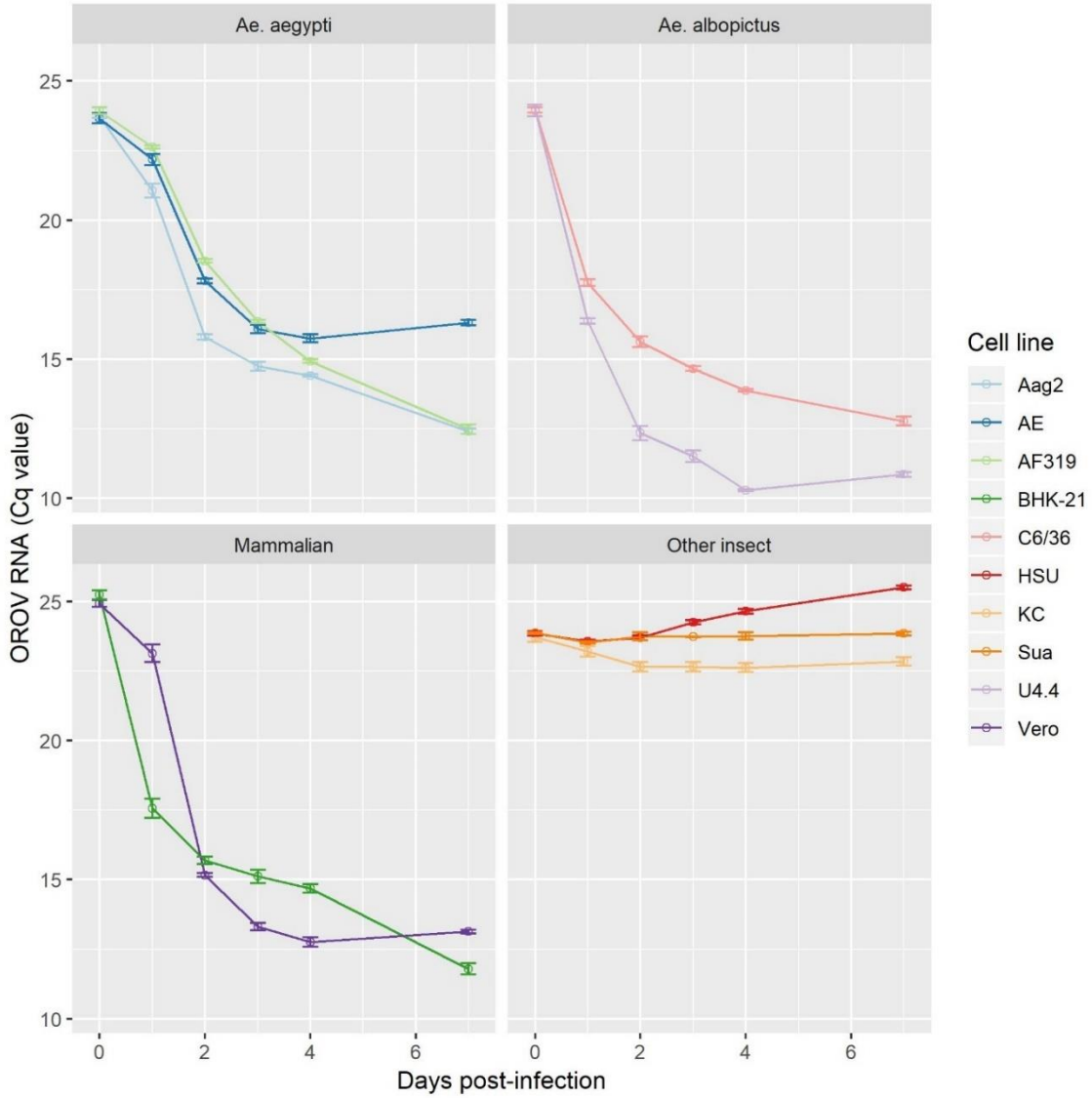

Figure 6.2 OROV genome replication in *Ae. aegypti, Ae. albopictus*, mammalian and other insect cell lines (HSU: *Cx. Quinquefasciatus*, Sua: *Anopheles gambiae* and KC: *Culicoides v. sonorensis*), assessed by relative quantity of OROV RNA measured at 0, 1, 2, 3, 4 and 7 days post-infection (dpi). Error bars represent the standard deviation from the mean of three replicates.

6.2.1.2 ASSESSMENT OF INFECTIOUS VIRUS IN CELL LINES SHOWING OROV GENOME REPLICATION

Infectious viral titres were assessed in cell lines that showed evidence of OROV genome replication by qRT-PCR. Viral titres in supernatants from *Ae. aegypti* cell lines increased from 1000-3000 pfu/mL at 0 dpi to between 2e+6 pfu/mL and 2e+7 pfu/mL at 4 dpi, with titres from Aag-2 cells approximately one log higher than the other cell lines (Figure 6.3). The higher quantity of OROV RNA measured in *Ae. albopictus* U4.4 cells compared to C6/36 cells at 4 dpi was reflected by a higher titre of infectious virus, which was almost 10-fold higher than that from C6/36 cells (Figure 6.3). From 0 to 4 dpi, viral titres increased to approximately 1e+6 pfu/mL in both mammalian cell lines (Figure 6.3).

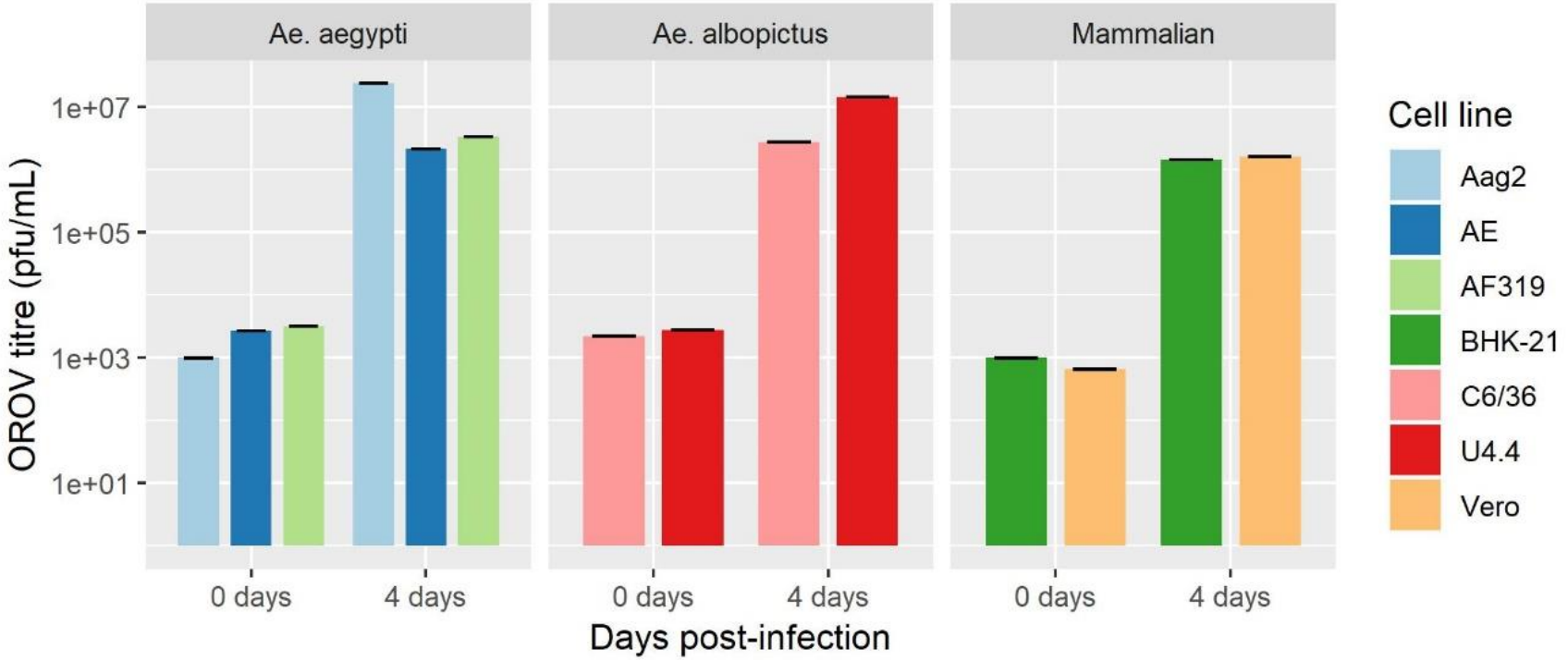

Figure 6.3 OROV replication in *Ae. aegypti, Ae. albopictus* and mammalian cell lines, assessed by measuring viral titre at 0 and 4 dpi. Error bars represent the standard deviation from the mean of three replicates.

6.2.2 OROV REPLICATION IN HUMAN CELLS

OROV replication in human primary cells and cell lines was assessed using an MOI of 0.1. Genome replication was assessed by measuring intracellular viral RNA using qRT-PCR and viral titres were measured in supernatants using a plaque assay.

6.2.2.1 ASSESSMENT OF OROV GENOME REPLICATION

An initial experiment assessed OROV growth in fibroblasts, hepatocytes and PBMCs over a 72-hour period. PBMCs isolated from seven healthy volunteers were used. OROV genome replication was observed in fibroblasts and hepatocytes, but not in PBMCs (Figure 6.4). OROV RNA in fibroblasts increased substantially between 0 and 24 hours posti-infection (hpi), after which it plateaued (Figure 6.4). In hepatocytes, OROV RNA increased between 0 and 24 hpi, plateaued, then decreased after 48 hours (Figure 6.4), probably reflecting the condition of the infected cells at this point in the experiment, although it was not possible to check for cytopathic effect (CPE) because of biosafety constraints within the CL3 laboratory. There was no evidence of OROV genome replication in PBMCs; the amount of OROV RNA remained the same from 0 to 24 hpi, then started to decrease (Figure 6.4).

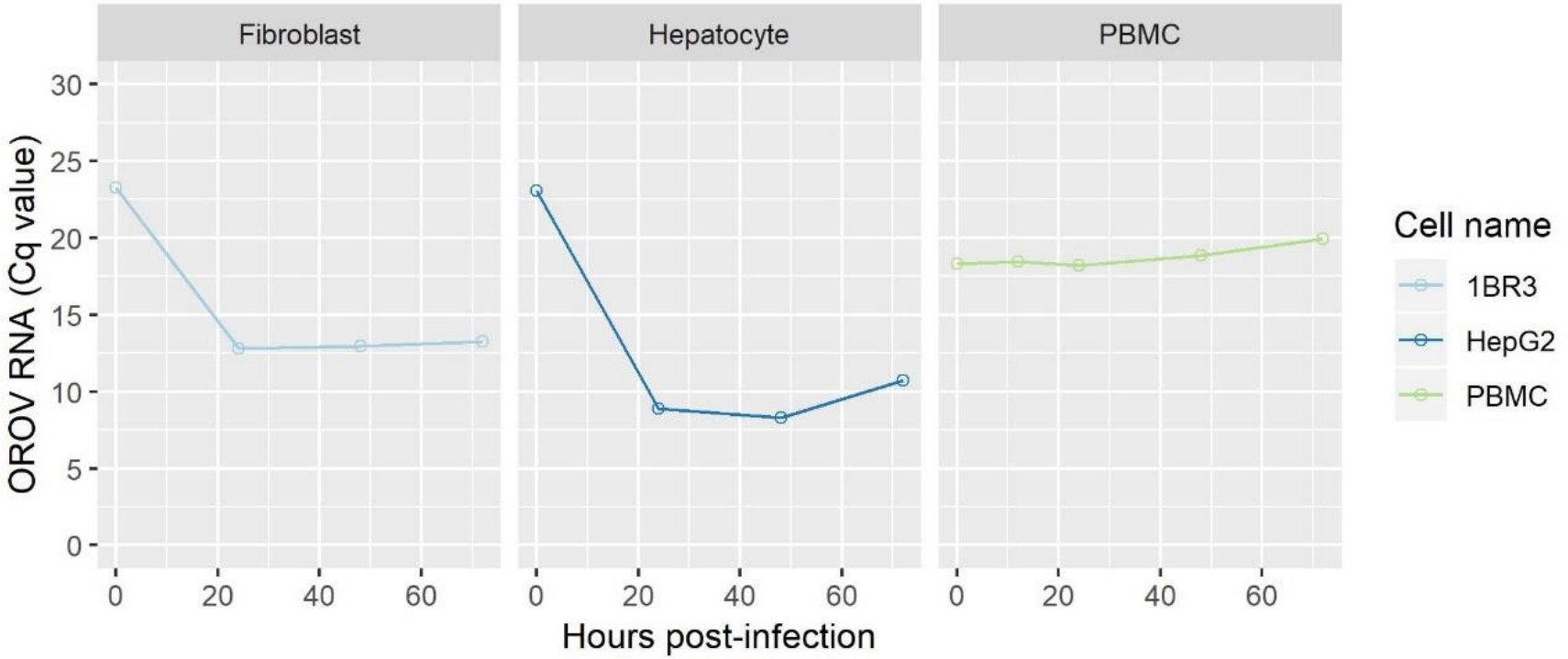

Figure 6.4 OROV genome replication in human fibroblasts, hepatocytes and PBMCs, assessed by relative quantity of OROV RNA measured at 0, 24, 48 and 72 hours post-infection (hpi).

Based on results from the initial 72-hour experiment, a second experiment was performed in triplicate, focussing on the 0-36 hpi period because the majority of virus genome replication was observed between 0-24 hours. PBMCs were not assessed further because of the absence of OROV replication observed previously. In addition to fibroblasts and hepatocytes, two primary keratinocyte cell lines were assessed.

OROV genome replication was first observed in fibroblasts between 6 and 12 hpi. Genome replication after 12 hpi is at a slower rate than that seen in the preceding 6 hours, and greater variation was observed between replicates at 12 and 36 hpi (Figure 6.5). Genome replication in hepatocytes was observed as early as 6 hpi, earlier than in fibroblasts (Figure 6.5). A roughly linear increase in OROV RNA was observed until 24 hpi, after which it began to plateau (Figure 6.5). For both primary keratinocyte cell lines, a small increase in OROV RNA was observed between 12 and 24 hpi, which then decreased again between 24 and 36 hpi (Figure 6.5).

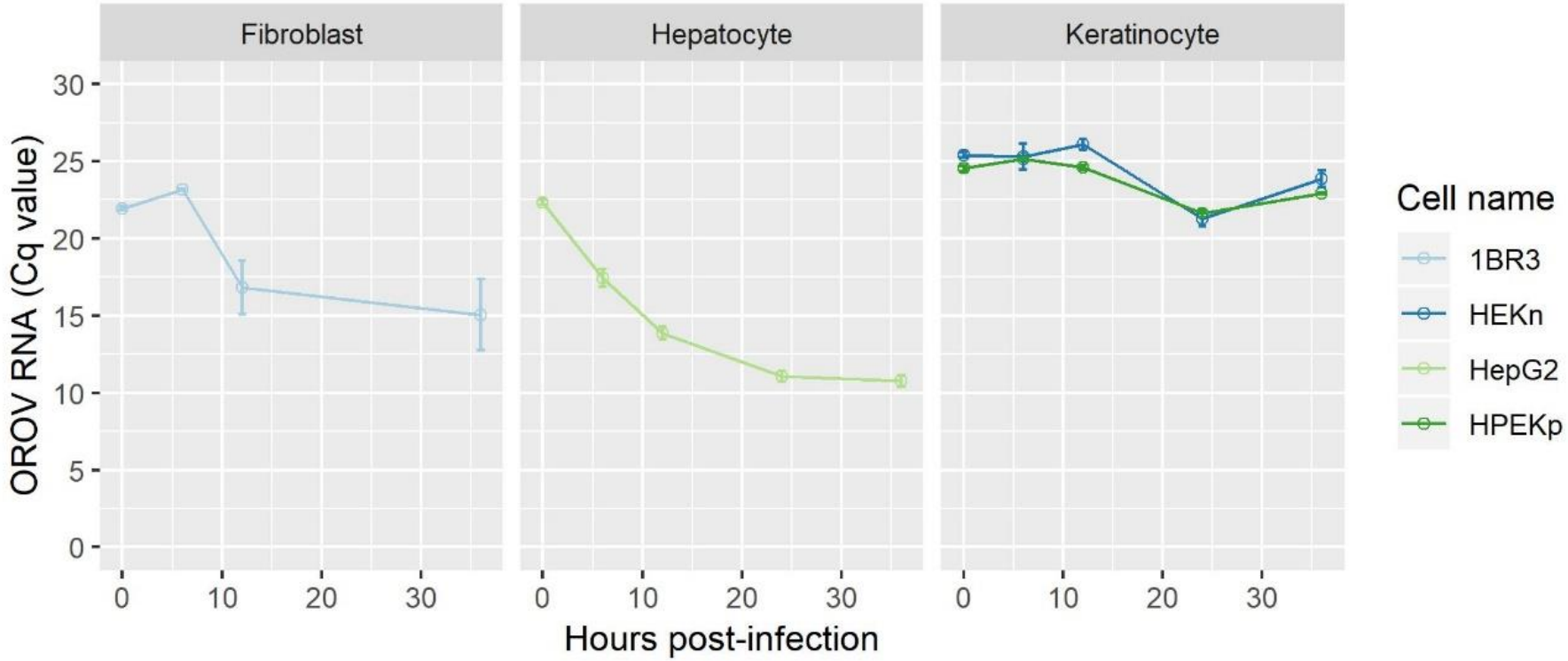

Figure 6.5 OROV genome replication in human fibroblasts, hepatocytes and keratinocytes, assessed by relative quantity of OROV RNA measured at 0, 12, 24, and 36 hours post-infection (hpi). Error bars represent the standard deviation from the mean of three replicates.

6.2.2.2 ASSESSMENT OF INFECTIOUS VIRUS IN CELL LINES WITH OROV GENOME REPLICATION

In agreement with the qRT-PCR data, a high viral titre was measured in fibroblasts at 24 hpi (1.2e+6 pfu/mL), a substantial increase from 0 hpi (2.2e+2 pfu/mL, Figure 6.6). Similarly, the viral titre in hepatocytes increased substantially by 24 hpi (Figure 6.6), also in agreement with the qRT-PCR data (Figure 6.5). There was no evidence of OROV replication in PBMCs (Figure 6.6). The relatively high titre of OROV observed at 0 dpi is related to the experimental design; it was not possible to remove the virus inoculum because the PBMCs were maintained in suspension rather than adhered to a plate. In both keratinocyte cell lines, no infectious virus was detected at either timepoint, suggesting that the virus did not replicate effectively in these cell types.

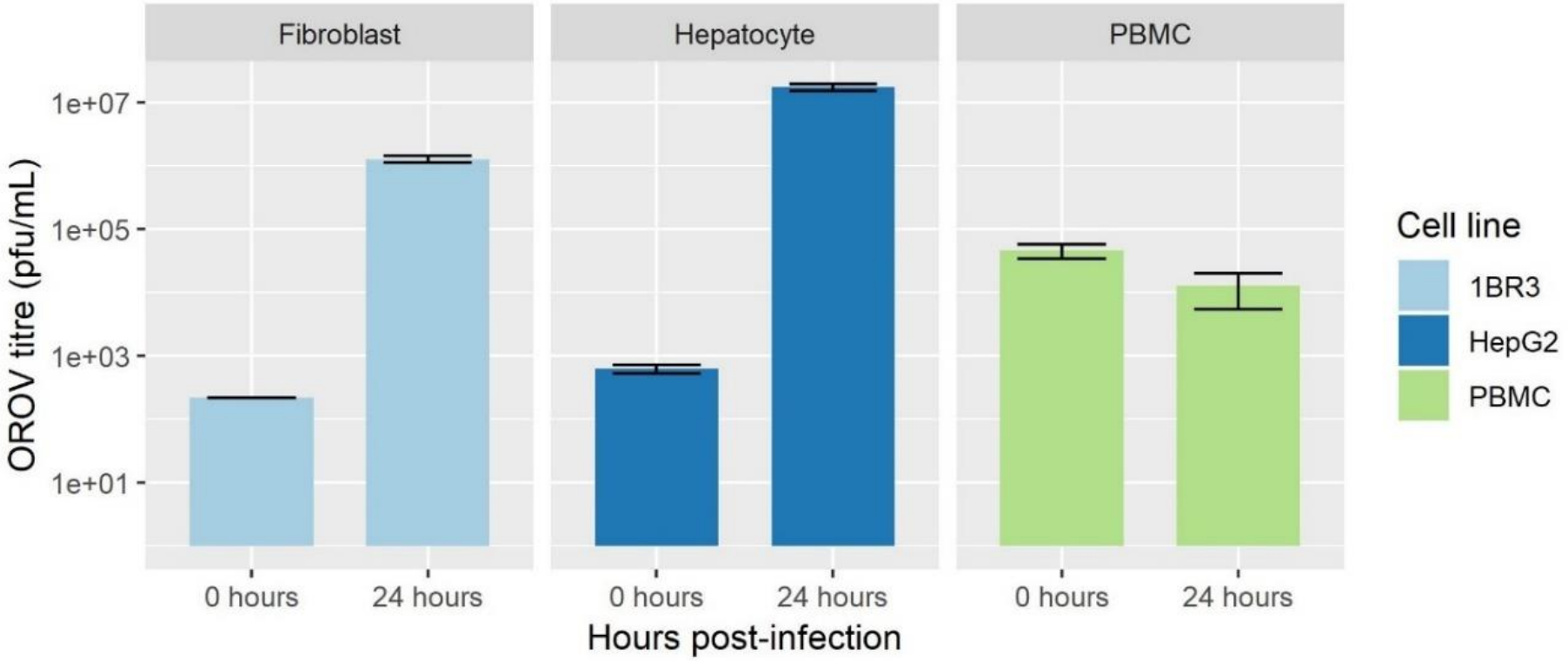

Figure 6.6 OROV replication in human fibroblasts, hepatocytes and PBMCs, assessed by viral titres measured at 0 and 4 dpi. Error bars represent the standard deviation from the mean of three replicates.

6.2.3 CELL VIABILITY

As previously stated, it was not possible to check for CPE because of biosafety constraints within the CL3 laboratory. As an alternative, cell viability counts using mock-infected cells were taken at each timepoint during the human cell time-course experiments, to control for lack of virus replication due to sub-optimal cell health. Mean cell viability (averaged across all experimental timepoints) of 70% and above was considered adequate, however, in some instances the low number of cells available for counting made it difficult to obtain a reliable viability count. Therefore, for cells that showed no evidence of OROV replication, the capability of these cell types to support OROV replication is not ruled out because it cannot be definitively said that the results were not influenced by sub-optimal cell health.

6.2.4 SUMMARY

OROV can replicate in cell lines derived from *Ae. aegypti* (*n*=3), *Ae. albopictus* (*n*=2), non-human mammals (*n*=2), and transformed human hepatocytes (*n*=1), as well as primary human fibroblasts (Table 6.1). No evidence of replication was observed in cell lines from *Anopheles gambiae*, *Culex quinquefasciatus*, *Culicoides v. sonorensis*, or in primary human keratinocytes or PBMCs (Table 6.1).

Cell name	Cell type	Species	OROV genome replication	Infectious OROV produced
Aag-2	Embryonic	*Aedes aegypti*	Yes	Yes
AE	Unknown	*Aedes aegypti*	Yes	Yes
AF319	Embryonic	*Aedes aegypti*	Yes	Yes
C6/36	Embryonic	*Aedes albopictus*	Yes	Yes
U4.4	Embryonic	*Aedes albopictus*	Yes	Yes
Sua4a-2	Larvae	*Anopheles gambiae*	No	No
HSU	Ovary	*Culex quinquefasciatus*	No	No
KC	Embryonic	*Culicoides v. sonorensis*	No	No
BHK-21	Kidney, fibroblast	Hamster	Yes	Yes
Vero	Kidney, epithelial	African green monkey	Yes	Yes
1BR3	Fibroblast	Human	Yes	Yes
HEKn	Keratinocyte	Human	No	No
HPEkp	Keratinocyte	Human	No	No
PBMC	PBMC	Human	No	No
HepG2	Liver, HCC	Human	Yes	Yes

Table 6.1 A summary of OROV replication results in all cell types tested.

6.3 DISCUSSION

6.3.1 OROV REPLICATES IN CELL LINES FROM *AEDES AEGYPTI* AND *AEDES ALBOPICTUS*

The experimental results described in this chapter demonstrated that wildtype Ecuadorian OROV is able to replicate in cell lines derived from *Ae. Aegypti* and *Ae. albopictus*; both important insect vectors of other arboviral diseases circulating both in Ecuador and globally. Few studies have looked at the capability of mosquito species *Aedes aegypti* and *Aedes albopictus* to transmit OROV. Screening of 311 *Aedes* mosquitoes (collected from the area local to the original febrile patient's residence in Trinidad) did not detect virus in any mosquito tested. OROV was recovered from *Aedes* mosquitoes parenterally inoculated with OROV in the laboratory (7/7 *Ae. scapularis* and 4/4 *Ae. serratus*), but transmission to mice did not occur (177). Another study investigating whether *Ae. albopictus* mosquitoes can become infected and transmit OROV in a laboratory setting detected virus in a small proportion of mosquitoes that had fed on a viraemic hamster, but none transmitted virus to mice (540). These studies were performed in the 1960s and 1990s, respectively, so further experiments using contemporary mosquitoes and OROV strains would provide better understanding of the picture today.

Ae. aegypti is considered to be the most important arboviral vector of the past century, in large part because of its ability to transmit multiple clinically important emerging viruses including DENV, CHIKV, YFV and ZIKV (473,541,542). This species is widespread throughout Ecuador, though not present at high altitudes, and does well in heavily urbanised environments where breeding sites tend to be plentiful (Figure 6.7) (543). The incidence of vector-borne disease in Ecuador has historically been highest in the western

coastal and interior regions of the country, which corresponds with the distribution of mosquito vector species (543).

AF319 is a clonal cell line derived from embryonic *Ae. aegypti* that has a defective RNA interference (RNAi) response resulting from an introduced homozygous Dicer 2 (Dcr2) mutation (544). Conversely, the Aag-2 *Ae. aegypti* cell line of embryonic origin is RNAi competent (545,546), whereas the origin and immunocompetence of AE cells is unknown. Despite the differences in RNAi competence, OROV replicated in all three cells lines, suggesting that OROV may be able to circumvent innate immunity pathways present in *Ae. aegypti* cells.

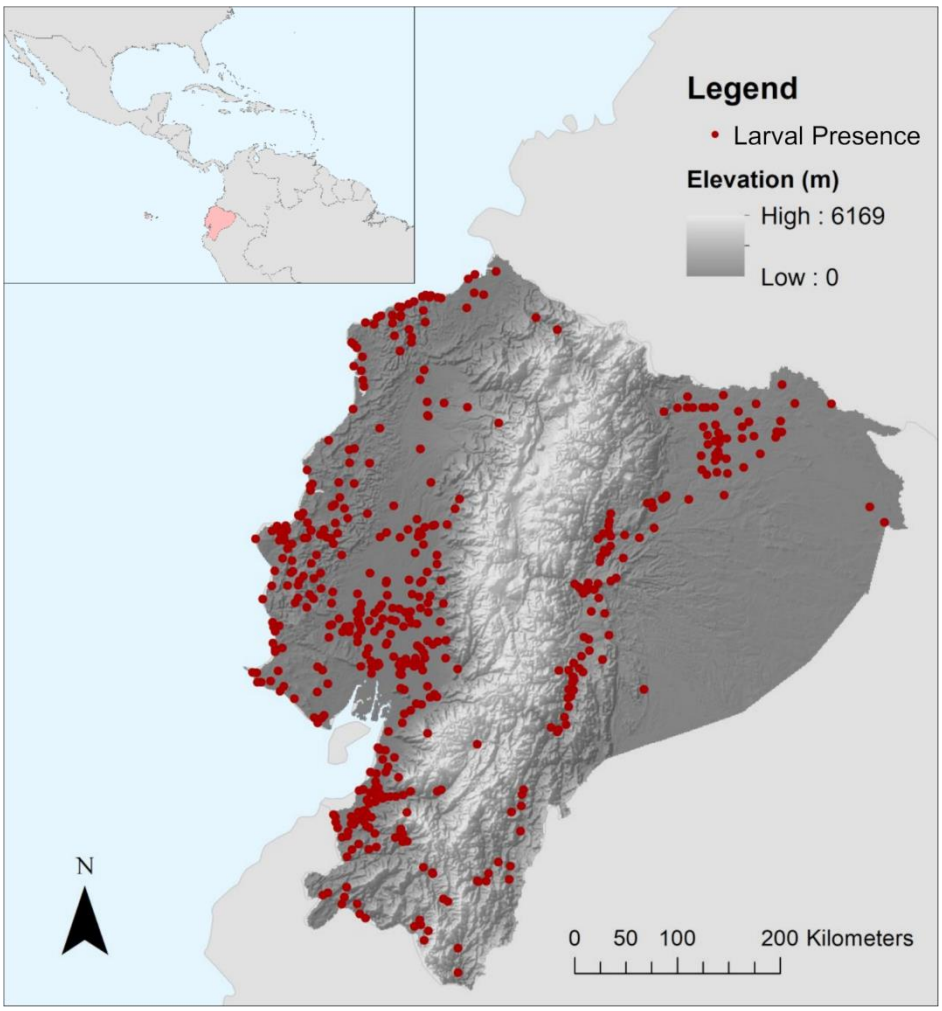

Figure 6.7 The ecological distribution of *Ae. aegypti* in Ecuador, based on household entomological surveys conducted by the Ecuadorian Ministerio de Salud Pública from 2000-2012. Reproduced from Lippi *et al.* (2019) (543).

Ae. albopictus, vector for CHIKV and DENV and a potential vector for a number of other arboviruses (547–549), was identified in Ecuador in 2017 for the first time in the highly populated city of Guayaquil on the Pacific coast (550). Its geographic distribution and contribution to arbovirus transmission across the country is unknown. C6/36 and U4.4 cell lines are both sub-clones of an original culture derived from embryonic *Ae. albopictus* (551–553). C6/36 cells are RNAi deficient due to a mutation in the Dcr2 gene

(554), whereas U4.4 cells have a fully functional RNAi response (555). Virus propagation in U4.4 cells usually results in much lower titres that those seen in C6/36 cells (556–558). Conversely, in this study higher levels of viral RNA and infectious OROV were observed in U4.4 cells compared to C6/36 cells, suggesting that OROV may be able to effectively circumvent *Ae. albopictus* innate immune defences to establish an infection.

The OROV replication observed in *Ae. aegypti* and *Ae. albopictus* cell lines suggests that these mosquito species have the potential to become infected with OROV. Whether or not they are competent vectors, meaning virus is capable of escaping the midgut and reaching the salivary glands where it can be transmitted to another host, is poorly understood due to the paucity of available data. The present data suggests that *in vivo* vector competence studies in both mosquito species, using a contemporary OROV strain, would be highly informative.

Cx. quinquefasciatus, a proposed secondary vector of OROV in urban epidemics and a known vector of flaviviruses West Nile virus and Saint Louis encephalitis virus (559–561), is prevalent in tropical and sub-tropical areas globally, including Ecuador (Figure 6.8) (562,563). OROV replication was not detected in the *Cx. quinquefasciatus* ovary-derived HSU cell line (564). This somewhat contradicts previous findings that *Cx. quinquefasciatus* mosquitoes can be infected in the laboratory (although this could result from differences between cell culture and the whole organism) (528), and is at odds with the isolation of OROV from *Cx. quinquefasciatus* mosquitoes collected in the field (180). However, the observation was based on a single experiment and further studies are needed to confirm the result.

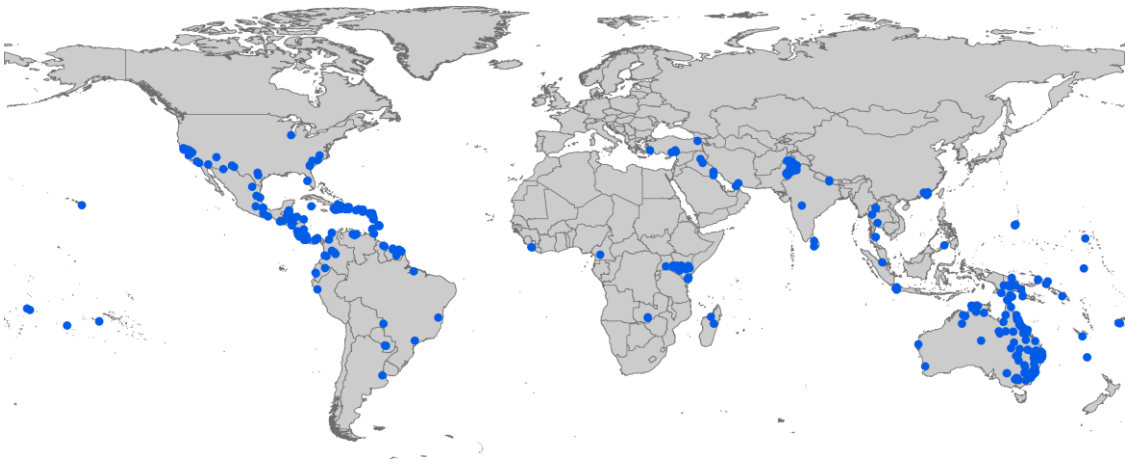

Figure 6.8 Distribution of *Cx. quinquefasciatus* based on 1402 occurrence records. Reproduced from Samy *et al.* (2016) (565).

Anopheles spp. mosquitoes are major vectors of *Plasmodium falciparum* and the primary species responsible for malaria transmission in South America is *Anopheles darlingi* (566,567). *Anopheles* spp. have been detected throughout Ecuador, although not at high altitudes (568). *Anopheles* spp. are vectors of O'nyong nyong virus (569) and a number of other pathogenic human viruses have been detected in them (570–572), including those belonging to the *Orthobunyavirus* genus (573,574). This study used *Anopheles gambiae*-derived (Sua4a-2) cells (575), though no evidence of OROV replication was observed.

To the best of the author's knowledge, no cell lines from *C. paraensis* have been established. Cell lines from related species *C. variipennis* and *C. v. sonorensis,* the vectors of bluetongue virus, are available and the present study used the *C. v. sonorensis*-derived KC cell line (576) to investigate OROV replication. The lack of replication seen may reflect the differences between *Culicoides* species, and further studies in *C. paraensis* would be useful to further elucidate the dynamics of infection in this vector

species. In agreement with previous studies (185,387–389), OROV replication was observed in mammalian cell lines Vero and BHK-21.

6.3.2 OROV REPLICATES IN PRIMARY HUMAN FIBROBLASTS AND A HUMAN HEPATOCYTE CELL LINE

It was hypothesised that fibroblasts and keratinocytes from human skin would support OROV replication. The skin is the primary site of infection following a bite from an infected vector, and presumably leads to OROV entering the blood stream and subsequent viraemia, but little is known about OROV replication in this site. Studies of other arboviruses with similar transmission routes showed that ZIKV replicates in human skin fibroblasts (577), and ZIKV and DENV-2 replicate in human keratinocytes (282). The present experiments showed that OROV replicates in normal, non-transformed adult primary human skin fibroblasts (1BR3 cells), corroborating the observation made by Varela *et al.* (391) and supporting the hypothesis that this cell type could be an initial replication site for OROV. Conversely, no replication was observed in two human primary epidermal keratinocyte cell types (HEKn and HPEKp cells).

OROV is hepatotropic in small animal models (182,189,393), but little is known about liver involvement in human disease, mainly because fatalities from OROV have not been recorded therefore there has been no opportunity to study this. Symptoms consistent with liver disease are not commonly reported in OROV patients, though a recent case study described hepatic manifestations including altered liver enzymes, secondary to OROV-associated aseptic meningoencephalitis (184). Furthermore, OROV replicates in the human hepatocarcinoma cell line HuH-7 (390). In this study, high levels of OROV replication were observed in a human hepatoma cell line (HepG2), reaching the highest

viral titre observed in any of the human cell lines tested, suggesting that human hepatocytes could be a site of OROV replication. It would be informative to repeat this experiment using primary human hepatocytes, which are more representative of normal human hepatocytes.

Contrary to previous observations that OROV was present in peripheral blood leukocytes from OROV-infected patients and can replicate in macrophage-like cells (390,536), no increase in OROV RNA nor infectious virus was detected from PBMCs isolated from seven healthy volunteers and infected with OROV. De Souza Luna *et al.* detected OROV RNA (using qRT-PCR) and OROV antigen (using indirect immunofluorescence, Figure 6.9) from buffy coats isolated from patient blood samples, but it was not determined exactly which cell types OROV antigen was observed in (536). The disparity between the present observation and that of de Souza Luna *et al.* could be explained by the difference in sample type. PBMCs (used in this study) are a mixed population of mononuclear cells comprising lymphocytes (T cells, B cells, NK cells) and monocytes. Peripheral blood leukocytes (used in the de Souza Luna *et al.* study) contain mononuclear cells in addition to granulocytes (neutrophils, basophils, and eosinophils) that have multi-lobed nuclei. If OROV antigen in the patients resided in granulocytes but not mononuclear cells, this could explain the different observations. Alternatively, a modest amount of OROV replication in PBMCs could have occurred undetected in the present experiment. It was not possible to remove OROV following inoculation without compromising the viability of the PBMCs, therefore substantial viral RNA and infectious virus was present from inoculation. If OROV replicated in a minor population of PBMCs, for example dendritic cells, this could be masked by the background level of OROV.

Performing indirect immunofluorescence or flow cytometric analysis on OROV-infected PBMCs would help to clarify this further.

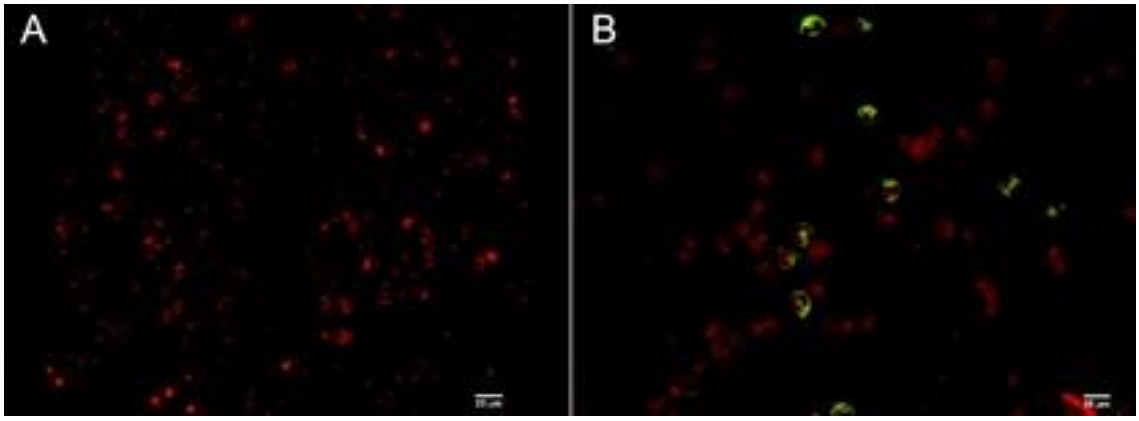

Figure 6.9 Indirect immunofluorescence for OROV performed on buffy coat smears. A) negative control, B) OROV-positive patient. Green = OROV antigen, red = cell nuclei. Modified from de Souza Luna et al. (2016) (536).

Previous studies of OROV replication kinetics in HeLa cells revealed that intracellular viral titres at 6 hpi were low, following which they rapidly increased, peaking at 24 hpi (388). In this study a similar pattern was observed in primary human fibroblasts, albeit through measuring intracellular OROV RNA. The low amount of viral RNA measured at 0-6 hpi probably reflected the virus eclipse phase, followed by substantial genome replication by 12 hpi. Interestingly, this eclipse phase is not observed in OROV-infected hepatocytes, suggesting that this happens earlier than 6 hpi, pointing to a faster replication cycle than that seen in other cell types.

Our experiments have some advantages over those performed previously. The virus used was a contemporary field strain that was isolated from a febrile patient and had

undergone minimal passages in cell culture. Most previous studies have used the OROV prototype strain BeAn19991 (Brazil 1960) (187,388–390,578), or recombinant viruses (185), which have limited relevance to current circulating strains. Where possible, primary cells were used that have biological relevance to the OROV mode of transmission, rather than transformed cell lines or less relevant cell types. Lack of OROV replication in the cell types tested in these studies does not rule out a role in OROV infection because the number of experiments and methods performed was limited. Rather, positive results demonstrate a potential role in the OROV life cycle that warrants further investigation.

6.3.3 LIMITATIONS

In vitro virus studies provide useful information under conditions in which is it relatively easy to control and manipulate variables. However, they do not represent a natural infection, in which there is far more complex interplay between virus, multiple cell types and tissues, and most importantly the host immune system. Results from the present *in vitro* studies of OROV replication should be viewed in this context and used to inform further studies.

6.3.4 FUTURE WORK

The experiments described in this chapter provide preliminary data on which further studies can be built to further elucidate the role of different insects in OROV

transmission, and the role of various human cell types in OROV infection and pathogenesis.

This study demonstrated that OROV replicates in cells from *Ae. aegypti* and *Ae. albopictus,* two important mosquito species that are known vectors of arboviral diseases and are widespread globally. The competence of these species in transmitting OROV is currently unknown, but the impact of OROV transmission by *Aedes* spp. on public health is likely to be significant. Based on this data, it is recommended that OROV vector competence studies in *Ae. aegypti* and *Ae. albopictus* are undertaken.

The dynamics of OROV in Ecuador are not understood. To better understand if and how OROV transmission is occurring in Esmeraldas and in Ecuador as a whole, active surveillance studies sampling insects from targeted areas should be undertaken. Screening captured insects for OROV RNA using the qRT-PCR assay developed in this project may identify insect species relevant to OROV transmission in Ecuador, leading to improved understanding of the risk factors associated with disease and how to control them to reduce the risk to public health.

This study showed that OROV is capable of replicating in primary human fibroblasts and a human hepatoma cell line, suggesting that these cell types that may be relevant to the course of infection in humans. Further studies to understand infection at the site of virus inoculation, the skin, would be informative for understanding how OROV interacts with the human innate immune system in order to escape the tissues and disseminate via the bloodstream. It is essential to study the mechanisms by which OROV infects humans and evades immune defences in order to develop effective therapies and vaccines in the future.

CHAPTER 7: DISCUSSION

7.1 SUMMARY OF FINDINGS

The major aims of this thesis were to: 1) establish whether pathogenic viruses were present in two cohorts of febrile patients from low- and middle-income countries, 2) characterise the viruses identified and 3) perform subsequent research to further knowledge relevant to emerging infectious disease. The third aim was dependant on virus identification results, which shaped the focus of the project as it progressed. The anticipated outcomes of the project were: 1) support for existing in-country laboratories by identifying circulating viruses and recommending additional assays to include in surveillance and diagnostic testing, 2) protection of UK public health from imported infectious diseases by identifying pathogens that may be a risk to those returning from endemic countries, and 3) enhancement of future surveillance efforts and collaborative research programmes by banking propagated, clinically significant viruses with national curated virus collections.

7.1.1 DISCOVERY OF OROV IN ECUADOR AND DEVELOPMENT OF DETECTION ASSAYS

The major outcome of this project has been the detection, isolation and sequencing of Oropouche virus for the first time in febrile patients from Ecuador. OROV was initially detected in a single patient who had remained in Esmeraldas province for more than 3 months and had a blood sample taken following seven days of fever and other symptoms. The clinical picture fitted that caused by multiple pathogens circulating in Ecuador, including DENV, ZIKV, and *Plasmodium*. Testing for DENV, CHIKV and ZIKV in-country yielded negative results, as did retrospective RT-PCR testing for a more extensive panel of pathogens. Metagenomic sequencing detected a substantial portion

of the OROV genome. Virus isolation confirmed the presence of infectious virus in the patient sample, and subsequent sequencing from the culture supernatant resulted in the first complete OROV genome sequence from Ecuador (380). An established OROV qRT-PCR assay (361), however, did not detect viral RNA in the patient sample. The availability of OROV genome sequence from the metagenomic sequencing data was crucial in identifying primer mismatches between the Ecuadorian OROV sequence and the assay reverse primer. The subsequent development of a modified qRT-PCR with high sensitivity for both Ecuadorian and prototype OROV strains demonstrated the utility of NGS data for the adaptation of detection assays. This modified assay was used to test the entire Ecuadorian patient cohort (*n*=196), detecting a total of six OROV-positive patients. Infectious virus was isolated from all positive patient plasma samples and subsequent sequencing generated complete genomes from all isolates. In addition to the OROV qRT-PCR, a multiplex tiling PCR primer scheme was developed that was capable of amplifying complete genome sequences from Ecuadorian and prototype OROV strains. This tool could be used to amplify and sequence OROV genomes from clinical samples containing low amounts of OROV RNA, providing important genomic information in OROV endemic countries.

The detection of large proportions of the OROV genome from samples with relatively high qRT-PCR Cq values (>30) shows that the metagenomic sequencing protocol used in this project has very good sensitivity for RNA viruses. A key difference from some previous protocols is the use of a SISPA primer with nine random nucleotides (9N) as opposed to six. A previous comparison of 6N and 12N SISPA primers for viral RNA sequencing demonstrated reduced bias and higher median sequence depth using the 12N primer (579). The use of 9N likely contributed to the high sensitivity for viral

sequences such as OROV, and future optimisation of the length of random sequence used could further improve viral detection.

The Ecuadorian OROV sequences were included in phylogenetic analyses of OROV genomic sequences in the wider context of South America (363). The Ecuadorian genomes clustered together in a monophyletic group and timescale analyses showed a most recent common ancestor that existed between 2008-2016 (363). This suggests that not all Ecuadorian OROV-positive patients were infected from the same source, but by different strains, making it likely that the virus has been circulating undetected in Ecuador for some time. This hypothesis fits with previous detections of anti-OROV antibodies in patients that are geographically and temporally distant from Esmeraldas (479,480), suggesting that there is unsampled OROV diversity within Ecuador. Entomological collections performed in Ecuador since 2009 have not identified the OROV urban vector *C. paraensis* in Esmeraldas, which is only present in the South and Amazon areas of the country. These observations led to the hypothesis that OROV transmission occurred in Esmeraldas during 2016, via an unknown insect vector.

7.1.2 ENHANCED KNOWLEDGE OF OROV PATHOGENESIS AND POTENTIAL VECTORS

Experimental work demonstrated that OROV can replicate in RNAi competent cell lines from *Ae. aegypti* and *Ae. albopictus*; both important mosquito vectors of other arboviruses (473,541,542,547–549) that have not been thoroughly investigated as vectors of OROV. Previously OROV has been isolated from the sylvatic mosquito *Aedes (Ochlerotatus) serratus* in Brazil (28). These preliminary findings warrant further investigation of the potential for *Aedes* spp. to transmit OROV; *in vivo* vector

competence studies would be highly informative. *Ae. aegypti* and *Ae. albopictus* are globally distributed, thrive in urban environments and are anthropophilic (580), making them highly effective vectors. If they are capable of transmitting OROV, establishment of the virus in a human-*Aedes* spp. transmission cycle could have extremely serious consequences for the spread of OROV globally.

Knowledge of OROV pathogenesis in humans is limited compared to other arboviruses. The hypothesis that OROV replicates in certain human cell types, identified based on the route of transmission, previous observations of pathogenesis and the clinical presentation of OROV infection, was tested. Experiments demonstrated (see Chapter 6) that OROV replicates in primary human fibroblasts, suggesting that this could be a key cell type for OROV replication early during infection, following inoculation into the skin via an insect vector. No evidence of replication in primary human epidermal keratinocytes, or PBMCs, was seen, however as discussed in chapter 6, further experiments are required to rule out these cell types as sites of replication. High titres of OROV were measured in a human hepatoma cell line, fitting with observations from animal models (182,393). Hamsters inoculated subcutaneously with OROV showed clinical signs including high temperature, lethargy and shivering, as well as histopathological evidence of meningoencephalitis and liver abnormalities, with OROV antigen and virions detected in cells from both organs (393). Further studies to investigate the role of fibroblasts and hepatocytes in OROV pathogenesis and immune response would enhance understanding of this emerging virus and help inform effective strategies for the development of vaccines and therapeutics.

7.1.3 RETROSPECTIVE TESTING IDENTIFIES EBOV IN FEBRILE SIERRA LEONEAN PATIENTS THAT TESTED NEGATIVE IN-COUNTRY

Febrile EBOV-negative Sierra Leonean patients that had a blood sample taken at an Ebola treatment centre were tested using RT-PCR/PCR assays and metagenomic sequencing, to identify pathogenic viruses co-circulating at the time of the West African Ebola virus outbreak in 2014-2015. Despite these patients testing negative for EBOV at the time of sampling, 8/120 tested positive and a further 10 tested inconclusive upon retrospective qRT-PCR testing. Metagenomic sequencing was performed on representative EBOV-positive samples which yielded almost 60% of the EBOV genome from one sample. Following further investigation, it was hypothesised that the low level of EBOV RNA in these samples was not detected in-country because a less sensitive qRT-PCR assay (Altona) was used in the field laboratories at the end of 2014. Sensitivity issues were identified in this assay (431), prompting a timely transition to a more sensitive assay (Trombley) in January 2015. Seven of the eight retrospective EBOV-positive samples were tested prior to January 2015 in-country and all had high Cq values (>30). This highlights the challenges and importance of assay selection and implementation in outbreak scenarios, and the requirement for ongoing assessment of assay performance. Aside from EBOV, RT-PCR/PCR tests identified *Plasmodium* and *Leptospira*, but no other viral infections.

7.1.4 IDENTIFICATION OF VIRUSES IN PCR-NEGATIVE FEBRILE PATIENTS USING METAGENOMIC SEQUENCING PROVIDES PROOF OF PRINCIPLE FOR THE APPROACH

Metagenomic sequencing of 17 RT-PCR/PCR-negative febrile Ecuadorian patient samples identified Hepatitis A virus in one patient, but no other pathogenic viruses.

Additionally, human pegivirus GB virus type C was identified in 2/6 febrile patients sampled in Esmeraldas in 2017. Metagenomic sequencing of 30 RT-PCR/PCR-negative febrile Sierra Leonean patient samples using the same approach identified Hepatitis B virus, human immunodeficiency virus type 1 and GBV-C in one, five and seven patients, respectively. Furthermore, one patient showed a co-infection of HBV and HIV, demonstrating the utility of the metagenomic approach for identifying multiple clinically important viruses.

7.2 TOWARDS PREVENTING AND CONTROLLING EMERGING INFECTIOUS DISEASE

Over recent decades an increase in the number of EID events has been recorded, even when controlling for increased reporting (5). The detection and isolation of OROV in patient samples from Ecuador demonstrates the ongoing emergence of EIDs into areas in which they have not previously been detected or the evidence for their existence is limited. Because of the relatively mild, self-limiting nature of Oropouche fever, it is reasonable to surmise that, following multiple negative test results, treatment of the OROV-positive patients in Esmeraldas would have been symptomatic (treating the symptoms rather than the cause of infection) and no further investigations would have been performed. It is in this way that infectious diseases can spread 'silently', undetected in areas where other endemic pathogens cause similar clinical spectrums of disease.

Understanding factors that drive the emergence and re-emergence of infectious disease is key to preventing and controlling EID events. An essential part of this is implementing effective surveillance systems in relevant countries. The identification of OROV in Ecuador and the development of effective molecular detection assays is the first-step towards understanding the dynamics of the virus in this country and neighbouring areas, and these tools could be integrated into testing protocols in hospitals and healthcare centres. Assay implementation and capacity building has begun through an ongoing collaboration with USFQ, involving training visits both in Ecuador and the UK, through which expertise in qRT-PCR and metagenomic sequencing was exchanged. In this way this project has fulfilled the anticipated outcome of supporting existing in-country laboratories by identifying a circulating virus and providing additional assays to include in surveillance and diagnostic testing. Furthermore, this assay has been adopted by the

PHE Rare and Imported Pathogens Laboratory, assisting diagnosis in returning UK travellers with febrile illness. This fulfils another anticipated outcome; to protect UK public health from imported infectious diseases by identifying pathogens that may be a risk to those returning from endemic countries.

Early detection of an EID event can help prevent further spread by controlling the outbreak at an earlier stage, when it is more manageable. Effective surveillance requires assays that are sensitive for currently circulating virus species and strains, which can be challenging in the case of RNA viruses that have a high rate of mutation. Taking advantage of newer technologies such as NGS could help detect EID events earlier. At present there are challenges associated with implementing a metagenomic sequencing approach as a frontline assay in a diagnostic setting, not least of which is the expense associated with the required technology and reagents, which can preclude its use in low- and middle-income countries. In addition, careful validation work must be performed, defining sensitivity and specificity, setting cut-off values and identifying robust negative and internal controls. Furthermore, ethical implications regarding human genome sequences need careful consideration. Although good progress is being made towards this goal, exemplified by the validated clinical metagenomic sequencing assay for pathogen detection from clinical CSF samples (334), at present the application is some-way off being ready for frontline use in many countries that experience EID occurrence. That being said, at the present time metagenomic sequencing could be used in prospective screening studies to help ensure that diagnostic assays are relevant and capable of detecting current strains, a problem highlighted in this project by the inability of an established OROV qRT-PCR to detect the Ecuadorian strain of OROV, and the subsequent assay modification made possible from the metagenomic sequencing data.

In this way, potential issues with current RT-PCR/PCR-based assays would be identified, allowing assay adaptation to ensure relevance to current circulating strains. This approach would require less stringent validation than frontline diagnostic use, and fewer sequencing tests would be required, reducing costs. This kind of screening could be performed using a portable sequencing device such as the ONT MinION, the initial set-up costs of which are substantially less expensive when compared to benchtop sequencing platforms such as Illumina.

Surveillance for OROV in relevant vector species could help define high risk areas for virus transmission and guide public health advice. The identification of OROV insect vectors in Ecuador, through collection and qRT-PCR testing, would help define OROV transmission dynamics in the country. A project recently funded by the National Institutes of Health and carried out at USFQ will investigate the prevalence of arboviruses in Ecuador over the next four years. This will include molecular testing of cohorts of arthropod species and febrile patients using the OROV qRT-PCR optimised during this project. Evidence of OROV replication in *Ae. aegypti* and *Ae. albopictus* cell lines suggests that collecting and testing these species for the presence of OROV, in addition to the established vector *C. paraensis* and proposed vector *Culex quinquefasciatus,* would be a good initial strategy for vector identification in Ecuador.

Effective treatments and vaccines help combat outbreaks of EID once they have been established. To develop these, basic research into virus pathogenesis and virus-host interactions is essential. Compared to some viral EIDs, OROV is mild in terms of the disease it causes in humans, however, the importance of understanding its pathogenesis should not be underestimated. Previously, other apparently mild or non-lethal infections have been associated with more serious syndromes, such as the recently

discovered link between ZIKV, Guillain-Barré syndrome and microcephaly (276–278), which was only uncovered following thousands of cases of infection. Furthermore, genome mutations can lead to changes in transmissibility, for example, mutations in the CHIKV envelope glycoproteins improved virus fitness in *Ae. albopictus*, resulting in widespread transmission and morbidity (56–58). Previous studies of OROV pathogenesis have mostly been undertaken using laboratory adapted virus strains and cell lines. This study used a contemporary Ecuadorian OROV strain that was isolated from a febrile patient, underwent minimal passages *in vitro* and therefore is more representative of strains circulating in nature. Furthermore, primary human cells were used to investigate virus tropism, identifying skin fibroblasts and a hepatocyte cell line as supportive of OROV replication. Further studies of the mechanisms that OROV uses to effectively enter, replicate, and evade immune responses in these cells could provide targets for future therapies.

As a result of the research activities carried out during this project, clinically significant virus isolates have been banked with the National Collection of Pathogenic Viruses, and genome sequences were made available online via the GenBank database (as described in chapters 4 and 5). This fulfils the anticipated outcome of enhancing future surveillance efforts and collaborative research programmes by banking propagated, clinically significant viruses with national curated virus collections.

7.3 SUMMARY

This project has made a novel contribution to the understanding of emerging infectious disease by providing conclusive evidence that OROV, a clinically important emerging arbovirus, is present in Ecuador, where (based on antibody evidence) it was suspected but not previously known to circulate. Furthermore, two molecular assays for the detection and characterisation of OROV have been developed and published, which can be adopted in relevant countries to enhance OROV surveillance and diagnosis. Novel suggestions for potential OROV insect vectors have arisen from experimental work, and human cell types with relevance to natural infection were identified. Through an ongoing collaboration with USFQ, the capacity for EID detection and surveillance has been improved in Ecuador through training delivery, including training in metagenomic sequencing. This project has demonstrated the utility of the metagenomic approach in detecting an emerging virus in a new area, as well as detecting established viral infections in febrile Sierra Leonean patients. I hope that this modest step forward in knowledge will provide a base for future research into OROV that may prevent the spread of the virus into new areas and lead to better control and reduced burden of disease in endemic countries.

APPENDICES

APPENDIX 1: SIERRA LEONEAN PLASMA SAMPLE METADATA

PHE ID	Sierra Leone ID	Laboratory of origin	Sample date	Sample type	District	Chiefdom	Ebola test result	Malaria rapid test result	Patient age	Sample status
SL-001	PL005748	Port Loko	03/04/2015	Blood	Kambia	nd	Negative	Negative	65	Follow-up
SL-002	PL005749	Port Loko	03/04/2015	Blood	Kambia	nd	Negative	Negative	32	Follow-up
SL-003	PL005734	Port Loko	02/04/2015	Blood	Kambia	Masungbala	Negative	Positive	20	Original
SL-004	PL005667	Port Loko	01/04/2015	Blood	Kambia	nd	Negative	Negative	24	Follow-up
SL-005	PL005733	Port Loko	02/04/2015	Blood	Kambia	Masungbala	Negative	Positive	20	Original
SL-006	PL005750	Port Loko	03/04/2015	Blood	Port Loko	Maforki	Negative	Negative	35	Follow-up
SL-007	PL005952	Port Loko	08/04/2015	Blood	Kambia	Tonko Limba	Negative	Negative	50	Original
SL-008	PL06005	Port Loko	10/04/2015	Blood	Port Loko	Marampa	Negative	Negative	37	Follow-up
SL-009	PL001324	Port Loko	03/01/2015	Blood	Port Loko	Kaffu Bullom	Negative	Negative	21	Original

SL-010	PL001383	Port Loko	04/01/2015	Blood	Port Loko	Marampa	Negative	Negative	16	Original
SL-011	PL000236	Port Loko	13/12/2014	Blood	Port Loko	Dibia	Negative	Negative	65	Original
SL-012	PL000298	Port Loko	13/12/2014	Blood	Port Loko	Lokomasama	Negative	Negative	35	Original
SL-013	PL000317	Port Loko	13/12/2014	Blood	Port Loko	Kaffu Bullom	Negative	Negative	28	Original
SL-014	PL000320	Port Loko	13/12/2014	Blood	Port Loko	Lokomasama	Negative	Negative	17	Original
SL-015	PL000055	Port Loko	07/12/2014	Blood	Port Loko	Kaffu Bullom	Negative	n/a	21	Original
SL-016	PL000076	Port Loko	08/12/2014	Blood	Kambia	Magbema	Negative	n/a	3	Original
SL-017	PL005543	Port Loko	29/03/2015	Blood	Kambia	Magbema	Negative	Negative	28	Original
SL-018	PL005466	Port Loko	28/03/2015	Blood	Kambia	Samu	Negative	Negative	15	Original
SL-019	PL005454	Port Loko	27/03/2015	Blood	Port Loko	nd	Negative	Negative	60	Original
SL-020	PL005453	Port Loko	27/03/2015	Blood	Port Loko	Maforki	Negative	Negative	25	Original
SL-021	PL005468	Port Loko	28/03/2015	Blood	Port Loko	Maforki	Negative	Negative	40	Original
SL-022	PL005471	Port Loko	28/03/2015	Blood	Port Loko	Lokomasam	Negative	Negative	45	Original
SL-023	PL005509	Port Loko	28/03/2015	Blood	Kambia	Tonko Limba	Negative	Negative	40	Original

SL-024	PL005532	Port Loko	29/03/2015	Blood	Port Loko	Tms	Negative	Negative	38	Original
SL-025	PL005595	Port Loko	30/03/2015	Blood	Port Loko	Marampa	Negative	Negative	25	Follow-up
SL-026	PL001205	Port Loko	02/01/2015	Blood	nd	nd	Negative	Positive	59	Original
SL-027	PL001204	Port Loko	02/01/2015	Blood	nd	nd	Negative	Positive	60	Original
SL-028	PL001202	Port Loko	02/01/2015	Blood	nd	nd	Negative	Positive	nd	Original
SL-029	PL004836	Port Loko	15/03/2015	Blood	Kambia	Magbema	Negative	Negative	75	Original
SL-030	PL004871	Port Loko	16/03/2015	Blood	Kambia	Magbema	Negative	Negative	40	Original
SL-031	PL004868	Port Loko	16/03/2015	Blood	Kambia	Magbema	Negative	Negative	4	Original
SL-032	PL004916	Port Loko	17/03/2015	Blood	Kambia	nd	Negative	Positive	29	Follow-up
SL-033	PL004853	Port Loko	16/03/2015	Blood	Port Loko	Maforki	Negative	Negative	38	Follow-up
SL-034	PL004840	Port Loko	16/03/2015	Blood	Port Loko	Kaffu Bullom	Negative	Negative	72	Follow-up
SL-035	PL004901	Port Loko	17/03/2015	Blood	Kambia	Magbema	Negative	Positive	28	Original
SL-036	PL004914	Port Loko	17/03/2015	Blood	Kambia	Tonko Limba	Negative	Negative	48	Original
SL-037	PL004838	Port Loko	15/03/2015	Blood	Kambia	Masungbala	Negative	Negative	28	Original

SL-038	PL004962	Port Loko	19/03/2015	Blood	Kambia	Gbinle-Dixing	Negative	Negative	45	Original
SL-039	PL004961	Port Loko	19/03/2015	Blood	Kambia	Masungbala	Negative	Negative	19	Original
SL-040	PL000867	Port Loko	25/12/2014	Blood	Port Loko	Maforki	Negative	n/a	35	Follow-up
SL-041	KT004988	Kerry Town	13/02/2015	Blood	nd	nd	Negative	Negative	20	Original
SL-042	KT004945	Kerry Town	12/02/2015	Blood	nd	nd	Negative	Negative	25	Original
SL-043	KT001763	Kerry Town	26/11/2014	Blood	WA	nd	Negative	n/a	56	Original
SL-044	KT001760	Kerry Town	26/11/2014	Blood	WA	nd	Negative	n/a	19	Original
SL-045	KT003310	Kerry Town	26/12/2014	Blood	nd	K/ARD 346	Negative	Negative	63	Original
SL-046	KT003381	Kerry Town	26/12/2014	Blood	Western Area Urb	nd	Negative	Negative	50	Original
SL-047	KT003702	Kerry Town	01/01/2015	Blood	Western Area Urb	nd	Negative	Negative	nd	Original
SL-048	KT003745	Kerry Town	02/01/2015	Blood	Western Area Rur	nd	Negative	Negative	45	Original
SL-049	KT003771	Kerry Town	03/01/2015	Blood	Western Area Rur	nd	Negative	Negative	40	Original

SL-050	KT003774	Kerry Town	03/01/2015	Blood	Western Area Urb	nd	Negative	Negative	18	Original
SL-051	KT003749	Kerry Town	03/01/2015	Blood	nd	369	Negative	n/a	25	Original
SL-052	KT003114	Kerry Town	22/12/2014	Blood	Western Area Urb	nd	Negative	Negative	24	Original
SL-053	KT003118	Kerry Town	22/12/2014	Blood	Western Area Urb	nd	Negative	Negative	36	Original
SL-054	KT005148	Kerry Town	19/02/2015	Blood	nd	nd	Negative	n/a	40	Follow-up
SL-055	KT005189	Kerry Town	20/02/2015	Blood	nd	nd	Negative	Negative	23	Original
SL-056	KT005165	Kerry Town	19/02/2015	Blood	nd	nd	Negative	Negative	24	Original
SL-057	KT005227	Kerry Town	21/02/2015	Blood	Western Area Rur	Waterloo - Waterloo Village A	Negative	Positive	25	Original
SL-058	KT005228	Kerry Town	21/02/2015	Blood	Western Area Urb	Urban	Negative	Negative	70	Original
SL-059	KT005231	Kerry Town	21/02/2015	Blood	nd	nd	Negative	Positive	47	Original
SL-060	KT005244	Kerry Town	22/02/2015	Blood	nd	nd	Negative	Negative	73	Original
SL-061	KT005239	Kerry Town	22/02/2015	Blood	nd	nd	Negative	n/a	28	Follow-up

SL-062	KT005732	Kerry Town	06/03/2015	Blood	Western Area Rur	nd	Negative	Negative	46	Original
SL-063	KT003555	Kerry Town	29/12/2014	Blood	Western Area Urb	nd	Negative	n/a	16	Original
SL-064	KT003592	Kerry Town	29/12/2014	Blood	Western Area Urb	nd	Negative	n/a	35	Original
SL-065	KT003593	Kerry Town	30/12/2014	Blood	Western Area Urb	nd	Negative	Negative	52	Original
SL-066	KT003635	Kerry Town	01/01/2015	Blood	nd	nd	Negative	n/a	53	Original
SL-067	KT003645	Kerry Town	31/12/2014	Blood	Western Area Urb	nd	Negative	n/a	29	Original
SL-068	KT004000	Kerry Town	11/01/2015	Blood	ODCH 2500 Holding Centre	nd	Negative	Positive	8	Original
SL-069	KT004048	Kerry Town	12/01/2015	Blood	Western Area Urb	Freetown	Negative	Negative	4	Original
SL-070	KT004019	Kerry Town	11/01/2015	Blood	Western Area Urb	nd	Negative	Negative	38	Original
SL-071	KT003877	Kerry Town	06/01/2015	Blood	Western Area Rur	nd	Negative	Negative	38	Original

SL-072	KT003889	Kerry Town	07/01/2015	Unknown swab	Western Area Rur	nd	Negative	n/a	3	Original
SL-073	KT003899	Kerry Town	07/01/2015	Blood	Western Area Urb	nd	Negative	n/a	40	Original
SL-074	KT004305	Kerry Town	20/01/2015	Blood	Western Area Urb	nd	Negative	Negative	32	Original
SL-075	KT004308	Kerry Town	20/01/2015	Blood	Western Area Urb	nd	Negative	Positive	19	Repeat
SL-076	KT004310	Kerry Town	20/01/2015	Blood	Western Area Urb	nd	Negative	Positive	16	Original
SL-077	KT006024	Kerry Town	19/03/2015	Blood	Western Area Urb	nd	Negative	n/a	48	Follow-up
SL-078	KT006068	Kerry Town	21/03/2015	Blood	Western Area Rur	nd	Negative	Negative	42	Original
SL-079	KT006071	Kerry Town	21/03/2015	Blood	Western Area Urb	nd	Negative	n/a	15	Follow-up
SL-080	KT005287	Kerry Town	23/02/2015	Blood	Western Area Rur	Waterloo	Negative	Negative	25	Original
SL-081	MK000727	Makeni	01/01/2015	Blood	nd	nd	Negative	Negative	nd	Original

SL-082	MK000730	Makeni	01/01/2015	Blood	Bombali	Gbanti Kamaranka	Negative	Negative	21	Original
SL-083	MK000712	Makeni	31/12/2014	Blood	Bombali	Bombali Sebora	Negative	Negative	30	Original
SL-084	MK000722	Makeni	01/01/2015	Blood	nd	nd	Negative	Negative	75	Follow-up
SL-085	MK000659	Makeni	30/12/2014	Blood	Bombali	Paki Masabong	Negative	Negative	31	Original
SL-086	MK000717	Makeni	31/12/2014	Blood	Bombali	Makari Gbanti	Negative	Negative	25	Original
SL-087	MK000683	Makeni	31/12/2014	Blood	nd	nd	Negative	Negative	60	Original
SL-088	MK000724	Makeni	01/01/2015	Blood	Port Loko	Kaffu Bullom	Negative	Negative	29	Original
SL-089	MK000720	Makeni	01/01/2015	Blood	Port Loko	Kaffu Bullom	Negative	Negative	8	Original
SL-090	MK000721	Makeni	01/01/2015	Blood	Port Loko	Koya	Negative	Negative	30	Original
SL-091	MK000176	Makeni	15/12/2014	Blood	Bombali	Makari Gbanti	Negative	Negative	17	Original
SL-092	MK000169	Makeni	15/12/2014	Blood	Bombali	Bombali Sebora	Negative	Negative	60	Original

SL-093	MK000173	Makeni	15/12/2014	Blood	Bombali	Bombali Sebora	Negative	Negative	17	Original
SL-094	MK000164	Makeni	15/12/2014	Blood	Bombali	Makari Gbanti	Negative	Negative	9	Original
SL-095	MK000174	Makeni	15/12/2014	Blood	Bombali	Makari Gbanti	Negative	Negative	44	Original
SL-096	MK000227	Makeni	16/12/2014	Blood	Bombali	Bombali Sebora	Negative	Negative	17	Original
SL-097	MK000225	Makeni	16/12/2014	Blood	Bombali	Sanda Loko	Negative	Negative	38	Original
SL-098	MK001870	Makeni	08/02/2015	Blood	nd	nd	Negative	Negative	70	Original
SL-099	MK001844	Makeni	07/02/2015	Blood	nd	nd	Negative	Negative	18	Original
SL-100	MK001879	Makeni	08/02/2015	Blood	Bombali	Paki Masabong	Negative	Negative	9	Original
SL-101	MK000863	Makeni	05/01/2015	Blood	nd	nd	Negative	Negative	23	Follow-up
SL-102	MK000862	Makeni	05/01/2015	Blood	nd	nd	Negative	Negative	65	Follow-up
SL-103	MK000992	Makeni	10/01/2015	Blood	nd	nd	Negative	Negative	30	Original
SL-104	MK000999	Makeni	10/01/2015	Blood	Bombali	Bombali Sebora	Negative	Negative	28	Original

SL-105	MK000968	Makeni	09/01/2015	Blood	nd	nd	Negative	Negative	56	Follow-up
SL-106	MK002142	Makeni	17/02/2015	Blood	Bombali	Paki Masabong	Negative	Positive	7	Original
SL-107	MK002052	Makeni	15/02/2015	Blood	nd	nd	Negative	n/a	20	Follow-up
SL-108	MK002064	Makeni	14/02/2015	Blood	Bombali	Paki Masabong	Negative	Positive	60	Original
SL-109	MK002137	Makeni	17/02/2015	Blood	Bombali	Gbanti-Kamarank	Negative	Negative	13	Original
SL-110	MK001420	Makeni	24/01/2015	Blood	Bombali	Bombali Sebora	Negative	Negative	39	Original
SL-111	MK001124	Makeni	14/01/2015	Blood	nd	nd	Negative	n/a	43	Follow-up
SL-112	MK001125	Makeni	14/01/2015	Blood	nd	nd	Negative	n/a	15	Follow-up
SL-113	MK001152	Makeni	15/01/2015	Blood	Bombali	Bombali Sebora	Negative	Negative	50	Original
SL-114	MK003121	Makeni	16/03/2015	Blood	Port Loko	Koya	Negative	n/a	52	Follow-up
SL-115	MK005603	Makeni	24/05/2015	Blood	Bombali	Bombali Sebora	Negative	Negative	32	Follow-up
SL-116	MK005604	Makeni	24/05/2015	Blood	Bombali	nd	Negative	Negative	30	Original

SL-117	MK005609	Makeni	23/05/2015	Blood	Tonkolili	Yoni	Negative	Negative	20	Original
SL-118	MK005610	Makeni	24/05/2015	Blood	Tonkolili	Gbonkolenken	Negative	Negative	1	Original
SL-119	MK005431	Makeni	20/05/2015	Blood	Tonkolili	Gbonkolenken	Negative	Positive	5 months	Original
SL-120	MK005432	Makeni	20/05/2015	Blood	Tonkolili	Gbonkolenken	Negative	Positive	10 months	Original

APPENDIX 2: ECUADORIAN PLASMA SAMPLE METADATA, 2016

Sex: M = male, F = female. Blank cells represent data that was not available.

Sample ID	Location	Date	Sex	Age	Fever	Days of fever	Headache	Joint pain	Muscle pain	Nausea	Previous ZIKV qPCR Cq (USFQ)
D-001	SECTOR centro	02/03/2016	F	3	Yes	3	Yes	No	No	No	No Cq
D-002	las palmas	02/03/2016	M	62	Yes	4	Yes	Yes	No	No	No Cq
D-003					Yes						No Cq
D-004	Catalago	10/02/2016	F	8	Yes		Yes	No	No	No	No Cq
D-005		22/01/2016	M	36	Yes		Yes	Yes	Yes	No	No Cq
D-006	Atacames	26/01/2016	M	29	Yes		Yes	Yes	Yes	Yes	No Cq
D-007		12/02/2016	M	36	Yes		Yes	Yes	Yes	No	No Cq
D-008	CS#2	26/01/2016	F	77	Yes		Yes	No	No	No	No Cq
D-009		01/03/2016	M		Yes						No Cq
D-010		29/02/2016	M	35	Yes		Yes	Yes	Yes	Yes	No Cq

D-011		29/02/2016	M		Yes		Yes	Yes	No	No	No Cq
D-012		03/03/2016	M	14	Yes	6	No	No	No	No	No Cq
D-013	Manabí	03/03/2016	M	17	Yes	5	No	No	No	No	No Cq
D-014	parada 12	03/03/2016	M	5	Yes	4	Yes	No	No	No	No Cq
D-015	Olmedo y Espejo	03/03/2016	M	9	Yes	6	Yes	No	No	No	No Cq
D-016	CS#2	03/03/2016	M	40	Yes	7	No	No	No	No	No Cq
D-017	Es	03/03/2016	M	14	Yes	3	No	No	No	No	No Cq
D-018	CS#2	20/02/2016	M	8	Yes	3	Yes	Yes	Yes	No	No Cq
D-019	CS#2	20/02/2016	M	11 months	Yes	8	Yes	Yes	Yes	No	No Cq
D-020	CS Santa	02/03/2016	F	48	Yes		Yes	Yes	Yes	No	No Cq
D-021	Eg	08/03/2016	F	46	Yes						No Cq
D-022	Eg	15/03/2016	F	66	Yes	7	Yes				No Cq
D-023	CS#1	25/02/2016	M	54	Yes		Yes	Yes	Yes		No Cq
D-025	IESS	14/03/2015	F	42	Yes	7	Yes	Yes	Yes		No Cq

D-026	C.Ext	17/03/2016	F	25	Yes		Yes				No Cq
D-027	Eg	19/03/2016	M	29	Yes	8	Yes	Yes	Yes		No Cq
D-028	IESS	21/03/2016	F	2	Yes	7	Yes	Yes			No Cq
D-029	Eg	28/03/2016	M	54	Yes	7	Yes	Yes	Yes	Yes	No Cq
D-030	C.ext	29/03/2016	M	45	Yes	3	Yes				No Cq
D-031	CS1	31/03/2016	F	20	Yes	7	Yes	Yes	Yes		No Cq
D-032	&	31/03/2016	F	44	Yes	6	Yes	Yes	Yes		No Cq
D-033	Cattelago	31/03/2016	F	16	Yes	6	Yes	Yes			No Cq
D-034	C.ext	31/03/2016	M	32	Yes	7	Yes	Yes			No Cq
D-035	C.ext	01/04/2016	M	64	Yes	6	Yes	Yes	Yes		No Cq
D-036	C.Ext	01/04/2016	M	48	Yes	8	Yes	Yes	Yes		No Cq
D-037	C.ext	01/04/2016	M	23	Yes		Yes				No Cq
D-038	CS1	01/04/2016	F	34	Yes	6	Yes	Yes			No Cq
D-039	CS tipo C	01/04/2016	F	50	Yes	8	Yes	Yes	Yes	Yes	No Cq

D-040	C. ext	04/04/2016	F	50	Yes	6	Yes	Yes	Yes	Yes	No Cq
D-041	C.ext	04/04/2016	F	32	Yes	32					No Cq
D-042	Muisne	04/04/2016	F	7	Yes	7					No Cq
D-043	Cs San rafael	05/04/2016	M	47	Yes	7					No Cq
D-044	C.ext CS 2	05/04/2016	F	22	Yes	8	Yes	Yes	Yes	Yes	No Cq
D-045	CS 1	05/04/2016	F	21	Yes	6	Yes	Yes			No Cq
D-047	C.ext		F	63	Yes	6	Yes	Yes	Yes		No Cq
D-048	Hospital		F	28	Yes	7	Yes	Yes			No Cq
D-049	CS1	07/04/2016	F	9	Yes	6	Yes	Yes			No Cq
D-050	Cottolego		F	72	Yes	6	Yes	Yes			No Cq
D-051	Santa Vans	08/04/2016	F	68	Yes	6	Yes	Yes			31.14
D-052	CS1	08/04/2016	M	21	Yes	5	Yes	Yes	Yes		No Cq
D-053	Cottolego		M	24	Yes	6	Yes	Yes			No Cq
D-054	RV		M	24	Yes	6	Yes	Yes			No Cq

D-055	RV		F	48	Yes	6	Yes	Yes			No Cq
D-057		13/04/2016	M	35	Yes	3	Yes	Yes	Yes		No Cq
D-058	C.ext	11/04/2016	M	2	Yes	7	Yes	Yes			No Cq
D-059	C.ext	11/04/2016	M				Yes	Yes	Yes	Yes	No Cq
D-060	C.ext	11/04/2016	M	66	Yes	6	Yes	Yes	Yes	Yes	25.21
D-061	C.ext	12/04/2016	M	45							No Cq
D-062	C.ext	12/04/2016	M	27		2	Yes	Yes			24.17
D-064	Cottolego	12/04/2016	F	23	Yes	5	Yes	Yes	Yes		No Cq
D-065	Cottolego		F	21	Yes	6	Yes	Yes	Yes		No Cq
D-066	C.ext	13/04/2016	F	43	Yes	7	Yes	Yes	Yes	Yes	No Cq
D-067	C.ext		F	35	Yes	6	Yes	Yes	Yes	Yes	No Cq
D-068	IESS		F	34	Yes	5	Yes	Yes	Yes	Yes	No Cq
D-069	C.ext		M	48	Yes	5	Yes	Yes	Yes	Yes	No Cq
D-070	Los Almendros	13/04/2016	M	34	Yes	6	Yes	Yes	Yes	Yes	No Cq

D-071	Eg	14/04/2016	F	21	Yes	7	Yes	Yes	Yes		34.74
D-072	CS1		F	41	Yes	6	Yes	Yes			No Cq
D-073	Los Almendros		F	32	Yes	6	Yes	Yes	Yes		No Cq
D-074	C.ext		F	14	Yes	7	Yes	Yes	Yes		No Cq
D-075	Eg		M	19	Yes	5	Yes	Yes	Yes	Yes	No Cq
D-076	CS1	15/04/2016	M	50	Yes	6	Yes	Yes			No Cq
D-077	HTDC		F	46	Yes	3	Yes	Yes			No Cq
D-078	HDTC		M	35	Yes	7	Yes	Yes	Yes	Yes	No Cq
D-079	HDTC		F	57	Yes	6	Yes	Yes	Yes	Yes	No Cq
D-080	HDTC		F	44	Yes	6	Yes	Yes			No Cq
D-081	Almendros		M	10	Yes	6	Yes	Yes			No Cq
D-082	Almendros		M	7	Yes	7	Yes	Yes			No Cq
D-083	Almendros		F	32	Yes	5	Yes	Yes			No Cq
D-084	Almendros		F	9	Yes	6	Yes	Yes			No Cq

D-085	HosNAE	16/04/2016	F	13	Yes	6	Yes				No Cq
D-086	C.ext	19/04/2016	M	18	Yes	6	Yes	Yes			No Cq
D-087	ISPOL		M	41	Yes	7	Yes	Yes	Yes	Yes	No Cq
D-088	CS1		M	52	Yes	6	Yes	Yes			No Cq
D-090	C.ext		F	37	Yes	6	Yes	Yes			No Cq
D-091	CS2	21/04/2016	F	37	Yes	4	Yes				No Cq
D-092	Cs2		F	10	Yes	5					No Cq
D-093	CS2		F	54	Yes	6					34.79
D-094	Hospital		M	57	Yes		Yes				No Cq
D-095	C.ext	22/04/2016	F	23	Yes	5					No Cq
D-096	CS2	22/04/2016	F	56	Yes	6					No Cq
D-097	San Pablo		F	22	Yes	5					No Cq
D-098	Arenal		F	20	Yes	6					No Cq
D-099	CS1		M	80	Yes	6					No Cq

D-100	San Pablo		F	25	Yes	5					No Cq
D-101	CS2		F	24	Yes	6	Yes				No Cq
D-102	San Pablo		F	6	Yes	6					37.07
D-103		26/04/2016	F		Yes	3					No Cq
D-104			F		Yes	8					No Cq
D-105			F		Yes	4					No Cq
D-106			F		Yes	4					No Cq
D-107			F		Yes	3					No Cq
D-108			M								No Cq
D-109			F		Yes	6					No Cq
D-110			F		Yes	4					36.39
D-111			F		Yes	4					36.36
D-112		27/04/2016	F		Yes	4					No Cq
D-113			F		Yes	3					32.39

D-114		28/04/2016	F		Yes	2					31.49
D-118		29/04/2016	F		Yes	3					No Cq
D-119			F		Yes	4					No Cq
D-121			F		Yes	3					27.63
D-122		04/05/2016	M		Yes	4					No Cq
D-123			F		Yes	4					No Cq
D-124			F		Yes	4					36.12
D-125			F		Yes	3					No Cq
D-126			F		Yes	2					29.08
D-127			F		Yes	3					No Cq
D-128			F		Yes	3					No Cq
D-129			F		Yes	5					No Cq
D-130			M								No Cq
D-131			F		Yes	4					No Cq

D-132			M								No Cq
D-133			M								No Cq
D-134			F								No Cq
D-135			F								33.37
D-136			F								No Cq
D-137			F								No Cq
D-138			F								No Cq
D-139			M								No Cq
D-140			F								32.4
D-141			M		Yes	3					33.11
D-142			M		Yes	4					No Cq
D-143			F		Yes	2					No Cq
D-144			F		Yes	3					No Cq
D-145			F		Yes	8					No Cq

D-146			M		Yes	4					34.48
D-147			F		Yes	2					No Cq
D-148			M		Yes	1					No Cq
D-149			F		Yes	1					31.98
D-150											No Cq
D-151			F		Yes	5					No Cq
D-152			M		Yes	4					No Cq
D-153			F		Yes	4					No Cq
D-154											No Cq
D-155			M		Yes	2					No Cq
D-156			M		Yes	3					No Cq
D-157			F		Yes	8					No Cq
D-158			F		Yes	6					No Cq
D-159			F		Yes	3					No Cq

D-160			M		Yes	3					No Cq
D-161			M		Yes	8					No Cq
D-162			F		Yes	3					No Cq
D-164			M		Yes	3					No Cq
D-166			F		Yes	5					No Cq
D-167			F		Yes	6					No Cq
D-168			F		Yes	3					No Cq
D-170			F		Yes	2					No Cq
D-171			F		Yes	2					No Cq
D-172			M		Yes	3					35.49
D-173			F		Yes	4					No Cq
D-174			M		Yes	6					No Cq
D-175			F		Yes	3					No Cq
D-176			F		Yes	4					32.37

D-177			M		Yes	3					No Cq
D-181			F		Yes	3					No Cq
D-182			F		Yes	4					No Cq
D-183			F		Yes	3					No Cq
D-184			F		Yes	3					No Cq
D-185			F		Yes	4					No Cq
D-186			M		Yes	4					No Cq
D-187			F		Yes	3					No Cq
D-189			M		Yes	3					No Cq
D-190			F		Yes	4					No Cq
D-191			F		Yes	2					No Cq
D-192			F		Yes	2					No Cq
D-193			F		Yes	6					No Cq
D-194			F		Yes	2					37.72

D-195			F		Yes	5					No Cq
D-196			F		Yes	4					No Cq
D-197			M		Yes	4					No Cq
D-198			F		Yes	3					No Cq
D-199			F		Yes	2					No Cq
D-200			M		Yes	2					No Cq
D-201			F		Yes	3					No Cq
D-202			F		Yes	3					No Cq
D-203			F		Yes	2					No Cq
D-204			F		Yes	3					No Cq
D-205			F		Yes	2					No Cq
D-206			M		Yes	4					No Cq
D-207			M		Yes	3					No Cq
D-208			F		Yes	3					No Cq

D-209			F		Yes	4					No Cq
D-210			M		Yes	3					No Cq
D-212			F		Yes	3					No Cq
D-213			M		Yes	5					No Cq

APPENDIX 3: ECUADORIAN PLASMA SAMPLE METADATA, 2017

Sex: M = male, F = female. Blank cells represent data that was not available.

Sample ID	Location	Date	Sex	Age	Fever	Days fever	Headache	Joint pain	Muscle pain	Nausea	Previous ZIKV qPCR (USFQ)
D214	Rioverde	17/03/2017	F	18	Yes	5					
D215	Borbon	02/04/2017	M	3	Yes	3					
D216	Rioverde/Palestina		M	3	Yes	5					
D217			M	64	Yes	5					
D218		18/04/2017	M	13							
D219		19/04/2017	F	55							
D220		23/05/2017		RN							
D221	HOSP	06/06/2017	M	22							
D222	CHAMNAGA-BORBON	08/06/2017	F	17	Yes	5					
D223	UCI	12/06/2017	F	25							

D224	HOSP	13/06/2017	F	62							
D225	LAS PALMAS	19/06/2017	F	23	Yes	5					
D226	HOSP	20/06/2017	F	75							
D227	QUITO	20/06/2017	F	60	Yes	4					
D228	QUNINDE	22/06/2017	M	17							
D229	QUININDE	22/06/2017	F	32	Yes	2					
D230	QUINIDE	22/06/2017	F	1							
D231	EMERG	25/06/2017	M	63							
D232	NUEVA ESPERANZA	27/06/2017	M	22	Yes	9					
D233	QUINIDE	27/06/2017	M	1	Yes	4					
D234	TOLITA 1	29/09/2017	F	21	Yes	9					
D235	LAGARTO-RIOVERDE	30/09/2017	F	53	Yes	3					
D236	QUNINDE	06/07/2017	F	23							
D237	CHONTADURO	06/07/2017	F	34	Yes	5					

D238	RIOVERDE	06/07/2017	M	4 months	Yes	3					
D239	ATACAMES	06/07/2017	M	20							
D240	ATACAMES	06/07/2017		50							
D241	SAN LORENZO	06/07/2017	F	36	Yes	5					
D242	BORBON	06/07/2017	M	4 months	Yes	10					
D243	MANABI	06/07/2017	M	29	Yes	6					
D244	QUINIDE	07/07/2017	M	20	Yes	4					
D245	MEJIA Y MALECON	10/07/2017	M	2	Yes	2					
D246	RIOVERDE	10/07/2017	M	4 months							
D247	LAS PALMAS	14/07/2017	M	8							
D248	SAN RAFAEL	14/07/2017	M	10							
D249	LAS PALMAS	14/07/2017	M	13							
D250	LAS PALMAS	14/07/2017	F	4							
D251											

D252											
D253											
D254											
D255											
D256											
D257											
D258											
D259											
D260											
D261											
D262											
D263											
D264											
D265											

D266											
D267											
D268											
D269											
D270											
D271											
D272											
D273											
D274											
D275											

APPENDIX 4: SIERRA LEONEAN FEBRILE PATIENT SAMPLE RT-PCR/PCR RESULTS

n=120. Green = Cq value <35.0, orange = Cq value 35.0 – 39.9, blue = testing performed in-country prior to this study. Samples that underwent metagenomic sequencing are indicated.

Sample ID	*Plasmodium* RDT (in-country)	*Plasmodium*	LASV	Pan-EBOV	Zaire EBOV	DENV 1-3	DENV 4	CHIKV	YFV	ZIKV	RVFV	CCHFV	*Leptospira*	*Rickettsia*	MS2 control	Metagenomics performed
SL-001	Neg	Neg	Neg	No Ct	No Ct	No Ct	No Ct	No Ct	No Ct	No Ct	No Ct	No Ct	No Ct	No Ct	30.11	
SL-002	Neg	Neg	Neg	No Ct	No Ct	No Ct	No Ct	No Ct	No Ct	No Ct	No Ct	No Ct	No Ct	No Ct	29.76	
SL-003	Pos	Neg	Neg	No Ct	No Ct	No Ct	No Ct	No Ct	No Ct	No Ct	No Ct	No Ct	No Ct	No Ct	30.78	
SL-004	Neg	Neg	Neg	No Ct	No Ct	No Ct	No Ct	No Ct	No Ct	No Ct	No Ct	No Ct	No Ct	No Ct	29.48	
SL-005	Pos	Weak pos	Neg	No Ct	34.02	No Ct	No Ct	No Ct	No Ct	No Ct	No Ct	No Ct	No Ct	No Ct	29.24	
SL-006	Neg	Neg	Neg	No Ct	36.04	No Ct	No Ct	No Ct	No Ct	No Ct	No Ct	No Ct	No Ct	No Ct	30.2	
SL-007	Neg	Neg	Neg	No Ct	No Ct	No Ct	No Ct	No Ct	No Ct	No Ct	No Ct	No Ct	No Ct	No Ct	30.33	Yes

SL-008	Neg	Neg	Neg	No Ct	No Ct	No Ct	No Ct	No Ct	No Ct	No Ct	No Ct	No Ct	No Ct	No Ct	30.46	
SL-009	Neg	Neg	Neg	No Ct	No Ct	No Ct	No Ct	No Ct	No Ct	No Ct	No Ct	No Ct	No Ct	No Ct	29.99	Yes
SL-010	Neg	Pos	Neg	No Ct	35.99	No Ct	No Ct	No Ct	No Ct	No Ct	No Ct	No Ct	No Ct	No Ct	31.31	
SL-011	Neg	Neg	Neg	No Ct	No Ct	No Ct	No Ct	No Ct	No Ct	No Ct	No Ct	No Ct	No Ct	No Ct	31.11	
SL-012	Neg	Neg	Neg	No Ct	No Ct	No Ct	No Ct	No Ct	No Ct	No Ct	No Ct	No Ct	No Ct	No Ct	31.14	
SL-013	Neg	Neg	Neg	No Ct	No Ct	No Ct	No Ct	No Ct	No Ct	No Ct	No Ct	No Ct	No Ct	No Ct	30.73	Yes
SL-014	Neg	Neg	Neg	No Ct	No Ct	No Ct	No Ct	No Ct	No Ct	No Ct	No Ct	No Ct	No Ct	No Ct	30.7	Yes
SL-015	n/a	Pos	Neg	No Ct	No Ct	No Ct	No Ct	No Ct	No Ct	No Ct	No Ct	No Ct	No Ct	No Ct	29.87	
SL-016	n/a	Pos	Neg	No Ct	No Ct	No Ct	No Ct	No Ct	No Ct	No Ct	No Ct	No Ct	No Ct	No Ct	29.87	
SL-017	Neg	Neg	Neg	No Ct	No Ct	No Ct	No Ct	No Ct	No Ct	No Ct	No Ct	No Ct	No Ct	No Ct	29.84	Yes
SL-018	Neg	Neg	Neg	No Ct	No Ct	No Ct	No Ct	No Ct	No Ct	No Ct	No Ct	No Ct	No Ct	No Ct	30.01	Yes
SL-019	Neg	Neg	Neg	No Ct	No Ct	No Ct	No Ct	No Ct	No Ct	No Ct	No Ct	No Ct	No Ct	No Ct	30.21	
SL-020	Neg	Neg	Neg	No Ct	No Ct	No Ct	No Ct	No Ct	No Ct	No Ct	No Ct	No Ct	No Ct	No Ct	30.07	
SL-021	Neg	Neg	Neg	No Ct	No Ct	No Ct	No Ct	No Ct	No Ct	No Ct	No Ct	No Ct	No Ct	No Ct	30.81	

SL-022	Neg	Neg	Neg	No Ct	No Ct	No Ct	No Ct	No Ct	No Ct	No Ct	No Ct	No Ct	36.3	No Ct	30.22	
SL-023	Neg	Neg	Neg	No Ct	No Ct	No Ct	No Ct	No Ct	No Ct	No Ct	No Ct	No Ct	No Ct	No Ct	31.17	Yes
SL-024	Neg	Neg	Neg	No Ct	No Ct	No Ct	No Ct	No Ct	No Ct	No Ct	No Ct	No Ct	No Ct	No Ct	30.75	Yes
SL-025	Neg	Neg	Neg	No Ct	No Ct	No Ct	No Ct	No Ct	No Ct	No Ct	No Ct	No Ct	No Ct	No Ct	30.19	
SL-026	Pos	Neg	Neg	No Ct	No Ct	No Ct	No Ct	No Ct	No Ct	No Ct	No Ct	No Ct	No Ct	No Ct	32.32	
SL-027	Pos	Neg	Neg	No Ct	No Ct	No Ct	No Ct	No Ct	No Ct	No Ct	No Ct	No Ct	No Ct	No Ct	31.91	
SL-028	Pos	Neg	Neg	No Ct	No Ct	No Ct	No Ct	No Ct	No Ct	No Ct	No Ct	No Ct	No Ct	No Ct	30.81	
SL-029	Neg	Neg	Neg	No Ct	No Ct	No Ct	No Ct	No Ct	No Ct	No Ct	No Ct	No Ct	No Ct	No Ct	31.56	Yes
SL-030	Neg	Neg	Neg	No Ct	No Ct	No Ct	No Ct	No Ct	No Ct	No Ct	No Ct	No Ct	No Ct	No Ct	31.81	
SL-031	Neg	Pos	Neg	No Ct	No Ct	No Ct	No Ct	No Ct	No Ct	No Ct	No Ct	No Ct	No Ct	No Ct	29.87	
SL-032	Pos	Inconclusive	Neg	No Ct	No Ct	No Ct	No Ct	No Ct	No Ct	No Ct	No Ct	No Ct	No Ct	No Ct	30.42	
SL-033	Neg	Neg	Neg	No Ct	No Ct	No Ct	No Ct	No Ct	No Ct	No Ct	No Ct	No Ct	No Ct	No Ct	32.25	
SL-034	Neg	Neg	Neg	No Ct	No Ct	No Ct	No Ct	No Ct	No Ct	No Ct	No Ct	No Ct	No Ct	No Ct	31.73	

SL-035	Pos	Inconclusive	Neg	No Ct	No Ct	No Ct	No Ct	No Ct	No Ct	No Ct	No Ct	No Ct	No Ct	No Ct	30.45	
SL-036	Neg	Neg	Neg	No Ct	No Ct	No Ct	No Ct	No Ct	No Ct	No Ct	No Ct	No Ct	No Ct	No Ct	30.31	
SL-037	Neg	Neg	Neg	No Ct	No Ct	No Ct	No Ct	No Ct	No Ct	No Ct	No Ct	No Ct	No Ct	No Ct	32.3	
SL-038	Neg	Neg	Neg	No Ct	No Ct	No Ct	No Ct	No Ct	No Ct	No Ct	No Ct	No Ct	No Ct	No Ct	30.89	
SL-039	Neg	Neg	Neg	No Ct	No Ct	No Ct	No Ct	No Ct	No Ct	No Ct	No Ct	No Ct	No Ct	No Ct	30.92	
SL-040	n/a	Neg	Neg	33.55	32.24	No Ct	No Ct	No Ct	No Ct	No Ct	No Ct	No Ct	No Ct	No Ct	29.75	
SL-041	Neg	Neg	Neg	No Ct	No Ct	No Ct	No Ct	No Ct	No Ct	No Ct	No Ct	No Ct	No Ct	No Ct	29.22	Yes
SL-042	Neg	Neg	Neg	No Ct	No Ct	No Ct	No Ct	No Ct	No Ct	No Ct	No Ct	No Ct	No Ct	No Ct	29.53	
SL-043	n/a	Neg	Neg	33.16	32.64	No Ct	No Ct	No Ct	No Ct	No Ct	No Ct	No Ct	No Ct	No Ct	29.69	Yes
SL-044	n/a	Neg	Neg	No Ct	No Ct	No Ct	No Ct	No Ct	No Ct	No Ct	No Ct	No Ct	No Ct	No Ct	29.5	Yes
SL-045	Neg	Pos	Neg	No Ct	No Ct	No Ct	No Ct	No Ct	No Ct	No Ct	No Ct	No Ct	No Ct	No Ct	30.58	
SL-046	Neg	Neg	Neg	No Ct	No Ct	No Ct	No Ct	No Ct	No Ct	No Ct	No Ct	No Ct	No Ct	No Ct	30.01	Yes
SL-047	Neg	Pos	Neg	No Ct	No Ct	No Ct	No Ct	No Ct	No Ct	No Ct	No Ct	No Ct	No Ct	No Ct	29.61	
SL-048	Neg	Neg	Neg	No Ct	No Ct	No Ct	No Ct	No Ct	No Ct	No Ct	No Ct	No Ct	No Ct	No Ct	29.75	

SL-049	Neg	Weak pos	Neg	No Ct	No Ct	No Ct	No Ct	No Ct	No Ct	No Ct	No Ct	No Ct	No Ct	No Ct	30.43	
SL-050	Neg	Neg	Neg	No Ct	36.14	No Ct	No Ct	No Ct	No Ct	No Ct	No Ct	No Ct	No Ct	No Ct	30.15	
SL-051	n/a	Neg	Neg	No Ct	35.96	No Ct	No Ct	No Ct	No Ct	No Ct	No Ct	No Ct	No Ct	No Ct	30.69	
SL-052	Neg	Weak pos	Neg	No Ct	No Ct	No Ct	No Ct	No Ct	No Ct	No Ct	No Ct	No Ct	No Ct	No Ct	29.61	
SL-053	Neg	Neg	Neg	34.43	34.01	No Ct	No Ct	No Ct	No Ct	No Ct	No Ct	No Ct	No Ct	No Ct	29.61	
SL-054	n/a	Neg	Neg	No Ct	No Ct	No Ct	No Ct	No Ct	No Ct	No Ct	No Ct	No Ct	No Ct	No Ct	31.47	
SL-055	Neg	Neg	Neg	No Ct	35.93	No Ct	No Ct	No Ct	No Ct	No Ct	No Ct	No Ct	No Ct	No Ct	30.53	
SL-056	Neg	Neg	Neg	No Ct	No Ct	No Ct	No Ct	No Ct	No Ct	No Ct	No Ct	No Ct	No Ct	No Ct	33.89	
SL-057	Pos	Pos	Neg	No Ct	No Ct	No Ct	No Ct	No Ct	No Ct	No Ct	No Ct	No Ct	No Ct	No Ct	30.95	
SL-058	Neg	Neg	Neg	No Ct	No Ct	No Ct	No Ct	No Ct	No Ct	No Ct	No Ct	No Ct	No Ct	No Ct	32.62	Yes
SL-059	Pos	Pos	Neg	No Ct	No Ct	No Ct	No Ct	No Ct	No Ct	No Ct	No Ct	No Ct	No Ct	No Ct	31.36	
SL-060	Neg	Neg	Neg	No Ct	No Ct	No Ct	No Ct	No Ct	No Ct	No Ct	No Ct	No Ct	No Ct	No Ct	31.06	
SL-061	n/a	Neg	Neg	No Ct	No Ct	No Ct	No Ct	No Ct	No Ct	No Ct	No Ct	No Ct	No Ct	No Ct	31.29	

SL-062	Neg	Neg	Neg	No Ct	No Ct	No Ct	No Ct	No Ct	No Ct	No Ct	No Ct	No Ct	No Ct	No Ct	30.54	
SL-063	n/a	Neg	Neg	No Ct	No Ct	No Ct	No Ct	No Ct	No Ct	No Ct	No Ct	No Ct	No Ct	No Ct	29.68	Yes
SL-064	n/a	Pos	Neg	No Ct	No Ct	No Ct	No Ct	No Ct	No Ct	No Ct	No Ct	No Ct	No Ct	No Ct	29.31	
SL-065	Neg	Neg	Neg	No Ct	No Ct	No Ct	No Ct	No Ct	No Ct	No Ct	No Ct	No Ct	No Ct	No Ct	29.88	Yes
SL-066	n/a	Neg	Neg	No Ct	No Ct	No Ct	No Ct	No Ct	No Ct	No Ct	No Ct	No Ct	No Ct	No Ct	29.7	
SL-067	n/a	Pos	Neg	No Ct	No Ct	No Ct	No Ct	No Ct	No Ct	No Ct	No Ct	No Ct	No Ct	No Ct	29.62	
SL-068	Pos	Pos	Neg	No Ct	No Ct	No Ct	No Ct	No Ct	No Ct	No Ct	No Ct	No Ct	No Ct	No Ct	29.63	
SL-069	Neg	Neg	Neg	No Ct	No Ct	No Ct	No Ct	No Ct	No Ct	No Ct	No Ct	No Ct	No Ct	No Ct	30.92	
SL-070	Neg	Neg	Neg	No Ct	35.82	No Ct	No Ct	No Ct	No Ct	No Ct	No Ct	No Ct	No Ct	No Ct	35.56	
SL-071	Neg	Neg	Neg	No Ct	No Ct	No Ct	No Ct	No Ct	No Ct	No Ct	No Ct	No Ct	No Ct	No Ct	30.05	Yes
SL-072	n/a	Pos	Neg	No Ct	No Ct	No Ct	No Ct	No Ct	No Ct	No Ct	No Ct	No Ct	No Ct	No Ct	29.26	
SL-073	n/a	Neg	Neg	No Ct	No Ct	No Ct	No Ct	No Ct	No Ct	No Ct	No Ct	No Ct	No Ct	No Ct	29.45	Yes
SL-074	Neg	Neg	Neg	No Ct	No Ct	No Ct	No Ct	No Ct	No Ct	No Ct	No Ct	No Ct	No Ct	No Ct	29.66	Yes
SL-075	Pos	Pos	Neg	No Ct	No Ct	No Ct	No Ct	No Ct	No Ct	No Ct	No Ct	No Ct	No Ct	No Ct	29.12	

SL-076	Pos	Pos	Neg	No Ct	36.54	No Ct	No Ct	No Ct	No Ct	No Ct	No Ct	No Ct	No Ct	No Ct	29.44	
SL-077	n/a	Neg	Neg	No Ct	34.83	No Ct	No Ct	No Ct	No Ct	No Ct	No Ct	No Ct	No Ct	No Ct	29.63	
SL-078	Neg	Neg	Neg	No Ct	No Ct	No Ct	No Ct	No Ct	No Ct	No Ct	No Ct	No Ct	No Ct	No Ct	29.61	Yes
SL-079	n/a	Neg	Neg	No Ct	35.34	No Ct	No Ct	No Ct	No Ct	No Ct	No Ct	No Ct	No Ct	No Ct	29.51	
SL-080	Neg	Neg	Neg	No Ct	No Ct	No Ct	No Ct	No Ct	No Ct	No Ct	No Ct	No Ct	No Ct	No Ct	29.74	Yes
SL-081	Neg	Pos	Neg	No Ct	No Ct	No Ct	No Ct	No Ct	No Ct	No Ct	No Ct	No Ct	No Ct	No Ct	28.79	
SL-082	Neg	Neg	Neg	No Ct	No Ct	No Ct	No Ct	No Ct	No Ct	No Ct	No Ct	No Ct	No Ct	No Ct	29.78	Yes
SL-083	Neg	Neg	Neg	No Ct	No Ct	No Ct	No Ct	No Ct	No Ct	No Ct	No Ct	No Ct	No Ct	No Ct	28.71	
SL-084	Neg	Neg	Neg	No Ct	No Ct	No Ct	No Ct	No Ct	No Ct	No Ct	No Ct	No Ct	No Ct	No Ct	29.54	
SL-085	Neg	Neg	Neg	No Ct	No Ct	No Ct	No Ct	No Ct	No Ct	No Ct	No Ct	No Ct	No Ct	No Ct	29.53	
SL-086	Neg	Neg	Neg	No Ct	No Ct	No Ct	No Ct	No Ct	No Ct	No Ct	No Ct	No Ct	No Ct	No Ct	28.66	Yes
SL-087	Neg	Neg	Neg	No Ct	No Ct	No Ct	No Ct	No Ct	No Ct	No Ct	No Ct	No Ct	No Ct	No Ct	29.03	
SL-088	Neg	Neg	Neg	No Ct	No Ct	No Ct	No Ct	No Ct	No Ct	No Ct	No Ct	No Ct	No Ct	No Ct	29.43	
SL-089	Neg	Neg	Neg	No Ct	No Ct	No Ct	No Ct	No Ct	No Ct	No Ct	No Ct	No Ct	No Ct	No Ct	29.54	

SL-090	Neg	Neg	Neg	34.76	33.31	No Ct	No Ct	No Ct	No Ct	No Ct	No Ct	No Ct	No Ct	No Ct	29.3	Yes
SL-091	Neg	Neg	Neg	No Ct	No Ct	No Ct	No Ct	No Ct	No Ct	No Ct	No Ct	No Ct	No Ct	No Ct	28.33	Yes
SL-092	Neg	Neg	Neg	No Ct	No Ct	No Ct	No Ct	No Ct	No Ct	No Ct	No Ct	No Ct	No Ct	No Ct	30.2	
SL-093	Neg	Neg	Neg	No Ct	No Ct	No Ct	No Ct	No Ct	No Ct	No Ct	No Ct	No Ct	No Ct	No Ct	30.18	Yes
SL-094	Neg	Neg	Neg	38.14	33.38	No Ct	No Ct	No Ct	No Ct	No Ct	No Ct	No Ct	No Ct	No Ct	28.19	
SL-095	Neg	Neg	Neg	No Ct	No Ct	No Ct	No Ct	No Ct	No Ct	No Ct	No Ct	No Ct	No Ct	No Ct	28.42	Yes
SL-096	Neg	Neg	Neg	32.21	30.85	No Ct	No Ct	No Ct	No Ct	No Ct	No Ct	No Ct	No Ct	No Ct	28.7	Yes
SL-097	Neg	Neg	Neg	No Ct	No Ct	No Ct	No Ct	No Ct	No Ct	No Ct	No Ct	No Ct	No Ct	No Ct	30.17	Yes
SL-098	Neg	Neg	Neg	No Ct	No Ct	No Ct	No Ct	No Ct	No Ct	No Ct	No Ct	No Ct	No Ct	No Ct	29.75	Yes
SL-099	Neg	Neg	Neg	No Ct	No Ct	No Ct	No Ct	No Ct	No Ct	No Ct	No Ct	No Ct	No Ct	No Ct	29.31	
SL-100	Neg	Pos	Neg	No Ct	No Ct	No Ct	No Ct	No Ct	No Ct	No Ct	No Ct	No Ct	No Ct	No Ct	29.19	
SL-101	Neg	Neg	Neg	No Ct	No Ct	No Ct	No Ct	No Ct	No Ct	No Ct	No Ct	No Ct	No Ct	No Ct	28.24	
SL-102	Neg	Neg	Neg	No Ct	No Ct	No Ct	No Ct	No Ct	No Ct	No Ct	No Ct	No Ct	No Ct	No Ct	27.71	
SL-103	Neg	Neg	Neg	No Ct	No Ct	No Ct	No Ct	No Ct	No Ct	No Ct	No Ct	No Ct	No Ct	No Ct	28.92	

SL-104	Neg	Neg	Neg	No Ct	No Ct	No Ct	No Ct	No Ct	No Ct	No Ct	No Ct	No Ct	No Ct	No Ct	29.72	Yes
SL-105	Neg	Neg	Neg	No Ct	No Ct	No Ct	No Ct	No Ct	No Ct	No Ct	No Ct	No Ct	No Ct	No Ct	31.65	
SL-106	Pos	Pos	Neg	No Ct	No Ct	No Ct	No Ct	No Ct	No Ct	No Ct	No Ct	No Ct	No Ct	No Ct	30.85	
SL-107	n/a	Neg	Neg	No Ct	No Ct	No Ct	No Ct	No Ct	No Ct	No Ct	No Ct	No Ct	No Ct	No Ct	29.43	
SL-108	Pos	Neg	Neg	No Ct	No Ct	No Ct	No Ct	No Ct	No Ct	No Ct	No Ct	No Ct	No Ct	No Ct	30.76	Yes
SL-109	Neg	Neg	Neg	No Ct	No Ct	No Ct	No Ct	No Ct	No Ct	No Ct	No Ct	No Ct	No Ct	No Ct	30.6	
SL-110	Neg	Neg	Neg	No Ct	No Ct	No Ct	No Ct	No Ct	No Ct	No Ct	No Ct	No Ct	No Ct	No Ct	29.1	Yes
SL-111	n/a	Neg	Neg	No Ct	34.81	No Ct	No Ct	No Ct	No Ct	No Ct	No Ct	No Ct	No Ct	No Ct	28.55	
SL-112	n/a	Neg	Neg	No Ct	35.38	No Ct	No Ct	No Ct	No Ct	No Ct	No Ct	No Ct	No Ct	No Ct	28.55	
SL-113	Neg	Neg	Neg	No Ct	No Ct	No Ct	No Ct	No Ct	No Ct	No Ct	No Ct	No Ct	No Ct	No Ct	30.41	Yes
SL-114	n/a	Neg	Neg	No Ct	No Ct	No Ct	No Ct	No Ct	No Ct	No Ct	No Ct	No Ct	No Ct	No Ct	29.53	
SL-115	Neg	Neg	Neg	No Ct	No Ct	No Ct	No Ct	No Ct	No Ct	No Ct	No Ct	No Ct	No Ct	No Ct	28.91	
SL-116	Neg	Neg	Neg	No Ct	No Ct	No Ct	No Ct	No Ct	No Ct	No Ct	No Ct	No Ct	No Ct	No Ct	30.11	Yes
SL-117	Neg	Neg	Neg	No Ct	No Ct	No Ct	No Ct	No Ct	No Ct	No Ct	No Ct	No Ct	No Ct	No Ct	29.22	Yes

SL-118	Neg	Neg	Neg	No Ct	No Ct	No Ct	No Ct	No Ct	No Ct	No Ct	No Ct	No Ct	No Ct	No Ct	29.69	
SL-119	Pos	Pos	Neg	No Ct	No Ct	No Ct	No Ct	No Ct	No Ct	No Ct	No Ct	No Ct	No Ct	No Ct	29.42	
SL-120	Pos	Pos	Neg	No Ct	No Ct	No Ct	No Ct	No Ct	No Ct	No Ct	No Ct	No Ct	No Ct	No Ct	29.79	

APPENDIX 5: *DE NOVO* ASSEMBLED SCAFFOLDS WITH PROTEIN SEQUENCE HOMOLOGY TO HUMAN VIRUSES

Identified from metagenomic sequencing data from Sierra Leonean plasma samples using Kaiju.

Sample ID	Scaffold ID	Scaffold length (bp)	Mean node coverage	Matching accessions	Family	Genus	Species
SL014	1	8949	124.3	NP_043570.1,	Pegivirus	Pegivirus C	GBV-C
SL014	869	342	2.1	NP_043570.1,	Pegivirus	Pegivirus C	GBV-C
SL017	4	2022	30.1	NP_057856.1,	Orthoretrovirinae	Lentivirus	HIV-1
SL017	5	1852	72.7	NP_057849.4,	Orthoretrovirinae	Lentivirus	HIV-1
SL017	37	1111	69.6	NP_057856.1,	Orthoretrovirinae	Lentivirus	HIV-1
SL017	79	907	37.9	NP_057849.4,	Orthoretrovirinae	Lentivirus	HIV-1
SL017	122	808	6.5	NP_057856.1,	Orthoretrovirinae	Lentivirus	HIV-1
SL017	158	741	48.6	NP_057852.2,	Orthoretrovirinae	Lentivirus	HIV-1
SL017	184	698	9.3	NP_057856.1,	Orthoretrovirinae	Lentivirus	HIV-1
SL017	334	554	76.5	NP_057849.4,NP_057850.1,	Orthoretrovirinae	Lentivirus	HIV-1
SL017	352	542	15.8	NP_057857.2,	Orthoretrovirinae	Lentivirus	HIV-1

SL017	391	518	8.1	NP_057849.4,NP_057850.1,	Orthoretrovirinae	Lentivirus	HIV-1
SL017	409	509	39.4	NP_057849.4,	Orthoretrovirinae	Lentivirus	HIV-1
SL017	480	474	8.7	NP_057857.2,	Orthoretrovirinae	Lentivirus	HIV-1
SL017	568	424	2.5	NP_057849.4,	Orthoretrovirinae	Lentivirus	HIV-1
SL017	597	413	8.5	NP_057856.1,	Orthoretrovirinae	Lentivirus	HIV-1
SL017	612	404	8.4	NP_057857.2,	Orthoretrovirinae	Lentivirus	HIV-1
SL017	621	399	3.4	NP_057852.2,	Orthoretrovirinae	Lentivirus	HIV-1
SL017	746	344	3.0	NP_057857.2,	Orthoretrovirinae	Lentivirus	HIV-1
SL017	769	337	3.4	NP_057849.4,	Orthoretrovirinae	Lentivirus	HIV-1
SL017	802	326	4.1	NP_057856.1,	Orthoretrovirinae	Lentivirus	HIV-1
SL017	810	324	5.9	NP_057849.4,NP_057850.1,	Orthoretrovirinae	Lentivirus	HIV-1
SL017	820	320	9.2	NP_057856.1,	Orthoretrovirinae	Lentivirus	HIV-1
SL017	835	315	5.2	NP_057856.1,	Orthoretrovirinae	Lentivirus	HIV-1
SL017	860	306	6.6	NP_057849.4,NP_057850.1,	Orthoretrovirinae	Lentivirus	HIV-1

SL024	2	2530	87.2	YP_009173866.1,	Hepadnaviridae	Orthohepadnavirus	HBV
SL024	279	599	12.1	YP_009173857.1,	Hepadnaviridae	Orthohepadnavirus	HBV
SL024	333	558	21.4	YP_009173867.1,	Hepadnaviridae	Orthohepadnavirus	HBV
SL024	13	1426	2.2	NP_057849.4,	Orthoretrovirinae	Lentivirus	HIV-1
SL024	137	767	2.8	NP_057849.4,	Orthoretrovirinae	Lentivirus	HIV-1
SL071	942	576	2.3	NP_043570.1,	Pegivirus	Pegivirus C	GBV-C
SL071	1049	532	3.1	NP_043570.1,	Pegivirus	Pegivirus C	GBV-C
SL071	1605	381	2.2	NP_043570.1,	Pegivirus	Pegivirus C	GBV-C
SL080	1	3249	14.6	NP_043570.1,	Pegivirus	Pegivirus C	GBV-C
SL080	2	2317	2.9	NP_043570.1,	Pegivirus	Pegivirus C	GBV-C
SL080	16	1499	5.4	NP_043570.1,	Pegivirus	Pegivirus C	GBV-C
SL080	24	1319	4.2	NP_043570.1,	Pegivirus	Pegivirus C	GBV-C
SL080	238	627	4.2	NP_043570.1,	Pegivirus	Pegivirus C	GBV-C
SL080	1035	323	2.1	NP_043570.1,	Pegivirus	Pegivirus C	GBV-C

SL093	1	5861	166.5	NP_043570.1,	Pegivirus	Pegivirus C	GBV-C
SL093	2	3221	260.1	NP_043570.1,	Pegivirus	Pegivirus C	GBV-C
SL093	1064	380	6.7	NP_043570.1,	Pegivirus	Pegivirus C	GBV-C
SL093	1261	314	3.2	NP_043570.1,	Pegivirus	Pegivirus C	GBV-C
SL096	2	2974	6.6	NP_066251.1,	Filoviridae	Ebolavirus	EBOV Zaire
SL096	22	1703	13.4	NP_066250.1,	Filoviridae	Ebolavirus	EBOV Zaire
SL096	186	906	7.3	NP_066243.1,	Filoviridae	Ebolavirus	EBOV Zaire
SL096	268	784	3.8	NP_066246.1,NP_066247.1,NP_066248.1,	Filoviridae	Ebolavirus	EBOV Zaire
SL096	289	752	2.2	NP_066251.1,	Filoviridae	Ebolavirus	EBOV Zaire
SL096	599	536	3.9	NP_066244.1,	Filoviridae	Ebolavirus	EBOV Zaire
SL097	9	1446	34.5	NP_057849.4,	Orthoretrovirinae	Lentivirus	HIV-1
SL097	23	1183	4.4	NP_057856.1,	Orthoretrovirinae	Lentivirus	HIV-1
SL097	28	1147	8.4	NP_057849.4,NP_057850.1,	Orthoretrovirinae	Lentivirus	HIV-1
SL097	30	1132	7.3	NP_057849.4,	Orthoretrovirinae	Lentivirus	HIV-1

SL097	33	1035	9.8	NP_057856.1,	Orthoretrovirinae	Lentivirus	HIV-1
SL097	36	950	11.1	NP_057849.4,NP_057850.1,	Orthoretrovirinae	Lentivirus	HIV-1
SL097	61	758	12.1	NP_057849.4,	Orthoretrovirinae	Lentivirus	HIV-1
SL097	63	749	20.3	NP_057849.4,	Orthoretrovirinae	Lentivirus	HIV-1
SL097	71	715	2.5	NP_057856.1,	Orthoretrovirinae	Lentivirus	HIV-1
SL097	81	663	3.0	NP_057856.1,	Orthoretrovirinae	Lentivirus	HIV-1
SL097	141	472	7.5	NP_057849.4,NP_057850.1,	Orthoretrovirinae	Lentivirus	HIV-1
SL097	169	408	3.8	NP_057849.4,	Orthoretrovirinae	Lentivirus	HIV-1
SL097	175	401	12.2	NP_057849.4,	Orthoretrovirinae	Lentivirus	HIV-1
SL097	206	322	10.5	NP_057849.4,	Orthoretrovirinae	Lentivirus	HIV-1
SL108	228	652	16.2	NP_059433.1,	Flaviviridae	Flavivirus	DENV-1
SL110	21	1258	29.6	NP_057857.2,	Orthoretrovirinae	Lentivirus	HIV-1
SL110	26	1239	192.0	NP_057849.4,NP_057850.1,	Orthoretrovirinae	Lentivirus	HIV-1
SL110	61	1016	94.3	NP_057849.4,	Orthoretrovirinae	Lentivirus	HIV-1

SL110	83	923	255.6	NP_057849.4,	Orthoretrovirinae	Lentivirus	HIV-1
SL110	96	878	107.2	NP_057856.1,	Orthoretrovirinae	Lentivirus	HIV-1
SL110	97	874	19.7	NP_057857.2,	Orthoretrovirinae	Lentivirus	HIV-1
SL110	120	793	128.6	NP_057856.1,	Orthoretrovirinae	Lentivirus	HIV-1
SL110	131	773	26.3	NP_057856.1,	Orthoretrovirinae	Lentivirus	HIV-1
SL110	136	766	102.4	NP_057856.1,	Orthoretrovirinae	Lentivirus	HIV-1
SL110	138	758	11.2	NP_057852.2,	Orthoretrovirinae	Lentivirus	HIV-1
SL110	164	717	5.9	NP_057849.4,	Orthoretrovirinae	Lentivirus	HIV-1
SL110	177	694	99.3	NP_057849.4,	Orthoretrovirinae	Lentivirus	HIV-1
SL110	192	665	10.4	NP_057849.4,	Orthoretrovirinae	Lentivirus	HIV-1
SL110	199	654	37.4	NP_057852.2,	Orthoretrovirinae	Lentivirus	HIV-1
SL110	206	647	12.7	NP_057857.2,	Orthoretrovirinae	Lentivirus	HIV-1
SL110	215	637	23.1	NP_057856.1,	Orthoretrovirinae	Lentivirus	HIV-1
SL110	218	634	16.1	NP_057852.2,	Orthoretrovirinae	Lentivirus	HIV-1

SL110	253	607	19.1	NP_057856.1,	Orthoretrovirinae	Lentivirus	HIV-1
SL110	255	604	10.9	NP_057856.1,	Orthoretrovirinae	Lentivirus	HIV-1
SL110	259	599	15.0	NP_057856.1,	Orthoretrovirinae	Lentivirus	HIV-1
SL110	261	598	7.4	NP_057850.1,	Orthoretrovirinae	Lentivirus	HIV-1
SL110	272	581	272.7	NP_057856.1,	Orthoretrovirinae	Lentivirus	HIV-1
SL110	289	561	2.5	NP_057857.2,	Orthoretrovirinae	Lentivirus	HIV-1
SL110	294	554	75.4	NP_057849.4,	Orthoretrovirinae	Lentivirus	HIV-1
SL110	296	551	10.4	NP_057850.1,	Orthoretrovirinae	Lentivirus	HIV-1
SL110	303	549	63.4	NP_057849.4,	Orthoretrovirinae	Lentivirus	HIV-1
SL110	316	541	353.4	NP_057853.1,	Orthoretrovirinae	Lentivirus	HIV-1
SL110	317	541	39.2	NP_057849.4,	Orthoretrovirinae	Lentivirus	HIV-1
SL110	323	532	2.3	NP_057856.1,	Orthoretrovirinae	Lentivirus	HIV-1
SL110	328	525	184.3	NP_057852.2,	Orthoretrovirinae	Lentivirus	HIV-1
SL110	331	524	5.8	NP_057856.1,	Orthoretrovirinae	Lentivirus	HIV-1

SL110	335	523	130.8	NP_057856.1,	Orthoretrovirinae	Lentivirus	HIV-1
SL110	342	517	4.1	NP_057849.4,	Orthoretrovirinae	Lentivirus	HIV-1
SL110	357	504	28.5	NP_057849.4,	Orthoretrovirinae	Lentivirus	HIV-1
SL110	363	498	24.0	NP_057849.4,	Orthoretrovirinae	Lentivirus	HIV-1
SL110	367	495	25.1	NP_057850.1,	Orthoretrovirinae	Lentivirus	HIV-1
SL110	368	494	96.1	NP_057849.4,	Orthoretrovirinae	Lentivirus	HIV-1
SL110	369	494	5.5	NP_057849.4,	Orthoretrovirinae	Lentivirus	HIV-1
SL110	376	491	7.4	NP_057850.1,	Orthoretrovirinae	Lentivirus	HIV-1
SL110	380	490	12.5	NP_057856.1,	Orthoretrovirinae	Lentivirus	HIV-1
SL110	383	488	92.3	NP_057856.1,	Orthoretrovirinae	Lentivirus	HIV-1
SL110	408	471	11.8	NP_057857.2,	Orthoretrovirinae	Lentivirus	HIV-1
SL110	411	469	9.3	NP_057849.4,NP_057850.1,	Orthoretrovirinae	Lentivirus	HIV-1
SL110	417	467	16.9	NP_057850.1,	Orthoretrovirinae	Lentivirus	HIV-1
SL110	443	451	22.3	NP_057852.2,	Orthoretrovirinae	Lentivirus	HIV-1

SL110	457	442	17.8	NP_057852.2,	Orthoretrovirinae	Lentivirus	HIV-1
SL110	481	421	8.3	NP_057849.4,NP_057850.1,	Orthoretrovirinae	Lentivirus	HIV-1
SL110	483	421	4.1	NP_057852.2,	Orthoretrovirinae	Lentivirus	HIV-1
SL110	487	418	82.6	NP_057849.4,	Orthoretrovirinae	Lentivirus	HIV-1
SL110	494	412	6.1	NP_057849.4,	Orthoretrovirinae	Lentivirus	HIV-1
SL110	499	409	40.6	NP_057850.1,	Orthoretrovirinae	Lentivirus	HIV-1
SL110	520	401	140.0	NP_057852.2,	Orthoretrovirinae	Lentivirus	HIV-1
SL110	521	401	14.1	NP_057852.2,	Orthoretrovirinae	Lentivirus	HIV-1
SL110	522	401	6.8	NP_057856.1,	Orthoretrovirinae	Lentivirus	HIV-1
SL110	528	399	6.2	NP_057852.2,	Orthoretrovirinae	Lentivirus	HIV-1
SL110	535	393	5.0	NP_057850.1,	Orthoretrovirinae	Lentivirus	HIV-1
SL110	540	390	51.8	NP_057852.2,	Orthoretrovirinae	Lentivirus	HIV-1
SL110	543	389	7.8	NP_057849.4,	Orthoretrovirinae	Lentivirus	HIV-1
SL110	548	385	46.0	NP_057856.1,	Orthoretrovirinae	Lentivirus	HIV-1

SL110	549	385	14.1	NP_057856.1,	Orthoretrovirinae	Lentivirus	HIV-1
SL110	558	379	38.1	NP_057856.1,	Orthoretrovirinae	Lentivirus	HIV-1
SL110	563	375	30.9	NP_057856.1,	Orthoretrovirinae	Lentivirus	HIV-1
SL110	564	375	11.6	NP_057849.4,	Orthoretrovirinae	Lentivirus	HIV-1
SL110	588	360	10.4	NP_057856.1,	Orthoretrovirinae	Lentivirus	HIV-1
SL110	600	355	9.9	NP_057849.4,	Orthoretrovirinae	Lentivirus	HIV-1
SL110	613	351	24.4	NP_057856.1,	Orthoretrovirinae	Lentivirus	HIV-1
SL110	614	351	9.3	YP_009028572.1,	Orthoretrovirinae	Lentivirus	HIV-1
SL110	618	350	103.5	NP_057851.1,	Orthoretrovirinae	Lentivirus	HIV-1
SL110	619	350	8.0	NP_057852.2,	Orthoretrovirinae	Lentivirus	HIV-1
SL110	632	345	23.0	NP_057849.4,	Orthoretrovirinae	Lentivirus	HIV-1
SL110	634	344	5.5	NP_057849.4,	Orthoretrovirinae	Lentivirus	HIV-1
SL110	640	342	66.6	NP_057856.1,	Orthoretrovirinae	Lentivirus	HIV-1
SL110	645	339	241.1	NP_057849.4,	Orthoretrovirinae	Lentivirus	HIV-1

SL110	654	337	95.1	NP_057856.1,	Orthoretrovirinae	Lentivirus	HIV-1
SL110	655	337	13.4	NP_057851.1,	Orthoretrovirinae	Lentivirus	HIV-1
SL110	656	337	7.7	NP_057849.4,	Orthoretrovirinae	Lentivirus	HIV-1
SL110	660	336	296.1	NP_057856.1,	Orthoretrovirinae	Lentivirus	HIV-1
SL110	665	333	6.7	NP_057856.1,	Orthoretrovirinae	Lentivirus	HIV-1
SL110	668	331	107.0	NP_057849.4,	Orthoretrovirinae	Lentivirus	HIV-1
SL110	674	329	13.2	NP_057849.4,	Orthoretrovirinae	Lentivirus	HIV-1
SL110	683	325	245.1	NP_057852.2,	Orthoretrovirinae	Lentivirus	HIV-1
SL110	692	322	6.3	YP_009028572.1,	Orthoretrovirinae	Lentivirus	HIV-1
SL110	696	321	50.1	NP_057856.1,	Orthoretrovirinae	Lentivirus	HIV-1
SL110	697	320	4.2	NP_057856.1,	Orthoretrovirinae	Lentivirus	HIV-1
SL110	698	319	146.1	NP_057856.1,	Orthoretrovirinae	Lentivirus	HIV-1
SL110	699	319	28.7	NP_057849.4,	Orthoretrovirinae	Lentivirus	HIV-1
SL110	700	319	20.9	NP_057849.4,	Orthoretrovirinae	Lentivirus	HIV-1

SL110	711	314	10.6	NP_057852.2,	Orthoretrovirinae	Lentivirus	HIV-1
SL110	712	314	4.9	NP_057856.1,	Orthoretrovirinae	Lentivirus	HIV-1
SL110	722	310	4.7	NP_057856.1,	Orthoretrovirinae	Lentivirus	HIV-1
SL110	726	309	21.8	NP_057849.4,	Orthoretrovirinae	Lentivirus	HIV-1
SL110	731	307	4.1	NP_057857.2,	Orthoretrovirinae	Lentivirus	HIV-1
SL117	312	878	3.4	YP_001129351.1,	Gammaherpesvirinae	Rhadinovirus	HHV-8

APPENDIX 6: ECUADORIAN FEBRILE PATIENT RT-PCR/PCR RESULTS, 2016.

Green = Cq value <35.0, orange = Cq value 35.0 – 39.9, blue = testing performed in-country, prior to this study. Samples that underwent metagenomic sequencing are indicated.

Sample ID	Previous ZIKV qRT-PCR (USFQ)	ZIKV	DENV 1-3	DENV 4	CHIKV	*Leptospira*	*Rickettsia*	*Plasmodium*	YFV	OROV	MAYV	MS2 control	Virus isolated	Metagenomic sequencing performed
D-001	No Ct	No Ct	No Ct	No Ct	No Ct	No Ct	No Ct	Negative	No Ct	No Ct	No Ct	28.87		Yes
D-002	No Ct	No Ct	No Ct	No Ct	No Ct	No Ct	No Ct	Negative	No Ct	No Ct	No Ct	28.93		Yes
D-003	No Ct	No Ct	No Ct	No Ct	No Ct	No Ct	No Ct	Negative	No Ct	No Ct	No Ct	28.62		
D-004	No Ct	No Ct	33.45	No Ct	No Ct	No Ct	No Ct	Negative	No Ct	No Ct	No Ct	28.27		
D-005	No Ct	No Ct	No Ct	No Ct	No Ct	No Ct	No Ct	Negative	No Ct	No Ct	No Ct	29.37		Yes
D-006	No Ct	No Ct	34.05	No Ct	No Ct	No Ct	No Ct	Negative	No Ct	No Ct	No Ct	27.71		
D-007	No Ct	No Ct	No Ct	No Ct	No Ct	No Ct	No Ct	Negative	No Ct	No Ct	No Ct	28.89		
D-008	No Ct	No Ct	No Ct	No Ct	No Ct	No Ct	No Ct	Negative	No Ct	No Ct	No Ct	28.87		
D-009	No Ct	No Ct	36.47	No Ct	No Ct	No Ct	No Ct	Negative	No Ct	No Ct	No Ct	28.86		

D-010	No Ct	No Ct	No Ct	No Ct	No Ct	No Ct	No Ct	Negative	No Ct	No Ct	No Ct	28.75		Yes
D-011	No Ct	No Ct	No Ct	No Ct	No Ct	No Ct	No Ct	Negative	No Ct	No Ct	No Ct	29.03		
D-012	No Ct	No Ct	No Ct	No Ct	No Ct	35.52	No Ct	Negative	No Ct	No Ct	No Ct	28.45		
D-013	No Ct	No Ct	No Ct	No Ct	No Ct	No Ct	No Ct	Negative	No Ct	No Ct	No Ct	28.41		
D-014	No Ct	No Ct	No Ct	No Ct	No Ct	No Ct	No Ct	Negative	No Ct	No Ct	No Ct	28.03		Yes
D-015	No Ct	No Ct	No Ct	No Ct	No Ct	No Ct	No Ct	Negative	No Ct	No Ct	No Ct	28.51		
D-016	No Ct	No Ct	No Ct	No Ct	No Ct	No Ct	No Ct	Negative	No Ct	No Ct	No Ct	28.50		
D-017	No Ct	No Ct	No Ct	No Ct	No Ct	33.64	No Ct	Negative	No Ct	No Ct	No Ct	28.42		
D-018	No Ct	No Ct	No Ct	No Ct	No Ct	No Ct	No Ct	Negative	No Ct	No Ct	No Ct	29.1		Yes
D-019	No Ct	No Ct	No Ct	No Ct	No Ct	No Ct	No Ct	Negative	No Ct	No Ct	No Ct	28.86		
D-020	No Ct	No Ct	No Ct	No Ct	No Ct	No Ct	No Ct	Negative	No Ct	No Ct	No Ct	28.46		Yes
D-021	No Ct	No Ct	No Ct	No Ct	No Ct	No Ct	No Ct	Negative	No Ct	No Ct	No Ct	28.25		
D-022	No Ct	No Ct	No Ct	No Ct	No Ct	No Ct	No Ct	Negative	No Ct	No Ct	No Ct	28.58		
D-023	No Ct	31.49	No Ct	No Ct	No Ct	No Ct	No Ct	Negative	No Ct	No Ct	No Ct	29.58		

D-025	No Ct	No Ct	No Ct	No Ct	No Ct	No Ct	No Ct	Negative	No Ct	No Ct	No Ct	29.79		
D-026	No Ct	No Ct	No Ct	No Ct	No Ct	No Ct	No Ct	Negative	No Ct	No Ct	No Ct	29.07		
D-027	No Ct	No Ct	No Ct	No Ct	No Ct	No Ct	No Ct	Negative	No Ct	No Ct	No Ct	28.95		
D-028	No Ct	No Ct	No Ct	No Ct	No Ct	No Ct	No Ct	Negative	No Ct	No Ct	No Ct	29.21		
D-029	No Ct	No Ct	No Ct	No Ct	No Ct	No Ct	No Ct	Negative	No Ct	No Ct	No Ct	29.61		Yes
D-030	No Ct	No Ct	No Ct	No Ct	No Ct	No Ct	No Ct	Negative	No Ct	No Ct	No Ct	28.87		Yes
D-031	No Ct	No Ct	No Ct	No Ct	No Ct	No Ct	No Ct	Negative	No Ct	No Ct	No Ct	28.87		
D-032	No Ct	No Ct	No Ct	No Ct	No Ct	No Ct	No Ct	Negative	No Ct	No Ct	No Ct	31.18		
D-033	No Ct	No Ct	No Ct	No Ct	No Ct	No Ct	No Ct	Negative	No Ct	No Ct	No Ct	27.9		
D-034	No Ct	No Ct	No Ct	No Ct	No Ct	No Ct	No Ct	Negative	No Ct	No Ct	No Ct	29.03		
D-035	No Ct	No Ct	No Ct	No Ct	No Ct	No Ct	No Ct	Negative	No Ct	No Ct	No Ct	29.26		Yes
D-036	No Ct	No Ct	No Ct	No Ct	No Ct	No Ct	No Ct	Negative	No Ct	No Ct	No Ct	29.55		
D-037	No Ct	No Ct	No Ct	No Ct	No Ct	No Ct	No Ct	Negative	No Ct	No Ct	No Ct	29.17		
D-038	No Ct	No Ct	No Ct	No Ct	No Ct	No Ct	No Ct	Negative	No Ct	No Ct	No Ct	29.31		

D-039	No Ct	34.66	No Ct	No Ct	No Ct	No Ct	No Ct	Negative	No Ct	No Ct	No Ct	28.71		
D-040	No Ct	No Ct	No Ct	No Ct	No Ct	No Ct	No Ct	Negative	No Ct	No Ct	No Ct	28.75		Yes
D-041	No Ct	36.5	No Ct	No Ct	No Ct	No Ct	No Ct	Negative	No Ct	No Ct	No Ct	29.59		
D-042	No Ct	No Ct	No Ct	No Ct	No Ct	No Ct	No Ct	Negative	No Ct	No Ct	No Ct	28.6		
D-043	No Ct	No Ct	No Ct	No Ct	No Ct	No Ct	No Ct	Negative	No Ct	No Ct	No Ct	29.49		
D-044	No Ct	No Ct	No Ct	No Ct	No Ct	No Ct	No Ct	Negative	No Ct	No Ct	No Ct	28.95		
D-045	No Ct	No Ct	No Ct	No Ct	No Ct	No Ct	No Ct	Negative	No Ct	No Ct	No Ct	29.21		
D-047	No Ct	No Ct	No Ct	No Ct	No Ct	No Ct	No Ct	Negative	No Ct	No Ct	No Ct	28.53		Yes
D-048	No Ct	No Ct	No Ct	No Ct	No Ct	No Ct	No Ct	Negative	No Ct	No Ct	No Ct	29.01		
D-049	No Ct	No Ct	No Ct	No Ct	No Ct	No Ct	No Ct	Negative	No Ct	No Ct	No Ct	29.01		
D-050	No Ct	No Ct	34.8	No Ct	No Ct	No Ct	No Ct	Negative	No Ct	No Ct	No Ct	29.00		
D-051	31.14	30.65	No Ct	No Ct	No Ct	No Ct	No Ct	Negative	No Ct	No Ct	No Ct	28.53		
D-052	No Ct	32.88	No Ct	No Ct	No Ct	No Ct	No Ct	Negative	No Ct	No Ct	No Ct	28.78		
D-053	No Ct	No Ct	No Ct	No Ct	No Ct	No Ct	No Ct	Negative	No Ct	No Ct	No Ct	28.78		

D-054	No Ct	No Ct	No Ct	No Ct	No Ct	No Ct	No Ct	Negative	No Ct	No Ct	No Ct	29.13		
D-055	No Ct	36.11	No Ct	No Ct	No Ct	No Ct	No Ct	Negative	No Ct	No Ct	No Ct	29.74		
D-057	No Ct	No Ct	No Ct	No Ct	No Ct	No Ct	No Ct	Negative	No Ct	25.66	No Ct	28.79	OROV	Yes
D-058	No Ct	No Ct	No Ct	No Ct	No Ct	No Ct	No Ct	Negative	No Ct	No Ct	No Ct	28.91		
D-059	No Ct	No Ct	No Ct	No Ct	No Ct	No Ct	No Ct	Negative	No Ct	No Ct	No Ct	28.90		
D-060	25.21	34.58	No Ct	No Ct	No Ct	No Ct	No Ct	Negative	No Ct	No Ct	No Ct	29.96		
D-061	No Ct	No Ct	No Ct	No Ct	No Ct	No Ct	No Ct	Negative	No Ct	No Ct	No Ct	29.11		
D-062	24.17	27.03	No Ct	No Ct	No Ct	No Ct	No Ct	Negative	No Ct	No Ct	No Ct	30.23		
D-064	No Ct	No Ct	No Ct	No Ct	No Ct	No Ct	No Ct	Negative	No Ct	No Ct	No Ct	31.46		
D-065	No Ct	No Ct	No Ct	No Ct	No Ct	No Ct	No Ct	Negative	No Ct	No Ct	No Ct	29.16		
D-066	No Ct	No Ct	No Ct	No Ct	No Ct	No Ct	No Ct	Negative	No Ct	No Ct	No Ct	29.47		
D-067	No Ct	No Ct	No Ct	No Ct	No Ct	No Ct	No Ct	Negative	No Ct	No Ct	No Ct	28.79		
D-068	No Ct	No Ct	No Ct	No Ct	No Ct	No Ct	No Ct	Negative	No Ct	No Ct	No Ct	28.95		
D-069	No Ct	No Ct	No Ct	No Ct	No Ct	No Ct	No Ct	Negative	No Ct	No Ct	No Ct	28.96		

D-070	No Ct	No Ct	No Ct	No Ct	No Ct	No Ct	No Ct	Negative	No Ct	No Ct	No Ct	29.12		
D-071	34.74	No Ct	No Ct	No Ct	No Ct	No Ct	No Ct	Negative	No Ct	No Ct	No Ct	28.38		
D-072	No Ct	No Ct	No Ct	No Ct	No Ct	No Ct	No Ct	Negative	No Ct	No Ct	No Ct	29.21		
D-073	No Ct	No Ct	No Ct	No Ct	No Ct	No Ct	No Ct	Negative	No Ct	No Ct	No Ct	29.16		
D-074	No Ct	No Ct	No Ct	No Ct	No Ct	No Ct	No Ct	Negative	No Ct	No Ct	No Ct	28.57		Yes
D-075	No Ct	No Ct	No Ct	No Ct	No Ct	No Ct	No Ct	Negative	No Ct	No Ct	No Ct	28.26		Yes
D-076	No Ct	No Ct	No Ct	No Ct	No Ct	No Ct	No Ct	Negative	No Ct	No Ct	No Ct	29.32		
D-077	No Ct	No Ct	No Ct	No Ct	No Ct	No Ct	No Ct	Negative	No Ct	No Ct	No Ct	29.21		
D-078	No Ct	No Ct	No Ct	No Ct	No Ct	No Ct	No Ct	Negative	No Ct	No Ct	No Ct	28.76		
D-079	No Ct	No Ct	No Ct	No Ct	No Ct	No Ct	No Ct	Negative	No Ct	No Ct	No Ct	28.84		
D-080	No Ct	37.14	No Ct	No Ct	No Ct	No Ct	No Ct	Negative	No Ct	No Ct	No Ct	29.54		
D-081	No Ct	No Ct	No Ct	No Ct	No Ct	No Ct	No Ct	Negative	No Ct	No Ct	No Ct	29.15		
D-082	No Ct	No Ct	No Ct	No Ct	No Ct	No Ct	No Ct	Negative	No Ct	No Ct	No Ct	29.17		
D-083	No Ct	No Ct	No Ct	No Ct	No Ct	No Ct	No Ct	Negative	No Ct	No Ct	No Ct	29.28		

D-084	No Ct	No Ct	No Ct	No Ct	No Ct	No Ct	No Ct	Negative	No Ct	No Ct	No Ct	29.36		
D-085	No Ct	No Ct	No Ct	No Ct	No Ct	No Ct	No Ct	Negative	No Ct	No Ct	No Ct	28.84		
D-086	No Ct	No Ct	No Ct	No Ct	No Ct	No Ct	No Ct	Negative	No Ct	No Ct	No Ct	29.06		
D-087	No Ct	No Ct	35.33	No Ct	36.63	No Ct	No Ct	Negative	No Ct	36.26	No Ct	29.45	OROV	Yes
D-088	No Ct	No Ct	No Ct	No Ct	No Ct	No Ct	No Ct	Negative	No Ct	No Ct	No Ct	29.31		
D-090	No Ct	No Ct	No Ct	No Ct	No Ct	No Ct	No Ct	Negative	No Ct	No Ct	No Ct	28.89		
D-091	No Ct	No Ct	No Ct	No Ct	No Ct	No Ct	No Ct	Negative	No Ct	No Ct	No Ct	28.64		Yes
D-092	No Ct	No Ct	No Ct	No Ct	No Ct	No Ct	No Ct	Negative	No Ct	No Ct	No Ct	29.02		
D-093	34.79	No Ct	No Ct	No Ct	No Ct	No Ct	No Ct	Negative	No Ct	No Ct	No Ct	28.36		
D-094	No Ct	No Ct	No Ct	No Ct	No Ct	No Ct	No Ct	Negative	No Ct	No Ct	No Ct	28.92		
D-095	No Ct	36.32	No Ct	No Ct	No Ct	No Ct	No Ct	Negative	No Ct	No Ct	No Ct	30.01		
D-096	No Ct	No Ct	No Ct	No Ct	No Ct	No Ct	No Ct	Negative	No Ct	No Ct	No Ct	29.89		
D-097	No Ct	No Ct	No Ct	No Ct	No Ct	No Ct	No Ct	Negative	No Ct	No Ct	No Ct	30.47		
D-098	No Ct	No Ct	No Ct	No Ct	No Ct	No Ct	No Ct	Negative	No Ct	No Ct	No Ct	28.90		

D-099	No Ct	34.97	38.27	No Ct	No Ct	No Ct	No Ct	Negative	No Ct	No Ct	No Ct	29.22		
D-100	No Ct	No Ct	No Ct	No Ct	No Ct	No Ct	No Ct	Negative	No Ct	No Ct	No Ct	29.05		
D-101	No Ct	No Ct	32.34	No Ct	No Ct	No Ct	No Ct	Negative	No Ct	No Ct	No Ct	27.72		
D-102	37.07	No Ct	No Ct	No Ct	No Ct	No Ct	No Ct	Negative	No Ct	No Ct	No Ct	28.37		
D-103	No Ct	No Ct	No Ct	No Ct	No Ct	No Ct	No Ct	Negative	No Ct	No Ct	No Ct	29.15		
D-104	No Ct	No Ct	No Ct	No Ct	No Ct	No Ct	No Ct	Negative	No Ct	No Ct	No Ct	29.96		
D-105	No Ct	No Ct	No Ct	No Ct	No Ct	No Ct	No Ct	Negative	No Ct	No Ct	No Ct	29.51		
D-106	No Ct	No Ct	No Ct	No Ct	No Ct	No Ct	No Ct	Negative	No Ct	No Ct	No Ct	29.99		
D-107	No Ct	No Ct	No Ct	No Ct	No Ct	No Ct	No Ct	Negative	No Ct	No Ct	No Ct	30.95		
D-108	No Ct	No Ct	No Ct	No Ct	No Ct	No Ct	No Ct	Negative	No Ct	No Ct	No Ct	28.38		
D-109	No Ct	37.41	No Ct	No Ct	No Ct	No Ct	No Ct	Negative	No Ct	No Ct	No Ct	31.55		
D-110	36.39	34.18	No Ct	No Ct	No Ct	No Ct	No Ct	Negative	No Ct	No Ct	No Ct	28.02		
D-111	36.36	34.67	No Ct	No Ct	No Ct	No Ct	No Ct	Negative	No Ct	No Ct	No Ct	27.63		
D-112	No Ct	No Ct	No Ct	No Ct	No Ct	No Ct	No Ct	Negative	No Ct	No Ct	No Ct	30.78		

D-113	32.39	30.18	No Ct	No Ct	No Ct	No Ct	No Ct	Negative	No Ct	No Ct	No Ct	28.66		
D-114	31.49	29.32	No Ct	No Ct	No Ct	No Ct	No Ct	Negative	No Ct	No Ct	No Ct	28.62		
D-118	No Ct	35.14	No Ct	No Ct	No Ct	No Ct	No Ct	Negative	No Ct	No Ct	No Ct	30.34		
D-119	No Ct	34.52	No Ct	No Ct	No Ct	No Ct	No Ct	Negative	No Ct	No Ct	No Ct	30.39		
D-121	27.63	26.74	No Ct	No Ct	No Ct	No Ct	No Ct	Negative	No Ct	No Ct	No Ct	28.55	ZIKV	
D-122	No Ct	No Ct	No Ct	No Ct	No Ct	No Ct	No Ct	Negative	No Ct	No Ct	No Ct	29.13		
D-123	No Ct	No Ct	No Ct	No Ct	No Ct	No Ct	No Ct	Negative	No Ct	No Ct	No Ct	30.05		
D-124	36.12	34.54	No Ct	No Ct	35.76	No Ct	No Ct	Negative	No Ct	No Ct	No Ct	28.55	ZIKV	Yes
D-125	No Ct	No Ct	No Ct	No Ct	No Ct	No Ct	No Ct	Negative	No Ct	No Ct	No Ct	29.80		
D-126	29.08	29.6	No Ct	No Ct	No Ct	No Ct	No Ct	Negative	No Ct	No Ct	No Ct	28.56		
D-127	No Ct	No Ct	No Ct	No Ct	No Ct	No Ct	No Ct	Negative	No Ct	No Ct	No Ct	29.39		
D-128	No Ct	No Ct	No Ct	No Ct	No Ct	No Ct	No Ct	Negative	No Ct	No Ct	No Ct	29.67		
D-129	No Ct	No Ct	No Ct	No Ct	No Ct	No Ct	No Ct	Negative	No Ct	No Ct	No Ct	29.04		
D-130	No Ct	No Ct	No Ct	No Ct	No Ct	No Ct	No Ct	Negative	No Ct	No Ct	No Ct	29.07		

D-131	No Ct	No Ct	No Ct	No Ct	No Ct	No Ct	No Ct	Negative	No Ct	No Ct	No Ct	29.71		Yes
D-132	No Ct	No Ct	No Ct	No Ct	No Ct	No Ct	No Ct	Negative	No Ct	No Ct	No Ct	29.20		
D-133	No Ct	No Ct	No Ct	No Ct	No Ct	No Ct	No Ct	Negative	No Ct	No Ct	No Ct	29.99		
D-134	No Ct	No Ct	No Ct	No Ct	No Ct	No Ct	No Ct	Negative	No Ct	No Ct	No Ct	29.51		
D-135	33.37	34.31	No Ct	No Ct	No Ct	No Ct	No Ct	Negative	No Ct	No Ct	No Ct	29.19		
D-136	No Ct	37.51	No Ct	No Ct	No Ct	No Ct	No Ct	Negative	No Ct	No Ct	No Ct	28.76		
D-137	No Ct	No Ct	No Ct	No Ct	No Ct	No Ct	No Ct	Negative	No Ct	No Ct	No Ct	28.75		
D-138	No Ct	No Ct	No Ct	No Ct	No Ct	No Ct	No Ct	Negative	No Ct	No Ct	No Ct	29.48		
D-139	No Ct	35.73	No Ct	No Ct	No Ct	No Ct	No Ct	Negative	No Ct	No Ct	No Ct	30.30		
D-140	32.4	34.02	No Ct	No Ct	No Ct	No Ct	No Ct	Negative	No Ct	No Ct	No Ct	29.57		
D-141	33.11	35.44	No Ct	No Ct	No Ct	No Ct	No Ct	Negative	No Ct	No Ct	No Ct	28.60		
D-142	No Ct	No Ct	No Ct	No Ct	No Ct	No Ct	No Ct	Negative	No Ct	No Ct	No Ct	29.11		
D-143	No Ct	No Ct	No Ct	No Ct	No Ct	No Ct	No Ct	Negative	No Ct	No Ct	No Ct	29.04		
D-144	No Ct	No Ct	No Ct	No Ct	No Ct	No Ct	No Ct	Negative	No Ct	No Ct	No Ct	30.19		

D-145	No Ct	No Ct	No Ct	No Ct	No Ct	No Ct	No Ct	Negative	No Ct	No Ct	No Ct	30.25		
D-146	34.48	32.95	No Ct	No Ct	No Ct	No Ct	No Ct	Negative	No Ct	No Ct	No Ct	28.17		
D-147	No Ct	No Ct	No Ct	No Ct	No Ct	No Ct	No Ct	Negative	No Ct	No Ct	No Ct	30.19		
D-148	No Ct	No Ct	No Ct	No Ct	No Ct	No Ct	No Ct	Negative	No Ct	No Ct	No Ct	29.69		
D-149	31.98	35.37	No Ct	No Ct	No Ct	No Ct	No Ct	Negative	No Ct	No Ct	No Ct	28.78		
D-150	No Ct	No Ct	No Ct	No Ct	No Ct	No Ct	No Ct	Negative	No Ct	No Ct	No Ct	28.10		
D-151	No Ct	No Ct	No Ct	No Ct	No Ct	No Ct	No Ct	Negative	No Ct	No Ct	No Ct	30.14		
D-152	No Ct	No Ct	No Ct	No Ct	No Ct	No Ct	No Ct	Negative	No Ct	No Ct	No Ct	29.07		
D-153	No Ct	No Ct	No Ct	No Ct	No Ct	No Ct	No Ct	Negative	No Ct	No Ct	No Ct	28.88		
D-154	No Ct	No Ct	No Ct	No Ct	No Ct	No Ct	No Ct	Negative	No Ct	No Ct	No Ct	28.15		
D-155	No Ct	No Ct	No Ct	No Ct	No Ct	No Ct	No Ct	Negative	No Ct	25.75	No Ct	29.98	OROV	Yes
D-156	No Ct	35.52	No Ct	No Ct	No Ct	No Ct	No Ct	Negative	No Ct	No Ct	No Ct	30.31		
D-157	No Ct	26.77	No Ct	No Ct	No Ct	No Ct	No Ct	Negative	No Ct	No Ct	No Ct	29.43		
D-158	No Ct	No Ct	No Ct	No Ct	No Ct	No Ct	No Ct	Negative	No Ct	No Ct	No Ct	30.32		

D-159	No Ct	No Ct	No Ct	No Ct	No Ct	No Ct	No Ct	Negative	No Ct	No Ct	No Ct	29.16		
D-160	No Ct	No Ct	No Ct	No Ct	No Ct	No Ct	No Ct	Negative	No Ct	No Ct	No Ct	29.30		
D-161	No Ct	No Ct	No Ct	No Ct	No Ct	No Ct	No Ct	Negative	No Ct	No Ct	No Ct	30.00		
D-162	No Ct	No Ct	No Ct	No Ct	No Ct	No Ct	No Ct	Negative	No Ct	No Ct	No Ct	28.47		
D-164	No Ct	No Ct	No Ct	No Ct	No Ct	No Ct	No Ct	Negative	No Ct	No Ct	No Ct	28.92		
D-166	No Ct	No Ct	No Ct	No Ct	No Ct	No Ct	No Ct	Negative	No Ct	No Ct	No Ct	28.53		
D-167	No Ct	No Ct	No Ct	No Ct	No Ct	No Ct	No Ct	Negative	No Ct	No Ct	No Ct	29.50		
D-168	No Ct	No Ct	No Ct	No Ct	No Ct	No Ct	No Ct	Negative	No Ct	No Ct	No Ct	29.48		
D-170	No Ct	No Ct	No Ct	No Ct	No Ct	No Ct	No Ct	Negative	No Ct	No Ct	No Ct	28.80		
D-171	No Ct	No Ct	No Ct	No Ct	No Ct	No Ct	No Ct	Negative	No Ct	26.75	No Ct	28.99	OROV	Yes
D-172	35.49	34.38	No Ct	No Ct	No Ct	No Ct	No Ct	Negative	No Ct	No Ct	No Ct	27.99		
D-173	No Ct	No Ct	No Ct	No Ct	No Ct	No Ct	No Ct	Negative	No Ct	No Ct	No Ct	28.99		
D-174	No Ct	No Ct	No Ct	No Ct	No Ct	No Ct	No Ct	Negative	No Ct	No Ct	No Ct	28.12		
D-175	No Ct	No Ct	No Ct	No Ct	No Ct	No Ct	No Ct	Negative	No Ct	No Ct	No Ct	29.38		

D-176	32.37	33.78	No Ct	No Ct	No Ct	No Ct	No Ct	Negative	No Ct	No Ct	No Ct	28.09		
D-177	No Ct	35.88	No Ct	No Ct	No Ct	No Ct	No Ct	Negative	No Ct	No Ct	No Ct	28.83		
D-181	No Ct	No Ct	No Ct	No Ct	No Ct	No Ct	No Ct	Negative	No Ct	No Ct	No Ct	29.98		
D-182	No Ct	No Ct	No Ct	No Ct	No Ct	No Ct	No Ct	Negative	No Ct	No Ct	No Ct	28.96		
D-183	No Ct	No Ct	No Ct	No Ct	No Ct	No Ct	No Ct	Negative	No Ct	No Ct	No Ct	30.16		
D-184	No Ct	No Ct	No Ct	No Ct	No Ct	No Ct	No Ct	Negative	No Ct	No Ct	No Ct	30.95		
D-185	No Ct	No Ct	No Ct	No Ct	No Ct	No Ct	No Ct	Negative	No Ct	No Ct	No Ct	30.14		
D-186	No Ct	35.29	No Ct	No Ct	No Ct	No Ct	No Ct	Negative	No Ct	No Ct	No Ct	30.46		
D-187	No Ct	No Ct	No Ct	No Ct	No Ct	No Ct	No Ct	Negative	No Ct	No Ct	No Ct	30.19		
D-189	No Ct	No Ct	No Ct	No Ct	No Ct	No Ct	No Ct	Negative	No Ct	No Ct	No Ct	30.44		
D-190	No Ct	No Ct	No Ct	No Ct	No Ct	No Ct	No Ct	Negative	No Ct	No Ct	No Ct	30.14		
D-191	No Ct	No Ct	No Ct	No Ct	No Ct	No Ct	No Ct	Negative	No Ct	No Ct	No Ct	30.50		
D-192	No Ct	No Ct	No Ct	No Ct	No Ct	No Ct	No Ct	Negative	No Ct	No Ct	No Ct	30.47		
D-193	No Ct	No Ct	No Ct	No Ct	No Ct	No Ct	No Ct	Negative	No Ct	No Ct	No Ct	29.88		

D-194	37.72	28.11	No Ct	No Ct	No Ct	No Ct	No Ct	Negative	No Ct	No Ct	No Ct	27.98		
D-195	No Ct	No Ct	No Ct	No Ct	No Ct	No Ct	No Ct	Negative	No Ct	No Ct	No Ct	29.85		
D-196	No Ct	No Ct	No Ct	No Ct	No Ct	No Ct	No Ct	Negative	No Ct	No Ct	No Ct	29.89		
D-197	No Ct	No Ct	No Ct	No Ct	No Ct	No Ct	No Ct	Negative	No Ct	No Ct	No Ct	30.25		
D-198	No Ct	No Ct	No Ct	No Ct	No Ct	No Ct	No Ct	Negative	No Ct	No Ct	No Ct	29.81		
D-199	No Ct	No Ct	No Ct	No Ct	No Ct	No Ct	No Ct	Negative	No Ct	No Ct	No Ct	30.09		
D-200	No Ct	No Ct	No Ct	No Ct	No Ct	No Ct	No Ct	Negative	No Ct	No Ct	No Ct	30.25		
D-201	No Ct	No Ct	No Ct	No Ct	No Ct	No Ct	No Ct	Negative	No Ct	No Ct	No Ct	30.31		
D-202	No Ct	No Ct	No Ct	No Ct	No Ct	No Ct	No Ct	Negative	No Ct	No Ct	No Ct	29.89		
D-203	No Ct	No Ct	No Ct	No Ct	No Ct	No Ct	No Ct	Negative	No Ct	No Ct	No Ct	30.35		
D-204	No Ct	No Ct	No Ct	No Ct	No Ct	No Ct	No Ct	Negative	No Ct	No Ct	No Ct	30.05		
D-205	No Ct	34.06	No Ct	No Ct	No Ct	No Ct	No Ct	Negative	No Ct	No Ct	No Ct	30.47		
D-206	No Ct	No Ct	No Ct	No Ct	No Ct	No Ct	No Ct	Negative	No Ct	30.87	No Ct	30.50	OROV	Yes
D-207	No Ct	No Ct	No Ct	No Ct	No Ct	No Ct	No Ct	Negative	No Ct	No Ct	No Ct	30.62		

D-208	No Ct	No Ct	No Ct	No Ct	No Ct	No Ct	No Ct	Negative	No Ct	No Ct	No Ct	31.10		
D-209	No Ct	37.44	No Ct	No Ct	No Ct	No Ct	No Ct	Negative	No Ct	No Ct	No Ct	30.24		
D-210	No Ct	No Ct	No Ct	No Ct	No Ct	No Ct	No Ct	Negative	No Ct	29.18	No Ct	30.29	OROV	Yes
D-212	No Ct	No Ct	No Ct	No Ct	No Ct	No Ct	No Ct	Negative	No Ct	No Ct	No Ct	30.89		
D-213	No Ct	No Ct	No Ct	No Ct	No Ct	No Ct	No Ct	Negative	No Ct	No Ct	No Ct	30.32		

APPENDIX 7: PRIMER MISMATCHES TO EXISITING OROV SEQUENCES

OROV N gene sequences were aligned with published OROV oligonucleotide sequences (361) and newly designed reverse primer Ec2R. The number of bases at which variation from the oligonucleotide sequence exists is indicated.

OROV strain	Variation from F primer	Variation from OROV R primer	Variation from Ec2R primer	Variation from probe
AM01_Manaus|1980	0	0	1	0
AM03_Manaus|1980	0	0	1	0
MA03_PortoFranco|1988	1	0	1	1
PA22_Belem|1980	0	0	1	1
PA28_SerraPelada|1994	0	0	1	1
PA27_SerraPelada|1994	0	1	1	1
PA39_Oriximina|1996	0	0	0	0
MA06_BarraDaCorda|1993	1	0	1	0
PA34_Oriximina|1996	0	0	1	0
PA38_Oriximina|1996	0	0	1	0
PA25_SerraPelada|1994	1	0	1	0
PA26_SerraPelada|1994	2	0	1	0
PA43_PortoDeMoz|2004	0	0	0	0
PA17_Belem|1979	0	1	0	0
PA29_Altamira|1994	0	1	0	0
PA14_Ananindeua|1978	1	1	0	1
RO05_Ariquemes|1991	0	1	0	0
PA50_Maracana|2006	0	0	0	0
PA44_PortoDeMoz|2004	0	0	0	0

PA49_MagalhaesBarata|2006	0	0	0	0
PA47_MagalhaesBarata|2006	0	1	0	0
PA41_Parauapebas|2003	0	0	0	0
PA42_Parauapebas|2003	0	0	0	0
PA05_Braganca|1967	0	1	0	1
PA03_Belem|1961	1	1	0	1
PA04_Belem|1961	1	1	0	1
PA06_Belem|1968	0	0	0	0
PA01_Ipixuna|1960	0	1	0	0
PA09_Maracana|1971	0	0	0	0
PA07_Maracana|1971	0	0	0	0
PA08_Maracana|1971	0	0	0	0
AC02_Xapuri|1996	0	1	0	0
MA02_PortoFranco|1988	1	0	0	0
RO01_MachadinhoDOeste|1990	1	1	0	0
MG01_ArinoH29086s|2000	0	0	0	0
OROV|087|Ecuador|2016	0	2	0	0
OROV|057v|Ecuador|2016	0	2	0	0
OROV|155v|Ecuador|2016	0	2	0	0
OROV|171v|Ecuador|2016	0	2	0	0
OROV|210v|Ecuador|2016	0	2	0	0
OROV|206v|Ecuador|2016	0	2	0	0
OROV|BeH389865|Brazil|1980	0	0	1	0
OROV|BeH505764|Brazil|1991	1	0	0	0
OROV|BeH543100|Brazil|1996	0	1	0	0

OROV|BeH498913|Brazil|1990	1	1	0	0
OROV|GML444672|Panama|1989	0	0	0	0
OROV|GML444477|Panama|1989	0	0	0	0
OROV|GML444479|Panama|1989	0	0	0	0
OROV|GML444911|Panama|1989	0	0	0	0
OROV|GML445252|Panama|1989	0	0	0	0
OROV|GML450093|Panama|1989	0	0	0	0
OROV|BeAn626990|Brazil|Callithrix|2000	0	0	0	0
OROV|BeH472433|Brazil|1988	1	0	0	0
OROV|BeH384192|Brazil|1980	0	0	1	1
OROV|BeH384193|Brazil|1980	0	0	1	1
OROV|BeH472435|Brazil|1988	1	0	1	1
OROV|BeH356898|Brazil|1978	0	0	1	1
OROV|BeH532490|Brazil|1994	0	1	1	1
OROV|BeH532500|Brazil|1994	0	0	1	1
OROV|BeH543091|Brazil|1996	0	0	1	1
OROV|BeH366781|Brazil|1979	1	0	1	1
OROV|BeH385591|Brazil|1980	0	0	1	1
OROV|BeAr473358|Brazil|Culicoides|1988	0	0	1	0
OROV|GML480914|Panama|1989	0	0	0	1
OROV|PAN481126|Panama|1999	0	0	0	1
OROV|TRVL9760|Trinidad_and_Tobago|1955	0	0	0	0
OROV|BeH29086_29090|Brazil|1961	0	0	0	0
OROV|BeH532314|Brazil|1994	1	0	1	0
OROV|BeH532422|Brazil|1994	2	0	1	0

OROV|BeAr136921|Brazil|Culex|1968	0	0	0	0
OROV|BeAn206119|Brazil|sloth|1971	0	0	0	0
OROV|BeAn208402|Brazil|sloth|1971	0	0	0	0
OROV|BeAn208819|Brazil|sloth|1971	0	0	0	0
OROV|BeAn208823|Brazil|sloth|1971	0	0	0	0
OROV|BeAn19991|Brazil|sloth|1960	0	0	0	0
OROV|BeAn19991c|Brazil|sloth|1960	0	0	0	0
OROV|BeH381114|Brazil|1980	0	0	0	0
OROV|BeH669315|Brazil|2003	0	0	0	0
OROV|BeH669314|Brazil|2003	0	0	0	0
OROV|BeH521086|Brazil|1993	1	0	1	0
OROV|BeH543733|Brazil|1996	0	0	1	0
OROV|BeH543857|Brazil|1996	0	0	0	0
OROV|BeH543639|Brazil|1996	0	0	1	0
OROV|BeH543880|Brazil|1996	0	0	1	0
OROV|BeH543760|Brazil|1996	0	0	1	0
OROV|BeH541863|Brazil|1996	0	0	1	0
OROV|BeH355186|Brazil|1978	0	0	1	0
OROV|BeH504514|Brazil|1991	0	0	1	0
OROV|BeH622544|Brazil|2002	0	0	1	0
OROV|BeH544552|Brazil|1996	0	0	1	0
OROV|BeH472204|Brazil|1988	0	0	1	0
OROV|BeH472200|Brazil|1988	0	0	1	0
OROV|BeH475248|Brazil|1988	0	0	1	0
OROV|BeH543618|Brazil|1996	0	0	1	0

OROV|BeH543087|Brazil|1996	0	0	1	0
OROV|BeH543033|Brazil|1996	0	0	1	0
OROV|BeH271815|Brazil|1975	0	0	0	0
OROV|BeH271078|Brazil|1975	0	0	0	0
OROV|BeH390233|Brazil|1980	0	0	0	0
OROV|BeH379693|Brazil|1980	0	0	0	0
OROV|BeH759531|Brazil|2009	1	0	0	0
OROV|BeH758669|Brazil|2009	0	0	0	0
OROV|BeH759018|Brazil|2009	0	0	0	0
OROV|BeH759525|Brazil|2009	1	0	0	0
OROV|BeH759023|Brazil|2009	0	0	0	0
OROV|BeH75955|Brazil|2009	0	0	0	0
OROV|BeH759021|Brazil|2009	0	0	0	0
OROV|BeH759022|Brazil|2009	0	0	0	0
OROV|BeH759024|Brazil|2009	0	0	0	0
OROV|BeH759025|Brazil|2009	0	0	0	0
OROV|BeH759040|Brazil|2009	0	0	0	0
OROV|BeH759146|Brazil|2009	0	0	0	0
OROV|BeH759529|Brazil|2009	0	0	0	0
OROV|BeH759620|Brazil|2009	0	0	0	0
OROV|BeH758687|Brazil|2009	0	0	0	0
OROV|BeH759541|Brazil|2009	0	0	0	0
OROV|BeH759042|Brazil|2009	0	0	0	0
OROV|BeH759044|Brazil|2009	0	0	0	0
OROV|BeH759038|Brazil|2009	0	0	0	0

OROV|BeH759041|Brazil|2009	0	0	0	0
OROV|BeH759043|Brazil|2009	0	0	0	0
OROV|BeH759483|Brazil|2009	0	0	0	0
OROV|BeH759562|Brazil|2009	0	0	0	0
OROV|BeH244576|Brazil|2009	0	1	0	0
OROV|BeH708717|Brazil|2009	0	0	0	0
OROV|BeH706890|Brazil|2009	0	0	0	1
OROV|BeH706893|Brazil|2009	0	0	0	1
OROV|BeAr366927|Brazil|Culicoides|1979	0	1	0	0
OROV|01_812_98|Peru|1998	0	0	0	0
OROV|IQT1690|Peru|1992	0	0	0	0
OROV|IQT1690b|Peru|1995	0	0	0	0
OROV|BeH707157|Brazil|2006	0	0	1	0
OROV|BeH682426|Brazil|2004	0	0	0	0
OROV|BeH708139|Brazil|2006	0	1	0	0
OROV|BeH505768|Brazil|1991	0	1	0	0
OROV|BeH505442|Brazil|1991	0	0	0	0
OROV|BeH505663|Brazil|1991	0	0	0	0
OROV|BeH682431|Brazil|2004	0	0	0	0
OROV|IQT7085|Peru|1998	0	0	0	0
OROV|BeH505805|Brazil|1991	0	0	0	0
OROV|DEI216|Peru|1992	0	0	0	0
OROV|OBS9478|Peru|2000	0	0	0	0
OROV|GML444839|Panama|1989	0	0	0	0
OROV|MD023|Peru|1994	0	0	0	0

OROV|IQT4083|Peru|1997	0	0	0	0
OROV|MD023|Peru|1993	0	0	0	0
OROV|IQT4083b|Peru|1997	0	0	0	0
OROV|IQE7894|Peru|2008	0	1	0	0
OROV|IQT7085b|Peru|1998	0	0	0	0
Count of 1 difference	17	20	41	21
Count of 2 difference	2	6	0	0
Count of >2 difference	0	0	0	0

APPENDIX 8: POSITIONS IN THE OROV GENOME AT WHICH SNPS WERE IDENTIFIED BETWEEN THE PATIENT AND CULTURED GENOMES, FOR EACH ISOLATE

Variance within each genome is also shown as the percentage of reads at that position showing a particular base. Seg. = segment. Seg. pos. = segment position. Cons. = consensus.

Isolate	Seg.	Seg. pos.	Patient cons.	Depth	A (%)	C (%)	G (%)	T (%)	Culture cons.	Depth	A (%)	C (%)	G (%)	T (%)
D-057	M	59	W	21	23.8	0.0	0.0	76.2	A	405	95.1	0.0	0.0	0.0
D-087	S	300	T	16	0.0	0.0	0.0	100.0	C	52430	0.0	99.9	0.0	0.0
D-087	M	59	T	23	0.0	0.0	0.0	100.0	A	85	96.5	0.0	0.0	0.0
D-087	M	307	Y	1055	0.0	23.7	0.0	76.3	T	2419	0.0	0.0	0.0	99.8
D-087	M	1565	Y	286	0.0	21.0	0.0	79.0	T	5365	0.0	0.0	0.0	99.8
D-087	M	1858	G	129	0.0	0.0	100.0	0.0	R	5135	55.5	0.0	44.4	0.0
D-087	M	3097	M	55	29.1	70.9	0.0	0.0	A	6677	99.7	0.0	0.0	0.0
D-087	M	3650	G	28	0.0	0.0	100.0	0.0	A	3710	99.8	0.0	0.0	0.0
D-087	L	122	G	8	0.0	0.0	100.0	0.0	C	2575	0.0	98.6	0.0	1.2

D-087	L	312	R	33	75.8	0.0	24.2	0.0	A	9936	99.8	0.0	0.0	0.0
D-087	L	1855	R	56	25.0	0.0	75.0	0.0	A	3997	99.4	0.0	0.0	0.0
D-087	L	3114	A	315	99.7	0.0	0.0	0.0	C	1923	0.0	99.9	0.0	0.0
D-087	L	3875	T	775	0.0	1.4	0.0	98.6	C	11091	0.0	99.9	0.0	0.0
D-155	S	107	G	19	5.3	0.0	94.7	0.0	A	4060	98.8	0.0	0.0	0.0
D-155	S	880	C	6	0.0	100.0	0.0	0.0	T	14890	0.0	0.0	0.0	99.7
D-155	M	160	G	17	17.6	0.0	82.4	0.0	A	10115	92.9	0.0	6.7	0.0
D-155	M	1586	K	35	0.0	0.0	22.9	77.1	G	49818	0.0	0.0	99.7	0.0
D-155	M	2191	R	14	71.4	0.0	28.6	0.0	G	46084	0.0	0.0	100.0	0.0
D-155	M	2821	W	729	30.0	0.0	0.0	70.0	T	59384	0.0	0.0	0.0	99.9
D-155	M	2931	M	370	23.2	76.8	0.0	0.0	C	55496	0.0	99.8	0.0	0.0
D-155	M	4033	C	123	0.0	98.4	1.6	0.0	G	8704	0.0	0.0	99.9	0.0
D-155	L	6	A	110	100.0	0.0	0.0	0.0	T	587	0.0	0.0	0.0	98.3
D-155	L	1483	R	10	70.0	0.0	30.0	0.0	A	49020	100.0	0.0	0.0	0.0

D-155	L	1664	R	185	65.4	0.0	34.6	0.0	A	45106	99.7	0.0	0.0	0.0
D-155	L	2219	R	119	73.9	0.0	26.1	0.0	A	13427	99.9	0.0	0.0	0.0
D-155	L	3321	S	57	0.0	45.6	54.4	0.0	C	19968	0.0	99.9	0.0	0.0
D-155	L	5126	K	4019	0.0	0.0	26.5	73.5	G	23406	0.0	0.0	99.9	0.0
D-155	L	6206	R	572	75.0	0.0	24.8	0.0	A	8425	99.5	0.0	0.0	0.0
D-171	S	41	G	5	0.0	0.0	100.0	0.0	A	1008	97.7	0.0	0.0	0.0
D-171	M	144	C	71	0.0	95.8	0.0	0.0	T	6256	0.0	0.0	0.0	99.8
D-171	M	1940	Y	2955	0.0	57.5	0.0	42.5	T	86762	0.0	0.0	0.0	99.6
D-171	L	5165	Y	1251	0.0	24.7	0.0	75.3	T	34965	0.0	0.0	0.0	99.7
D-171	L	6298	Y	483	0.0	70.6	0.0	29.4	T	7615	0.0	0.0	0.0	99.4
D-171	L	6308	M	61	44.3	55.7	0.0	0.0	A	7409	99.6	0.0	0.0	0.0
D-206	M	1060	T	9	0.0	0.0	0.0	88.9	A	43090	99.8	0.0	0.0	0.0
D-206	M	3968	C	43	0.0	100.0	0.0	0.0	T	15874	0.0	0.0	0.0	99.6
D-206	L	208	G	109	0.0	0.0	100.0	0.0	T	21634	0.0	0.0	0.0	99.1

D-206	L	222	Y	2013	0.0	69.0	0.0	30.9	C	35017	0.0	98.4	0.0	0.0
D-206	L	223	Y	2040	0.0	31.2	0.0	68.8	T	35739	0.0	1.8	0.0	97.0
D-206	L	1041	R	8270	21.0	0.0	79.0	0.0	G	48064	0.0	0.0	99.6	0.0
D-206	L	2143	S	1024	0.0	63.8	36.1	0.0	C	15102	0.0	99.7	0.0	0.0
D-206	L	4093	R	368	75.8	0.0	24.2	0.0	A	27954	99.7	0.0	0.0	0.0
D-206	L	4381	S	110	0.0	66.4	33.6	0.0	G	30517	0.0	0.0	99.9	0.0
D-210	M	3929	Y	5066	0.0	53.2	0.0	46.8	C	17041	0.0	100.0	0.0	0.0
D-210	M	4376	W	230	53.0	0.0	0.0	46.5	T	365	0.0	0.0	0.0	99.5
D-210	L	91	T	49	0.0	0.0	0.0	98.0	C	5779	0.0	99.7	0.0	0.0
D-210	L	217	W	4454	29.8	0.0	0.0	68.4	T	25397	0.0	1.3	0.0	94.0
D-210	L	3238	R	4655	70.3	0.0	29.7	0.0	A	26664	99.8	0.0	0.0	0.0
D-210	L	4111	R	466	36.3	0.0	63.7	0.0	G	29698	0.0	0.0	99.9	0.0
D-210	L	5585	G	967	2.5	0.0	97.5	0.0	A	20436	99.8	0.0	0.0	0.0

APPENDIX 9: MULTIPLEX TILING PCR PRIMER DETAILS

Tm = melting temperature.

Primer name	Sequence (5’ to 3’)	Primer pool	Length	Tm	GC%	Genome segment	Segment start position	Segment end position
OROV_S_1_LEFT	CATTTTCAACGATGTACCACAACGG	1	25	61.34	44	S	55	80
OROV_S_1_RIGHT	TACAACCCTTCACCTCTGCCAA	1	22	61.56	50	S	435	413
OROV_S_2_LEFT	TGTCAGGATACCTAGCTCGCTG	2	22	61.33	54.55	S	327	349
OROV_S_2_RIGHT	TCCAAATTGGCGCAAGAAGTCT	2	22	61.08	45.45	S	728	706
OROV_S_3_LEFT	GGATGCGTGAAGAAATAGTTGCTG	1	24	60.73	45.83	S	615	639
OROV_S_3_RIGHT	GTGTGCTCCCAATTCAAAAATACGT	1	25	60.79	40	S	948	923
OROV_M_1_LEFT	GCAACAAACAGTGACAATGGCG	2	22	61.67	50	M	16	37
OROV_M_1_RIGHT	ACTGGGTTGCATTCAGACCAAT	2	22	60.49	45.45	M	300	278
OROV_M_2_LEFT	TGTTAAGAGTACAACTGCCTTTAGTAAGA	1	29	60.44	34.48	M	195	224
OROV_M_2_RIGHT	CAACCCCTATGCTGTCGAAAGC	1	22	61.83	54.55	M	594	572

OROV_M_3_LEFT	GTCGGAACTACTTCAACATCAGGT	2	24	60.56	45.83	M	457	481
OROV_M_3_RIGHT	TGGGCAGCTAGTAAAAGGGTGT	2	22	61.63	50	M	847	825
OROV_M_4_LEFT	CTTCTGCCATTGTTTTATCCAGTAACC	1	27	60.84	40.74	M	739	766
OROV_M_4_RIGHT	ATTCACCTGCTCTGCCAGTTCT	1	22	61.95	50	M	1099	1077
OROV_M_5_LEFT	TGGCTTAATATTGATGGAATTTGTTTCACC	2	30	61.42	33.33	M	996	1026
OROV_M_5_RIGHT	GCAAGATTCCCTTTGAACATGCA	2	23	60.31	43.48	M	1384	1361
OROV_M_6_LEFT	GACTAACAAATGCGGGAGTTGC	1	22	60.41	50	M	1278	1300
OROV_M_6_RIGHT	TCATTCTGTGTGCATCTTGAGCA	1	23	60.81	43.48	M	1697	1674
OROV_M_7_LEFT	TGATCTGCTTTCAAAGAACTTAATCACA	2	28	60.01	32.14	M	1584	1612
OROV_M_7_RIGHT	AGTCAGACCTATAAGCTGCAGCA	2	23	61.45	47.83	M	1946	1923
OROV_M_8_LEFT	GCAGCAGGCATAATTACAAAATGATATGT	1	29	61.38	34.48	M	1814	1843
OROV_M_8_RIGHT	AGGGGTTTGACTTAGGAATTTCGT	1	24	60.2	41.67	M	2201	2177
OROV_M_9_LEFT	TGGTCGGTGTGCTAAAATTTGCT	2	23	61.56	43.48	M	2090	2113
OROV_M_9_RIGHT	ATACCAGTTTGCATGTCGGCAG	2	22	61.52	50	M	2502	2480

OROV_M_10_LEFT	GCCACTGCAACTTAGAATTTACTGC	1	25	61.13	44	M	2393	2418
OROV_M_10_RIGHT	TGTTCCTATTTCGGATTCAATTGCCT	1	26	61.31	38.46	M	2800	2774
OROV_M_11_LEFT	TGCAACTGGGACAAGACTTATAAGG	2	25	60.8	44	M	2698	2723
OROV_M_11_RIGHT	AGGTCCAGTTGTGTACACTTTCTG	2	24	60.68	45.83	M	3058	3034
OROV_M_12_LEFT	TTAGGCGTCGGCTACCACTTAG	1	22	61.84	54.55	M	2944	2966
OROV_M_12_RIGHT	TGAAAAGATGCACTCAATTTATCCCCA	1	27	61.46	37.04	M	3381	3354
OROV_M_13_LEFT	AAAAGATTGGTAGTGAAGCATCGC	2	24	60.14	41.67	M	3260	3284
OROV_M_13_RIGHT	TGGATTCAGTCTGGTGCAAGAC	2	22	60.55	50	M	3625	3603
OROV_M_14_LEFT	TGGGTCTGGCAATCCTAAATTTGA	1	24	60.51	41.67	M	3513	3537
OROV_M_14_RIGHT	TGGGGTGAGATTACAATGTTGCT	1	23	60.25	43.48	M	3903	3880
OROV_M_15_LEFT	GCTGAAGGCATATCATGTTCTATAAATGC	2	29	61.27	37.93	M	3796	3825
OROV_M_15_RIGHT	AGCCCAATATTTCCCTAATCCTGAAA	2	26	60.36	38.46	M	4159	4133
OROV_M_16_LEFT	AAAAGAAGAAGACCTCCAATGTGGA	1	25	60.4	40	M	4053	4078
OROV_M_16_RIGHT	AGTGTGCTACCAACAACAATTTTTGAC	1	27	61.53	37.04	M	4384	4358

OROV_L_1_LEFT	ACAATCTCAAAATGTCGCAACTGTT	2	25	60.45	36	L	33	57
OROV_L_1_RIGHT	TTATCAGGTGTGCAAAAGCGCA	2	22	61.65	45.45	L	276	254
OROV_L_2_LEFT	CAGAGCTGCAAACCTTGAGTATAGA	1	25	60.63	44	L	168	193
OROV_L_2_RIGHT	TCATCATCCCGGAATTTGCCAA	1	22	60.62	45.45	L	564	542
OROV_L_3_LEFT	AGATTTCATGAATACAATCGGGCCA	2	25	60.92	40	L	465	490
OROV_L_3_RIGHT	CAGCCAGCTGAAATTTGGTCCT	2	22	61.41	50	L	879	857
OROV_L_4_LEFT	AGGGAGTGATGTCTAAGTATGGTGA	1	25	60.58	44	L	758	783
OROV_L_4_RIGHT	TGCACCGGTTCTATTTTCCTGT	1	22	60.22	45.45	L	1191	1169
OROV_L_5_LEFT	TGATGGATATATCGTCAGACATCAAAAAGT	2	30	61.08	33.33	L	1082	1112
OROV_L_5_RIGHT	CCCACATTTCTACACTGCAGGC	2	22	61.77	54.55	L	1511	1489
OROV_L_6_LEFT	CAAGTCACACATAACTTGTCTCAAGTT	1	27	60.2	37.04	L	1408	1435
OROV_L_6_RIGHT	GCCTGTTGTTGTCTTGAAAGTGG	1	23	60.73	47.83	L	1789	1766
OROV_L_7_LEFT	GCTTAGTGATGCCAAGCTCAGA	2	22	60.68	50	L	1655	1677
OROV_L_7_RIGHT	GCTAGAAACTGCCAATGAGTTCATG	2	25	60.68	44	L	2023	1998

OROV_L_8_LEFT	AGAGTCTAGAGTTTGATAAGTTACTAGGCT	1	30	60.99	36.67	L	1898	1928
OROV_L_8_RIGHT	TGCTTTTCATGCAATCCTTTGGAA	1	24	60.2	37.5	L	2310	2286
OROV_L_9_LEFT	AAATCCATTTGGTTCCCGGGAA	2	22	60.49	45.45	L	2212	2234
OROV_L_9_RIGHT	ACCAATTTTAATGCATGATTTCGAGCT	2	27	60.85	33.33	L	2572	2545
OROV_L_10_LEFT	TAATTTTGTGAGGAGCCGGGTG	1	22	60.88	50	L	2472	2494
OROV_L_10_RIGHT	TGTCCTTTGTTGAAGAACCCGA	1	22	60.09	45.45	L	2886	2864
OROV_L_11_LEFT	TGAGGATTTGAAACAATCTATCCCAGA	2	27	60.31	37.04	L	2709	2736
OROV_L_11_RIGHT	AAGACCCGGATTGCAGGTTTTC	2	22	61.4	50	L	3122	3100
OROV_L_12_LEFT	TGATAAGCGAACCAGGTGACTCT	1	23	61.38	47.83	L	2996	3019
OROV_L_12_RIGHT	ACCCTCTGGTCCAATATCGTAGTG	1	24	61.48	50	L	3357	3333
OROV_L_13_LEFT	TCTTATATCCTGCTGAGAGGAAGAGA	2	26	60.18	42.31	L	3248	3274
OROV_L_13_RIGHT	ACATTGTCATCTGGCAACTTGTTTTG	2	26	61.4	38.46	L	3618	3592
OROV_L_14_LEFT	ACATTATTAGAGGGGGAAGCCCT	1	23	60.64	47.83	L	3517	3540
OROV_L_14_RIGHT	ACGTGGTGTGAGTTATCCAGTGA	1	23	61.57	47.83	L	3923	3900

OROV_L_15_LEFT	AGGCTATCTGCAACACAAACCG	2	22	61.45	50	L	3826	3848
OROV_L_15_RIGHT	AAGCCTCAGAATGTCGATCTGC	2	22	60.74	50	L	4195	4173
OROV_L_16_LEFT	AGGAAACTATCATCTCCAATCTTGCA	1	26	60.35	38.46	L	4087	4113
OROV_L_16_RIGHT	TGTGCTGGATTTTGTATTGACAGAGA	1	26	60.97	38.46	L	4518	4492
OROV_L_17_LEFT	TCCAGAGTTATTGGTCACAAAAGGTG	2	26	61.41	42.31	L	4404	4430
OROV_L_17_RIGHT	GCATTTTGCATGCTGATTGTCCT	2	23	60.93	43.48	L	4835	4812
OROV_L_18_LEFT	CGCCTTCTGTCTCATGAATGATCC	1	24	61.56	50	L	4725	4749
OROV_L_18_RIGHT	TCGTAACACACTTGGTAAAATCTAGTCA	1	28	60.69	35.71	L	5094	5066
OROV_L_19_LEFT	TCATACAAAGCACAAAACTCAGAGAGA	2	27	60.9	37.04	L	4967	4994
OROV_L_19_RIGHT	TCAGATGCCAAGAAAGTATCGGC	2	23	60.99	47.83	L	5349	5326
OROV_L_20_LEFT	ACACAAGGCACAAATCTCGTCC	1	22	61.39	50	L	5247	5269
OROV_L_20_RIGHT	AGCTGCCTGGAATAGCCACTTA	1	22	61.49	50	L	5619	5597
OROV_L_21_LEFT	AGTTTGATGCAGATAAATCAGACGAAAA	2	28	60.32	32.14	L	5507	5535
OROV_L_21_RIGHT	TACTGCAACAGGACACACAGGA	2	22	61.54	50	L	5926	5904

OROV_L_22_LEFT	GGTACTTCTATTCTATATTGCCCACCC	1	27	60.8	44.44	L	5813	5840
OROV_L_22_RIGHT	GCCATTTGGTCATTTTCACTGCC	1	23	61.42	47.83	L	6225	6202
OROV_L_23_LEFT	GTTAATGAAATCCACATCCTTATTGAGCT	2	29	60.44	34.48	L	6111	6140
OROV_L_23_RIGHT	TCTGTGGACCACTGATTCGTCT	2	22	61.08	50	L	6495	6473
OROV_L_24_LEFT	TCGACTTTCTTGACATGGGGTTT	1	23	60.43	43.48	L	6392	6415
OROV_L_24_RIGHT	CTGCCAGTGATCTTTTCTCGCT	1	22	60.93	50	L	6752	6730

BIBLIOGRAPHY

1. Murray CJL, Barber RM, Foreman KJ, Ozgoren AA, Abd-Allah F, Abera SF, et al. Global, regional, and national disability-adjusted life years (DALYs) for 306 diseases and injuries and healthy life expectancy (HALE) for 188 countries, 1990–2013: quantifying the epidemiological transition. The Lancet. 2015 Nov 28;386(10009):2145–91.

2. Reperant LA, Osterhaus ADME. AIDS, Avian flu, SARS, MERS, Ebola, Zika… what next? Vaccine. 2017 Aug 16;35(35 Pt A):4470–4.

3. Halliday JEB, Hampson K, Hanley N, Lembo T, Sharp JP, Haydon DT, et al. Driving improvements in emerging disease surveillance through locally relevant capacity strengthening. Science. 2017 14;357(6347):146–8.

4. World Health Organisation, Regional Office for South-East Asia. A brief guide to emerging infectious diseases and zoonoses [Internet]. 2014 [cited 2019 Nov 2]. Available from: https://apps.who.int/iris/handle/10665/204722

5. Jones KE, Patel NG, Levy MA, Storeygard A, Balk D, Gittleman JL, et al. Global trends in emerging infectious diseases. Nature. 2008 Feb 21;451(7181):990–3.

6. Woolhouse M, Gaunt E. Ecological origins of novel human pathogens. Crit Rev Microbiol. 2007;33(4):231–42.

7. Choi KH. Viral Polymerases. Adv Exp Med Biol. 2012;726:267–304.

8. Domingo E, Holland JJ. RNA virus mutations and fitness for survival. Annu Rev Microbiol. 1997;51:151–78.

9. Jenkins GM, Rambaut A, Pybus OG, Holmes EC. Rates of molecular evolution in RNA viruses: a quantitative phylogenetic analysis. J Mol Evol. 2002 Feb;54(2):156–65.

10. Hanada K, Suzuki Y, Gojobori T. A large variation in the rates of synonymous substitution for RNA viruses and its relationship to a diversity of viral infection and transmission modes. Mol Biol Evol. 2004 Jun;21(6):1074–80.

11. Hockett RD, Kilby JM, Derdeyn CA, Saag MS, Sillers M, Squires K, et al. Constant mean viral copy number per infected cell in tissues regardless of high, low, or undetectable plasma HIV RNA. J Exp Med. 1999 May 17;189(10):1545–54.

12. Huang SW, Hung SJ, Wang JR. Application of deep sequencing methods for inferring viral population diversity. J Virol Methods. 2019;266:95–102.

13. World Health Organization. Zoonoses [Internet]. [cited 2019 Nov 22]. Available from: http://www.who.int/topics/zoonoses/en/

14. Gardy JL, Loman NJ. Towards a genomics-informed, real-time, global pathogen surveillance system. Nat Rev Genet. 2018 Jan;19(1):9–20.

15. Morse SS, Mazet JAK, Woolhouse M, Parrish CR, Carroll D, Karesh WB, et al. Prediction and prevention of the next pandemic zoonosis. Lancet. 2012 Dec 1;380(9857):1956–65.

16. Institute of Medicine Committee on Emerging Microbial Threats to Health. Emerging Infections: Microbial Threats to Health in the United States. National Academies Press; 1992. 309 p.

17. Institute of Medicine (US) Committee on Emerging Microbial Threats to Health in the 21st Century. Microbial Threats to Health: Emergence, Detection, and Response [Internet]. Smolinski MS, Hamburg MA, Lederberg J, editors. Washington (DC): National Academies Press (US); 2003 [cited 2019 Nov 22]. Available from: http://www.ncbi.nlm.nih.gov/books/NBK221486/

18. Murray KA, Preston N, Allen T, Zambrana-Torrelio C, Hosseini PR, Daszak P. Global biogeography of human infectious diseases. Proc Natl Acad Sci USA. 2015 Oct 13;112(41):12746–51.

19. Bogich TL, Chunara R, Scales D, Chan E, Pinheiro LC, Chmura AA, et al. Preventing pandemics via international development: a systems approach. PLOS Medicine. 2012 Dec 11;9(12):e1001354.

20. Ann Marie Kimball. Emerging infections of international public health importance [Internet]. University of Washington Department of Health Services. 2004 [cited 2019 Nov 22]. Available from: https://depts.washington.edu/eminf/2004/mod1topic1/

21. Sippy R, Herrera D, Gaus D, Gangnon RE, Patz JA, Osorio JE. Seasonal patterns of dengue fever in rural Ecuador: 2009-2016. PLoS Negl Trop Dis [Internet]. 2019 May 6 [cited 2019 Oct 31];13(5). Available from: https://www.ncbi.nlm.nih.gov/pmc/articles/PMC6522062/

22. Bhatt S, Gething PW, Brady OJ, Messina JP, Farlow AW, Moyes CL, et al. The global distribution and burden of dengue. Nature. 2013 Apr 25;496(7446):504–7.

23. Tun-Lin W, Burkot TR, Kay BH. Effects of temperature and larval diet on development rates and survival of the dengue vector Aedes aegypti in north Queensland, Australia. Med Vet Entomol. 2000 Mar;14(1):31–7.

24. Johansson MA. Chikungunya on the move. Trends in parasitology. 2015 Feb;31(2):43.

25. Charrel RN, Lamballerie X de, Raoult D. Seasonality of mosquitoes and chikungunya in Italy. The Lancet Infectious Diseases. 2008 Jan 1;8(1):5–6.

26. Huber JH, Childs ML, Caldwell JM, Mordecai EA. Seasonal temperature variation influences climate suitability for dengue, chikungunya, and Zika transmission.

PLoS Neglected Tropical Diseases [Internet]. 2018 May [cited 2019 Apr 14];12(5). Available from: https://www.ncbi.nlm.nih.gov/pmc/articles/PMC5963813/

27. Geoghegan JL, Walker PJ, Duchemin JB, Jeanne I, Holmes EC. Seasonal drivers of the epidemiology of arthropod-borne viruses in Australia. PLoS Neglected Tropical Diseases [Internet]. 2014 Nov [cited 2019 Apr 14];8(11). Available from: https://www.ncbi.nlm.nih.gov/pmc/articles/PMC4239014/

28. Travassos da Rosa JF, de Souza WM, de Paula Pinheiro F, Figueiredo ML, Cardoso JF, Acrani GO, et al. Oropouche virus: clinical, epidemiological, and molecular aspects of a neglected Orthobunyavirus. Am J Trop Med Hyg. 2017 Feb 6;

29. Hallam HJ, Hallam S, Rodriguez SE, Barrett ADT, Beasley DWC, Chua A, et al. Baseline mapping of Lassa fever virology, epidemiology and vaccine research and development. npj Vaccines. 2018 Mar 20;3(1):11.

30. Isere EE, Fatiregun A, Ilesanmi O, Ijarotimi I, Egube B, Adejugbagbe A, et al. Lessons learnt from epidemiological investigation of lassa fever outbreak in a southwest state of Nigeria December 2015 to April 2016. PLoS Curr [Internet]. 2018 Jun 29 [cited 2018 Jul 2]; Available from: http://currents.plos.org/outbreaks/article/lessons-learnt-from-epidemiological-investigation-of-lassa-fever-outbreak-in-a-southwest-state-of-nigeria-december-2015-to-april-2016/

31. Epopa PS, Collins CM, North A, Millogo AA, Benedict MQ, Tripet F, et al. Seasonal malaria vector and transmission dynamics in western Burkina Faso. Malar J. 2019 Apr 2;18(1):113.

32. Schmidt JP, Park AW, Kramer AM, Han BA, Alexander LW, Drake JM. Spatiotemporal fluctuations and triggers of Ebola virus spillover. Emerging Infectious Diseases journal. 2017 Mar;23(3):415–22.

33. Pinzon JE, Wilson JM, Tucker CJ, Arthur R, Jahrling PB, Formenty P. Trigger events: enviroclimatic coupling of Ebola hemorrhagic fever outbreaks. Am J Trop Med Hyg. 2004 Nov;71(5):664–74.

34. Tucker CJ, Wilson J, Mahoney R, Anyamba A, Linthicum K, Myers M. Climatic and ecological context of the 1994-1996 Ebola outbreaks. Photogrammetric Engineering and Remote Sensing. 2002 Feb;78(2):6.

35. World Health Organization. WHO factsheet on HIV/AIDS [Internet]. 2019 [cited 2019 Nov 22]. Available from: https://www.who.int/news-room/fact-sheets/detail/hiv-aids

36. World Health Organization. WHO factsheet “The top 10 causes of death” [Internet]. 2018 [cited 2019 Nov 22]. Available from: https://www.who.int/news-room/fact-sheets/detail/the-top-10-causes-of-death

37. King DA, Peckham C, Waage JK, Brownlie J, Woolhouse MEJ. Epidemiology. Infectious diseases: preparing for the future. Science. 2006 Sep 8;313(5792):1392–3.

38. Hui DSC, Chan MCH, Wu AK, Ng PC. Severe acute respiratory syndrome (SARS): epidemiology and clinical features. Postgrad Med J. 2004 Jul;80(945):373–81.

39. Fineberg HV. Pandemic preparedness and response - lessons from the H1N1 influenza of 2009. N Engl J Med. 2014 Apr 3;370(14):1335–42.

40. Carroll MW, Matthews DA, Hiscox JA, Elmore MJ, Pollakis G, Rambaut A, et al. Temporal and spatial analysis of the 2014-2015 Ebola virus outbreak in West Africa. Nature. 2015 Aug 6;524(7563):97–101.

41. Coltart CEM, Lindsey B, Ghinai I, Johnson AM, Heymann DL. The Ebola outbreak, 2013-2016: old lessons for new epidemics. Philos Trans R Soc Lond, B, Biol Sci. 2017 May 26;372(1721).

42. Grubaugh ND, Ladner JT, Kraemer MUG, Dudas G, Tan AL, Gangavarapu K, et al. Genomic epidemiology reveals multiple introductions of Zika virus into the United States. Nature. 2017 15;546(7658):401–5.

43. Giron S, Franke F, Decoppet A, Cadiou B, Travaglini T, Thirion L, et al. Vector-borne transmission of Zika virus in Europe, southern France, August 2019. Eurosurveillance. 2019 Nov 7;24(45):1900655.

44. Robinson ML, Manabe YC. Reducing uncertainty for acute febrile illness in resource-limited settings: the current diagnostic landscape. Am J Trop Med Hyg. 2017 Jun;96(6):1285–95.

45. Institute for Health Metrics and Evaluation. GBD Compare | IHME Viz Hub [Internet]. 2017 [cited 2019 Aug 11]. Available from: http://vizhub.healthdata.org/gbd-compare

46. Allwinn R, Doerr HW, Emmerich P, Schmitz H, Preiser W. Cross-reactivity in flavivirus serology: new implications of an old finding? Med Microbiol Immunol. 2002 Mar;190(4):199–202.

47. Tanabe ISB, Tanabe ELL, Santos EC, Martins WV, Araújo IMTC, Cavalcante MCA, et al. Cellular and molecular immune response to chikungunya virus infection. Front Cell Infect Microbiol. 2018 Oct;10(8):345.

48. Brown JR, Bharucha T, Breuer J. Encephalitis diagnosis using metagenomics: application of next generation sequencing for undiagnosed cases. J Infect. 2018 Mar;76(3):225–40.

49. International Committee on Taxonomy of Viruses (ICTV). Virus Taxonomy: 2018b Release [Internet]. 2018 [cited 2019 Apr 14]. Available from: https://talk.ictvonline.org/taxonomy/

50. Mason PJ, Haddow AJ. An epidemic of virus disease in Southern Province, Tanganyika Territory, in 1952-53; an additional note on Chikungunya virus isolations and serum antibodies. Trans R Soc Trop Med Hyg. 1957 May;51(3):238–40.

51. Ross RW. The Newala epidemic: III. The virus: isolation, pathogenic properties and relationship to the epidemic. The Journal of Hygiene. 1956 Jun;54(2):177–91.

52. Vairo F, Haider N, Kock R, Ntoumi F, Ippolito G, Zumla A. Chikungunya: epidemiology, pathogenesis, clinical features, management, and prevention. Infect Dis Clin North Am. 2019 Dec;33(4):1003–25.

53. World Health Organization. WHO factsheet on Chikungunya [Internet]. 2017 [cited 2018 Jun 26]. Available from: http://www.who.int/news-room/fact-sheets/detail/chikungunya

54. Weaver SC, Winegar R, Manger ID, Forrester NL. Alphaviruses: Population genetics and determinants of emergence. Antiviral Res. 2012 Jun;94(3):242–57.

55. Althouse BM, Guerbois M, Cummings DAT, Diop OM, Faye O, Faye A, et al. Role of monkeys in the sylvatic cycle of chikungunya virus in Senegal. Nature Communications. 2018 Mar 13;9(1):1–10.

56. Tsetsarkin KA, Weaver SC. Sequential adaptive mutations enhance efficient vector switching by chikungunya virus and its epidemic emergence. PLoS Pathog [Internet]. 2011 Dec 8 [cited 2019 Nov 11];7(12). Available from: https://www.ncbi.nlm.nih.gov/pmc/articles/PMC3234230/

57. Tsetsarkin KA, Vanlandingham DL, McGee CE, Higgs S. A single mutation in chikungunya virus affects vector specificity and epidemic potential. PLoS Pathog. 2007 Dec;3(12):e201.

58. Vazeille M, Moutailler S, Coudrier D, Rousseaux C, Khun H, Huerre M, et al. Two chikungunya isolates from the outbreak of La Reunion (Indian Ocean) exhibit different patterns of infection in the mosquito, Aedes albopictus. PLoS One [Internet]. 2007 Nov 14 [cited 2019 Nov 11];2(11). Available from: https://www.ncbi.nlm.nih.gov/pmc/articles/PMC2064959/

59. Center for Disease Control and Prevention. Chikungunya virus geographic distribution [Internet]. 2019 [cited 2019 Nov 11]. Available from: https://www.cdc.gov/chikungunya/geo/index.html

60. Tsetsarkin KA, Chen R, Sherman MB, Weaver SC. Chikungunya virus: evolution and genetic determinants of emergence. Curr Opin Virol. 2011 Oct 1;1(4):310–7.

61. Noridah O, Paranthaman V, Nayar SK, Masliza M, Ranjit K, Norizah I, et al. Outbreak of chikungunya due to virus of Central/East African genotype in Malaysia. Med J Malaysia. 2007 Oct;62(4):323–8.

62. Rezza G, Nicoletti L, Angelini R, Romi R, Finarelli AC, Panning M, et al. Infection with chikungunya virus in Italy: an outbreak in a temperate region. Lancet. 2007 Dec 1;370(9602):1840–6.

63. Grandadam M, Caro V, Plumet S, Thiberge J-M, Souarès Y, Failloux A-B, et al. Chikungunya Virus, Southeastern France. Emerg Infect Dis. 2011 May;17(5):910–3.

64. Wahid B, Ali A, Rafique S, Idrees M. Global expansion of chikungunya virus: mapping the 64-year history. Int J Infect Dis. 2017 May;58:69–76.

65. Neto ASL, Sousa GS, Nascimento OJ, Castro MC. Chikungunya-attributable deaths: A neglected outcome of a neglected disease. PLOS Neglected Tropical Diseases. 2019 Sep 12;13(9):e0007575.

66. Powers AM, Logue CH. Changing patterns of chikungunya virus: re-emergence of a zoonotic arbovirus. J Gen Virol. 2007 Sep;88(Pt 9):2363–77.

67. Ganesan VK, Duan B, Reid SP. Chikungunya virus: pathophysiology, mechanism, and modeling. Viruses. 2017 01;9(12).

68. Sourisseau M, Schilte C, Casartelli N, Trouillet C, Guivel-Benhassine F, Rudnicka D, et al. Characterization of reemerging chikungunya virus. PLoS Pathog. 2007 Jun;3(6):e89.

69. Yactayo S, Staples JE, Millot V, Cibrelus L, Ramon-Pardo P. Epidemiology of Chikungunya in the Americas. J Infect Dis. 2016 Dec 15;214(suppl 5):S441–5.

70. Natrajan MS, Rojas A, Waggoner JJ. Beyond fever and pain: diagnostic methods for chikungunya virus. J Clin Microbiol. 2019 Jun;57(6).

71. Jerome H, Taylor C, Sreenu VB, Klymenko T, Jackson C, Davis C, et al. Metagenomic next-generation sequencing aids the diagnosis of viral infections in febrile returning travellers. J Infect. 2019 Oct;79(4):383–8.

72. Her Z, Malleret B, Chan M, Ong EKS, Wong S-C, Kwek DJC, et al. Active infection of human blood monocytes by Chikungunya virus triggers an innate immune response. J Immunol. 2010 May 15;184(10):5903–13.

73. Chen W, Foo S-S, Sims NA, Herrero LJ, Walsh NC, Mahalingam S. Arthritogenic alphaviruses: new insights into arthritis and bone pathology. Trends Microbiol. 2015 Jan;23(1):35–43.

74. Anderson CR, Downs WG, Wattley GH, Ahin NW, Reese AA. Mayaro virus: a new human disease agent. II. Isolation from blood of patients in Trinidad, B.W.I. Am J Trop Med Hyg. 1957 Nov;6(6):1012–6.

75. Halsey ES, Siles C, Guevara C, Vilcarromero S, Jhonston EJ, Ramal C, et al. Mayaro virus infection, Amazon Basin region, Peru, 2010-2013. Emerging Infect Dis. 2013 Nov;19(11):1839–42.

76. Powers AM, Aguilar PV, Chandler LJ, Brault AC, Meakins TA, Watts D, et al. Genetic relationships among Mayaro and Una viruses suggest distinct patterns of transmission. Am J Trop Med Hyg. 2006 Sep;75(3):461–9.

77. Causey OR, Maroja OM. Mayaro virus: a new human disease agent. III. Investigation of an epidemic of acute febrile illness on the river Guama in Pará, Brazil, and isolation of Mayaro virus as causative agent. Am J Trop Med Hyg. 1957 Nov;6(6):1017–23.

78. Schaeffer M, Gajdusek DC, Lema AB, Eichenwald H. Epidemic jungle fevers among Okinawan colonists in the Bolivian rain forest. I. Epidemiology. Am J Trop Med Hyg. 1959 May;8(3):372–96.

79. LeDuc JW, Pinheiro FP, Travassos da Rosa AP. An outbreak of Mayaro virus disease in Belterra, Brazil. II. Epidemiology. Am J Trop Med Hyg. 1981 May;30(3):682–8.

80. Pinheiro FP, Freitas RB, Travassos da Rosa JF, Gabbay YB, Mello WA, LeDuc JW. An outbreak of Mayaro virus disease in Belterra, Brazil. I. Clinical and virological findings. Am J Trop Med Hyg. 1981 May;30(3):674–81.

81. Downs WG, Anderson CR. Distribution of immunity to mayaro virus infection in the West Indies. West Indian Medical Journal. 1958;7(3):190–4.

82. Aitken TH, Downs WG, Anderson CR, Spence L, Casals J. Mayaro virus isolated from a Trinidadian mosquito, Mansonia venezuelensis. Science. 1960 Apr 1;131(3405):986.

83. Groot H, Morales A, Vidales H. Virus isolations from forest mosquitoes in San Vicente de Chucuri, Colombia. Am J Trop Med Hyg. 1961 May;10:397–402.

84. Karbaat J, Jonkers AH, Spence L. Arbovirus infections in Dutch military personnel stationed in Surinam: a preliminary study. Trop Geogr Med. 1964 Dec;16:370–6.

85. Talarmin A, Chandler LJ, Kazanji M, de Thoisy B, Debon P, Lelarge J, et al. Mayaro virus fever in French Guiana: isolation, identification, and seroprevalence. Am J Trop Med Hyg. 1998 Sep;59(3):452–6.

86. de Thoisy B, Gardon J, Salas RA, Morvan J, Kazanji M. Mayaro virus in wild mammals, French Guiana. Emerging Infect Dis. 2003 Oct;9(10):1326–9.

87. Izurieta RO, Macaluso M, Watts DM, Tesh RB, Guerra B, Cruz LM, et al. Hunting in the rainforest and mayaro virus infection: An emerging Alphavirus in Ecuador. J Glob Infect Dis. 2011 Oct;3(4):317–23.

88. Terzian ACB, Auguste AJ, Vedovello D, Ferreira MU, da Silva-Nunes M, Sperança MA, et al. Isolation and characterization of Mayaro virus from a human in Acre, Brazil. Am J Trop Med Hyg. 2015 Feb;92(2):401–4.

89. Navarrete-Espinosa J, Gómez-Dantés H. [Arbovirus causing hemorrhagic fever at IMSS]. Rev Med Inst Mex Seguro Soc. 2006 Aug;44(4):347–53.

90. White SK, Mavian C, Elbadry MA, Beau De Rochars VM, Paisie T, Telisma T, et al. Detection and phylogenetic characterization of arbovirus dual-infections among persons during a chikungunya fever outbreak, Haiti 2014. PLoS Negl Trop Dis. 2018;12(5):e0006505.

91. Lednicky J, Rochars VMBD, Elbadry M, Loeb J, Telisma T, Chavannes S, et al. Mayaro virus in child with acute febrile illness, Haiti, 2015. Emerging Infectious Diseases. 2016 Nov;22(11):2000–2.

92. Hoch AL, Peterson NE, LeDuc JW, Pinheiro FP. An outbreak of Mayaro virus disease in Belterra, Brazil. III. Entomological and ecological studies. Am J Trop Med Hyg. 1981 May;30(3):689–98.

93. Vasconcelos PFC, Calisher CH. Emergence of human arboviral diseases in the Americas, 2000-2016. Vector Borne Zoonotic Dis. 2016;16(5):295–301.

94. Long KC, Ziegler SA, Thangamani S, Hausser NL, Kochel TJ, Higgs S, et al. Experimental transmission of Mayaro virus by Aedes aegypti. Am J Trop Med Hyg. 2011 Oct;85(4):750–7.

95. Auguste AJ, Liria J, Forrester N, Giambalvo D, Moncada M, Long K, et al. Evolutionary and Ecological Characterization of mayaro virus strains isolated during an outbreak, Venezuela, 2010. Emerging Infectious Diseases. 21(10):1742–50.

96. Pezzi L, Rodriguez-Morales AJ, Reusken CB, Ribeiro GS, LaBeaud AD, Lourenço-de-Oliveira R, et al. GloPID-R report on chikungunya, o'nyong-nyong and Mayaro virus, part 3: Epidemiological distribution of Mayaro virus. Antiviral Res. 2019 Sep 20;172:104610.

97. Paniz-Mondolfi AE, Rodriguez-Morales AJ, Blohm G, Marquez M, Villamil-Gomez WE. ChikDenMaZika Syndrome: the challenge of diagnosing arboviral infections in the midst of concurrent epidemics. Ann Clin Microbiol Antimicrob [Internet]. 2016 Jul 22 [cited 2019 Nov 11];15. Available from: https://www.ncbi.nlm.nih.gov/pmc/articles/PMC4957883/

98. Pezzi L, Reusken CB, Weaver SC, Drexler JF, Busch M, LaBeaud AD, et al. GloPID-R report on Chikungunya, O'nyong-nyong and Mayaro virus, part I: Biological diagnostics. Antiviral Res. 2019 Jun;166:66–81.

99. Santiago FW, Halsey ES, Siles C, Vilcarromero S, Guevara C, Silvas JA, et al. Long-term arthralgia after mayaro virus infection correlates with sustained pro-inflammatory cytokine response. PLOS Neglected Tropical Diseases. 2015 Oct 23;9(10):e0004104.

100. Assunção-Miranda I, Cruz-Oliveira C, Da Poian AT. Molecular mechanisms involved in the pathogenesis of alphavirus-induced arthritis. Biomed Res Int. 2013;2013:973516.

101. Hallam SJ, Koma T, Maruyama J, Paessler S. Review of Mammarenavirus biology and replication. Front Microbiol [Internet]. 2018 Aug 3 [cited 2019 Mar 29];9. Available from: https://www.ncbi.nlm.nih.gov/pmc/articles/PMC6085440/

102. Frame JD, Baldwin JM, Gocke DJ, Troup JM. Lassa fever, a new virus disease of man from West Africa. I. Clinical description and pathological findings. Am J Trop Med Hyg. 1970 Jul;19(4):670–6.

103. Center for Disease Control and Prevention. Lassa fever [Internet]. 2019 [cited 2019 Mar 29]. Available from: https://www.cdc.gov/vhf/lassa/index.html

104. World Health Organization. Lassa fever [Internet]. [cited 2019 Aug 16]. Available from: http://www.who.int/emergencies/diseases/lassa-fever/en/

105. Akpede GO, Asogun DA, Okogbenin SA, Okokhere PO. Lassa fever outbreaks in Nigeria. Expert Rev Anti Infect Ther. 2018;16(9):663–6.

106. Asogun DA, Günther S, Akpede GO, Ihekweazu C, Zumla A. Lassa Fever: epidemiology, clinical features, diagnosis, management and prevention. Infect Dis Clin North Am. 2019 Dec;33(4):933–51.

107. Kofman A, Choi MJ, Rollin PE. Lassa fever in travelers from West Africa, 1969–2016. Emerging Infectious Diseases [Internet]. 2019 Feb [cited 2019 Nov 11];25(2). Available from: https://wwwnc.cdc.gov/eid/article/25/2/18-0836_article

108. Nikisins S, Rieger T, Patel P, Müller R, Günther S, Niedrig M. International external quality assessment study for molecular detection of Lassa virus. PLOS Neglected Tropical Diseases. 2015 May 21;9(5):e0003793.

109. Monath TP, Newhouse VF, Kemp GE, Setzer HW, Cacciapuoti A. Lassa virus isolation from Mastomys natalensis rodents during an epidemic in Sierra Leone. Science. 1974 Jul 19;185(4147):263–5.

110. Okokhere P, Colubri A, Azubike C, Iruolagbe C, Osazuwa O, Tabrizi S, et al. Clinical and laboratory predictors of Lassa fever outcome in a dedicated treatment facility in Nigeria: a retrospective, observational cohort study. Lancet Infect Dis. 2018;18(6):684–95.

111. Bausch DG, Demby AH, Coulibaly M, Kanu J, Goba A, Bah A, et al. Lassa fever in Guinea: I. Epidemiology of human disease and clinical observations. Vector Borne Zoonotic Dis. 2001;1(4):269–81.

112. Knobloch J, McCormick JB, Webb PA, Dietrich M, Schumacher HH, Dennis E. Clinical observations in 42 patients with Lassa fever. Tropenmed Parasitol. 1980 Dec;31(4):389–98.

113. McCormick JB, King IJ, Webb PA, Johnson KM, O'Sullivan R, Smith ES, et al. A case-control study of the clinical diagnosis and course of Lassa fever. J Infect Dis. 1987 Mar;155(3):445–55.

114. Shaffer JG, Grant DS, Schieffelin JS, Boisen ML, Goba A, Hartnett JN, et al. Lassa fever in post-conflict Sierra Leone. PLoS Negl Trop Dis [Internet]. 2014 Mar 20 [cited 2019 Nov 11];8(3). Available from: https://www.ncbi.nlm.nih.gov/pmc/articles/PMC3961205/

115. Peters CJ, Liu CT, Anderson GW, Morrill JC, Jahrling PB. Pathogenesis of viral hemorrhagic fevers: Rift Valley fever and Lassa fever contrasted. Rev Infect Dis. 1989 Jun;11 Suppl 4:S743-749.

116. McCormick JB, King IJ, Webb PA, Scribner CL, Craven RB, Johnson KM, et al. Lassa fever. Effective therapy with ribavirin. N Engl J Med. 1986 Jan 2;314(1):20–6.

117. Mire CE, Cross RW, Geisbert JB, Borisevich V, Agans KN, Deer DJ, et al. Human-monoclonal-antibody therapy protects nonhuman primates against advanced Lassa fever. Nat Med. 2017 Oct;23(10):1146–9.

118. Robinson JE, Hastie KM, Cross RW, Yenni RE, Elliott DH, Rouelle JA, et al. Most neutralizing human monoclonal antibodies target novel epitopes requiring both Lassa virus glycoprotein subunits. Nat Commun [Internet]. 2016 May 10 [cited 2019 Nov 11];7. Available from: https://www.ncbi.nlm.nih.gov/pmc/articles/PMC4866400/

119. Liao BS, Byl FM, Adour KK. Audiometric comparison of Lassa fever hearing loss and idiopathic sudden hearing loss: evidence for viral cause. Otolaryngol Head Neck Surg. 1992 Mar;106(3):226–9.

120. Okokhere PO, Ibekwe TS, Akpede GO. Sensorineural hearing loss in Lassa fever: two case reports. J Med Case Rep. 2009 Jan 29;3:36.

121. Charrel RN, de Lamballerie X, Emonet S. Phylogeny of the genus Arenavirus. Curr Opin Microbiol. 2008 Aug;11(4):362–8.

122. Whitmer SLM, Strecker T, Cadar D, Dienes H-P, Faber K, Patel K, et al. New Lineage of Lassa Virus, Togo, 2016. Emerg Infect Dis. 2018 Mar;24(3):599–602.

123. Raabe V, Koehler J. Laboratory Diagnosis of Lassa Fever. J Clin Microbiol. 2017;55(6):1629–37.

124. Radoshitzky SR, Abraham J, Spiropoulou CF, Kuhn JH, Nguyen D, Li W, et al. Transferrin receptor 1 is a cellular receptor for New World haemorrhagic fever arenaviruses. Nature. 2007 Mar 1;446(7131):92–6.

125. Rojek JM, Sanchez AB, Nguyen NT, de la Torre J-C, Kunz S. Different mechanisms of cell entry by human-pathogenic Old World and New World arenaviruses. J Virol. 2008 Aug;82(15):7677–87.

126. de Manzione N, Salas RA, Paredes H, Godoy O, Rojas L, Araoz F, et al. Venezuelan hemorrhagic fever: clinical and epidemiological studies of 165 cases. Clin Infect Dis. 1998 Feb;26(2):308–13.

127. Patterson M, Grant A, Paessler S. Epidemiology and pathogenesis of Bolivian hemorrhagic fever. Curr Opin Virol. 2014 Apr;0:82–90.

128. Hoogstraal H. The epidemiology of tick-borne Crimean-Congo hemorrhagic fever in Asia, Europe, and Africa. J Med Entomol. 1979 May 22;15(4):307–417.

129. Chumakov MP. A short story of the investigation of the virus of Crimean hemorrhagic fever. Tr Inst Polio Virusn Entsefalitov Akad Med Nauk SSSR. 1965;7:193–6.

130. Akinci E, Bodur H, Sunbul M, Leblebicioglu H. Prognostic factors, pathophysiology and novel biomarkers in Crimean-Congo hemorrhagic fever. Antiviral Research. 2016 Aug 1;132:233–43.

131. Shayan S, Bokaean M, Shahrivar MR, Chinikar S. Crimean-Congo Hemorrhagic Fever. Lab Med. 2015;46(3):180–9.

132. Bodur H, Akinci E, Ascioglu S, Öngürü P, Uyar Y. Subclinical infections with Crimean-Congo hemorrhagic fever virus, Turkey. Emerg Infect Dis. 2012 Apr;18(4):640–2.

133. Leblebicioglu H, Ozaras R, Sunbul M. Crimean-Congo hemorrhagic fever: A neglected infectious disease with potential nosocomial infection threat. Am J Infect Control. 2017 Jul 1;45(7):815–6.

134. Koksal I, Yilmaz G, Aksoy F, Aydin H, Yavuz I, Iskender S, et al. The efficacy of ribavirin in the treatment of Crimean-Congo hemorrhagic fever in Eastern Black Sea region in Turkey. J Clin Virol. 2010 Jan;47(1):65–8.

135. Bente DA, Forrester NL, Watts DM, McAuley AJ, Whitehouse CA, Bray M. Crimean-Congo hemorrhagic fever: history, epidemiology, pathogenesis, clinical syndrome and genetic diversity. Antiviral Res. 2013 Oct;100(1):159–89.

136. Mousavi-Jazi M, Karlberg H, Papa A, Christova I, Mirazimi A. Healthy individuals' immune response to the Bulgarian Crimean-Congo hemorrhagic fever virus vaccine. Vaccine. 2012 Sep 28;30(44):6225–9.

137. Papa A, Bino S, Velo E, Harxhi A, Kota M, Antoniadis A. Cytokine levels in Crimean-Congo hemorrhagic fever. J Clin Virol. 2006 Aug;36(4):272–6.

138. Ergonul O, Tuncbilek S, Baykam N, Celikbas A, Dokuzoguz B. Evaluation of serum levels of interleukin (IL)-6, IL-10, and tumor necrosis factor-alpha in patients with Crimean-Congo hemorrhagic fever. J Infect Dis. 2006 Apr 1;193(7):941–4.

139. Jonsson CB, Figueiredo LTM, Vapalahti O. A global perspective on hantavirus ecology, epidemiology, and disease. Clin Microbiol Rev. 2010 Apr;23(2):412–41.

140. Klempa B. Hantaviruses and climate change. Clin Microbiol Infect. 2009 Jun;15(6):518–23.

141. Plyusnin A, Morzunov SP. Virus evolution and genetic diversity of hantaviruses and their rodent hosts. Curr Top Microbiol Immunol. 2001;256:47–75.

142. Brummer-Korvenkontio M, Vaheri A, Hovi T, von Bonsdorff CH, Vuorimies J, Manni T, et al. Nephropathia epidemica: detection of antigen in bank voles and serologic diagnosis of human infection. J Infect Dis. 1980 Feb;141(2):131–4.

143. Avsic-Zupanc T, Xiao SY, Stojanovic R, Gligic A, van der Groen G, LeDuc JW. Characterization of Dobrava virus: a Hantavirus from Slovenia, Yugoslavia. J Med Virol. 1992 Oct;38(2):132–7.

144. Lee PW, Gibbs JC, Gajdusek DC, Hsiang CM, Hsiung GD. Identification of epidemic haemorrhagic fever with renal syndrome in China with Korean haemorrhagic fever. Lancet. 1980 May;1(8176):1025–6.

145. Nichol ST, Spiropoulou CF, Morzunov S, Rollin PE, Ksiazek TG, Feldmann H, et al. Genetic identification of a hantavirus associated with an outbreak of acute respiratory illness. Science. 1993 Nov 5;262(5135):914–7.

146. Bi Z, Formenty PBH, Roth CE. Hantavirus infection: a review and global update. J Infect Dev Ctries. 2008 Feb 1;2(1):3–23.

147. Tian H, Stenseth NChr. The ecological dynamics of hantavirus diseases: From environmental variability to disease prevention largely based on data from China. PLoS Negl Trop Dis [Internet]. 2019 Feb 21 [cited 2019 Apr 14];13(2). Available from: https://www.ncbi.nlm.nih.gov/pmc/articles/PMC6383869/

148. Vaheri A, Henttonen H, Voutilainen L, Mustonen J, Sironen T, Vapalahti O. Hantavirus infections in Europe and their impact on public health. Rev Med Virol. 2013 Jan;23(1):35–49.

149. Jameson LJ, Logue CH, Atkinson B, Baker N, Galbraith SE, Carroll MW, et al. The continued emergence of hantaviruses: isolation of a Seoul virus implicated in human disease, United Kingdom, October 2012. Euro Surveill. 2013 Jan 3;18(1):4–7.

150. McElhinney LM, Marston DA, Pounder KC, Goharriz H, Wise EL, Verner-Carlsson J, et al. High prevalence of Seoul hantavirus in a breeding colony of pet rats. Epidemiology & Infection. 2017 Nov;145(15):3115–24.

151. Taori S, Jameson L, Campbell A, Drew P, McCarthy N, Hart J, et al. UK hantavirus, renal failure, and pet rats. The Lancet. 2013 Mar 23;381(9871):1070.

152. Martinez-Valdebenito C, Calvo M, Vial C, Mansilla R, Marco C, Palma RE, et al. Person-to-person household and nosocomial transmission of Andes hantavirus, southern Chile, 2011. Emerg Infect Dis. 2014 Oct;20(10):1629–36.

153. Avšič-Županc T, Saksida A, Korva M. Hantavirus infections. Clinical Microbiology and Infection. 2019 Apr 1;21:e6–16.

154. Hjelle B, Jenison S, Torrez-Martinez N, Herring B, Quan S, Polito A, et al. Rapid and specific detection of Sin Nombre virus antibodies in patients with hantavirus pulmonary syndrome by a strip immunoblot assay suitable for field diagnosis. J Clin Microbiol. 1997 Mar;35(3):600–8.

155. Hujakka H, Koistinen V, Kuronen I, Eerikäinen P, Parviainen M, Lundkvist A, et al. Diagnostic rapid tests for acute hantavirus infections: specific tests for Hantaan, Dobrava and Puumala viruses versus a hantavirus combination test. J Virol Methods. 2003 Mar;108(1):117–22.

156. Evander M, Eriksson I, Pettersson L, Juto P, Ahlm C, Olsson GE, et al. Puumala hantavirus viremia diagnosed by real-time reverse transcriptase PCR using samples from patients with hemorrhagic fever and renal syndrome. J Clin Microbiol. 2007 Aug;45(8):2491–7.

157. Ferres M, Vial P, Marco C, Yanez L, Godoy P, Castillo C, et al. Prospective evaluation of household contacts of persons with hantavirus cardiopulmonary syndrome in chile. J Infect Dis. 2007 Jun 1;195(11):1563–71.

158. Matthys V, Mackow ER. Hantavirus regulation of type I interferon responses. Advances in Virology. 2012 Jul;2012(524024):9.

159. Raftery MJ, Kraus AA, Ulrich R, Krüger DH, Schönrich G. Hantavirus infection of dendritic cells. J Virol. 2002 Nov;76(21):10724–33.

160. Krüger DH, Schönrich G, Klempa B. Human pathogenic hantaviruses and prevention of infection. Hum Vaccin. 2011 Jun;7(6):685–93.

161. Daubney R, Hudson JR, Garnham PC. Enzootic hepatitis or rift valley fever. An undescribed virus disease of sheep cattle and man from east africa. The Journal of Pathology and Bacteriology. 1931;34(4):545–79.

162. Hartman A. Rift Valley Fever. Clin Lab Med. 2017;37(2):285–301.

163. World Health Organization. WHO factsheet on Rift Valley fever [Internet]. 201802-19 [cited 2018 Jun 26]. Available from: http://www.who.int/news-room/fact-sheets/detail/rift-valley-fever

164. Linthicum KJ, Britch SC, Anyamba A. Rift Valley fever: an emerging mosquito-borne disease. Annu Rev Entomol. 2016;61:395–415.

165. Boiro I, Konstaninov OK, Numerov AD. [Isolation of Rift Valley fever virus from bats in the Republic of Guinea]. Bull Soc Pathol Exot Filiales. 1987;80(1):62–7.

166. Dondona AC, Aschenborn O, Pinoni C, Di Gialleonardo L, Maseke A, Bortone G, et al. Rift Valley fever virus among wild ruminants, Etosha national park, Namibia, 2011. Emerg Infect Dis. 2016 Jan;22(1):128–30.

167. Davies FG, Koros J, Mbugua H. Rift Valley fever in Kenya: the presence of antibody to the virus in camels (Camelus dromedarius). J Hyg (Lond). 1985 Apr;94(2):241–4.

168. Nichol ST BB, Reynes JM. Rift Valley Fever. In: Hunter's Tropical Medicine and Emerging Infectious Disease. Elsevier Health Sciences; 2012.

169. Rusnak JM, Gibbs P, Boudreau E, Clizbe DP, Pittman P. Immunogenicity and safety of an inactivated Rift Valley fever vaccine in a 19-year study. Vaccine. 2011 Apr 12;29(17):3222–9.

170. Randall R, Binn LN, Harrison VR. Immunization against Rift Valley fever virus. Studies on the immunogenicity of lyophilized formalin-inactivated vaccine. J Immunol. 1964 Aug;93:293–9.

171. Njenga MK, Njagi L, Thumbi SM, Kahariri S, Githinji J, Omondi E, et al. Randomized controlled field trial to assess the immunogenicity and safety of rift valley fever clone 13 vaccine in livestock. PLoS Negl Trop Dis. 2015 Mar;9(3):e0003550.

172. Dulal P, Wright D, Ashfield R, Hill AVS, Charleston B, Warimwe GM. Potency of a thermostabilised chimpanzee adenovirus Rift Valley Fever vaccine in cattle. Vaccine. 2016 Apr 29;34(20):2296–8.

173. Warimwe GM, Gesharisha J, Carr BV, Otieno S, Otingah K, Wright D, et al. Chimpanzee adenovirus vaccine provides multispecies protection against Rift Valley fever. Sci Rep. 2016 Feb 5;6:20617.

174. Ly HJ, Ikegami T. Rift Valley fever virus NSs protein functions and the similarity to other bunyavirus NSs proteins. Virol J. 2016 02;13:118.

175. Wuerth JD, Weber F. Phleboviruses and the type I interferon response. Viruses. 2016 22;8(6).

176. Elliott RM. Orthobunyaviruses: recent genetic and structural insights. Nat Rev Micro. 2014 Oct;12(10):673–85.

177. Anderson CR, Spence L, Downs WG, Aitken THG. Oropouche virus: a new human disease agent from Trinidad, West Indies. The American Journal of Tropical Medicine and Hygiene. 1961;10(4):574–8.

178. World Health Organization. Disease outbreak news. Oropouche virus disease - Peru [Internet]. 2016 [cited 2018 Apr 23]. Available from: http://www.who.int/csr/don/03-june-2016-oropouche-peru/en/

179. Ladner JT, Savji N, Lofts L, Travassos da Rosa A, Wiley MR, Gestole MC, et al. Genomic and phylogenetic characterization of viruses included in the Manzanilla and Oropouche species complexes of the genus Orthobunyavirus, family Bunyaviridae. J Gen Virol. 2014 May;95(Pt 5):1055–66.

180. Cardoso BF, Serra OP, Heinen LB da S, Zuchi N, Souza VC de, Naveca FG, et al. Detection of Oropouche virus segment S in patients and in Culex quinquefasciatus in the state of Mato Grosso, Brazil. Memórias do Instituto Oswaldo Cruz. 2015 Sep;110(6):745–54.

181. Pinheiro FP, Travassos da Rosa AP, Gomes ML, LeDuc JW, Hoch AL. Transmission of Oropouche virus from man to hamster by the midge Culicoides paraensis. Science. 1982 Mar 5;215(4537):1251–3.

182. Sakkas H, Bozidis P, Franks A, Papadopoulou C. Oropouche Fever: A Review. Viruses. 2018 Apr 4;10(4).

183. Bastos M de S, Figueiredo LTM, Naveca FG, Monte RL, Lessa N, Pinto de Figueiredo RM, et al. Identification of Oropouche Orthobunyavirus in the cerebrospinal fluid of three patients in the Amazonas, Brazil. Am J Trop Med Hyg. 2012 Apr;86(4):732–5.

184. Vernal S, Martini CCR, da Fonseca BAL. Oropouche virus–associated aseptic meningoencephalitis, southeastern Brazil. Emerg Infect Dis. 2019 Feb;25(2):380–2.

185. Tilston-Lunel NL, Acrani GO, Randall RE, Elliott RM. Generation of recombinant Oropouche viruses lacking the nonstructural protein NSm or NSs. J Virol. 2016 Feb 11;90(5):2616–27.

186. Acrani GO, Tilston-Lunel NL, Spiegel M, Weidmann M, Dilcher M, Andrade da Silva DE, et al. Establishment of a minigenome system for Oropouche virus reveals the S genome segment to be significantly longer than reported previously. J Gen Virol. 2015 Mar;96(Pt 3):513–23.

187. Acrani GO, Gomes R, Proença-Módena JL, da Silva AF, Carminati PO, Silva ML, et al. Apoptosis induced by Oropouche virus infection in HeLa cells is dependent on virus protein expression. Virus Res. 2010 Apr;149(1):56–63.

188. Santos RI, Bueno-Júnior LS, Ruggiero RN, Almeida MF, Silva ML, Paula FE, et al. Spread of Oropouche virus into the central nervous system in mouse. Viruses. 2014 Oct 10;6(10):3827–36.

189. Proenca-Modena JL, Sesti-Costa R, Pinto AK, Richner JM, Lazear HM, Lucas T, et al. Oropouche virus infection and pathogenesis are restricted by MAVS, IRF-3, IRF-7, and type I interferon signaling pathways in nonmyeloid cells. J Virol. 2015 May;89(9):4720–37.

190. International Committee on Taxonomy of Viruses (ICTV). Filoviridae, ICTV ninth report; 2009 taxonomy release [Internet]. 2011 [cited 2019 Apr 4]. Available from: https://talk.ictvonline.org/ictv-reports/ictv_9th_report/negative-sense-rna-viruses-2011/w/negrna_viruses/197/filoviridae

191. Center for Disease Control and Prevention. Ebola virus disease distribution map: Cases of Ebola virus disease in Africa Since 1976 [Internet]. 2018 [cited 2019 Mar 29]. Available from: https://www.cdc.gov/vhf/ebola/history/distribution-map.html

192. World Health Organization. Ebola situation reports: archive [Internet]. 2016 [cited 2018 Feb 1]. Available from: http://www.who.int/csr/disease/ebola/situation-reports/archive/en/

193. World Health Organization. Ebola health update - DRC, 2019 [Internet]. 2019 [cited 2019 Dec 16]. Available from: https://www.who.int/emergencies/diseases/ebola/drc-2019

194. World Health Organization. WHO factsheet on Ebola virus disease [Internet]. 2019 [cited 2019 Apr 1]. Available from: https://www.who.int/news-room/fact-sheets/detail/ebola-virus-disease

195. Nsio J, Kapetshi J, Makiala S, Raymond F, Tshapenda G, Boucher N, et al. 2017 outbreak of Ebola virus disease in Northern Democratic Republic of Congo. J Infect Dis. 2019 Apr 3;

196. Laing ED, Mendenhall IH, Linster M, Low DHW, Chen Y, Yan L, et al. Serologic evidence of fruit bat exposure to Filoviruses, Singapore, 2011–2016. Emerg Infect Dis. 2018 Jan;24(1):122–6.

197. Hayman DTS, Emmerich P, Yu M, Wang L-F, Suu-Ire R, Fooks AR, et al. Long-term survival of an urban fruit bat seropositive for Ebola and Lagos bat viruses. PLoS One [Internet]. 2010 Aug 4 [cited 2019 Mar 29];5(8). Available from: https://www.ncbi.nlm.nih.gov/pmc/articles/PMC2915915/

198. Jayme SI, Field HE, de Jong C, Olival KJ, Marsh G, Tagtag AM, et al. Molecular evidence of Ebola Reston virus infection in Philippine bats. Virol J [Internet]. 2015 Jul 17 [cited 2019 Mar 29];12. Available from: https://www.ncbi.nlm.nih.gov/pmc/articles/PMC4504098/

199. Ogawa H, Miyamoto H, Nakayama E, Yoshida R, Nakamura I, Sawa H, et al. Seroepidemiological prevalence of multiple species of Filoviruses in fruit bats (Eidolon helvum) migrating in Africa. J Infect Dis. 2015 Oct 1;212 Suppl 2:S101-108.

200. Pourrut X, Souris M, Towner JS, Rollin PE, Nichol ST, Gonzalez J-P, et al. Large serological survey showing cocirculation of Ebola and Marburg viruses in Gabonese bat populations, and a high seroprevalence of both viruses in Rousettus aegyptiacus. BMC Infect Dis. 2009 Sep 28;9:159.

201. Biek R, Walsh PD, Leroy EM, Real LA. Recent common ancestry of Ebola Zaire virus found in a bat reservoir. PLoS Pathog [Internet]. 2006 Oct [cited 2019 Mar 29];2(10). Available from: https://www.ncbi.nlm.nih.gov/pmc/articles/PMC1626099/

202. Swanepoel R, Leman PA, Burt FJ, Zachariades NA, Braack LE, Ksiazek TG, et al. Experimental inoculation of plants and animals with Ebola virus. Emerg Infect Dis. 1996;2(4):321–5.

203. Clark DJ, Tyson J, Sails AD, Krishna S, Staines HM. The current landscape of nucleic acid tests for filovirus detection. J Clin Virol. 2018;103:27–36.

204. World Health Organization Regional Office for Africa. Ebola Virus Disease [Internet]. [cited 2019 Apr 1]. Available from: https://www.afro.who.int/health-topics/ebola-virus-disease

205. Feldmann H, Geisbert TW. Ebola haemorrhagic fever. Lancet. 2011 Mar 5;377(9768):849–62.

206. Nyakarahuka L, Kankya C, Krontveit R, Mayer B, Mwiine FN, Lutwama J, et al. How severe and prevalent are Ebola and Marburg viruses? A systematic review and meta-analysis of the case fatality rates and seroprevalence. BMC Infect Dis. 2016 25;16(1):708.

207. Reece S, Brown CS, Dunning J, Chand MA, Zambon MC, Jacobs M. The UK's multidisciplinary response to an Ebola epidemic. Clin Med (Lond). 2017 Jul;17(4):332–7.

208. World Health Organization, Institut National pour la Recherche Biomedicale. Preliminary results on the efficacy of rVSV-ZEBOV-GP Ebola vaccine using the ring vaccination strategy in the control of an Ebola outbreak in the Democratic Republic of the Congo [Internet]. WHO; 2019 Apr [cited 2019 Nov 16] p. 4. Available from: https://www.who.int/csr/resources/publications/ebola/ebola-ring-vaccination-results-12-april-2019.pdf

209. Kasereka MC, Sawatzky J, Hawkes MT. Ebola epidemic in war-torn Democratic Republic of Congo, 2018: Acceptability and patient satisfaction of the recombinant Vesicular Stomatitis Virus - Zaire Ebolavirus Vaccine. Vaccine. 2019 Apr 10;37(16):2174–8.

210. Espeland EM, Tsai C-W, Larsen J, Disbrow GL. Safeguarding against Ebola: Vaccines and therapeutics to be stockpiled for future outbreaks. PLoS Negl Trop Dis. 2018;12(4):e0006275.

211. Francisco EM. First vaccine to protect against Ebola [Internet]. European Medicines Agency. 2019 [cited 2019 Nov 25]. Available from: https://www.ema.europa.eu/en/news/first-vaccine-protect-against-ebola

212. World Health Organization. WHO prequalifies Ebola vaccine, paving the way for its use in high-risk countries [Internet]. 2019 [cited 2019 Nov 16]. Available from: https://www.who.int/news-room/detail/12-11-2019-who-prequalifies-ebola-vaccine-paving-the-way-for-its-use-in-high-risk-countries

213. Mohamadzadeh M, Chen L, Schmaljohn A. How Ebola and Marburg viruses battle the immune system. Nature Reviews Immunology. 2007;7:556–67.

214. Reid SP, Leung LW, Hartman AL, Martinez O, Shaw ML, Carbonnelle C, et al. Ebola virus VP24 binds karyopherin alpha1 and blocks STAT1 nuclear accumulation. J Virol. 2006 Jun;80(11):5156–67.

215. World Health Organization. Marburg virus disease [Internet]. [cited 2019 Apr 4]. Available from: http://www.who.int/csr/disease/marburg/en/

216. Normile D. Tropical medicine. Surprising new dengue virus throws a spanner in disease control efforts. Science. 2013 Oct 25;342(6157):415.

217. Higuera A, Ramírez JD. Molecular epidemiology of dengue, yellow fever, Zika and Chikungunya arboviruses: An update. Acta Trop. 2019 Feb;190:99–111.

218. World Health Organization. WHO factsheet on dengue and severe dengue [Internet]. 2019 [cited 2019 Nov 4]. Available from: http://www.who.int/news-room/fact-sheets/detail/dengue-and-severe-dengue

219. Wilson ME, Chen LH. Dengue: update on epidemiology. Curr Infect Dis Rep. 2015 Jan;17(1):457.

220. Tan PC, Rajasingam G, Devi S, Omar SZ. Dengue infection in pregnancy: prevalence, vertical transmission, and pregnancy outcome. Obstet Gynecol. 2008 May;111(5):1111–7.

221. Special Programme for Research and Training in Tropical Diseases, World Health Organization, editors. Dengue: guidelines for diagnosis, treatment, prevention, and control. Geneva: World Health Organization; 2009. 147 p.

222. Culshaw A, Mongkolsapaya J, Screaton GR. The immunopathology of dengue and Zika virus infections. Curr Opin Immunol. 2017 Oct;48:1–6.

223. Zompi S, Harris E. Animal models of dengue virus infection. Viruses. 2012 Jan 9;4(1):62–82.

224. Littaua R, Kurane I, Ennis FA. Human IgG Fc receptor II mediates antibody-dependent enhancement of dengue virus infection. J Immunol. 1990 Apr 15;144(8):3183–6.

225. Morens DM, Larsen LK, Halstead SB. Study of the distribution of antibody-dependent enhancement determinants on dengue 2 isolates using dengue 2-derived monoclonal antibodies. J Med Virol. 1987 Jun;22(2):163–7.

226. Boonnak K, Slike BM, Burgess TH, Mason RM, Wu S-J, Sun P, et al. Role of dendritic cells in antibody-dependent enhancement of dengue virus infection. J Virol. 2008 Apr;82(8):3939–51.

227. Priyamvada L, Quicke KM, Hudson WH, Onlamoon N, Sewatanon J, Edupuganti S, et al. Human antibody responses after dengue virus infection are highly cross-reactive to Zika virus. Proc Natl Acad Sci USA. 2016 12;113(28):7852–7.

228. Paul LM, Carlin ER, Jenkins MM, Tan AL, Barcellona CM, Nicholson CO, et al. Dengue virus antibodies enhance Zika virus infection. Clin Transl Immunology. 2016 Dec 16;5(12):e117.

229. World Health Organization. WHO factsheet on Japanese encephalitis [Internet]. 2019 [cited 2019 May 9]. Available from: http://www.who.int/news-room/fact-sheets/detail/japanese-encephalitis

230. Schuh AJ, Ward MJ, Brown AJL, Barrett ADT. Phylogeography of Japanese encephalitis virus: Genotype Is associated with climate. PLOS Neglected Tropical Diseases. 2013 Aug 29;7(8):e2411.

231. Caldwell JP, Chen LH, Hamer DH. Evolving epidemiology of Japanese encephalitis: implications for vaccination. Curr Infect Dis Rep. 2018 Jun 29;20(9):30.

232. Wang H, Liang G. Epidemiology of Japanese encephalitis: past, present, and future prospects. Ther Clin Risk Manag. 2015;11:435–48.

233. Kleinert RDV, Montoya-Diaz E, Khera T, Welsch K, Tegtmeyer B, Hoehl S, et al. Yellow fever: integrating current knowledge with technological innovations to identify strategies for controlling a re-emerging virus. Viruses. 2019 Oct 17;11(10).

234. Johnston LJ, Halliday GM, King NJ. Langerhans cells migrate to local lymph nodes following cutaneous infection with an arbovirus. J Invest Dermatol. 2000 Mar;114(3):560–8.

235. Yang KD, Yeh W-T, Chen R-F, Chuon H-L, Tsai H-P, Yao C-W, et al. A model to study neurotropism and persistency of Japanese encephalitis virus infection in human neuroblastoma cells and leukocytes. J Gen Virol. 2004 Mar;85(Pt 3):635–42.

236. Mathur A, Bharadwaj M, Kulshreshtha R, Rawat S, Jain A, Chaturvedi UC. Immunopathological study of spleen during Japanese encephalitis virus infection in mice. Br J Exp Pathol. 1988 Jun;69(3):423–32.

237. Lannes N, Summerfield A, Filgueira L. Regulation of inflammation in Japanese encephalitis. Journal of Neuroinflammation [Internet]. 2017 Aug [cited 2018 Jun 25];14(1). Available from: https://www.ncbi.nlm.nih.gov/pubmed/28807053

238. Lindqvist R, Upadhyay A, Överby AK. Tick-borne flaviviruses and the type I interferon response. Viruses. 2018 Jun 21;10(7).

239. Kellman EM, Offerdahl DK, Melik W, Bloom ME. Viral determinants of virulence in tick-borne flaviviruses. Viruses. 2018 Jun 16;10(6):329.

240. Public Health England. Tick-borne encephalitis virus detected in ticks in the UK [Internet]. 2019 [cited 2019 Nov 16]. Available from: https://www.gov.uk/government/news/tick-borne-encephalitis-virus-detected-in-ticks-in-the-uk

241. Holding M, Dowall SD, Medlock JM, Carter DP, Pullan ST, Lewis J, et al. Tick-borne encephalitis virus, United Kingdom. Emerging Infectious Diseases [Internet]. 2020 Jan [cited 2019 Nov 25];26(1). Available from: https://wwwnc.cdc.gov/eid/article/26/1/19-1085_article

242. World Health Organization. Tick-borne encephalitis [Internet]. 2014 [cited 2019 Nov 16]. Available from: https://www.who.int/immunization/diseases/tick_encephalitis/en/

243. Dobler G, Gniel D, Petermann R, Pfeffer M. Epidemiology and distribution of tick-borne encephalitis. Wien Med Wochenschr. 2012 Jun;162(11–12):230–8.

244. Veje M, Studahl M, Johansson M, Johansson P, Nolskog P, Bergström T. Diagnosing tick-borne encephalitis: a re-evaluation of notified cases. Eur J Clin Microbiol Infect Dis. 2018;37(2):339–44.

245. Luo H, Wang T. Recent advances in understanding West Nile virus host immunity and viral pathogenesis. F1000Res. 2018;7:338.

246. World Health Organization. WHO factsheet on West Nile virus [Internet]. 2017 [cited 2018 Jun 25]. Available from: http://www.who.int/news-room/fact-sheets/detail/west-nile-virus

247. Hadfield J, Brito AF, Swetnam DM, Vogels CBF, Tokarz RE, Andersen KG, et al. Twenty years of West Nile virus spread and evolution in the Americas visualized by Nextstrain. PLoS Pathog [Internet]. 2019 Oct 31 [cited 2019 Nov 17];15(10). Available from: https://www.ncbi.nlm.nih.gov/pmc/articles/PMC6822705/

248. George TL, Harrigan RJ, LaManna JA, DeSante DF, Saracco JF, Smith TB. Persistent impacts of West Nile virus on North American bird populations. Proc Natl Acad Sci USA. 2015 Nov 17;112(46):14290–4.

249. LaDeau SL, Kilpatrick AM, Marra PP. West Nile virus emergence and large-scale declines of North American bird populations. Nature. 2007 Jun 7;447(7145):710–3.

250. Sardelis MR, Turell MJ, Dohm DJ, O'Guinn ML. Vector competence of selected North American Culex and Coquillettidia mosquitoes for West Nile virus. Emerging Infect Dis. 2001 Dec;7(6):1018–22.

251. Turell MJ, O'Guinn M, Oliver J. Potential for New York mosquitoes to transmit West Nile virus. Am J Trop Med Hyg. 2000 Mar;62(3):413–4.

252. Garber C, Vasek MJ, Vollmer LL, Sun T, Jiang X, Klein RS. Astrocytes decrease adult neurogenesis during virus-induced memory dysfunction via IL-1. Nat Immunol. 2018 Feb;19(2):151–61.

253. World Health Organization. WHO factsheet on yellow fever [Internet]. 2019 [cited 2018 Jun 25]. Available from: http://www.who.int/news-room/fact-sheets/detail/yellow-fever

254. Onyango CO, Ofula VO, Sang RC, Konongoi SL, Sow A, De Cock KM, et al. Yellow fever outbreak, Imatong, southern Sudan. Emerg Infect Dis. 2004 Jun;10(6):1064–8.

255. Douam F, Ploss A. Yellow fever virus: knowledge gaps impeding the fight against an old foe. Trends Microbiol. 2018 Nov;26(11):913–28.

256. Waggoner JJ, Rojas A, Pinsky BA. Yellow fever virus: diagnostics for a persistent arboviral threat. J Clin Microbiol [Internet]. 2018 Sep 25 [cited 2019 Nov 17];56(10). Available from: https://www.ncbi.nlm.nih.gov/pmc/articles/PMC6156298/

257. Monath TP, Vasconcelos PFC. Yellow fever. Journal of Clinical Virology. 2015 Mar 1;64:160–73.

258. Shearer FM, Moyes CL, Pigott DM, Brady OJ, Marinho F, Deshpande A, et al. Global yellow fever vaccination coverage from 1970 to 2016: an adjusted retrospective analysis. Lancet Infect Dis. 2017;17(11):1209–17.

259. Garske T, Van Kerkhove MD, Yactayo S, Ronveaux O, Lewis RF, Staples JE, et al. Yellow Fever in Africa: estimating the burden of disease and impact of mass vaccination from outbreak and serological data. PLoS Med. 2014 May;11(5):e1001638.

260. Quaresma JAS, Pagliari C, Medeiros DBA, Duarte MIS, Vasconcelos PFC. Immunity and immune response, pathology and pathologic changes: progress and challenges in the immunopathology of yellow fever. Rev Med Virol. 2013 Sep;23(5):305–18.

261. Lefeuvre A, Contamin H, Decelle T, Fournier C, Lang J, Deubel V, et al. Host-cell interaction of attenuated and wild-type strains of yellow fever virus can be differentiated at early stages of hepatocyte infection. Microbes Infect. 2006 May;8(6):1530–8.

262. Barba-Spaeth G, Longman RS, Albert ML, Rice CM. Live attenuated yellow fever 17D infects human DCs and allows for presentation of endogenous and recombinant T cell epitopes. J Exp Med. 2005 Nov 7;202(9):1179–84.

263. Cong Y, McArthur MA, Cohen M, Jahrling PB, Janosko KB, Josleyn N, et al. Characterization of Yellow Fever virus infection of human and non-human primate antigen presenting cells and their interaction with CD4+ T Cells. PLoS Negl Trop Dis. 2016;10(5):e0004709.

264. McLinden JH, Bhattarai N, Stapleton JT, Chang Q, Kaufman TM, Cassel SL, et al. Yellow Fever virus, but not Zika virus or dengue virus, inhibits T-cell receptor-mediated T-Cell function by an RNA-based mechanism. J Infect Dis. 2017 27;216(9):1164–75.

265. Woodson SE, Freiberg AN, Holbrook MR. Differential cytokine responses from primary human Kupffer cells following infection with wild-type or vaccine strain yellow fever virus. Virology. 2011 Mar 30;412(1):188–95.

266. Khaiboullina SF, Rizvanov AA, Holbrook MR, St Jeor S. Yellow fever virus strains Asibi and 17D-204 infect human umbilical cord endothelial cells and induce novel changes in gene expression. Virology. 2005 Nov 25;342(2):167–76.

267. Quaresma JAS, Barros VLRS, Pagliari C, Fernandes ER, Guedes F, Takakura CFH, et al. Revisiting the liver in human yellow fever: virus-induced apoptosis in hepatocytes associated with TGF-beta, TNF-alpha and NK cells activity. Virology. 2006 Feb 5;345(1):22–30.

268. Engelmann F, Josset L, Girke T, Park B, Barron A, Dewane J, et al. Pathophysiologic and transcriptomic analyses of viscerotropic yellow fever in a rhesus macaque model. PLoS Negl Trop Dis. 2014;8(11):e3295.

269. Gutiérrez-Bugallo G, Piedra LA, Rodriguez M, Bisset JA, Lourenço-de-Oliveira R, Weaver SC, et al. Vector-borne transmission and evolution of Zika virus. Nat Ecol Evol. 2019;3(4):561–9.

270. Duffy MR, Chen T-H, Hancock WT, Powers AM, Kool JL, Lanciotti RS, et al. Zika virus outbreak on Yap Island, Federated States of Micronesia. N Engl J Med. 2009 Jun 11;360(24):2536–43.

271. Musso D, Bossin H, Mallet HP, Besnard M, Broult J, Baudouin L, et al. Zika virus in French Polynesia 2013-14: anatomy of a completed outbreak. Lancet Infect Dis. 2018;18(5):e172–82.

272. Pan American Health Organization. Archive by disease - Zika virus infection [Internet]. 2015 [cited 2019 Apr 6]. Available from: https://www.paho.org/hq/index.php?option=com_content&view=article&id=10898:2015-archive-by-disease-zika-virus-infection&Itemid=41443&lang=en

273. Mittal R, Nguyen D, Debs LH, Patel AP, Liu G, Jhaveri VM, et al. Zika virus: an emerging global health threat. Front Cell Infect Microbiol. 2017;7:486.

274. Depoux A, Philibert A, Rabier S, Philippe H-J, Fontanet A, Flahault A. A multi-faceted pandemic: a review of the state of knowledge on the Zika virus. Public Health Rev. 2018;39:10.

275. Cragan JD, Mai CT, Petersen EE, Liberman RF, Forestieri NE, Stevens AC, et al. Baseline prevalence of birth defects associated with congenital Zika virus infection - Massachusetts, North Carolina, and Atlanta, Georgia, 2013-2014. MMWR Morb Mortal Wkly Rep. 2017 Mar 3;66(8):219–22.

276. Cauchemez S, Besnard M, Bompard P, Dub T, Guillemette-Artur P, Eyrolle-Guignot D, et al. Association between Zika virus and microcephaly in French Polynesia, 2013-15: a retrospective study. Lancet. 2016 May 21;387(10033):2125–32.

277. de Araújo TVB, Rodrigues LC, de Alencar Ximenes RA, de Barros Miranda-Filho D, Montarroyos UR, de Melo APL, et al. Association between Zika virus infection and microcephaly in Brazil, January to May, 2016: preliminary report of a case-control study. Lancet Infect Dis. 2016 Dec;16(12):1356–63.

278. Cao-Lormeau V, Blake A, Mons S, Lastere S, Roche C, Vanhomwegen J, et al. Guillain-Barré syndrome outbreak caused by Zika virus infection in French Polynesia. Lancet. 2016 Apr 9;387(10027):1531–9.

279. Gunawardana SA, Shaw RH. Cross-reactive dengue virus-derived monoclonal antibodies to Zika virus envelope protein: Panacea or Pandora's box? BMC Infect Dis. 2018 Dec 10;18(1):641.

280. World Health Organization. Zika virus [Internet]. [cited 2019 Nov 17]. Available from: https://www.who.int/news-room/fact-sheets/detail/zika-virus

281. World Health Organization Regional Office for Africa. Laboratory testing for Zika virus infection [Internet]. WHO. 2016 [cited 2019 Nov 17]. Available from: http://www.who.int/csr/resources/publications/zika/laboratory-testing/en/

282. Hamel R, Dejarnac O, Wichit S, Ekchariyawat P, Neyret A, Luplertlop N, et al. Biology of Zika virus infection in human skin cells. J Virol. 2015 Jun 17;89(17):8880–96.

283. Tappe D, Pérez-Girón JV, Zammarchi L, Rissland J, Ferreira DF, Jaenisch T, et al. Cytokine kinetics of Zika virus-infected patients from acute to reconvalescent phase. Med Microbiol Immunol. 2016 Jun;205(3):269–73.

284. Wangdi K, Kasturiaratchi K, Nery SV, Lau CL, Gray DJ, Clements ACA. Diversity of infectious aetiologies of acute undifferentiated febrile illnesses in south and Southeast Asia: a systematic review. BMC Infectious Diseases. 2019 Jul 4;19(1):577.

285. Iroh Tam P-Y, Obaro SK, Storch G. Challenges in the etiology and diagnosis of acute febrile illness in children in low- and middle-income countries. J Pediatric Infect Dis Soc. 2016 Jun 1;5(2):190–205.

286. World Health Organization. This year's World malaria report at a glance [Internet]. 2018 [cited 2019 Nov 25]. Available from: http://www.who.int/malaria/media/world-malaria-report-2018/en/

287. World Health Organization. Malaria [Internet]. [cited 2019 Nov 25]. Available from: http://www.who.int/malaria/en/

288. Molina-Cruz A, Zilversmit MM, Neafsey DE, Hartl DL, Barillas-Mury C. Mosquito vectors and the globalization of Plasmodium falciparum malaria. Annu Rev Genet. 2016 Nov 23;50:447–65.

289. World Health Organization. Leptospirosis Burden Epidemiology Reference Group (LERG) [Internet]. [cited 2019 Mar 27]. Available from: https://www.who.int/zoonoses/diseases/lerg/en/index2.html

290. WHO | Leptospirosis [Internet]. WHO. [cited 2019 Aug 16]. Available from: http://www.who.int/topics/leptospirosis/en/

291. World Health Organization. WHO factsheet on Typhoid [Internet]. 2018 [cited 2019 Nov 25]. Available from: https://www.who.int/news-room/fact-sheets/detail/typhoid

292. Center for Disease Control and Prevention. Typhus fevers, scrub typhus [Internet]. 2019 [cited 2019 Nov 25]. Available from: https://www.cdc.gov/typhus/scrub/index.html

293. Luce-Fedrow A, Lehman ML, Kelly DJ, Mullins K, Maina AN, Stewart RL, et al. A review of scrub typhus (Orientia tsutsugamushi and related organisms): then, now, and tomorrow. Trop Med Infect Dis [Internet]. 2018 Jan 17 [cited 2019 Nov 25];3(1). Available from: https://www.ncbi.nlm.nih.gov/pmc/articles/PMC6136631/

294. Xu J. Next-generation sequencing: Current technologies and applications. Norfolk, UK: Caister Academic Press; 2014. 172 p.

295. Pareek CS. An overview of next-generation genome sequencing platforms. In: Next-generation sequencing: Current technologies and applications. Norfolk, UK: Caister Academic Press; 2014.

296. Wetterstrand KA. DNA sequencing costs: Data from the NHGRI Genome Sequencing Program (GSP) [Internet]. [cited 2019 Nov 21]. Available from: https://www.genome.gov/about-genomics/fact-sheets/DNA-Sequencing-Costs-Data

297. Derocles S, Bohan D, Dumbrell A, Massol F, Pauvert C, Plantegenest M, et al. Biomonitoring for the 21st century: integrating next-generation sequencing into ecological network analysis. In: Advances in Ecological Research [Internet]. Elsevier Academic Press; 2018. p. 1–62. Available from: https://doi.org/10.1016/bs.aecr.2017.12.001

298. Tyson JR, O'Neil NJ, Jain M, Olsen HE, Hieter P, Snutch TP. MinION-based long-read sequencing and assembly extends the Caenorhabditis elegans reference genome. Genome Res. 2018 Feb;28(2):266–74.

299. Plesivkova D, Richards R, Harbison S. A review of the potential of the MinION™ single-molecule sequencing system for forensic applications. Wiley Interdisciplinary Reviews: Forensic Science. 2019;1(1):e1323.

300. Illumina Inc. MiSeq system datasheet [Internet]. 2018 [cited 2019 Nov 20]. Available from: https://www.illumina.com/documents/products/datasheets/datasheet_miseq.pdf

301. Oxford Nanopore Technologies. MinION [Internet]. 2018 [cited 2019 Nov 20]. Available from: http://nanoporetech.com/products/minion

302. Brown S. Sequencing-by-synthesis: Explaining the Illumina sequencing technology [Internet]. 2017 [cited 2019 Nov 20]. Available from:

https://bitesizebio.com/13546/sequencing-by-synthesis-explaining-the-illumina-sequencing-technology/

303. Göpfrich K, Judge K. Decoding DNA with a pocket-sized sequencer [Internet]. 2018 [cited 2019 Nov 20]. Available from: https://www.scienceinschool.org/content/decoding-dna-pocket-sized-sequencer

304. Goodwin S, McPherson JD, McCombie WR. Coming of age: ten years of next-generation sequencing technologies. Nat Rev Genet. 2016 17;17(6):333–51.

305. Marston DA, McElhinney LM, Ellis RJ, Horton DL, Wise EL, Leech SL, et al. Next generation sequencing of viral RNA genomes. BMC Genomics. 2013 Jul 4;14:444.

306. Viehweger A, Krautwurst S, Lamkiewicz K, Madhugiri R, Ziebuhr J, Hölzer M, et al. Direct RNA nanopore sequencing of full-length coronavirus genomes provides novel insights into structural variants and enables modification analysis. Genome Res. 2019;29(9):1545–54.

307. Keller MW, Rambo-Martin BL, Wilson MM, Ridenour CA, Shepard SS, Stark TJ, et al. Direct RNA sequencing of the coding complete influenza A virus genome. Sci Rep. 2018 26;8(1):14408.

308. Greninger AL. A decade of RNA virus metagenomics is (not) enough. Virus Res. 2017 Oct 18;244:218–29.

309. Wongsurawat T, Jenjaroenpun P, Taylor MK, Lee J, Tolardo AL, Parvathareddy J, et al. Rapid sequencing of multiple RNA viruses in their native form. Front Microbiol. 2019 Feb;10:260.

310. Yang Y, Walls SD, Gross SM, Schroth GP, Jarman RG, Hang J. Targeted sequencing of respiratory viruses in clinical specimens for pathogen identification and genome-wide analysis. Methods Mol Biol. 2018;1838:125–40.

311. Ladner JT, Grubaugh ND, Pybus OG, Andersen KG. Precision epidemiology for infectious disease control. Nat Med. 2019;25(2):206–11.

312. Rivera MC, Izard J. Metagenomics for microbiology. Elsevier Academic Press; 2015. 188 p.

313. Chiu CY, Miller SA. Clinical metagenomics. Nat Rev Genet. 2019;20(6):341–55.

314. Kallies R, Hölzer M, Brizola Toscan R, Nunes da Rocha U, Anders J, Marz M, et al. Evaluation of sequencing library preparation protocols for viral metagenomic analysis from pristine aquifer groundwaters. Viruses. 2019 Jun;11(6):484.

315. Karlsson OE, Belák S, Granberg F. The effect of preprocessing by sequence-independent, single-primer amplification (SISPA) on metagenomic detection of viruses. Biosecur Bioterror. 2013 Sep;11 Suppl 1:S227-234.

316. Wilson MR, Naccache SN, Samayoa E, Biagtan M, Bashir H, Yu G, et al. Actionable diagnosis of neuroleptospirosis by next-generation sequencing. New England Journal of Medicine. 2014 Jun 19;370(25):2408–17.

317. Naccache SN, Peggs KS, Mattes FM, Phadke R, Garson JA, Grant P, et al. Diagnosis of neuroinvasive astrovirus infection in an immunocompromised adult with encephalitis by unbiased next-generation sequencing. Clin Infect Dis. 2015 Mar 15;60(6):919–23.

318. Greninger AL, Chen EC, Sittler T, Scheinerman A, Roubinian N, Yu G, et al. A metagenomic analysis of pandemic influenza A (2009 H1N1) infection in patients from North America. PLoS ONE. 2010 Oct 18;5(10):e13381.

319. Greninger AL, Naccache SN, Messacar K, Clayton A, Yu G, Somasekar S, et al. A novel outbreak enterovirus D68 strain associated with acute flaccid myelitis cases in the USA (2012-14): a retrospective cohort study. Lancet Infect Dis. 2015 Jun;15(6):671–82.

320. Naccache SN, Federman S, Veeraraghavan N, Zaharia M, Lee D, Samayoa E, et al. A cloud-compatible bioinformatics pipeline for ultrarapid pathogen identification from next-generation sequencing of clinical samples. Genome Res. 2014 Jul;24(7):1180–92.

321. Kafetzopoulou LE, Efthymiadis K, Lewandowski K, Crook A, Carter D, Osborne J, et al. Assessment of metagenomic Nanopore and Illumina sequencing for recovering whole genome sequences of chikungunya and dengue viruses directly from clinical samples. Euro Surveill. 2018 Dec;23(50).

322. Greninger AL, Naccache SN, Federman S, Yu G, Mbala P, Bres V, et al. Rapid metagenomic identification of viral pathogens in clinical samples by real-time nanopore sequencing analysis. Genome Med. 2015 Sep 29;7:99.

323. Djikeng A, Halpin R, Kuzmickas R, Depasse J, Feldblyum J, Sengamalay N, et al. Viral genome sequencing by random priming methods. BMC Genomics. 2008 Jan 7;9:5.

324. Chrzastek K, Lee D-H, Smith D, Sharma P, Suarez DL, Pantin-Jackwood M, et al. Use of Sequence-Independent, Single-Primer-Amplification (SISPA) for rapid detection, identification, and characterization of avian RNA viruses. Virology. 2017;509:159–66.

325. Goya S, Valinotto LE, Tittarelli E, Rojo GL, Nabaes Jodar MS, Greninger AL, et al. An optimized methodology for whole genome sequencing of RNA respiratory viruses from nasopharyngeal aspirates. PLoS One [Internet]. 2018 Jun 25 [cited 2019 Dec 21];13(6). Available from: https://www.ncbi.nlm.nih.gov/pmc/articles/PMC6016902/

326. Kim D, Song L, Breitwieser FP, Salzberg SL. Centrifuge: rapid and sensitive classification of metagenomic sequences. Genome Res. 2016 Dec;26(12):1721–9.

327. Bankevich A, Nurk S, Antipov D, Gurevich AA, Dvorkin M, Kulikov AS, et al. SPAdes: a new genome assembly algorithm and its applications to single-cell sequencing. J Comput Biol. 2012 May;19(5):455–77.

328. Menzel P, Ng KL, Krogh A. Fast and sensitive taxonomic classification for metagenomics with Kaiju. Nat Commun. 2016 Apr 13;7:11257.

329. Li H, Durbin R. Fast and accurate long-read alignment with Burrows–Wheeler transform. Bioinformatics. 2010 Mar 1;26(5):589–95.

330. Grumaz S, Stevens P, Grumaz C, Decker SO, Weigand MA, Hofer S, et al. Next-generation sequencing diagnostics of bacteremia in septic patients. Genome Medicine. 2016 Jul 1;8(1):73.

331. Doan T, Wilson MR, Crawford ED, Chow ED, Khan LM, Knopp KA, et al. Illuminating uveitis: metagenomic deep sequencing identifies common and rare pathogens. Genome Medicine. 2016 Aug 25;8(1):90.

332. Pendleton KM, Erb-Downward JR, Bao Y, Branton WR, Falkowski NR, Newton DW, et al. Rapid pathogen identification in bacterial pneumonia using real-time metagenomics. Am J Respir Crit Care Med. 2017 May 5;196(12):1610–2.

333. Li Y, Wang H, Nie K, Zhang C, Zhang Y, Wang J, et al. VIP: an integrated pipeline for metagenomics of virus identification and discovery. Sci Rep [Internet]. 2016 Mar 30;6. Available from: https://www.ncbi.nlm.nih.gov/pmc/articles/PMC4824449/

334. Miller S, Naccache SN, Samayoa E, Messacar K, Arevalo S, Federman S, et al. Laboratory validation of a clinical metagenomic sequencing assay for pathogen detection in cerebrospinal fluid. Genome Res. 2019;29(5):831–42.

335. Lewandowski K, Xu Y, Pullan ST, Lumley SF, Foster D, Sanderson N, et al. Metagenomic Nanopore sequencing of influenza virus direct from clinical respiratory samples. Journal of Clinical Microbiology [Internet]. 2019 Dec 23 [cited 2020 Jan 1];58(1). Available from: https://jcm.asm.org/content/58/1/e00963-19

336. Kopylova E, Navas-Molina JA, Mercier C, Xu ZZ, Mahé F, He Y, et al. Open-source sequence clustering methods improve the state of the art. mSystems. 2016 Feb;1(1).

337. Westcott SL, Schloss PD. De novo clustering methods outperform reference-based methods for assigning 16S rRNA gene sequences to operational taxonomic units. PeerJ. 2015;3:e1487.

338. Boers SA, Jansen R, Hays JP. Understanding and overcoming the pitfalls and biases of next-generation sequencing (NGS) methods for use in the routine clinical microbiological diagnostic laboratory. Eur J Clin Microbiol Infect Dis. 2019 Jun;38(6):1059–70.

339. Anthony SJ, Islam A, Johnson C, Navarrete-Macias I, Liang E, Jain K, et al. Non-random patterns in viral diversity. Nature Communications. 2015 Sep 22;6(1):1–7.

340. Shi M, Lin X-D, Tian J-H, Chen L-J, Chen X, Li C-X, et al. Redefining the invertebrate RNA virosphere. Nature. 2016 Dec 22;540(7634):539–43.

341. Hoffmann B, Tappe D, Höper D, Herden C, Boldt A, Mawrin C, et al. A variegated squirrel bornavirus associated with fatal human encephalitis. 2015 Jul 8;373:154–62.

342. McMullan LK, Folk SM, Kelly AJ, MacNeil A, Goldsmith CS, Metcalfe MG, et al. A new phlebovirus associated with severe febrile illness in Missouri. New England Journal of Medicine. 2012 Aug 30;367(9):834–41.

343. Quick J, Loman NJ, Duraffour S, Simpson JT, Severi E, Cowley L, et al. Real-time, portable genome sequencing for Ebola surveillance. Nature. 2016 Feb 11;530(7589):228–32.

344. Weaver SC, Costa F, Garcia-Blanco MA, Ko AI, Ribeiro GS, Saade G, et al. Zika virus: History, emergence, biology, and prospects for control. Antiviral Res. 2016;130:69–80.

345. Kraemer MUG, Faria NR, Reiner RC, Golding N, Nikolay B, Stasse S, et al. Spread of yellow fever virus outbreak in Angola and the Democratic Republic of the Congo 2015-16: a modelling study. Lancet Infect Dis. 2017;17(3):330–8.

346. Faria NR, Kraemer MUG, Hill SC, Goes de Jesus J, Aguiar RS, Iani FCM, et al. Genomic and epidemiological monitoring of yellow fever virus transmission potential. Science. 2018 31;361(6405):894–9.

347. Andersen KG, Shapiro BJ, Matranga CB, Sealfon R, Lin AE, Moses LM, et al. Clinical sequencing uncovers origins and evolution of Lassa virus. Cell. 2015 Aug 13;162(4):738–50.

348. Kafetzopoulou LE, Pullan ST, Lemey P, Suchard MA, Ehichioya DU, Pahlmann M, et al. Metagenomic sequencing at the epicenter of the Nigeria 2018 Lassa fever outbreak. Science. 2019 04;363(6422):74–7.

349. Metsky HC, Matranga CB, Wohl S, Schaffner SF, Freije CA, Winnicki SM, et al. Zika virus evolution and spread in the Americas. Nature. 2017 15;546(7658):411–5.

350. Faria NR, Quick J, Claro IM, Thézé J, de Jesus JG, Giovanetti M, et al. Establishment and cryptic transmission of Zika virus in Brazil and the Americas. Nature. 2017 15;546(7658):406–10.

351. Quick J, Grubaugh ND, Pullan ST, Claro IM, Smith AD, Gangavarapu K, et al. Multiplex PCR method for MinION and Illumina sequencing of Zika and other virus genomes directly from clinical samples. Nat Protoc. 2017 Jun;12(6):1261–76.

352. World Health Organization. Zika Strategic Response Plan [Internet]. WHO. 2016 [cited 2019 Apr 18]. Available from: http://www.who.int/emergencies/zika-virus/strategic-response-plan/en/

353. Myers N, Mittermeier RA, Mittermeier CG, da Fonseca GA, Kent J. Biodiversity hotspots for conservation priorities. Nature. 2000 Feb 24;403(6772):853–8.

354. Hannigan B, Whitworth J, Carroll M, Roberts A, Bruce C, Samba T, et al. The Ministry of Health and Sanitation, Sierra Leone - Public Health England (MOHS-PHE) Ebola Biobank. Wellcome Open Res. 2019;4:115.

355. Trombley AR, Wachter L, Garrison J, Buckley-Beason VA, Jahrling J, Hensley LE, et al. Comprehensive panel of real-time TaqMan polymerase chain reaction assays for detection and absolute quantification of filoviruses, arenaviruses, and New World hantaviruses. Am J Trop Med Hyg. 2010 May;82(5):954–60.

356. Panning M, Laue T, Olschlager S, Eickmann M, Becker S, Raith S, et al. Diagnostic reverse-transcription polymerase chain reaction kit for filoviruses based on the strain collections of all European biosafety level 4 laboratories. J Infect Dis. 2007 Nov 15;196 Suppl 2:S199-204.

357. Edwards CJ, Welch SR, Chamberlain J, Hewson R, Tolley H, Cane PA, et al. Molecular diagnosis and analysis of Chikungunya virus. J Clin Virol. 2007 Aug;39(4):271–5.

358. Drosten C, Göttig S, Schilling S, Asper M, Panning M, Schmitz H, et al. Rapid detection and quantification of RNA of Ebola and Marburg viruses, Lassa virus, Crimean-Congo hemorrhagic fever virus, Rift Valley fever virus, dengue virus, and yellow fever virus by real-time reverse transcription-PCR. J Clin Microbiol. 2002 Jul;40(7):2323–30.

359. Olschläger S, Lelke M, Emmerich P, Panning M, Drosten C, Hass M, et al. Improved detection of Lassa virus by reverse transcription-PCR targeting the 5' region of S RNA. J Clin Microbiol. 2010 Jun;48(6):2009–13.

360. Powers A, Roehrig JT. Chapter 2: Alphaviruses. In: Diagnostic Virology Protocols. 2nd ed. Humana Press; 2010. p. 23–4.

361. Weidmann M, Rudaz V, Nunes MRT, Vasconcelos PFC, Hufert FT. Rapid detection of human pathogenic orthobunyaviruses. J Clin Microbiol. 2003 Jul;41(7):3299–305.

362. Ciceron L, Jaureguiberry G, Gay F, Danis M. Development of a Plasmodium PCR for monitoring efficacy of antimalarial treatment. J Clin Microbiol. 1999 Jan;37(1):35–8.

363. Gutierrez B, Wise EL, Pullan ST, Logue CH, Bowden TA, Escalera-Zamudio M, et al. The evolutionary dynamics of Oropouche Virus in South America. J Virol. 2019 Dec 4;

364. Paris DH, Blacksell SD, Stenos J, Graves SR, Unsworth NB, Phetsouvanh R, et al. Real-time multiplex PCR assay for detection and differentiation of rickettsiae and orientiae. Trans R Soc Trop Med Hyg. 2008 Feb;102(2):186–93.

365. Pyke AT, Daly MT, Cameron JN, Moore PR, Taylor CT, Hewitson GR, et al. Imported Zika virus infection from the Cook Islands into Australia, 2014. PLoS Curr [Internet]. 2014 Jun 2 [cited 2018 Apr 25];6. Available from: http://currents.plos.org/outbreaks/article/imported-zika-virus-infection-from-the-cook-islands-into-australia-2014/

366. Illumina. Nextera DNA library prep reference guide (15027987 v01) [Internet]. 2016 [cited 2019 Dec 2]. Available from: https://support.illumina.com/content/dam/illumina-support/documents/documentation/chemistry_documentation/samplepreps_nextera/nexteradna/nextera-dna-library-prep-reference-guide-15027987-01.pdf

367. Bolger AM, Lohse M, Usadel B. Trimmomatic: a flexible trimmer for Illumina sequence data. Bioinformatics. 2014 Aug 1;30(15):2114–20.

368. Goecks J, Nekrutenko A, Taylor J, Galaxy Team. Galaxy: a comprehensive approach for supporting accessible, reproducible, and transparent computational research in the life sciences. Genome Biol. 2010;11(8):R86.

369. Breitwieser FP, Salzberg SL. Pavian: Interactive analysis of metagenomics data for microbiomics and pathogen identification. bioRxiv. 2016 Oct 31;084715.

370. Li H, Handsaker B, Wysoker A, Fennell T, Ruan J, Homer N, et al. The Sequence Alignment/Map format and SAMtools. Bioinformatics. 2009 Aug 15;25(16):2078–9.

371. Penedos AR, Myers R, Hadef B, Aladin F, Brown KE. Assessment of the utility of whole genome sequencing of Measles virus in the characterisation of outbreaks. PLOS ONE. 2015 Nov 16;10(11):e0143081.

372. Forrester NL, Palacios G, Tesh RB, Savji N, Guzman H, Sherman M, et al. Genome-scale phylogeny of the Alphavirus genus suggests a marine origin. J Virol. 2012 Mar;86(5):2729–38.

373. Garmiri P, Loua A, Haba N, Candotti D, Allain J-P. Deletions and recombinations in the core region of hepatitis B virus genotype E strains from asymptomatic blood donors in Guinea, west Africa. J Gen Virol. 2009 Oct;90(Pt 10):2442–51.

374. Bird BH, Khristova ML, Rollin PE, Ksiazek TG, Nichol ST. Complete genome analysis of 33 ecologically and biologically diverse Rift Valley fever virus strains reveals widespread virus movement and low genetic diversity due to recent common ancestry. J Virol. 2007 Mar;81(6):2805–16.

375. Stock NK, Laraway H, Faye O, Diallo M, Niedrig M, Sall AA. Biological and phylogenetic characteristics of yellow fever virus lineages from West Africa. J Virol. 2013 Mar;87(5):2895–907.

376. Herrera BB, Chang CA, Hamel DJ, Mboup S, Ndiaye D, Imade G, et al. Continued transmission of Zika virus in humans in West Africa, 1992-2016. J Infect Dis. 2017 15;215(10):1546–50.

377. de Wachter R, Merregaert J, Vandenberghe A, Contreras R, Fiers W. Studies on the bacteriophage MS2. The untranslated 5'-terminal nucleotide sequence preceding the first cistron. Eur J Biochem. 1971 Oct 14;22(3):400–14.

378. Ho DTW, Chan DPC, Lam CY, Liang DC, Lee SS, Kam JKM. At the advancing front of Chikungunya fever in Asia: Two imported cases in Hong Kong with novel amino acid changes. J Microbiol Immunol Infect. 2018 Jun;51(3):419–21.

379. Nakayama E, Tajima S, Kotaki A, Shibasaki K-I, Itokawa K, Kato K, et al. A summary of the imported cases of Chikungunya fever in Japan from 2006 to June 2016. J Travel Med. 2018 Jan 1;25(1).

380. Wise EL, Pullan ST, Márquez S, Paz V, Mosquera JD, Zapata S, et al. Isolation of Oropouche virus from febrile patient, Ecuador. Emerging Infect Dis. 2018 May;24(5):935–7.

381. Stewart-Ibarra AM, Ryan SJ, Kenneson A, King CA, Abbott M, Barbachano-Guerrero A, et al. The burden of dengue fever and chikungunya in southern coastal Ecuador: epidemiology, clinical presentation, and phylogenetics from the first two years of a prospective study. Am J Trop Med Hyg. 2018 May;98(5):1444–59.

382. Gómez MM, Abreu FVS de, Santos AACD, Mello IS, Santos MP, Ribeiro IP, et al. Genomic and structural features of the yellow fever virus from the 2016-2017 Brazilian outbreak. J Gen Virol. 2018;99(4):536–48.

383. Koren S, Walenz BP, Berlin K, Miller JR, Bergman NH, Phillippy AM. Canu: scalable and accurate long-read assembly via adaptive k-mer weighting and repeat separation. Genome Res. 2017;27(5):722–36.

384. Bell TG, Yousif M, Kramvis A. Bioinformatic curation and alignment of genotyped hepatitis B virus (HBV) sequence data from the GenBank public database. Springerplus. 2016 Oct 28;5(1):1896.

385. Siepel AC, Halpern AL, Macken C, Korber BT. A computer program designed to screen rapidly for HIV type 1 intersubtype recombinant sequences. AIDS Res Hum Retroviruses. 1995 Nov;11(11):1413–6.

386. Yendewa GA, Sahr F, Lakoh S, Ruiz M, Patiño L, Tabernilla A, et al. Prevalence of drug resistance mutations among ART-naive and -experienced HIV-infected patients in Sierra Leone. J Antimicrob Chemother. 2019 Jul 1;74(7):2024–9.

387. Tilston-Lunel NL, Hughes J, Acrani GO, da Silva DEA, Azevedo RSS, Rodrigues SG, et al. Genetic analysis of members of the species Oropouche virus and identification of a novel M segment sequence. J Gen Virol. 2015 Jul;96(Pt 7):1636–50.

388. Barbosa NS, Mendonça LR, Dias MVS, Pontelli MC, da Silva EZM, Criado MF, et al. ESCRT machinery components are required for Orthobunyavirus particle production in Golgi compartments. PLoS Pathog. 2018 May 3;14(5):e1007047.

389. Proenca-Modena JL, Hyde JL, Sesti-Costa R, Lucas T, Pinto AK, Richner JM, et al. Interferon-regulatory factor 5-dependent signaling restricts Orthobunyavirus dissemination to the central nervous system. J Virol. 2016 01;90(1):189–205.

390. Geddes VEV, Oliveira AS de, Tanuri A, Arruda E, Ribeiro-Alves M, Aguiar RS. MicroRNA and cellular targets profiling reveal miR-217 and miR-576-3p as proviral factors during Oropouche infection. PLOS Neglected Tropical Diseases. 2018 May 29;12(5):e0006508.

391. Varela M, Piras IM, Mullan C, Shi X, Tilston-Lunel NL, Pinto RM, et al. Sensitivity to BST-2 restriction correlates with Orthobunyavirus host range. Virology. 2017 Sep;509:121–30.

392. Araújo R, Dias LB, Araújo MT, Pinheiro F, Oliva OF. [Ultrastructural changes in the hamster liver after experimental inoculation with Oropouche arbovirus (type BeAn 19991)]. Rev Inst Med Trop Sao Paulo. 1978 Feb;20(1):45–54.

393. Rodrigues AH, Santos RI, Arisi GM, Bernardes ES, Silva ML, Rossi MA, et al. Oropouche virus experimental infection in the golden hamster (Mesocrisetus auratus). Virus Res. 2011 Jan;155(1):35–41.

394. The World Bank Group. World development indicators, DataBank [Internet]. [cited 2018 Feb 1]. Available from: http://databank.worldbank.org/data/reports.aspx?source=world-development-indicators

395. Central Intelligence Agency. Sierra Leone: the world factbook [Internet]. [cited 2019 Apr 18]. Available from: https://www.cia.gov/library/publications/the-world-factbook/geos/sl.html

396. The World Bank Group. World bank country and lending groups [Internet]. [cited 2018 Feb 1]. Available from: https://datahelpdesk.worldbank.org/knowledgebase/articles/906519-world-bank-country-and-lending-groups

397. The World Health Organization. Sierra Leone [Internet]. WHO. [cited 2019 Nov 24]. Available from: http://www.who.int/countries/sle/en/

398. Center for Disease Control and Prevention. CDC global health - Sierra Leone [Internet]. 2019 [cited 2019 Jun 13]. Available from: https://www.cdc.gov/globalhealth/countries/sierra-leone/default.htm

399. World Health Organization. Sierra Leone Annual Report 2017 [Internet]. [cited 2019 Jun 13]. Available from: https://www.afro.who.int/publications/world-health-organization-sierra-leone-annual-report-2017

400. World Health Organization, Regional Office for Africa. Sierra Leone [Internet]. WHO | Regional Office for Africa. [cited 2019 Nov 24]. Available from: https://www.afro.who.int/countries/sierra-leone

401. Yendewa GA, Poveda E, Yendewa SA, Sahr F, Quiñones-Mateu ME, Salata RA. HIV/AIDS in Sierra Leone: Characterizing the hidden epidemic. AIDS Rev. 2018 Jun;20(2):104–13.

402. UNAIDS. Sierra Leone [Internet]. 2019 [cited 2019 Aug 26]. Available from: https://www.unaids.org/en/regionscountries/countries/sierraleone

403. World Health Organization, Regional Office for Africa. Report on key populations in African HIV/AIDS: national strategic plans [Internet]. 2018 Jul [cited 2019 Dec 5]. Report No.: WHO/AF/CDS/HIV/02, 2018. Available from: https://apps.who.int/iris/bitstream/handle/10665/275494/WHO-AF-CDS-HIV-02.2018-eng.pdf?ua=1

404. Shaffer JG, Schieffelin JS, Gbakie M, Alhasan F, Roberts NB, Goba A, et al. A medical records and data capture and management system for Lassa fever in Sierra Leone: Approach, implementation, and challenges. PLoS One [Internet]. 2019 Mar 28 [cited 2019 Nov 25];14(3). Available from: https://www.ncbi.nlm.nih.gov/pmc/articles/PMC6438490/

405. Boisen ML, Schieffelin JS, Goba A, Oottamasathien D, Jones AB, Shaffer JG, et al. Multiple circulating infections can mimic the early stages of viral hemorrhagic fevers and possible human exposure to filoviruses in Sierra Leone prior to the 2014 outbreak. Viral Immunology. 2014 Dec 22;28(1):19–31.

406. World Health Organization. 2014 West African Ebola outbreak: feature map [Internet]. [cited 2019 Apr 4]. Available from: https://www.who.int/features/ebola/storymap/en/

407. Baize S, Pannetier D, Oestereich L, Rieger T, Koivogui L, Magassouba N, et al. Emergence of Zaire Ebola virus disease in Guinea. New England Journal of Medicine. 2014 Oct 9;371(15):1418–25.

408. Government of the United Kingdom. How the UK government is responding to Ebola [Internet]. [cited 2019 Apr 4]. Available from: https://www.gov.uk/government/topical-events/ebola-virus-government-response/about

409. Kerber R, Krumkamp R, Diallo B, Jaeger A, Rudolf M, Lanini S, et al. Analysis of diagnostic findings from the European mobile laboratory in Guéckédou, Guinea, March 2014 through March 2015. J Infect Dis. 2016 Oct 15;214(suppl 3):S250–7.

410. Logue CH, Lewis SM, Lansley A, Fraser S, Shieber C, Shah S, et al. Case study: design and implementation of training for scientists deploying to Ebola diagnostic field laboratories in Sierra Leone: October 2014 to February 2016. Philos Trans R Soc Lond, B, Biol Sci. 2017 May 26;372(1721).

411. O'Shea MK, Clay KA, Craig DG, Matthews SW, Kao RLC, Fletcher TE, et al. Diagnosis of febrile illnesses other than Ebola virus disease at an Ebola treatment unit in Sierra Leone. Clin Infect Dis. 2015 Sep 1;61(5):795–8.

412. Gire SK, Goba A, Andersen KG, Sealfon RSG, Park DJ, Kanneh L, et al. Genomic surveillance elucidates Ebola virus origin and transmission during the 2014 outbreak. Science. 2014 Sep 12;345(6202):1369–72.

413. Lauck M, Bailey AL, Andersen KG, Goldberg TL, Sabeti PC, O'Connor DH. GB virus C coinfections in West African Ebola patients. J Virol. 2014 Dec 3;89(4):2425–9.

414. Tamura K, Nei M. Estimation of the number of nucleotide substitutions in the control region of mitochondrial DNA in humans and chimpanzees. Mol Biol Evol. 1993 May;10(3):512–26.

415. Kumar S, Stecher G, Tamura K. MEGA7: molecular evolutionary genetics analysis version 7.0 for bigger datasets. Mol Biol Evol. 2016;33(7):1870–4.

416. Abbott. BinaxNOW Malaria [Internet]. [cited 2019 Aug 28]. Available from: https://www.alere.com/en/home/product-details/binaxnow-malaria.html

417. Abbott. SD BIOLINE Malaria Ag P.f/Pan [Internet]. [cited 2019 Aug 28]. Available from: https://www.alere.com/en/home/product-details/sd-bioline-malaria-ag-p-f-pan.html

418. Wanja EW, Kuya N, Moranga C, Hickman M, Johnson JD, Moseti C, et al. Field evaluation of diagnostic performance of malaria rapid diagnostic tests in western Kenya. Malar J [Internet]. 2016 Sep 7 [cited 2019 Aug 28];15(1). Available from: https://www.ncbi.nlm.nih.gov/pmc/articles/PMC5015256/

419. Spengler JR, Bergeron É, Spiropoulou CF. Crimean-Congo hemorrhagic fever and expansion from endemic regions. Curr Opin Virol. 2019 Feb;34:70–8.

420. World Health Organization. Rift Valley fever [Internet]. [cited 2019 Aug 16]. Available from: http://www.who.int/emergencies/diseases/rift-valley-fever/en/

421. World Health Organization. WHO factsheet on Zika virus [Internet]. 2018 [cited 2019 Nov 17]. Available from: https://www.who.int/news-room/fact-sheets/detail/zika-virus

422. World Health Organization. Yellow fever in Sierra Leone [Internet]. [cited 2019 Aug 16]. Available from: https://www.who.int/csr/don/2011_03_11/en/

423. Parola P, Paddock CD, Socolovschi C, Labruna MB, Mediannikov O, Kernif T, et al. Update on tick-borne Rickettsioses around the world: a geographic approach. Clin Microbiol Rev. 2013 Oct;26(4):657–702.

424. Redus MA, Parker RA, McDade JE. Prevalence and distribution of spotted fever and typhus infections in Sierra Leone and Ivory Coast. Int J Zoonoses. 1986 Jun;13(2):104–11.

425. World Health Organization. Chikungunya [Internet]. [cited 2019 Aug 16]. Available from: http://www.who.int/denguecontrol/arbo-viral/other_arboviral_chikungunya/en/

426. Ng LC, Hapuarachchi HC. Tracing the path of Chikungunya virus--evolution and adaptation. Infect Genet Evol. 2010 Oct;10(7):876–85.

427. Burt FJ, Rolph MS, Rulli NE, Mahalingam S, Heise MT. Chikungunya: a re-emerging virus. Lancet. 2012 Feb 18;379(9816):662–71.

428. Staples JE, Breiman RF, Powers AM. Chikungunya fever: an epidemiological review of a re-emerging infectious disease. Clin Infect Dis. 2009 Sep 15;49(6):942–8.

429. Robin Y, Mouchet J. [Serological and entomological study on yellow fever in Sierra Leone]. Bull Soc Pathol Exot Filiales. 1975 Jun;68(3):249–58.

430. Ansumana R, Jacobsen KH, Leski TA, Covington AL, Bangura U, Hodges MH, et al. Reemergence of chikungunya virus in Bo, Sierra Leone. Emerging Infect Dis. 2013 Jul;19(7):1108–10.

431. Broadhurst MJ, Kelly JD, Miller A, Semper A, Bailey D, Groppelli E, et al. ReEBOV Antigen Rapid Test kit for point-of-care and laboratory-based testing for Ebola virus disease: a field validation study. The Lancet. 2015 Aug 29;386(9996):867–74.

432. World Health Organization. Global hepatitis report, 2017 [Internet]. 2017 [cited 2019 Aug 26]. Available from: http://apps.who.int/iris/bitstream/10665/255016/1/9789241565455-eng.pdf?ua=1

433. Hodges M, Sanders E, Aitken C. Seroprevalence of hepatitis markers; HAV, HBV, HCV and HEV amongst primary school children in Freetown, Sierra Leone. West Afr J Med. 1998 Mar;17(1):36–7.

434. Wurie IM, Wurie AT, Gevao SM. Sero-prevalence of hepatitis B virus among middle to high socio-economic antenatal population in Sierra Leone. West Afr J Med. 2005 Mar;24(1):18–20.

435. García-Tardón N, Gresnigt TM, Fofanah AB, Grobusch MP. Hepatitis B and C in Tonkolili province, Sierra Leone. Lancet. 2017 Sep 23;390(10101):1485.

436. Velkov S, Ott JJ, Protzer U, Michler T. The global hepatitis B virus genotype distribution approximated from available genotyping data. Genes [Internet]. 2018 Oct 15 [cited 2019 Aug 26];9(10). Available from: https://www.ncbi.nlm.nih.gov/pmc/articles/PMC6210291/

437. Liu WJ, Hu H-Y, Su Q-D, Zhang Z, Liu Y, Sun Y-L, et al. HIV prevalence in suspected Ebola cases during the 2014-2016 Ebola epidemic in Sierra Leone. Infect Dis Poverty. 2019 Mar 4;8(1):15.

438. Taylor BS, Sobieszczyk ME, McCutchan FE, Hammer SM. The challenge of HIV-1 subtype diversity. N Engl J Med. 2008 Apr 10;358(15):1590–602.

439. Luk K-C, Berg MG, Naccache SN, Kabre B, Federman S, Mbanya D, et al. Utility of metagenomic next-generation sequencing for characterization of HIV and human pegivirus diversity. PLOS ONE. 2015 Nov 23;10(11):e0141723.

440. Stapleton JT, Foung S, Muerhoff AS, Bukh J, Simmonds P. The GB viruses: a review and proposed classification of GBV-A, GBV-C (HGV), and GBV-D in genus Pegivirus within the family Flaviviridae. J Gen Virol. 2011 Feb;92(Pt 2):233–46.

441. Blair CS, Davidson F, Lycett C, McDonald DM, Haydon GH, Yap PL, et al. Prevalence, incidence, and clinical characteristics of hepatitis G virus/GB virus C infection in Scottish blood donors. J Infect Dis. 1998 Dec;178(6):1779–82.

442. Gutierrez RA, Dawson GJ, Knigge MF, Melvin SL, Heynen CA, Kyrk CR, et al. Seroprevalence of GB virus C and persistence of RNA and antibody. J Med Virol. 1997 Oct;53(2):167–73.

443. Pilot-Matias TJ, Carrick RJ, Coleman PF, Leary TP, Surowy TK, Simons JN, et al. Expression of the GB virus C E2 glycoprotein using the Semliki Forest virus vector system and its utility as a serologic marker. Virology. 1996 Nov 15;225(2):282–92.

444. Tacke M, Schmolke S, Schlueter V, Sauleda S, Esteban JI, Tanaka E, et al. Humoral immune response to the E2 protein of hepatitis G virus is associated with long-term recovery from infection and reveals a high frequency of hepatitis G virus exposure among healthy blood donors. Hepatology. 1997 Dec;26(6):1626–33.

445. Mohr EL, Stapleton JT. GB virus type C interactions with HIV: the role of envelope glycoproteins. J Viral Hepat. 2009 Nov;16(11):757–68.

446. Polgreen PM, Xiang J, Chang Q, Stapleton JT. GB virus type C/hepatitis G virus: a non-pathogenic flavivirus associated with prolonged survival in HIV-infected individuals. Microbes Infect. 2003 Nov;5(13):1255–61.

447. Zhang W, Chaloner K, Tillmann HL, Williams CF, Stapleton JT. Effect of early and late GB virus C viraemia on survival of HIV-infected individuals: a meta-analysis. HIV Med. 2006 Apr;7(3):173–80.

448. Stapleton JT, Martinson JA, Klinzman D, Xiang J, Desai SN, Landay A. GB virus C infection and B-cell, natural killer cell, and monocyte activation markers in HIV-infected individuals. AIDS. 2013 Jul 17;27(11):1829–32.

449. Rosseel T, Pardon B, Clercq KD, Ozhelvaci O, Borm SV. False-positive results in metagenomic virus discovery: a strong case for follow-up diagnosis. Transboundary and Emerging Diseases. 2014;61(4):293–9.

450. Lewandowski K, Bell A, Miles R, Carne S, Wooldridge D, Manso C, et al. The effect of nucleic acid extraction platforms and sample storage on the integrity of viral RNA for use in whole genome sequencing. J Mol Diagn. 2017;19(2):303–12.

451. Verheyen J, Kaiser R, Bozic M, Timmen-Wego M, Maier BK, Kessler HH. Extraction of viral nucleic acids: comparison of five automated nucleic acid extraction platforms. J Clin Virol. 2012 Jul;54(3):255–9.

452. Central Intelligence Agency. Ecuador - the world factbook [Internet]. [cited 2019 Apr 6]. Available from: https://www.cia.gov/library/publications/the-world-factbook/geos/ec.html

453. TUBS. Español: Mapa de las provincias de Ecuador [Internet]. 2014 [cited 2019 Nov 28]. Available from: https://commons.wikimedia.org/wiki/File:Ecuador,_administrative_divisions_-_es_-_colored.svg

454. Tandon A, Murray CJ, Lauer JA, Evans DB. Measuring overall health system performance for 191 countries [Internet]. World Health Organization; [cited 2019 Dec 2] p. 23. (GPE Discussion Paper Series). Report No.: 30. Available from: https://www.who.int/healthinfo/paper30.pdf

455. Aldulaimi S, Mora FE. A primary care system to improve health care efficiency: lessons from Ecuador. J Am Board Fam Med. 2017 Jun;30(3):380–3.

456. Pan American Health Organization. Health systems profile - Ecuador [Internet]. 2008 [cited 2019 Dec 2] p. 68. Available from: http://www1.paho.org/hq/dmdocuments/2010/Health_System_Profile-Ecuador_2008.pdf

457. World Health Organization. Ecuador [Internet]. [cited 2019 Nov 25]. Available from: http://www.who.int/countries/ecu/en/

458. Pan American Health Organization. PAHO/WHO Data - Visualization [Internet]. 2018 [cited 2019 Nov 3]. Available from: http://www.paho.org/data/index.php/en/indicators/visualization.html

459. Pan American Health Organization. PAHO/WHO Data - Leading causes of death [Internet]. 2017 [cited 2019 Nov 25]. Available from: http://www.paho.org/data/index.php/en/indicators-mortality/mnu-lcd-en.html

460. UNAIDS. Ecuador [Internet]. [cited 2019 Nov 25]. Available from: https://www.unaids.org/en/regionscountries/countries/ecuador

461. World Health Organization. Ecuador tuberculosis profile [Internet]. [cited 2019 Nov 25]. Available from: https://extranet.who.int/sree/Reports?op=Replet&name=%2FWHO_HQ_Reports%2FG2%2FPROD%2FEXT%2FTBCountryProfile&ISO2=EC&LAN=EN&outtype=html

462. Pan American Health Organisation, World Health Organization, Regional Office for the Americas. Tuberculosis in the Americas 2018 [Internet]. 2018 [cited 2019 Nov 25]. Report No.: PAHO/CDE/18-036. Available from:

http://iris.paho.org/xmlui/bitstream/handle/123456789/49510/PAHOCDE18036_eng?sequence=1&isAllowed=y

463. Cartelle Gestal M, Holban AM, Escalante S, Cevallos M. Epidemiology of tropical neglected diseases in Ecuador in the last 20 years. PLoS One [Internet]. 2015 Sep 22 [cited 2019 Nov 25];10(9). Available from: https://www.ncbi.nlm.nih.gov/pmc/articles/PMC4579123/

464. Castilho JG, Carnieli PJ, Durymanova EA, Fahl W de O, Oliveira R de N, Macedo CI, et al. Human rabies transmitted by vampire bats: antigenic and genetic characterization of rabies virus isolates from the Amazon region (Brazil and Ecuador). Virus Research. 2010 Oct;153(1):100–5.

465. Lee DN, Papeş M, Bussche RAVD. Present and potential future distribution of common vampire bats in the Americas and the associated risk to cattle. PLOS ONE. 2012 Aug 10;7(8):e42466.

466. World Health Organization. World malaria report 2011 [Internet]. 2011 [cited 2018 May 9]. Available from: http://www.who.int/malaria/publications/atoz/9789241564403/en/

467. World Health Organization. World malaria report 2018 [Internet]. 2018 Nov [cited 2019 Dec 2] p. 210. Available from: https://www.who.int/malaria/publications/world-malaria-report-2018/report/en/

468. Cifuentes SG, Trostle J, Trueba G, Milbrath M, Baldeón ME, Coloma J, et al. Transition in the cause of fever from malaria to dengue, Northwestern Ecuador, 1990-2011. Emerging Infect Dis. 2013 Oct;19(10):1642–5.

469. Ramos-Castañeda J, Barreto Dos Santos F, Martínez-Vega R, Galvão de Araujo JM, Joint G, Sarti E. Dengue in Latin America: Systematic review of molecular epidemiological trends. PLoS Negl Trop Dis. 2017 Jan;11(1):e0005224.

470. Eisenberg JNS, Cevallos W, Ponce K, Levy K, Bates SJ, Scott JC, et al. Environmental change and infectious disease: how new roads affect the transmission of diarrheal pathogens in rural Ecuador. Proc Natl Acad Sci USA. 2006 Dec 19;103(51):19460–5.

471. Eisenberg JNS, Goldstick J, Cevallos W, Trueba G, Levy K, Scott J, et al. In-roads to the spread of antibiotic resistance: regional patterns of microbial transmission in northern coastal Ecuador. J R Soc Interface. 2012 May 7;9(70):1029–39.

472. Stewart-Ibarra AM, Lowe R. Climate and non-climate drivers of dengue epidemics in southern coastal ecuador. Am J Trop Med Hyg. 2013 May;88(5):971–81.

473. Stewart-Ibarra AM, Ryan SJ, Beltrán E, Mejía R, Silva M, Muñoz A. Dengue vector dynamics (Aedes aegypti) influenced by climate and social factors in Ecuador: implications for targeted control. PLoS ONE. 2013;8(11):e78263.

474. Cevallos V, Ponce P, Waggoner JJ, Pinsky BA, Coloma J, Quiroga C, et al. Zika and Chikungunya virus detection in naturally infected Aedes aegypti in Ecuador. Acta Trop. 2018 Jan;177:74–80.

475. Pan American Health Organization, World Health Organization, Regional Office for the Americas. Zika - epidemiological report, Ecuador. [Internet]. 2017 Sep [cited 2019 Jun 4] p. 5. Available from: http://www.paho.org/hq/index.php?option=com_docman&task=doc_view&gid=35027&Itemid=270&lang=en.

476. Zambrano H, Waggoner JJ, Almeida C, Rivera L, Benjamin JQ, Pinsky BA. Zika virus and chikungunya virus coInfections: a series of three cases from a single center in Ecuador. Am J Trop Med Hyg. 2016 Oct 5;95(4):894–6.

477. Pan American Health Organization. PAHO/WHO data - Chikungunya weekly report [Internet]. 2019 [cited 2019 Nov 3]. Available from: http://www.paho.org/data/index.php/en/mnu-topics/chikv-en/550-chikv-weekly-en.html

478. Demeester R, Bottieau E, Van Esbroeck M, Pourkarim MR, Maes P, Clement J. Hantavirus nephropathy as a pseudo-import pathology from Ecuador. Eur J Clin Microbiol Infect Dis. 2010 Jan;29(1):59–62.

479. Forshey BM, Guevara C, Laguna-Torres VA, Cespedes M, Vargas J, Gianella A, et al. Arboviral etiologies of acute febrile illnesses in Western South America, 2000-2007. PLoS Negl Trop Dis. 2010 Aug 10;4(8):e787.

480. Manock SR, Jacobsen KH, de Bravo NB, Russell KL, Negrete M, Olson JG, et al. Etiology of acute undifferentiated febrile illness in the Amazon basin of Ecuador. Am J Trop Med Hyg. 2009 Jul;81(1):146–51.

481. Márquez S, Carrera J, Pullan ST, Lewandowski K, Paz V, Loman N, et al. First complete genome sequences of Zika virus isolated from febrile patient Sera in Ecuador. Genome Announc. 2017 Feb 23;5(8).

482. Barzon L, Trevisan M, Sinigaglia A, Lavezzo E, Palù G. Zika virus: from pathogenesis to disease control. FEMS Microbiol Lett. 2016 Sep;363(18).

483. Center for Disease Control and Prevention. Zika virus, 2016 case counts [Internet]. 2019 [cited 2019 Apr 25]. Available from: https://www.cdc.gov/zika/reporting/2016-case-counts.html

484. O'Reilly KM, Lowe R, Edmunds WJ, Mayaud P, Kucharski A, Eggo RM, et al. Projecting the end of the Zika virus epidemic in Latin America: a modelling analysis. BMC Medicine. 2018 Oct 3;16(1):180.

485. Reina Ortiz M, Le NK, Sharma V, Hoare I, Quizhpe E, Teran E, et al. Post-earthquake Zika virus surge: Disaster and public health threat amid climatic conduciveness. Sci Rep. 2017 Nov 13;7(1):15408.

486. International Organization for Migration. Displaced Ecuador earthquake survivors face lack of water, sanitation, funding [Internet]. 2016 [cited 2019 Apr 11]. Available from: https://www.iom.int/news/displaced-ecuador-earthquake-survivors-face-lack-water-sanitation-funding

487. Gharbi M, Pillai DR, Lau R, Hubert V, Khairnar K, Existe A, et al. Chloroquine-resistant malaria in travelers returning from Haiti after 2010 earthquake. Emerging Infect Dis. 2012 Aug;18(8):1346–9.

488. Polonsky J, Luquero F, Francois G, Rousseau C, Caleo G, Ciglenecki I, et al. Public health surveillance after the 2010 haiti earthquake: the experience of médecins sans frontières. PLoS Curr. 2013 Jan 7;5.

489. Aguilar PV, Barrett AD, Saeed MF, Watts DM, Russell K, Guevara C, et al. Iquitos virus: a novel reassortant Orthobunyavirus associated with human illness in Peru. PLOS Neglected Tropical Diseases. 2011 Sep 20;5(9):e1315.

490. Instituto Nacional de Estadística y Censos del Ecuador. Esmeraldas (Canton, Ecuador) - Population statistics, charts, map and location [Internet]. 2019 [cited 2019 Oct 31]. Available from: https://www.citypopulation.de/php/ecuador-admin.php?adm2id=0801

491. Stewart-Ibarra AM, Muñoz ÁG, Ryan SJ, Ayala EB, Borbor-Cordova MJ, Finkelstein JL, et al. Spatiotemporal clustering, climate periodicity, and social-ecological risk factors for dengue during an outbreak in Machala, Ecuador, in 2010. BMC Infect Dis. 2014 Nov 25;14:610.

492. Pan American Health Organization, World Health Organization, Regional Office for the Americas. PAHO/WHO data - dengue cases [Internet]. 2015 [cited 2019 Oct 31]. Available from: http://www.paho.org/data/index.php/en/mnu-topics/indicadores-dengue-en/dengue-nacional-en/252-dengue-pais-ano-en.html?start=2

493. Null J. El Niño and La Niña years and intensities [Internet]. 2019 [cited 2019 Nov 3]. Available from: https://ggweather.com/enso/oni.htm

494. Gerrard SR, Li L, Barrett AD, Nichol ST. Ngari virus is a Bunyamwera virus reassortant that can be associated with large outbreaks of hemorrhagic fever in Africa. J Virol. 2004 Aug;78(16):8922–6.

495. Saeed MF, Wang H, Suderman M, Beasley DW, Travassos da Rosa A, Li L, et al. Jatobal virus is a reassortant containing the small RNA of Oropouche virus. Virus Res. 2001 Sep;77(1):25–30.

496. Graf EH, Simmon KE, Tardif KD, Hymas W, Flygare S, Eilbeck K, et al. Unbiased detection of respiratory viruses by use of RNA sequencing-sased metagenomics: a systematic comparison to a commercial PCR panel. J Clin Microbiol. 2016 Apr;54(4):1000–7.

497. Sardi SI, Somasekar S, Naccache SN, Bandeira AC, Tauro LB, Campos GS, et al. Coinfections of Zika and chikungunya viruses in Bahia, Brazil, identified by metagenomic next-generation sequencing. J Clin Microbiol. 2016 Jan 9;54(9):2348–53.

498. Yozwiak NL, Skewes-Cox P, Stenglein MD, Balmaseda A, Harris E, DeRisi JL. Virus identification in unknown tropical febrile illness cases using deep sequencing. PLoS Negl Trop Dis. 2012;6(2):e1485.

499. Vaughan G, Goncalves Rossi LM, Forbi JC, de Paula VS, Purdy MA, Xia G, et al. Hepatitis A virus: host interactions, molecular epidemiology and evolution. Infect Genet Evol. 2014 Jan;21:227–43.

500. Jacobsen KH, Wiersma ST. Hepatitis A virus seroprevalence by age and world region, 1990 and 2005. Vaccine. 2010 Sep 24;28(41):6653–7.

501. Guerrero-Latorre L, Romero B, Bonifaz E, Timoneda N, Rusiñol M, Girones R, et al. Quito's virome: Metagenomic analysis of viral diversity in urban streams of Ecuador's capital city. Science of The Total Environment. 2018 Dec 15;645:1334–43.

502. Enfermedades zoonoticas 1994-2016 [Internet]. Tableau Software. [cited 2019 Oct 31]. Available from: https://public.tableau.com/views/cronicas_2016/ANUARIO?%3Aembed=y&%3AshowVizHome=no&%3Adisplay_count=y&%3Adisplay_static_image=y&%3AbootstrapWhenNotified=true

503. Romero-Sandoval N, Cifuentes L, León G, Lecaro P, Ortiz-Rico C, Cooper P, et al. High rates of exposures to waterborne pathogens in indigenous communities in the Amazon region of Ecuador. Am J Trop Med Hyg. 2019 Jul;101(1):45–50.

504. Pinheiro F, Pinheiro M, Bensabath G, Causey OR, Shope RE (last). Epidemia de viìrus Oropouche em Beleìm. Revista do Serviço Especial de Sauìde Puìblica. 1962;12:13–23.

505. Pinheiro FP, Travassos da Rosa AP, Travassos da Rosa JF, Ishak R, Freitas RB, Gomes ML, et al. Oropouche virus. I. A review of clinical, epidemiological, and ecological findings. Am J Trop Med Hyg. 1981 Jan;30(1):149–60.

506. LeDuc J, Pinheiro F. Oropouche fever. In: Monath T, editor. The Arboviruses: epidemiology and ecology. Boca Raton, FL: CRC Press Inc; 1986.

507. Pinheiro F, Travassos da Rosa A. Arboviral zoonoses of Central and South America. In: Beran G, editor. Handbook of Zoonoses. Boca Raton, FL: CRC Press; 1994. p. 201–25.

508. Pinheiro FP, Travassos da Rosa AP, Travassos da Rosa JF, Bensabath G. An outbreak of Oropouche virus diease in the vicinity of santarem, para, barzil. Tropenmed Parasitol. 1976 Jun;27(2):213–23.

509. Vasconcelos PF, Travassos Da Rosa JF, Guerreiro SC, Dégallier N, Travassos Da Rosa ES, Travassos Da Rosa AP. [1st register of an epidemic caused by Oropouche virus in the states of Maranhão and Goiás, Brazil]. Rev Inst Med Trop Sao Paulo. 1989 Aug;31(4):271–8.

510. Dixon KE, Travassos da Rosa AP, Travassos da Rosa JF, Llewellyn CH. Oropouche virus. II. Epidemiological observations during an epidemic in Santarém, Pará, Brazil in 1975. Am J Trop Med Hyg. 1981 Jan;30(1):161–4.

511. Vasconcelos HB, Azevedo RSS, Casseb SM, Nunes-Neto JP, Chiang JO, Cantuária PC, et al. Oropouche fever epidemic in Northern Brazil: epidemiology and molecular characterization of isolates. J Clin Virol. 2009 Feb;44(2):129–33.

512. Naveca FG, Nascimento VA, Souza VC, de Figueiredo RMP. Human Orthobunyavirus infections, Tefé, Amazonas, Brazil. PLoS Curr. 2018 Mar 22;10.

513. Watts DM, Phillips I, Callahan JD, Griebenow W, Hyams KC, Hayes CG. Oropouche virus transmission in the Amazon River basin of Peru. Am J Trop Med Hyg. 1997 Feb;56(2):148–52.

514. Baisley KJ, Watts DM, Munstermann LE, Wilson ML. Epidemiology of endemic Oropouche virus transmission in upper Amazonian Peru. Am J Trop Med Hyg. 1998 Nov;59(5):710–6.

515. Silva-Caso W, Aguilar-Luis MA, Palomares-Reyes C, Mazulis F, Weilg C, Del Valle LJ, et al. First outbreak of Oropouche Fever reported in a non-endemic western region of the Peruvian Amazon. Molecular diagnosis and clinical characteristics. Int J Infect Dis. 2019 Apr 13;

516. Romero-Alvarez D, Escobar LE. Vegetation loss and the 2016 Oropouche fever outbreak in Peru. Mem Inst Oswaldo Cruz. 2017 Apr;112(4):292–8.

517. Naveca FG, Nascimento VA do, Souza VC de, Nunes BTD, Rodrigues DSG, Vasconcelos PF da C. Multiplexed reverse transcription real-time polymerase chain reaction for simultaneous detection of Mayaro, Oropouche, and Oropouche-like viruses. Mem Inst Oswaldo Cruz. 2017 Jul;112(7):510–3.

518. Camarão A, Swanepoel R, Boinas F, Quan M. Development and analytical validation of a group-specific RT-qPCR assay for the detection of the Simbu serogroup orthobunyaviruses. J Virol Methods. 2019 Sep;271:113685.

519. Moreli ML, Aquino VH, Cruz ACR, Figueiredo LTM. Diagnosis of Oropouche virus infection by RT-nested-PCR. J Med Virol. 2002 Jan;66(1):139–42.

520. Nunes MRT, de Souza WM, Savji N, Figueiredo ML, Cardoso JF, da Silva SP, et al. Oropouche orthobunyavirus: Genetic characterization of full-length genomes and development of molecular methods to discriminate natural reassortments. Infect Genet Evol. 2019;68:16–22.

521. Saeed MF, Wang H, Nunes M, Vasconcelos PF, Weaver SC, Shope RE, et al. Nucleotide sequences and phylogeny of the nucleocapsid gene of Oropouche virus. J Gen Virol. 2000 Mar;81(Pt 3):743–8.

522. Rojas A, Stittleburg V, Cardozo F, Bopp N, Cantero C, López S, et al. Real-time RT-PCR for the detection and quantitation of Oropouche virus. Diagn Microbiol Infect Dis. 2019 Sep 9;114894.

523. Burton DR. Antibodies, viruses and vaccines. Nature Reviews Immunology. 2002 Sep;2(9):706–13.

524. Dudas G, Bedford T. The ability of single genes vs full genomes to resolve time and space in outbreak analysis. BMC Evol Biol. 2019 Dec 26;19(1):232.

525. World Health Organization. Disease outbreaks [Internet]. [cited 2019 Dec 17]. Available from: https://www.who.int/environmental_health_emergencies/disease_outbreaks/en/

526. McPhee DA, Della-Porta AJ. Biochemical and serological comparisons of Australian bunyaviruses belonging to the Simbu serogroup. J Gen Virol. 1988 May;69 (Pt 5):1007–17.

527. Kinney RM, Calisher CH. Antigenic relationships among Simbu serogroup (Bunyaviridae) viruses. Am J Trop Med Hyg. 1981 Nov;30(6):1307–18.

528. Hoch AL, Pinheiro FP, Roberts DR, Gomes ML. Laboratory transmission of Oropouche virus by Culex Quinquefasciatus Say. Bull Pan Am Health Organ. 1987;21(1):55–61.

529. Virus Pathogen Database and Analysis Resource. Peribunyaviridae [Internet]. 2019 [cited 2019 Dec 11]. Available from: https://www.viprbrc.org/brc/aboutPathogen.spg?decorator=peribunya

530. International Committee on Taxonomy of Viruses (ICTV). Genus: Orthobunyavirus [Internet]. International Committee on Taxonomy of Viruses (ICTV). [cited 2019 Dec 11]. Available from: https://talk.ictvonline.org/ictv-reports/ictv_online_report/negative-sense-rna-viruses/bunyavirales/w/peribunyaviridae/1238/genus-orthobunyavirus

531. da Silva Azevedo R do S, Nunes MRT, Chiang JO, Bensabath G, Vasconcelos HB, Pinto AY das N, et al. Reemergence of Oropouche Fever, Northern Brazil. Emerg Infect Dis. 2007 Jun;13(6):912–5.

532. De Figueiredo RMP, Thatcher BD, de Lima ML, Almeida TC, Alecrim WD, Guerra MV de F. [Exanthematous diseases and the first epidemic of dengue to occur in Manaus, Amazonas State, Brazil, during 1998-1999]. Rev Soc Bras Med Trop. 2004 Dec;37(6):476–9.

533. Nunes M, Martins L, Rodrigues S, Chiang J, Azevedo R do S da S, da Rosa A, et al. Oropouche virus isolation, southeast Brazil. Emerging Infect Dis. 2005 Oct;11(10):1610–3.

534. Pinheiro FP, Hoch AL, Gomes ML, Roberts DR. Oropouche virus. IV. Laboratory transmission by Culicoides paraensis. Am J Trop Med Hyg. 1981 Jan;30(1):172–6.

535. Goeldi E. Os mosquitos no Pará. Reunião de quatro trabalhos sobre os mosquitos indigenas, principalmente as especies que molestam o homem. Mem Mus Goeldi Hist Nat Ethnogr. 1905;4:1–154.

536. de Souza Luna LK, Rodrigues AH, Santos RIM, Sesti-Costa R, Criado MF, Martins RB, et al. Oropouche virus is detected in peripheral blood leukocytes from patients. J Med Virol. 2017 Jun;89(6):1108–11.

537. Bastos MS, Lessa N, Naveca FG, Monte RL, Braga WS, Figueiredo LTM, et al. Detection of Herpesvirus, Enterovirus, and Arbovirus infection in patients with suspected central nervous system viral infection in the Western Brazilian Amazon. J Med Virol. 2014 Sep;86(9):1522–7.

538. Nascimento VA do, Santos JHA, Monteiro DC da S, Pessoa KP, Cardoso AJL, Souza VC de, et al. Oropouche virus detection in saliva and urine. bioRxiv. 2019 Sep 8;758839.

539. Fonseca LM dos S, Carvalho RH, Bandeira AC, Sardi SI, Campos GS. Detection of Oropouche virus in saliva and urine samples of febrile patients in Salvador, Bahia, Brazil. Jpn J Infect Dis. 2019 Nov 29;JJID.2019.296.

540. Smith GC, Francy DB. Laboratory studies of a Brazilian strain of Aedes albopictus as a potential vector of Mayaro and Oropouche viruses. J Am Mosq Control Assoc. 1991 Mar;7(1):89–93.

541. Fontenille D, Diallo M, Mondo M, Ndiaye M, Thonnon J. First evidence of natural vertical transmission of yellow fever virus in Aedes aegypti, its epidemic vector. Trans R Soc Trop Med Hyg. 1997 Oct;91(5):533–5.

542. Campbell LP, Luther C, Moo-Llanes D, Ramsey JM, Danis-Lozano R, Peterson AT. Climate change influences on global distributions of dengue and chikungunya virus vectors. Philos Trans R Soc Lond B Biol Sci [Internet]. 2015 Apr 5 [cited 2019 Nov 13];370(1665). Available from: https://www.ncbi.nlm.nih.gov/pmc/articles/PMC4342968/

543. Lippi CA, Stewart-Ibarra AM, Loor MEFB, Zambrano JED, Lopez NAE, Blackburn JK, et al. Geographic shifts in Aedes aegypti habitat suitability in Ecuador using larval surveillance data and ecological niche modeling: Implications of climate change for public health vector control. PLOS Neglected Tropical Diseases. 2019 Apr 17;13(4):e0007322.

544. Varjak M, Maringer K, Watson M, Sreenu VB, Fredericks AC, Pondeville E, et al. Aedes aegypti Piwi4 Is a noncanonical PIWI protein involved in antiviral responses. mSphere. 2017 Jun;2(3).

545. Peleg J. Growth of arboviruses in primary tissue culture of Aedes aegypti embryos. Am J Trop Med Hyg. 1968 Mar;17(2):219–23.

546. Barletta ABF, Silva MCLN, Sorgine MHF. Validation of Aedes aegypti Aag-2 cells as a model for insect immune studies. Parasites & Vectors. 2012 Jul 24;5(1):148.

547. Medlock JM, Hansford KM, Schaffner F, Versteirt V, Hendrickx G, Zeller H, et al. A review of the invasive mosquitoes in Europe: ecology, public health risks, and control options. Vector Borne Zoonotic Dis. 2012 Jun;12(6):435–47.

548. Wong P-SJ, Li MI, Chong C-S, Ng L-C, Tan C-H. Aedes (Stegomyia) albopictus (Skuse): a potential vector of Zika virus in Singapore. PLoS Negl Trop Dis. 2013;7(8):e2348.

549. Amraoui F, Vazeille M, Failloux AB. French Aedes albopictus are able to transmit yellow fever virus. Euro Surveill. 2016 Sep 29;21(39).

550. Ponce P, Morales D, Argoti A, Cevallos VE. First report of Aedes (Stegomyia) albopictus (Skuse) (Diptera: Culicidae), the Asian tiger mosquito, in Ecuador. J Med Entomol. 2018 Jan;55(1):248–9.

551. Igarashi A. Isolation of a Singh's Aedes albopictus cell clone sensitive to Dengue and Chikungunya viruses. J Gen Virol. 1978 Sep;40(3):531–44.

552. Miller ML, Brown DT. Morphogenesis of Sindbis virus in three subclones of Aedes albopictus (mosquito) cells. J Virol. 1992 Jul;66(7):4180–90.

553. Singh K. Cell cultures derived from larvae of Aedes albopictus (Skuse) and Aedes aegypti (L.). Curr Sci India. 1967;36:506–8.

554. Brackney DE, Scott JC, Sagawa F, Woodward JE, Miller NA, Schilkey FD, et al. C6/36 Aedes albopictus cells have a dysfunctional antiviral RNA interference response. PLoS Negl Trop Dis. 2010 Oct 26;4(10):e856.

555. Weger-Lucarelli J, Rückert C, Grubaugh ND, Misencik MJ, Armstrong PM, Stenglein MD, et al. Adventitious viruses persistently infect three commonly used mosquito cell lines. Virology. 2018;521:175–80.

556. Paradkar PN, Trinidad L, Voysey R, Duchemin J-B, Walker PJ. Secreted Vago restricts West Nile virus infection in Culex mosquito cells by activating the Jak-STAT pathway. Proc Natl Acad Sci USA. 2012 Nov 13;109(46):18915–20.

557. Scott JC, Brackney DE, Campbell CL, Bondu-Hawkins V, Hjelle B, Ebel GD, et al. Comparison of dengue virus type 2-specific small RNAs from RNA interference-competent and -incompetent mosquito cells. PLoS Negl Trop Dis. 2010 Oct 26;4(10):e848.

558. Siu RWC, Fragkoudis R, Simmonds P, Donald CL, Chase-Topping ME, Barry G, et al. Antiviral RNA interference responses induced by Semliki Forest virus infection of mosquito cells: characterization, origin, and frequency-dependent functions of virus-derived small interfering RNAs. J Virol. 2011 Mar;85(6):2907–17.

559. Rutledge CR, Day JF, Lord CC, Stark LM, Tabachnick WJ. West Nile virus infection rates in Culex nigripalpus (Diptera: Culicidae) do not reflect transmission rates in Florida. J Med Entomol. 2003 May;40(3):253–8.

560. Vitek CJ, Richards SL, Mores CN, Day JF, Lord CC. Arbovirus transmission by Culex nigripalpus in Florida, 2005. J Med Entomol. 2008 May;45(3):483–93.

561. Hribar LJ, Vlach JJ, Demay DJ, Stark LM, Stoner RL, Godsey MS, et al. Mosquitoes infected with West Nile Virus in the Florida Keys, Monroe County, Florida, USA. J Med Entomol. 2003 May 1;40(3):361–3.

562. Andreadis TG. The contribution of Culex pipiens complex mosquitoes to transmission and persistence of West Nile virus in North America. J Am Mosq Control Assoc. 2012 Dec;28(4 Suppl):137–51.

563. Kramer LD, Styer LM, Ebel GD. A global perspective on the epidemiology of West Nile virus. Annu Rev Entomol. 2008;53:61–81.

564. Hsu SH, Mao WH, Cross JH. Establishment of a line of cells derived from ovarian tissue of Clex quinquefasciatus Say. J Med Entomol. 1970 Dec;7(6):703–7.

565. Samy AM, Elaagip AH, Kenawy MA, Ayres CFJ, Peterson AT, Soliman DE. Climate change influences on the global potential distribution of the mosquito Culex quinquefasciatus, vector of West Nile Virus and Lymphatic Filariasis. PLOS ONE. 2016 Oct 3;11(10):e0163863.

566. Batista EP, Costa EF, Silva AA. Anopheles darlingi (Diptera: Culicidae) displays increased attractiveness to infected individuals with Plasmodium vivax gametocytes. Parasites & Vectors. 2014 May 29;7(1):251.

567. Molina-Cruz A, Barillas-Mury C. The remarkable journey of adaptation of the Plasmodium falciparum malaria parasite to New World anopheline mosquitoes. Mem Inst Oswaldo Cruz. 2014;109(5):662–7.

568. Padilla O, Rosas P, Moreno W, Toulkeridis T. Modeling of the ecological niches of the anopheles spp in Ecuador by the use of geo-informatic tools. Spat Spatiotemporal Epidemiol. 2017;21:1–11.

569. Rezza G, Chen R, Weaver SC. O'nyong-nyong fever: a neglected mosquito-borne viral disease. Pathog Glob Health. 2017 Sep;111(6):271–5.

570. Su C-L, Yang C-F, Teng H-J, Lu L-C, Lin C, Tsai K-H, et al. Molecular epidemiology of Japanese encephalitis virus in mosquitoes in Taiwan during 2005–2012. PLOS Neglected Tropical Diseases. 2014 Oct 2;8(10):e3122.

571. Maquart M, Boyer S, Rakotoharinome VM, Ravaomanana J, Tantely ML, Heraud J-M, et al. High prevalence of West Nile virus in domestic birds and detection in 2 new mosquito species in Madagascar. PLoS ONE. 2016;11(1):e0147589.

572. Ratovonjato J, Olive M-M, Tantely LM, Andrianaivolambo L, Tata E, Razainirina J, et al. Detection, isolation, and genetic characterization of Rift Valley fever virus from Anopheles (Anopheles) coustani, Anopheles (Anopheles) squamosus, and Culex (Culex) antennatus of the Haute Matsiatra region, Madagascar. Vector Borne Zoonotic Dis. 2011 Jun;11(6):753–9.

573. Williams MC, Woodall JP, Corbet PS. Nyando virus: A hitherto undescribed virus isolated from Anopheles funestus giles collected in Kenya. Arch Gesamte Virusforsch. 1965 Jun 1;15(3):422–7.

574. Jöst H, Bialonski A, Schmetz C, Günther S, Becker N, Schmidt-Chanasit J. Isolation and phylogenetic analysis of Batai virus, Germany. Am J Trop Med Hyg. 2011 Feb 4;84(2):241–3.

575. Müller HM, Dimopoulos G, Blass C, Kafatos FC. A hemocyte-like cell line established from the malaria vector Anopheles gambiae expresses six prophenoloxidase genes. J Biol Chem. 1999 Apr 23;274(17):11727–35.

576. Wechsler SJ, McHolland LE, Wilson WC. A RNA virus in cells from Culicoides variipennis. J Invertebr Pathol. 1991 Mar;57(2):200–5.

577. López-González M, Meza-Sánchez D, García-Cordero J, Bustos-Arriaga J, Vélez-Del Valle C, Marsch-Moreno M, et al. Human keratinocyte cultures (HaCaT) can be infected by DENV, triggering innate immune responses that include IFNλ and LL37. Immunobiology. 2018;223(11):608–17.

578. Livonesi MC, De Sousa RLM, Badra SJ, Figueiredo LTM. In vitro and in vivo studies of ribavirin action on Brazilian Orthobunyavirus. Am J Trop Med Hyg. 2006 Nov;75(5):1011–6.

579. Rosseel T, Van Borm S, Vandenbussche F, Hoffmann B, van den Berg T, Beer M, et al. The Origin of Biased Sequence Depth in Sequence-Independent Nucleic Acid Amplification and Optimization for Efficient Massive Parallel Sequencing. PLoS One [Internet]. 2013 Sep 26 [cited 2020 Jul 7];8(9). Available from: https://www.ncbi.nlm.nih.gov/pmc/articles/PMC3784409/

580. Kamal M, Kenawy MA, Rady MH, Khaled AS, Samy AM. Mapping the global potential distributions of two arboviral vectors Aedes aegypti and Ae. albopictus under changing climate. PLOS ONE. 2018 Dec 31;13(12):e0210122.